Langmuir-Blodgett Film Formation of Polymerisable Amphiphilic Metal Complexes

(A structural investigation)

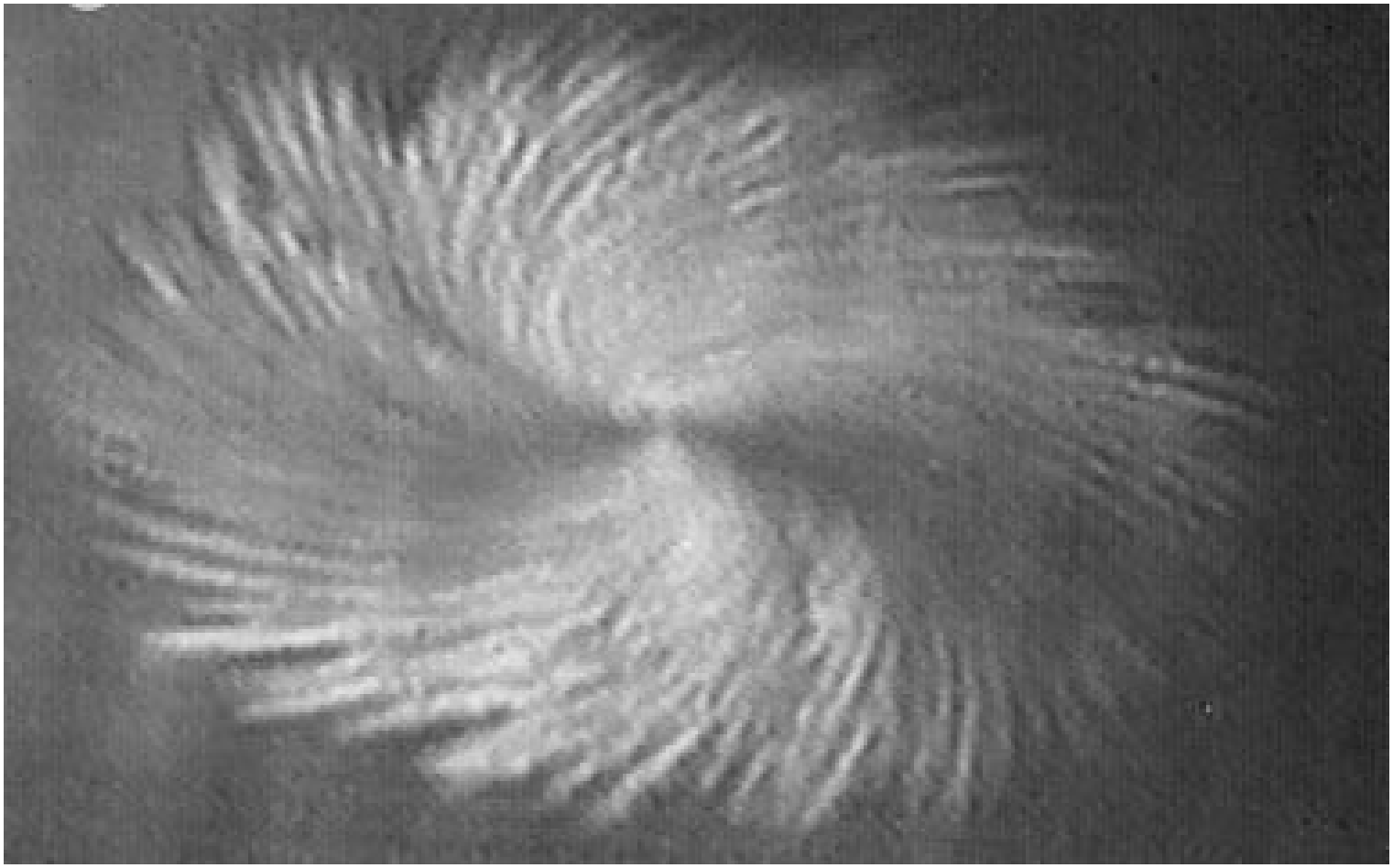

Peter Werkman

Langmuir-Blodgett Film Formation of Polymerisable Amphiphilic Metal Complexes

(A structural investigation)

P.J. Werkman

Quality assessment committee: Prof.dr. G.A. Sawatzky
Prof.dr. J.B.F.N. Engberts
Prof.dr. E.J.R. Sudhölter

Langmuir-Blodgett Film Formation of Polymerisable Amphiphilic Metal Complexes
(A structural investigation)
P.J. Werkman
Ph.D. Thesis
University of Groningen, The Netherlands
January 1998

Cover: BAM image of a crystalline domain of the ester pyridine amphiphile formed upon compression of a monolayer film of the amphiphile on a 5 mM $Cu(ClO_4)_2$ subphase.

ISBN 90-367-0799-4

This research was supported by the Netherlands Foundation for Chemical Research (SON) with financial aid of the Netherlands Organisation for Scientific Research (NWO).

Rijks*universiteit* Groningen

Langmuir-Blodgett Film Formation of Polymerisable Amphiphilic Metal Complexes

(A structural investigation)

Proefschrift

ter verkrijging van het doctoraat in de
Wiskunde en Natuurwetenschappen
aan de Rijksuniversiteit Groningen
op gezag van de
Rector Magnificus Dr. F. van der Woude
in het openbaar te verdedigen op
vrijdag 9 januari 1998
des namiddags te 4.15 uur

door

Pieter Johannes Werkman

geboren op 20 juni 1969
te Leek

Promotor: Prof.dr. A.J. Schouten

Ter nagedachtenis aan mijn vader
Voor mijn moeder

Dankwoord

Na 5 jaar is er dan een eind gekomen aan mijn promotietijd. Het is dus een goed moment om de vele mensen te bedanken die allemaal op hun eigen manier hebben bijgedragen aan het tot stand komen van dit proefschrift.

In de eerste plaats wil in mijn promotor, Prof.dr. Arend Jan Schouten, bedanken voor de mogelijkheid die hij me heeft geboden om in zijn groep dit promotieonderzoek uit te voeren. De grote mate van vrijheid in het onderzoek en het vertrouwen dat ik van je kreeg heb ik erg gewaardeerd.

De hoofdvakstudenten, Ad Schasfoort, Wilhelm Veehof en Hans Wilms hebben veel inzet en doorzettingsvermogen getoond. Jullie inspanningen zijn niet voor niets geweest en zijn in de verschillende hoofdstukken van dit proefschrift weer te vinden. Bedankt!

Verder wil ik de leden van de leescommissie, Prof.dr. G.A. Sawatzky, Prof.dr. J.B.F.N. Engberts en Prof.dr. E.J.R. Sudhölter bedanken voor de snelle en kritische beoordeling van het manuscript. Professor Sudhölter wil ik ook nog bedanken voor de gelegenheid die hij mij heeft gegeven om samen met Marina Noordegraaf en Peter “Hindley Street the Party Street” Kimkes Brewster angle metingen aan monolagen te verrichten in zijn laboratorium aan de L.U. Wageningen.

Voor verschillende karakterisatiemethoden moest een beroep worden gedaan op andere vakgroepen. Frans van der Horst coördineerde altijd (in goed overleg) de meettijd van de diffractometer zodat de noodzakelijke SAXR metingen konden worden verricht. Deze taak had Arend Heeres wat betreft de XPS apparatuur. Hartelijk dank daarvoor. Gert Oostergetel wil ik graag bedanken voor het me bijbrengen van de beginselen van elektronen microscopie en het maken van de elektronen diffractie patronen van enkele monolagen.

Jannes Hommes, Jan Ebels en Harm Draaijer worden bedankt voor de vele elementanalyes en het meedenken over het koper(I)-vraagstuk.

Voor de prettige werksfeer op het lab ben ik vele (ex-) aio’s, oio’s en studenten dank verschuldigd. In dit geval wil ik in het bijzonder de groep Schouten bedanken. Berend, Joke, Maarten, Ulrich, Gerthé, Jannie, Robert, Patrick, Evelyne, Kati en Richard, bedankt!

Een speciaal woord van dank gaat uit naar Reinie. Onvermoeibaar en tot laat in de avond voerde hij de verschillende XPS metingen voor mij uit wat uiteindelijk leidde tot de oplossing van het koper(I)-probleem. Maar ook onze biljart en barbecue avonden zal ik niet snel vergeten. Wat dat betreft mag ook Gerard met z'n onovertroffen "kip uit de oven" niet onvermeld blijven.

Mijn "fietsvader" Joop Vorenkamp en natuurlijk Marcel "la Redoute" Teerenstra wil ik met name bedanken voor de vele fietskilometers die we samen hebben afgelegd. Joop als we nog eens samen gaan fietsen mag jij steeds een bandje voor en wat Marcel betreft, driemaal is scheepsrecht.

Jannette en Betty wil ik bedanken voor het in goede banen leiden van mijn engels in dit boekje en in de verschillende artikelen.

Natuurlijk was er buiten het lab ook een leven. Naast de gezelligheid van mijn voetbalploeg kon ik altijd terugvallen op de steun en gezelligheid van mijn vrienden: Theo, Monique, Mark, Hetty, Anton, Christina, Bob, Karin en natuurlijk mijn broeder Wim. Hiervoor hartelijk dank.

Mijn moeder wil ik bedanken voor alle liefde, steun en vertrouwen die ze me altijd heeft gegeven ook op momenten in haar leven dat ze het zelf niet zo gemakkelijk had.

Tenslotte bedank ik Baukje voor de steun en de liefde die ik altijd van haar kreeg. Maar ook voor het doorstaan van het afreageren van mijn frustraties als er weer eens wat experimenten mislukt waren en tijdens het schrijven van dit boekje.

Peter.

Contents

Chapter 1

General introduction

Summary

In this first chapter an introduction will be given into the principles of the Langmuir-Blodgett technique. Two well-known techniques to visualise the morphology of a monolayer during compression (fluorescence and Brewster angle microscopy) are pointed out briefly. Different routes for the preparation of polymer LB films will be discussed and while in the present study diacetylene group containing amphiphiles are used, the history of Langmuir-Blodgett mono- and multilayers of diacetylene group containing amphiphiles is briefly reviewed. The possibility of incorporation of metal ions into Langmuir monolayers by different approaches will be discussed. The method of complex formation of metal ions with amphiphilic ligands will be considered in more detail, because polymerisable amphiphilic ligands will be used throughout this thesis. Finally, an outline of the thesis is given.

Historical introduction

Molecular ordered thin organic films, ranging in thickness from about a few nanometers (a monolayer) to several hundred nanometers, show a considerable technological promise. Highly ordered organic films can be prepared easily by means of the Langmuir-Blodgett technique, by which multilayers of a particular compound can be built up from monolayers, transferred from the air-water interface onto a solid substrate. The thickness of these multilayers (LB films) can easily be controlled by the size of the compound and the number of deposited layers.

The first documented experiment on the effect of oily films on a water surface, was written by Benjamin Francklin [1] in 1774. But in 1891, Agnes Pockels [2] was the first to describe a method to manipulate oily films at the air-water interface by means of movable "barriers". A few years later Raleigh [1,3,4] proposed that the films prepared by Pockels at the air-water interface were one molecule thick. In 1917, Langmuir [4,5] developed the experimental (surface balance) and theoretical concepts which underlie our modern understanding of the behaviour of molecules in a monolayer at the air-water interface. The first studies on multiple deposition of long aliphatic carboxylic acids onto a solid substrate have been carried out by Katherine Blodgett [6,7,8]. The early investigations have been mainly related to the interfacial phenomena, but nowadays the interest is shifted to functional LB films with potential applications [9] in thin film optics, as sensors and transducers, as protective layers, as patternable materials, for surface preparation and modification, for chemically modified electrodes and as models for biological membranes.

Traditionally, LB films have been prepared from low molecular-weight compounds, like fatty acids. These organic films have a poor mechanical, thermal and chemical stability, which reduces their application in practical devices. One way to overcome these obstacles is to make use of polymeric LB films, which enhances the thermal, mechanical and chemical stability of these multilayer films [9,10,11].

Monolayer formation

The monolayer characteristics of a compound can easily be obtained by measuring surface pressure-area (Π-A) isotherms at the air-water interface. A dilute solution of the compound (dissolved in a volatile solvent) is spread at the air-water interface on a Langmuir trough. The solvent evaporates leaving a monolayer of the compound at the air-water interface [1,3].

Materials suitable for the formation of monolayers at the air-water interface are amphiphiles bearing a hydrophilic (“water loving”) headgroup and a hydrophobic (“water hating”) tail. Classical monolayer forming materials are fatty acids (like arachidic or stearic acid) with a carboxylic headgroup and a long alkyl chain.

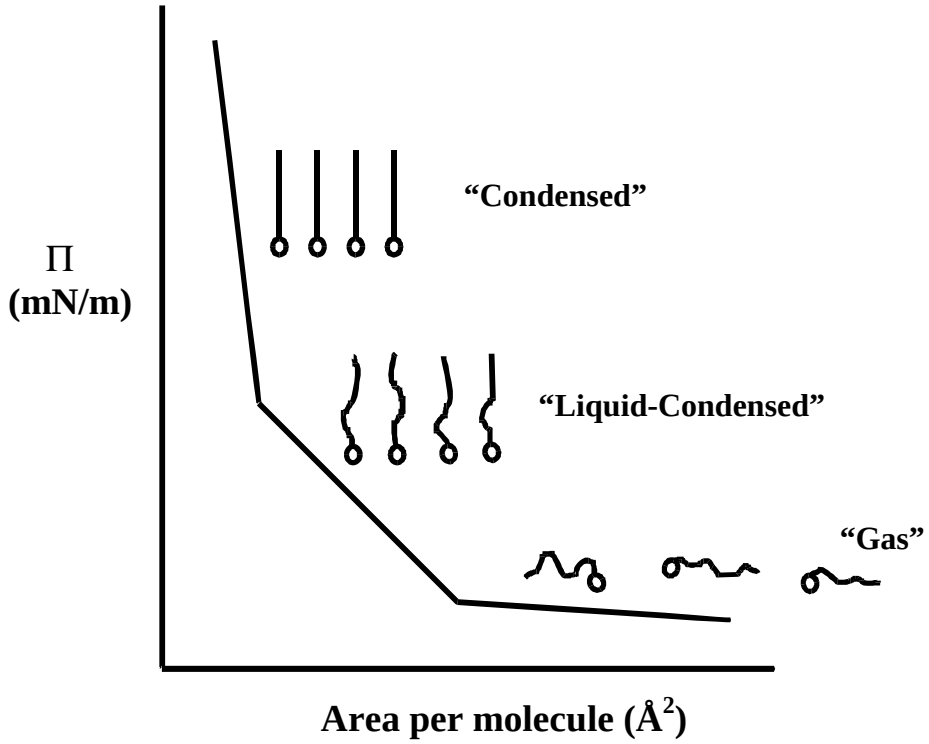

Figure 1.1: *An example of a surface pressure-area isotherm.*

In Figure 1.1, an example of a surface pressure-area isotherm can be seen. When the compound is spread at the air-water interface, a “gaseous” (G) monolayer is formed, in which the molecules occupy a large area per molecule. The molecules hardly feel each other and due to thermal motions the gaseous monolayer will have surface pressures (Π) up to 0.1 mN·m^{-1}. Upon compression of the monolayer (by moving the barriers towards each other) the area per molecule decreases and at a certain area per molecule the surface pressure starts to increase because the molecules exert a repulsive effect on each other. At that point the “liquid-condensed” (LC) region of the isotherm is reached. This LC phase is more compressible, lower pressure condensed phase. When the area per molecule is reduced even further, at a certain point there is a sharp discontinuity of the slope of the Π-A isotherm. The surface pressure increases very rapidly with a small change in area per molecule. This is called the “condensed” region of the isotherm, in which the molecules are arranged in their closest possible packing which is highly incompressible. In this region the monolayer is considered as

a two-dimensional crystal in which the aliphatic tails have a regular arrangement. In some cases the surface pressure already starts to rise at molecular areas which are much larger then those required for a close packing of the molecules (already at molecular areas which are typically two or three times as large as the molecular cross-section). At that point the "liquid-expanded" (LE) region of the isotherm is reached. In this region of the isotherm, the aliphatic tails have a random, irregular (liquid-like) orientation and are intertwined. Isotherms which only have a LE region and were no LC or condensed region is observed are frequently observed for amphiphiles in which some disruption of the aliphatic chain causes a difficulty in packing, as in the case of 2- ethylpalmitic acid [1,3].

The morphological changes of monolayers upon compression can easily be visualised by means of fluorescence or Brewster angle microscopy (BAM). The fluorescence technique was introduced by Tscharner and McConnel [12-15] in 1981 and by Lösche and Möhwald [16,17]. This technique relies on fluorescent probes, like NBD-DPPE (N-(7-nitro-2-1,3-benzoxadiazol-4-yl)dipalmitoyl-L-α-phosphatidylethanolamine), which are incorporated into the molecular films at concentrations in the order of 1 mol%. The fluorescent probe dissolves in the LE phase, so the condensed phase will appear as dark floating objects in a bright, two-dimensional liquid. In this way it became possible to visualise coexisting phases and domain structures that were previously only inferred from surface pressure-area isotherms or surface potentials. LC phases with a wide variety of sizes and shapes were observed which depended on the chemical composition of the amphiphile, temperature, surface pressure and on concentrations of impurities. This brings us to the critical point of the fluorescent probe which causes some problems. For instance, a high fluorescent probe concentration may lead to artifacts because it may disturb the local environment of the probe [16-18] and increase the number of nucleation sites, which could for instance result in a drastic reduction in size of the LC domains [19].

Two groups separately developed the Brewster angle microscope (BAM) in 1991 [20,21]. The BAM technique allows a direct visualisation of the monolayer without addition of special probes. The operation of the BAM is based on the well-known fact that, for a pure Fresnel interface, the reflectivity of the in-plane polarisation component becomes zero at the Brewster angle (53^o for the air-water interface). So, when the water surface (which is almost a pure Fresnel interface) is illuminated under the Brewster angle with monochromatic p-polarised light, the reflectivity can be as low as 10^{-7}, and the water surface will appear dark [18,21,22]. The reflectivity is not exactly zero because of the presence of some roughness caused by capillary waves. The reflected light is very sensitive to the interfacial properties. When a monolayer (with refractive index n_2) is present at the air-water interface, this will

have a large effect on the Brewster angle condition and the reflectivity is not zero anymore but increases. Regions of the monolayer which differ in density or orientation of the molecules on the air-water interface will show up by virtue of their optical contrast. A detailed description of the different experimental setups has been published elsewhere [18-20,22]. A lot of reports have been published on the formation of liquid-condensed domains at the plateau region of the isotherms of esters, alcohols, phospholipids, polymers [22,23] and other amphiphilic compounds [20,21,24-27] for which all kind of textures could be observed. These include for instance, circular, spiral and branched structures.

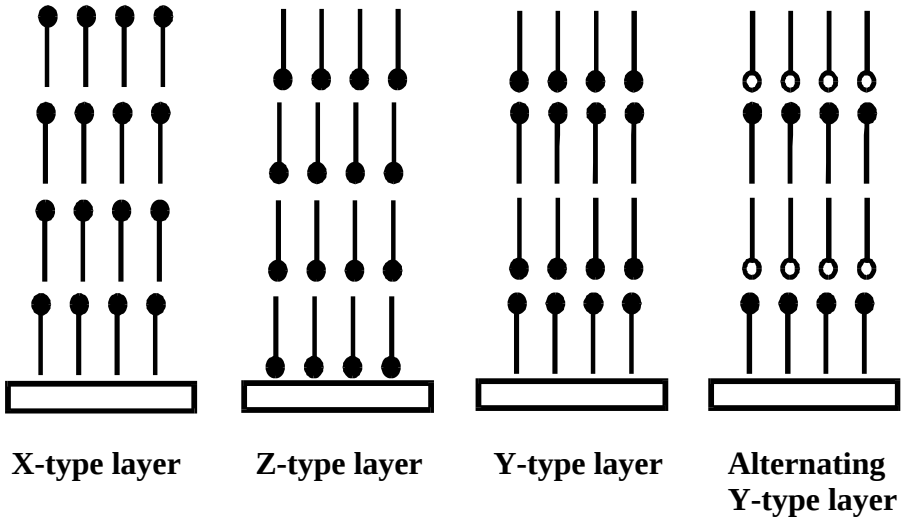

Figure 1.2: *Multilayer structures that can be obtained by the Langmuir-Blodgett technique.*

Monolayers at the air-water interface can easily be deposited onto solid substrates when the monolayer is in the oriented state at a certain surface pressure, by dipping a substrate perpendicularly through the water surface. Depending on the structure of the amphiphile or surface pressure at which the monolayers are transferred, transfer of the monolayer may occur only during the downstroke (X-type deposition), only during the upstroke (Z-type deposition) or both during down- and upstroke (Y-type deposition). The corresponding multilayer structures can be seen in Figure 1.2. Also noncentrosymmetric, alternating multilayers can be built up using an alternate layer trough, producing supramolecular structures ("superlattices"). Y-type multilayers films are the thermodynamically most stable multilayers with the hydrophilic head to head and hydrophobic tail to tail arrangement. Although there have been a lot of reports on multilayers built up with a X- or Z-type deposition, these multilayers often exhibit a Y-type structure as was concluded by several researchers from X-ray diffraction

measurements [1,3,28-31]. In those cases the molecules must have "turned over" to form a thermodynamically more stable Y-type structure. There are only a few reports on stable Z-type multilayers films of low molecular-weight compounds. For instance, Ashwell et al. [32] showed that the addition of a second hydrophobic endgroup to a hydrophilic chromophore resulted in LB films with a stable Z-type arrangement up to 100 layers and Popovitz-Biro et al. [33] incorporated a second amide bond along the aliphatic chain of the amphiphile, in order to stabilise the Z-type multilayer structure by means of hydrogen-bond formation between the amide bonds of neighbouring molecules.

Polymer Langmuir-Blodgett films

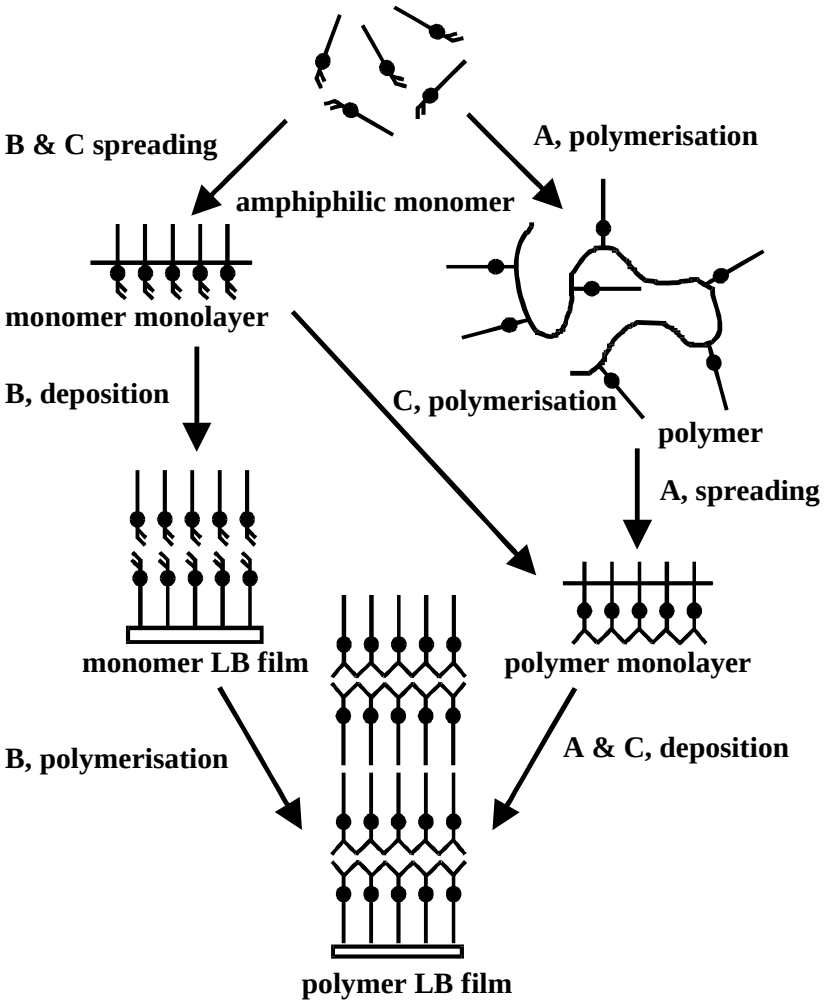

Figure 1.3: *Three routes for the preparation of polymer LB films.*

In Figure 1.3, schematically 3 routes are shown for the preparation of polymer LB films. *Route A*: an amphiphile is synthesised and subsequently polymerised by conventional polymerisation methods after which the formed polymer is spread at the air-water interface, followed by deposition onto solid substrates. In the literature a large amount of studies have been reported on the formation of polymer LB films following this route, like poly(octadecylmethacrylaat) [34], poly(octadecylacrylaat) [34], poly(isobutylmethacrylaat) [35], poly(methylmethacrylaat) [36,37], poly(N-alkylacrylamides) [38], poly(isocyanides) [39,40], etc..

Route B: an amphiphilic monomer is spread at the air-water interface and a condensed monolayer is formed. This monolayer is subsequently transferred onto solid substrates after which the monomer LB film is polymerised by means of the appropriate treatment, like UV light, electron beam or γ-irradiation or by a heat treatment. A disadvantage of this method is that the formed polymer films sometimes have cracks and defects caused by internal stress and reorganisation due to the polymerisation under restricted mobility conditions of the LB film. The polymerisation of polymerisable LB films has been studied mainly with amphiphiles containing double or triple bonds in the aliphatic tail, whereas also a few polycondensations in LB multilayers have been carried out employing long-chain esters or amino acids [41-43]. So, a lot of papers have been published about the polymerisation of vinyl amphiphiles, like vinyl stearate [44], octadecyl acrylate [45], octadecyl methacrylate [46], α-octadecyl acrylamide [47] and octadecyl fumaric and maleic esters [48], in LB films. The first application of polymerisable LB films of vinyl amphiphiles to a high resolution negative resist has been investigated by Barraud et al. [49,50]. Also diene amphiphiles have been used for this route. Ringsdorf et al. [51], for instance, studied the photopolymerisation of octadiene and docosadiene derivatives having various groups. This polymerisation proceeds in two steps, first a soluble polymer is formed by visible light irradiation and the subsequent UV irradiation results in a insoluble polymer network due to crosslinking.

A variety of diacetylenic amphiphiles have been synthesised and studied systematically. It was found by Tieke et al. [11,52] that diacetylenic acids containing more than 20 carbon atoms and having a melting point above 45 ^{o}C, were suitable for the formation of stable LB multilayers.

Route C is a intermediate between route A and B, the monomer monolayer is formed in the same way as in route B but the monomer monolayer is polymerised at the air-water interface and subsequently transferred onto solid substrates, forming a polymer LB film.

In this thesis, *route B* is used for the preparation of polymer LB films with amphiphiles which contain a diacetylene functionality in the aliphatic chain. A more detailed description

on the formation of LB films of diacetylene group containing amphiphles, will be given in the next section.

LB films of diacetylene group containing amphiphiles

The polymerisation of diacetylenes has been first studied in the solid state by Wegner [53,54]. The mechanism of the polymerisation has been studied well and proceeds via a 1,4 addition to the triple bond (Fig. 1.4).

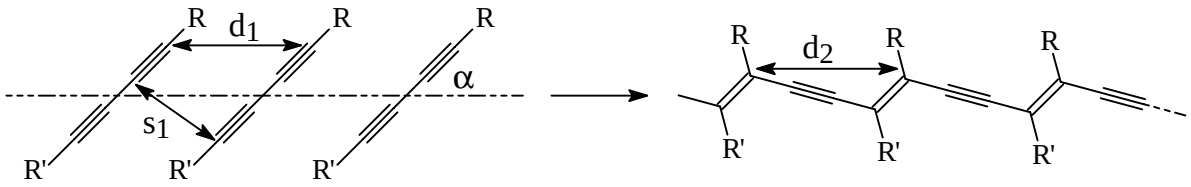

Figure 1.4: *The topochemical principle in diacetylene polymerisation.*

The polymerisation of diacetylenes is a topochemical reaction, so, the molecules must be regularly packed in a specific arrangement as shown in Figure 1.4. The topochemical polymerisation can only occur when a) the difference between the translational period in the monomer (d_1) and polymer (d_2) approaches zero, so, for reactive diacetylenes d_1 is between 4.7 and 5.2 Å and d_2 is almost constantly 4.93 Å [4,55-57], b) s_1 is smaller than 4.0 Å, with a lower limit of 3.4 Å and c) the angle (α) between the diacetylene rod and the translational vector is close to 45^o ($\pm 5^o$). Since diyne polymerisation is known to proceed strictly under lattice control, the differences in reactivity between diacetylene compounds, can be explained by small variations of packing geometry's of the monomers.

Polymerisation of diacetylenes occurs by means of UV irradiation, X- or γ-rays, electron beam or by thermal treatment. Upon polymerisation a one-dimensional, rigid backbone is formed with an extended π-conjugation. Absorption spectra of the polymerised multilayers show a strong π to π^* absorption with λ_{max} = 620 nm for the blue form of the polymer and at higher conversions, absorption's at λ_{max} = 500 and 540 nm for the red form of the polymer [56-58]. The polymerisation of diacetylenes is accompanied by a reorientation of the side chains, which leads to a lesser extend of conjugation at high conversions.

The early systematic studies on diacetylene amphiphiles have been carried out by Tieke et al. [55,59,60] and by Day and Ringsdorf [61,62].

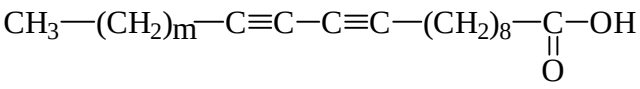

They showed that polydiacetylenic multilayers films of diacetylenes with m ≥ 8 were very stable and had interesting physical properties, e.g., photoconductivity [63,64].

The morphology and molecular packing of the diacetylene monolayers polymerised at the air-water interface, have been studied by Lando et al. [65,66] using transmission electron microscopy and electron diffraction while Putman et al. [67] used atomic force microscopy to investigate the molecular packing of LB films of diacetylenes and polydiacetylenes. Both groups found that the polymeric films had a fibrous texture and the cracks in the film were parallel to the chain axis director.

Lieser et al. [52,68,69] used electron diffraction and small angle X-ray diffraction techniques to study the structure of the monomer and polymer LB films of diacetylene monocarboxylic acids with different lengths of the aliphatic chain and different locations of the triple bonds along the aliphatic chain (near the hydrophilic head or in the middle of the aliphatic chain). They found that the aliphatic chain had a large tilt angle (α) with respect to the surface normal, ranging from 41 to 20^{o}, depending on the structure of the diacetylene compound.

Raman [70] and FT-IR spectroscopy [71] revealed that during the polymerisation process the polydiacetylene backbone keeps a fully extended conformation without any interruptions of its conjugation, forming the blue form of the polymer. When the polymerisation proceeds, the regular plane of the all-trans alkyl chain is converted into a more irregular one containing gauche conformations. The latter conformation causes some interruptions in the fully extended conjugated backbone of the polymer and a reduction of the average conjugation length, resulting in the formation of the red form of the polymer.

Bubeck et al. [72] reported that the photopolymerisation of diacetylene LB films can be sensitised by surface active dyes, like cyanine, acridine and anthraquinone, incorporated in the multilayers.

After these fundamental studies other diacetylene group containing amphiphiles were synthesised, like lipids containing two aliphatic tails [53,73], phospholipids [74], ferrocene group containing amphiphiles [75], amphiphiles with an amino acid headgroup [76], a phenyl headgroup [77], pyridine [78] and bipyridine [78] groups containing amphiphilic diacetylene

compounds. Polydiacetylene LB films have a wide range of potential applications in non-linear optics (second- and third-harmonic generation), biosensors, lubrication of magnetic tape, fabrication of integrated circuits using microlithography and semiconductor devices such as photovoltaic cells [9,55,67].

Incorporation of metal ions into LB films

Nowadays, there is a great interest in functional LB films. There are different approaches for the preparation of functional multilayer films. Amphiphiles or polymers can be synthesised having a functionality in the side chain or the hydrophilic headgroup, like the azo group [3,79,80], cyanine dye [81], merocyanine dye [82], pyridinium TCNQ salt [83], but also functional amphiphiles can be mixed with polymers as was shown by Schoondorp et al. [84], who made LB films of amylose esters with alkyl side groups mixed with specially designed amphiphilic NLO-dyes which showed almost ideal second-harmonic generation (SHG) properties. Kimkes et al. [85] showed that polymers containing an azo group in the polymer backbone, substituted with long aliphatic chains are suitable for the formation of functional LB films.

Another approach for the preparation of functional LB films, is to introduce metal ions. Metal ions can introduce special semiconducting, magnetic or quantum physical properties to the LB films [3,9,10]. There are several ways to introduce metal ions into monolayers at the air-water interface. For instance, metal ions dissolved in the subphase, can form salts with carboxylic groups of amphiphiles or polymers at a distinct pH range as was already shown by Katherine Blodgett in 1935 [6-8]. Divalent cations (like Pb(II), Ca(II), Cd(II), etc.) stabilise the monolayers of fatty acids (like arachidic and stearic acid) due to the crosslinking action of the metal ions and triply charged cations tend to give extremely rigid monolayers with a high shear modulus [3].

The metal ions can also coordinate to a ligand which is incorporated in an amphiphile or polymer. Coordination of metal ions to the amphiphilic ligand can take place in the solution, as was shown by Armand et al. for pentacyanoferrate(III) coordinated to a pyridine amphiphile [86,87] or iron (II) complexes with a triazole amphiphile [88]. They have spread the presynthesised metal complexes at the air-water interface and built up multilayers of the pentacyanoferrate(III) complex, but in the case of the triazole amphiphile stable monolayers were not formed with the iron(II) ions, because the iron ions diffused into the aqueous subphase. The same approach was used by Aroca et al. [89,90]. They have spread metal

complexes (Cu(II), Pd(II), Mg(II) , Zn(II)) of phthalocyanines substituted with alkyl chain at the air water interface and subsequently built up multilayers of these metal complexes.

Coordination of metal ions to amphiphilic ligands can also take place at the air-water interface. When metal ions are dissolved in an aqueous subphase and the amphiphilic ligands are subsequently spread on the metal ion containing subphase complexation takes place and the metal ions are incorporated into the monolayer at the air-water interface, as is shown in Figure 1.5. The Gouy-Chapman-Stern model has been used to describe the electric double layer between the amphiphilic ligand and the aqueous salt solution.

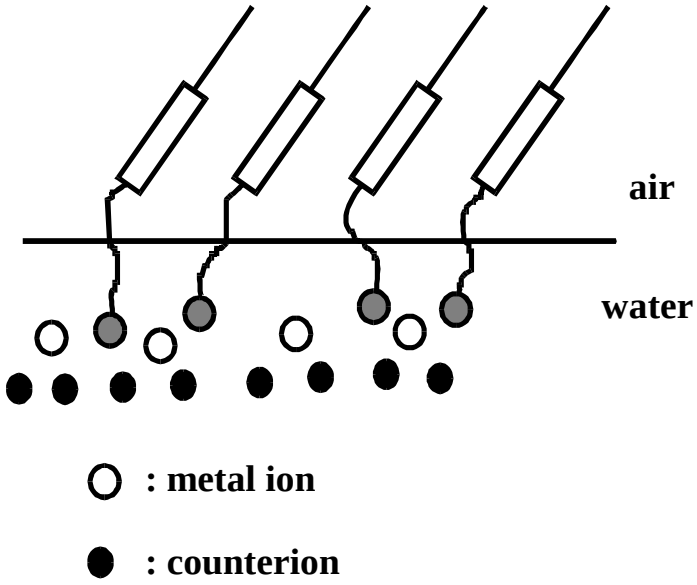

Figure 1.5: *Schematic representation of the metal complex monolayer at the air-water interface.*

The formed metal complexes can be transferred onto solid substrates, forming a functional LB film. The latter approach is used in the studies described in this thesis and there has been a growing interest in the latter approach in the last decade. All kinds of ligands were used for this purpose, like crownethers, 18-crown-6 [91,92] (Scheme 1.1, **1**), which has a affinity sequence for metal ions of $K^+ > Cs^+ > Na^+$, porphyrin [93,94] (Scheme 1.1, **2**), phthalocyanine [95] (Scheme 1.1 I, **3**), dithiooxamide [96] (Scheme 1.1, **4**), forming a coordination polymer network with Cu(II) ions at the air-water interface, pyridine [97,98] (Scheme 1.1, **5**), bipyridine [99] (Scheme 1.1, **6**) and imidazole [100] (Scheme 1.1, **7**).

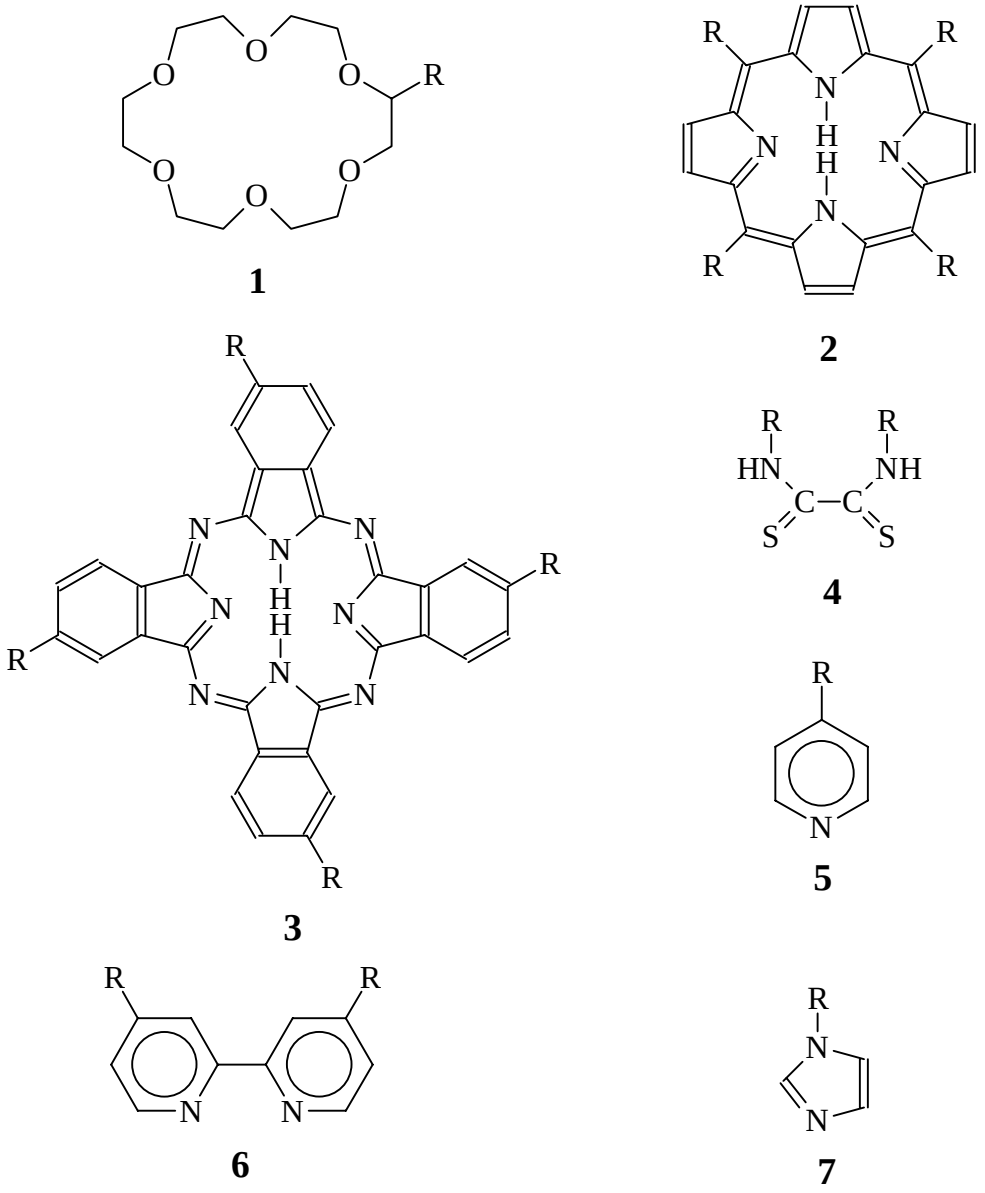

Scheme 1.1

Addition of metal ions to the subphase changed the form of the isotherms, indicating that complexation had taken place and when multilayers of the metal complexes were built up, the presence of metal ions could be proven by means of XPS measurements. For instance, Caminati et al. [97,101] studied the monolayer behaviour of nonadecylpyridine on subphases containing Ni(II), Cu(II) and Co(II) ions. The monolayers on the metal ion containing subphase had a larger collapse pressure than on an aqueous subphase, so, upon complexation a more stable monolayer was formed. LB films were built up containing metal ions as was

proven by UV/Vis absorption and XPS measurements. Van Esch et al. [100] studied the monolayer characteristics of chiral and achiral N-substituted imidazole derivatives containing two aliphatic chains. These amphiphiles formed stable monolayers at the air-water interface and upon addition of small amounts of transition metal ions (10^{-7} M) a change in the isotherms was measured, suggesting that the ions bind to the imidazole ligand. Fluorescence microscopy experiments were performed also and revealed that condensed domains had been formed when the monolayer was compressed into the LE to LC phase transition.

Multilayers containing metal ions have a number of potential applications, like new types of chemical sensors as was already shown by Petty et al. [92,102] who made LB films of phthalocyanine amphiphiles containing Cu(II) or Ni(II) ions, which acted as an optical sensor for toluene vapours, whereas Gu et al. [103] built up gas sensors of porphyrin containing LB films which were sensitive to gases like NO_2, NH_3, CO and H_2S. Caminati et al. [101] have built a sensor of a LB film of nonadecylpyridine which was sensitive to metal ions like Co(II), Ni(II) and Cu(II). Metal ion containing LB films are also of interest as novel supramolecular catalytical systems [100]. Zhang et al. [104] showed that LB films of Cr(III) or Mn(III) ions containing porphyrin amphiphiles have photovoltaic properties and exhibit a particular photovoltaic response with different central ions, under an external field.

The metal ions inside LB films can easily be converted with the gases H_2S, H_2Se and H_2Te into their corresponding metal sulphides, metal selenides and metal tellurides, respectively, as was shown by Barraud et al. [105,106] in 1986 and by Urquhart et al. [107,108] in later years. The sulphides, selenides and tellurides form nanoparticles or in the case of copper sulphide, a layer between the hydrophilic headgroups of the amphiphiles inside the multilayer. The formed semiconductor particles have large third-order nonlinear optical effects [109] and might have practical use in the development of optoelectronic devices, such as optical switches, infrared detectors or photovoltaics [110,111]. So, LB films of polymer coordination complexes deserve more attention from the organic and physical point of view because of the great variety of potential applications.

Aim and outline of the thesis

The scope of this thesis is to obtain a better understanding of the complexation behaviour of polymerisable amphiphilic ligands at the air-water interface and to built up multilayer and alternating multilayer films of the formed metal complexes. Different amphiphilic ligands were synthesised which contained a diacetylene functionality in the

aliphatic tail in order to polymerise the LB film upon UV irradiation, forming a semiconductive polymer LB film with enhanced mechanical, thermal and chemical stability compared to the monomer LB film.

In *Chapter 2*, the monolayer characteristics of a diacetylene group containing dithiooxamide amphiphile (amphiphile A) with two aliphatic tails are discussed. Upon complexation with Cu(II) ions, a stable two-dimensional polymer coordination network is formed at the air-water interface, which could be transferred onto solid substrates, whereas on an aqueous subphase the amphiphile itself did not form a stable monolayer.

In *Chapter 3*, the monolayer characteristics of the amphiphile 4-(10,12-pentacosadiynamidomethyl)pyridine (amphiphile B) upon complexation with Cu(II) ions under different conditions will be discussed.

The structure of LB films of Cu(II) and Cd(II) ion complexes of amphiphile B will be studied in *Chapter 4*. Depending on the type of metal ion or counter ion, the structure of the multilayers is altered which has an enormous influence on the polymerisation properties of these multilayers. With perchlorate as counter ion, the layer structure of Cu(II) ions containing LB films is preserved during the polymerisation process, while with chloride as counter ion no regular layer pattern could be observed after exposure to UV light. During the XPS experiments, X-ray induced copper reduction took place and the rate of the copper reduction depended on the type of counter ion. Multilayers containing Cd(II) ions, had a much larger tilt angle of the aliphatic tails with respect to the surface normal.

Chapter 5 will deal with the monolayer characteristics of the amphiphile, 4-(10,12-pentacosadiynoatomethyl)pyridine (amphiphile C) upon coordination with Cu(II) ions under different conditions. Furthermore, the structure of the Cu(II) ions containing LB films will be discussed, before and after exposure to UV light.

In *Chapter 6*, the influence of hydrogen bonding between neighbouring molecules, on the stability of monolayers of pyridine amphiphiles (B and C) will be studied by means of surface pressure-area isotherms and Brewster angle microscopy. Furthermore, the formation of condensed domains is nicely shown in the plateau region of the isotherm. The morphology of the formed domains strongly depended on the structure of the amphiphile and the type of counter ion.

Complexation at the air-water interface took place at much lower concentrations of metal ions ($5 \cdot 10^{-7}$ M) when imidazole was used as a ligand, as is described in *Chapter 7*. The amphiphile N-(10,12-pentacosadiynamidopropyl)imidazole (amphiphile D) formed metal complexes with all kinds of metal ions, following the series: Ni(II) < Cd(II) ≅ Co(II) < Zn(II)

< Cu(II). Multilayers of Cu(II) ion complexes had a poor layer structure which was preserved during the polymerisation process.

Chapter 8 will deal with the construction of alternating multilayers of 10,12-pentacosadiynoic acid (amphiphile E) and amphiphile B from a 5 mM $CdBr_2$ subphase. The multilayers had a good distinct layer pattern which is maintained upon UV irradiation.

Finally, in *Chapter 9*, the formation of copper sulphide layers in a LB film of the copper complex of amphiphile B will be studied. Different types of copper sulphide were formed inside these multilayers when the type of counter ion was changed. The layer structure was preserved during the formation of the copper sulphide layers.

Parts of this work have been published: Chapter 3 [112] or have been submitted for publication: Chapter 2 [113], Chapter 4 [114], Chapter 5 [115], Chapter 6 [116], Chapter 7 [117], Chapter 8 [118] and Chapter 9 [119].

References

1. G.L. Gaines, Jr., *Insoluble monolayers at liquid-gas interfaces*, Interscience, New York **1996**.
2. A. Pockels, *Nature* **1891**, *43*, 473.
3. G. Roberts, *Langmuir-Blodgett films*, Plenum Press, New York and London **1990**.
4. U. Ulman, *An introduction to ultrathin organic films: from Langmuir-Blodgett to self-assembly*, Academic Press, Inc., Boston **1991**.
5. I. Langmuir, *J. Am. Chem. Soc.* **1917**, *39*, 1848.
6. K.B. Blodgett, *J. Am. Chem. Soc.* **1935**, *57*, 1007.
7. K.B. Blodgett and I. Langmuir, *Phys. Rev.* **1937**, *51*, 964.
8. K.B. Blodgett, *J. Phys. Chem.* **1937**, *41*, 975.
9. J.D. Swalen, D.L. Allara, J.D. Andrade, E.A. Chandross, S. Garoff, J. Israelachvili, T.J. McCarthy, R. Murray, R.F. Pease, J.F. Rabolt, K.J. Wynne and H. Yu, *Langmuir* **1987**, *3*, 932.
10. T. Miyashita, *Prog. Polym. Sci.* **1993**, *18*, 263.
11. B. Tieke, G. Lieser and G. Wegner, *J. Polym. Sci.: Polym. Chem. Ed.* **1979**, *17*, 1631.
12. V. von Tscharner and H.M. McConnel, *Biophys. J.* **1981**, *36*, 4009.
13. R.W. Weis and H.M. McConnel, *Nature* **1984**, *310*, 47.
14. H.M. McConnel, D. Keller and H. Gaub, *J. Phys. Chem.* **1986**, *90*, 1717.
15. H.M. McConnel, *Annu. Rev. Phys. Chem.* **1991**, *42*, 171.

16. M. Lösche, E. Sackman and H. Möhwald, *Ber. Bunsenges. Phys. Chem.* **1983**, *87*, 848.
17. M. Lösche and H. Möhwald, *Rev. Sci. Instrum.* **1984**, *55*, 1968.
18. M.A. Cohen Stuart, R.A.J. Wegh, J.M. Kroon and E.J.R. Sudhölter, *Langmuir* **1996**, *12*, 2863.
19. N.A.J.M. Sommerdijk, *Thesis*, University of Nijmegen, The Netherlands **1995**.
20. D. Hönig and D. Möbius, *J. Phys. Chem.* **1991**, *95*, 4590.
21. S. Hénon and J. Meunier, *J. Rev. Sci. Instrum.* **1991**, *62*, 936.
22. S. Hénon and J. Meunier, *Thin Solid Films* **1993**, *234*, 471.
23. Y.S. Kang, S. Rishud, J.F. Rabolt and P. Stroeve, *Langmuir* **1996**, *12*, 4345.
24. D. Hönig, G.A. Overbeck and D. Möbius, *Adv. Mater.* **1992**, *4*, 419.
25. D. Hönig and D. Möbius, *Thin Solid Films* **1992**, *210-211*, 64.
26. D. Vollhardt, U. Gehlert and S. Siegel, *Colloids Surfaces A: Physicochem Eng. Aspects* **1993**, *76*, 187.
27. U. Gehlert and D. Vollhardt, *Langmuir* **1997**, *13*, 277.
28. I. Fankucken, *Phys. Rev.* **1938**, *53*, 909.
29. S. Bernstein, *J. Am. Chem. Soc.* **1938**, *60*, 1511.
30. M. Kuhn and D. Möbius, *Angew. Chem., Int. Ed. Engl.* **1971**, *10*, 620.
31. E.P. Hönig, *J. Colloid Interface Sci.* **1973**, *43*, 66.
32. G.A. Ashwell, P.D. Jackson and W.A. Crossland, *Nature* **1994**, *368*, 438.
33. R. Popovitz-Biro, K. Hill, E. Shavit, D.J. Hung, M. Lahav, L. Leiserowitz, J. Sagiv, H. Hsiung, G.R. Merendith, and H. Vanherzeele, *J. Am. Chem. Soc.* **1990**, *112*, 2498.
34. S.J. Mumby, J.D. Swalen and J.F. Rabolt, *Macromolecules* **1986**, *19*, 1054.
35. K. Naito, *J. Colloid Interface Sci.* **1989**, *131*, 218.
36. R.H.G. Brinkhuis and A.J. Schouten, *Macromolecules* **1991**, *24*, 1487.
37. R.H.G. Brinkhuis and A.J. Schouten, *Macromolecules* **1991**, *24*, 1496.
38. T. Miyashita, Y. Mizuta and M. Matsuda, *Br. Polym. J.* **1990**, *22*, 327.
39. M.N. Teerenstra, E.J. Vorenkamp, R.J.M. Nolte and A.J. Schouten, *Thin Solid Films* **1991**, *196*, 153.
40. M.N. Teerenstra, E.J. Vorenkamp, A.J. Schouten, R.J.M. Nolte, C.A. Walree, J.F. van de Pol and J.W. Zwikker, *Thin Solid Films* **1992**, *210-211*, 496.
41. K. Fukuda, Y. Shibasaki and H. Nakara, *J. Macromolec. Sci. Chem.* **1981**, *A15*, 999.
42. K. Fukuda, Y. Shibasaki and N. Nakara, *Thin Solid Films* **1989**, *179*, 103.
43. T. Miyashita, N. Nishikawa, A. Orikasa and M. Ono, *Chem. Lett.* **1991**, 969.
44. A. Cemel, T. Fort and J.B. Lando, J. Polym Sci., Polym. Chem. Ed. **1972**, *10*, 2061.
45. K. Fukuda and Y. Shibasaki, *Thin Solid Films* **1980**, *68*, 55.
46. M. Hatada and M. Nishi, *J. Polym. Sci., Polym. Chem. Ed.* **1977**, *15*, 927.

47. A. Banderjie and J.B. Lando, *Thin Solid Films* **1980**, *68*, 67.
48. D. Naegele, J.B. Lando and H. Ringsdorf, *Macromolecules* **1977**, *10*, 1339.
49. A. Barraud, C. Rosilio and A. Ruaudel-Teixier, *J. Colloid Interface Sci.* **1977**, *62*, 509.
50. A. Barraud, C. Rosilio and A. Ruaudel-Teixier, *Thin Solid Films* **1980**, *68*, 91.
51. A. Laschewsky and H. Ringsdorf, *Macromolecules* **1988**, *21*, 1936.
52. B. Tieke and G. Lieser, *J. Colloid Interface Sci.* **1982**, *88*, 471.
53. G. Wegner, *Z. Naturforsch., Teil B* **1969**, *24*, 824.
54. G. Wegner, *Pure Appl. Chem.* **1977**, *49*, 443.
55. B. Tieke, *Adv. Polym. Sci.* **1985**, *71*, 79.
56. H.D. Göbel, *Thesis*, Technische Universität München, Germany **1989**.
57. D. Bloor and R.R. Change (Ed.), *Polydiacetylenes*, NATO ASI Series, Serie E: Applied Sciences, Martinus Nijhoff Publishers, Dordrecht New York and London **1985**, 102.
58. A.A. Deckert, L. Fallon, L. Kiernan, C. Chashin, A. Perrone and T. Encalarde, *Langmuir* **1994**, *10*, 1948.
59. B. Tieke, G. Wegner, D. Naegele and H. Ringsdorf, *Angew. Chem. Int. Ed. Engl.* **1976**, *15*, 764.
60. B. Tieke, H.-J. Graf, G. Wegner, D. Naegele, H. Ringsdorf, A. Banerjie, D.R. Day and J.B. Lando, *Colloid & Polym. Sci.* **1977**, *255*, 521.
61. D.R. Day and H. Ringsdorf, *J. Polym. Sci., Polym. Lett. Ed.* **1978**, *16*, 205.
62. D.R. Day and H. Ringsdorf, *Makromol. Chem.* **1979**, *80*, 1059.
63. K. Lochner, H. Baessler,. B. Tieke and G. Wegner, *Phys. Status Solidi B* **1978**, *88*, 653.
64. D.R. Day and J.B. Lando, *J. Appl. Polym. Chem.* **1981**, *26*, 1605.
65. D.R. Day and J.B. Lando, *Macromolecules* **1980**, *13*, 1478.
66. M. Sarkar and J.B. Lando, *Thin Solid Films* **1983**, *99*, 119.
67. C.A.J. Putman, H.G. Hansma, H.E. Gaub and P.K. Hansma, *Langmuir* **1992**, *8*, 3014.
68. G. Lieser, B. Tieke and G. Wegner, *Thin Solid Films* **1980**, *68*, 77.
69. B. Tieke, G. Lieser and K. Weiss, *Thin Solid Films* **1983**, *99*, 95.
70. B. Tieke and D. Bloor, *Macromol. Chem.* **1979**, *180*, 2275.
71. A. Saito, Y. Urai and K. Itoh, *Langmuir* **1996**, *12*, 3938.
72. C. Bubeck, K. Weiss and B. Tieke, *Thin Solid Films* **1983**, *99*, 103.
73. H.D. Göbel and H. Möhwald, *Thin Solid Films* **1988**, *159*, 63.
74. M.A. Markowitz, G.-M. Chow and A. Singh, *Langmuir* **1994**, *10*, 4095.
75. F. Fukuda and H. Nakahara, *Colloid Surfaces A: Physicochem. Eng. Aspects* **1995**, *102*, 57.

76. T.E. Wilson and M.D. Bednarski, *Langmuir* **1992**, *8*, 2361.
77. Y. Yoshioka, H. Nakahara and K. Fukuda, *Thin Solid Films* **1985**, *133*, 11.
78. B. Tieke and K. Weiss, *Colloid & Polym. Sci.* **1985**, *263*, 576.
79. M.N. Teerenstra, *Thesis*, University of Groningen, The Netherlands **1995**.
80. O.A. Aktipetrov, N.N. Akhimediev, E.D. Mishina and V.R. Novak, *JEPT Lett.* **1983**, *40*, 207.
81. H. Kuhn, *Pure Appl. Chem.* **1979**, *51*, 341.
82. M. Sugi, M. Saito, T. Fukui and S. Iizima, *Thin Solid Films* **1983**, *199*, 17.
83. A. Ruaudel-Teixier, M. Vandenvyver and A. Barraud, *Mol. Cryst. Liq. Cryst.* **1985**, *120*, 319.
84. M.A. Schoondorp, *Thesis*, University of Groningen, The Netherlands **1992**.
85. P.K. Kimkes, *Thesis*, University of Groningen, The Netherlands **1995**.
86. F. Armand, S. Okada, K. Yase, H. Matsuda, H. Nakanishi, H. Sakuragi and K. Tokumaru, *Jpn. J. Appl. Phys.* **1993**, *32*, 1186.
87. F. Armand, H. Sakuragi, K. Tokumaru, S. Okada, K. Yase, H. Matsuda, H. Nakanishi, T. Yamada, K. Kajikawa and H. Takezoe, *Thin Solid Films* **1994**, *245*, 202.
88. F. Armand, C. Badoux, P. Bonville, A. Ruaudel-Teixier and O. Kahn, *Langmuir* **1995**, *11*, 3467.
89. M.I Gobernado-Mitri and R. Aroca, *Langmuir* **1993**, *9*, 2185.
90. C.A. Jennings, G.J. Kovacs and R. Aroca, *Langmuir* **1993**, *9*, 2151.
91. H. Matsunara, K. Furusawa, S. Inokuma and T. Kuwumara, *Chem. Lett.* **1986**, 453.
92. I.G. Lednev and M.C. Petty, *Adv. Mater.* **1996**, *8*, 615.
93. E. Satori, M.P. Fontana, M. Costa, E. Dalcanale and V. Paganuzzi, *Thin Solid Films* **1996**, *284-285*, 204.
94. R. Jones, R.H. Tredgold and P. Hodge, *Thin Solid Films* **1983**, *99*, 25.
95. L. Kalvoda and E. Brynda, *Thin Solid Films* **1993**, *232*, 120.
96. A. Suzuki, K. Ohkawa, S. Kanda, M. Emoto and S. Watari, *Bull. Chem. Soc. Japan* **1975**, *48*, 2634.
97. G. Caminati, E. Margheri and G. Gabrielli, *Thin Solid Films* **1994**, *244*, 905.
98. G. Caminati, D. Berti, G. Gabrielli, S. Leponati, R. Rolandi, M.G. Ponzi-Bossi and B. Yang, *Thin Solid Films* **1996**, *284-285*, 181.
99. G. Sprintschnik, H.W. Sprintschnik, P.P. Kirsch and P.G. Whitten, *J. Am. Chem. Soc.* **1976**, *133*, 1.
100. J.H. van Esch, R.J.M. Nolte, H. Ringsdorf and G. Wildburg, *Langmuir* **1994**, *10*, 1955.
101. C. Caminati, E. Margheri, G. Gabrielli, *Progr. Colloid Polym. Sci.* **1994**, *97*, 12.
102. C. Granito, J.N. Wilde, M.C. Petty, S. Houghton and P.J. Iredale, *Thin Solid Films*

1996, *284-285*, 98.
103. C. Gu, L. Swa. T. Zhang and T. Li, *Thin Solid Films* **1996**, *284-285*, 863.
104. J. Zhang, D. Wang, T. Shi, B. Wang, J. Sun and T. Li, *Thin Solid Films* **1996**, *284-285*, 596.
105. A. Ruaudel-Teixier, J. Leloup and A. Barraud, *Mol. Cryst. Liq. Cryst.* **1986**, *134*, 347.
106. J. Leloup, A. Ruaudel-Tiexier and A. Barraud, *Thin Solid Films* **1992**, *210-211*, 407.
107. F. Griezer, D.N. Furlong, D. Scoberg, I. Ichinose, N. Kiizuka and T. Kunitake, *J. Chem. Soc. Faraday Trans.* **1992**, *88*, 2207.
108. D.J. Elliot, D.N. Furlong, T.R. Gengenbach, F. Griezer, R.S. Urquhart, C.L. Hoffman and J.F. Rabolt, *Colloid Surfaces A: Physicochem. Eng. Aspects* **1995**, *103*, 207.
109. D.J. Elliot, D.N. Furlong, T.R. Gengenbach, F. Griezer, R.S. Urquhart, C.L. Hoffman and J.F. Rabolt, *Langmuir* **1995**, *11*, 4773.
110. M.T.S. Nair and P.K. Nair, *Semicond. Sci. Technol.* **1989**, *4*, 191.
111. Y. Wang and N. Herron, *J. Phys. Chem.* **1991**, *95*, 525.
112. P.J. Werkman and A.J. Schouten, *Thin Solid Films* **1996**, *284-285*, 24.
113. P.J.Werkman, A. Schasfoort and A.J. Schouten, *submitted to Thin Solid Films.*
114. P.J. Werkman, R.H. Wieringa, E.J Vorenkamp and A.J. Schouten, *submitted to Langmuir.*
115. P.J. Werkman, H. Wilms, R.H. Wieringa and A.J. Schouten, *submitted to Thin Solid Films.*
116. P.J. Werkman, A.J. Schouten, M.A. Noordegraaf, P. Kimkes and E.J.R. Sudhölter, *submitted to Langmuir.*
117. P.J. Werkman, H. Wilms, R.H. Wieringa , A.J. Schouten and G.T. Oostergetel, s*ubmitted to Langmuir*.
118. P.J. Werkman, R.H. Wieringa and A.J. Schouten, *accepted by Langmuir.*
119. P.J. Werkman, R.H. Wieringa and A.J. Schouten, *submitted to Thin Solid Films.*

Chapter 2

Langmuir-Blodgett films of a polymerisable N,N'-disubstituted dithiooxamide coordination compound

Summary

The monolayer properties of the amphiphile N,N'-bis(10,12-pentacosadiynyl-oxycarbonylmethyl)dithiooxamide at the air-water interface were studied by measuring surface pressure-area isotherms. The amphiphile itself does not form stable monolayers on an aqueous subphase but when Cu(II) ions are added to the subphase a coordination polymer is formed, which forms stable monolayers at the air-water interface. The monolayer stability is strongly influenced by the counter ion, pH and temperature of the subphase. Electron microscopy shows that at a low surface pressure (about 2 $mN \cdot m^{-1}$) a monolayer of loosely packed islands is formed. When the surface pressure has increased a more homogeneous monolayer is formed with small holes which disappear when the monolayer is stabilised at a constant surface pressure for a few hours.

The monolayers of the coordination polymer can be transferred onto solid substrates by a Y-type transfer. The presence of Cu(II) ions is confirmed by XPS measurements and UV/Vis spectroscopy shows a strong absorption at 370 nm, indicating that a strongly conjugated coordination polymer is formed at the air-water interface. SAXR measurements reveal that the LB films have a rather irregular layer structure and upon exposure to UV light, the diacetylene groups are only partly converted to polydiacetylene, moreover, the coordination polymer is partly destroyed.

Introduction

Katherine Blodgett has already shown in 1935 [1,2] that metal ions (like Pb(II), Ca(II), Cd(II) etc.) dissolved in the subphase, had an enormous influence on the stability of monolayers of fatty acids at the air-water interface. Due to the crosslinking action of metal ions, the monolayer stability of stearic acid had been enhanced and metal stearate monolayers could easily be transferred onto solid substrates.

Nowadays, there is a growing interest in functional Langmuir-Blodgett (LB) films [3,4]. These films can be prepared by transferring functional amphiphiles or polymers onto solid substrates from the air-water interface. Also metal ions with special properties can be incorporated into LB films. In this way, semiconductive, magnetic and quantum physical properties can be introduced into LB films. These multilayer films have potential applications as sensors, in catalytical systems and in microelectronical devices [5,6].

The metal ions can be introduced into the LB film by means of salt formation with carboxylic groups of the amphiphile or polymer, as we have already mentioned. But in recent years, there is a growing interest in coordination of metal ions with amphiphiles or polymers, having a ligand group. For the latter approach, all kinds of ligands, like pyridine [7,8,9], imidazole [10], crown ethers [11], phthalocyanines [12] and porphyrins [13], have been used.

Dithiooxamide ($H_2NC(=S)C(=S)NH_2$) has been discovered more than one and a half century ago by Gay-Lussac [14]. The compound has a wide range of applications as reported in literature [15], but the transition metal complexes of the compound have received most attention because of the semiconductive [16,17], magnetic [16,17] and spectroscopic [18-20] properties of these complexes. Dithiooxamide compounds form two-dimensional coordination polymer networks with Ni(II), Cu(II) and Co(II) ions in solution [21,22]. Suzuki et al. [23] and Sasakawa et al. [24] showed that by introducing aliphatic tails on the nitrogen atoms, a stable copper coordination polymer network can be formed at the air-water interface. When these monolayers were transferred onto solid substrates, the formed multilayers had special electrical properties with anisotropy in the conductivity related to the dipping direction of the LB film [24].

In this Chapter the monolayer characteristics of the amphiphile N,N'-bis(10,12-pentacosadiynyloxycarbonylmethyl)dithiooxamide (Scheme 2.1A) on an aqueous subphase and a Cu(II) ions containing subphase are described. Scheme 2.1B shows the expected situation during the complexation process [23]. The amphiphile contains a diacetylene functionality in the aliphatic chain, so upon exposure to UV light a one-dimensional, rigid, polymer backbone can be formed which should result in an improved thermal and mechanical stability of the LB film [25,26]. It will be shown that only stable monolayers are formed when the subphase contains Cu(II) ions and by changing the counter ion a more complete

complexation can be obtained. Furthermore, multilayers of the polymer coordination network were built up and the presence of Cu(II) ions inside the multilayers is proven by XPS measurements. Small angle X-ray reflection (SAXR) measurements reveal that the multilayers have a poor distinct layer structure and UV/Vis spectroscopy shows that upon exposure to UV light (λ = 300 nm), the coordination polymer network of the LB film was partly destroyed and only a small amount of diacetylene groups was converted into the corresponding polydiacetylene.

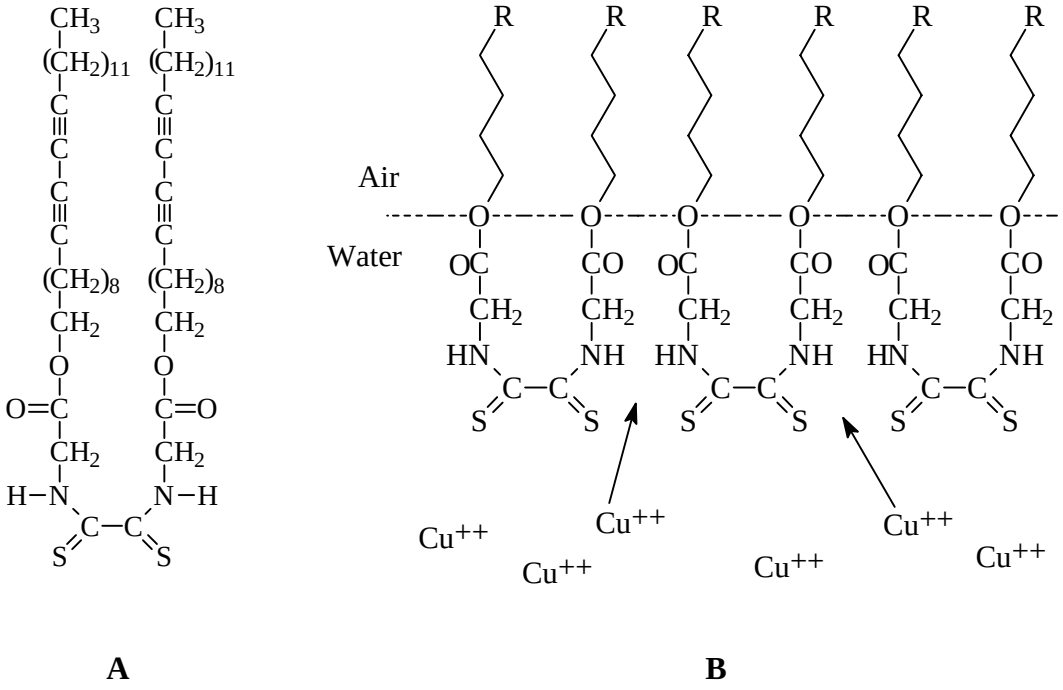

A **B**

Scheme 2.1: A, *the amphiphile*, **B**, *the suggested situation during the complexation process.*

Experimental

Materials

To a stirred brown solution of N,N'-bis(carboxymethyl)dithiooxamide (Pfaltz & Bauer, inc., 99%, 1.00 g, 4.24 mmol) in 4 ml DMF (Merck, 99%, stored over 4Å mol.sieves) at 40 ^{o}C under nitrogen atmosphere, 1.5 g CsOH (Acros, 98%, 8.50 mmol) was added. The

mixture was stirred for 16 hours and a green precipitate was formed. After 16 hours the solvent was removed under reduced pressure.

150 mg (0.30 mmol) of the sticky green product was added to 10 ml of DMF (Merck, 99%, stored over 4Å mol.sieves) at 60 ^{o}C under nitrogen atmosphere and the suspension was stirred for 30 minutes after which a solution of 300 mg 1-bromo-10,12-pentacosadiyne (Tokyo Kasai, 99%, 0.71 mmol) was added dropwise. The mixture was stirred for 2 days after which the solvent was removed under reduced pressure. The crude product was dissolved in chloroform (Merck p.a.) and purified by column chromatography (Silicagel 60 (Merck), eluent chloroform) and a twofold recrystallisation from acetone (Merck p.a.). Yield: 150 mg (0.16 mmol, 54%) (Scheme 2.2).

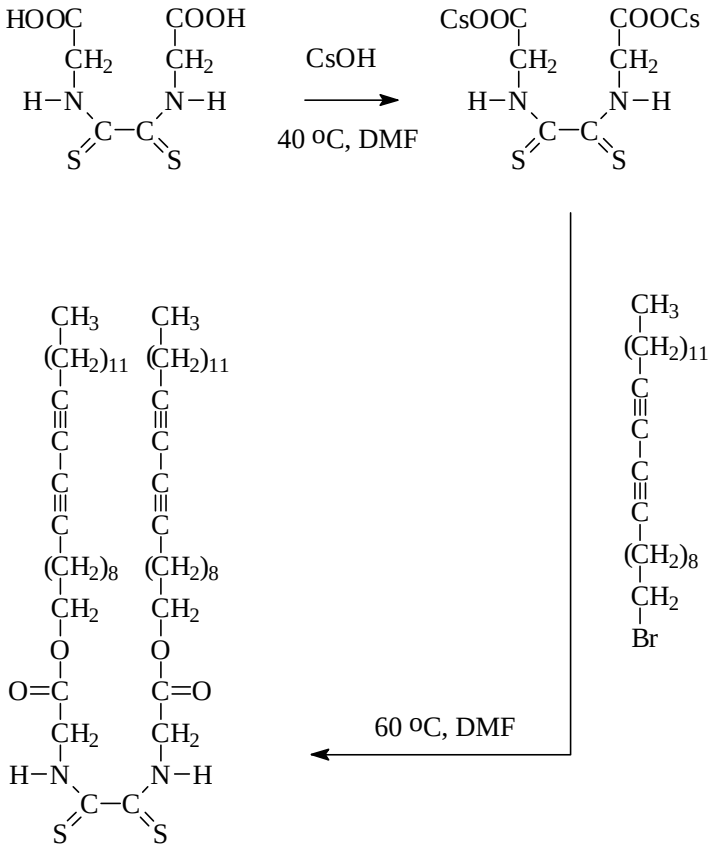

Scheme 2.2

Elemental analysis: Calc. for $C_{56}H_{92}N_2O_4S_2$: C 73.04; H 10.00; N 3.04; S 6.96. Found: C 72.78; H 9.94; N 3.03; S 6.94.
IR: ν (cm^{-1}): 3187 (ν NH), 2920 (ν_a CH_2), 2850 (ν_s CH_2), 1730 (ν C=O), 1547 (δ NH), 1468 (δ CH_2), 1325 (ν N–C=S), 1223 (ν_a C–O–C), 880 (ν C=S).
^{1}H NMR (200 MHz): δ 0.87 (t, 6H), 1.19-1.58 (br, 64H), 1.71 (m, 4H), 2.26 (t, 8H), 4.25 (t, 4H), 4.43 (d, 4H).
T_m = 84.9 ^{o}C, T_c = 51.0 ^{o}C.

$Cu(ClO_4)_2$ (Acros, 98%) and $CuCl_2$ (Merck, 99%) were used without further purification. HCl (Merck, 37%) and NaOH (Merck p.a.) were used to adjust the pH of the subphase.

Langmuir-Blodgett mono- and multilayers

The monolayer properties were studied by measuring the surface pressure-area isotherms using a commercially available computer controlled Lauda-Filmbalance (FW 2). The water used for the subphase was purified by a reversed-osmosis system (Elgastat spectrum SC 30) and subsequent filtration through a Milli-Q purification system. The amphiphile was dissolved in toluene (Merck, p.a.), at a concentration of 0.1 wt%, and the isotherms were recorded with a compression speed of 10 $Å^2$·(molecule·min)$^{-1}$ at different temperatures. Glass slides, quartz slides and silicon wafers, used as substrates, were subsequently treated with a mixture of H_2O_2 (30%) / NH_3 (25%) / H_2O (1:1:5 v/v) for 30 minutes at 60 ^{o}C, ultrasonically treated with a mixture of HCl (37%) / H_2O (1:6 v/v) for 15 minutes, washed several times with Milli-Q water, again ultrasonically cleaned with methanol (Merck p.a.), methanol / chloroform (3:1 v/v) mixture and chloroform (Merck p.a.) for 15 minutes, and finally stored in methanol. Before use the substrates were hydrophobised by treating them with a mixture of chloroform and hexamethyldisilazane (Acros, 97%) (4:1 v/v) at 50 ^{o}C, and finally rinsed with chloroform. After stabilisation at a constant temperature and surface pressure, the monolayer was transferred onto solid substrates with a dipping rate of 3 mm·min^{-1} for the down and upstroke.

Polymerisation

The multilayers were polymerised using a Rayonette Photochemical Reactor which contained UV lamps (300 nm, 16W). The polymerisation was carried out under an argon atmosphere. The distance of the lamps to the centre of the photochemical reactor was 12 cm.

UV/Vis spectroscopy

UV/Vis absorption spectra of the multilayers on glass, were recorded on a SLM-Aminco 300 diode-array UV/Vis spectrophotometer.

XPS measurements

XPS measurements were obtained using a X-Probe 300 of Surface Sciences Instruments spectrometer with monochromated AlK_α radiation with energy of 1486.6 eV. Measurements were carried out with a resolution of 1.8 eV and 0.5 eV for the overall and narrow scan, respectively, and a take-off angle of 45^o. Bindings energy values were referred to the aliphatic carbon 1S line, taken as 287.0 eV.

Small angle X-ray reflection (SAXR) measurements

Small angle X-ray reflection measurements were performed with a Philips PW1830 generator and a Philips PW1820 diffractometer in a $\theta/2\theta$ geometry, using CuK_α radiation (λ = 1.542 Å).

Electron microscopy

Samples for transmission electron microscopy (TEM) were prepared by transferring the monolayer, at different surface pressures onto a carbon coated copper grid by a manual horizontal lifting method. The samples were Pt-shadowed at an angle of 20^o. TEM micrographs were recorded with a Philips EM 300 instrument using an acceleration voltage of 80 kV at a magnification of 2900×.

Results and discussion

Monolayer behaviour

In order to study the monolayer characteristics of the amphiphile, surface pressure-area isotherms were recorded, as is shown in Figure 2.1, on an aqueous subphase (2.1A) and on subphases containing 5 mM Cu(II) ions with Cl^- (2.1B) and ClO_4^- (2.1C) as counter ions. It can be seen clearly that the amphiphile does not form a stable monolayer at the air-water interface on an aqueous subphase, because the limiting area is about 30 $Å^2 \cdot molecule^{-1}$, which

is too small for an amphiphile containing two aliphatic tails. A dithiooxamide amphiphile with two aliphatic tails should occupy at least a limiting area that is twice the value for the cross-section of an aliphatic chain, 20 $Å^2 \cdot chain^{-1}$ [27] and for a diacetylene functionality containing aliphatic tail, this value is even larger [28], about 23 $Å^2 \cdot$chain.

When Cu(II) ions were added to the subphase, the surface pressure starts to rise at a much larger area per molecule (Fig. 2.1B and C) and a limiting area of 61.3 $Å^2 \cdot molecule^{-1}$ is found. This value corresponds well with the model proposed by Suzuki et al. [23] (Fig.2.2) for a monolayer of a stereospecific dithiooxamide coordination polymer at the air-water interface. They calculated an area per dithiooxamide-Cu unit of about 60-70 $Å^2$. Collapse pressures of 28.0 and 42.8 $mN \cdot m^{-1}$ have been found for the monolayers of the amphiphile with Cl^- and ClO_4^- as counter ions, respectively, so when perchlorate is used as a counter ion a more stable monolayer is formed. Upon complexation a charged monolayer is formed and to meet the condition of electroneutrality, negatively charged anions absorb to the positively charged monolayer and a Stern layer will be formed [29]. The specific interaction energy (ϕ) is higher for anions when they are larger, more easily polarisable and have a lower hydration number. The specific absorption of these anions will be enhanced, so a more complete complexation can take place. For this reason, the use of the bigger, more easily polarisable ClO_4^- anions instead of the Cl^- anions results in a more complete complexation and a more stable monolayer.

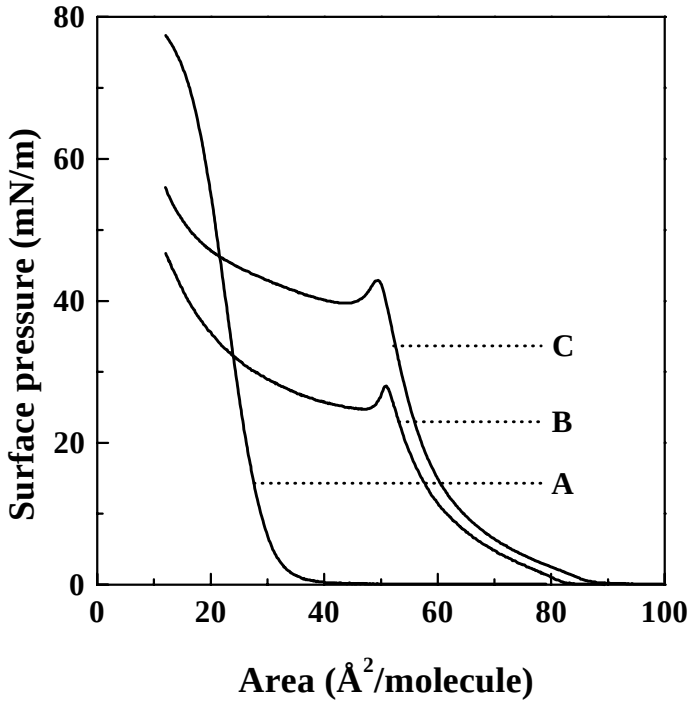

Figure 2.1: *Surface pressure-area isotherms of the amphiphile at 18.7 ^oC on different subphases: aqueous (A), 5 mM $CuCl_2$ (B) and 5 mM $Cu(ClO_4)_2$ (C).*

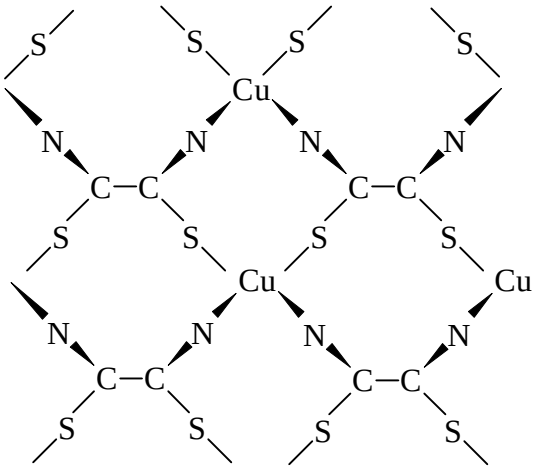

Figure 2.2: *Schematic representation of the stereospecific dithiooxamide coordination polymers at the air-water interface.*

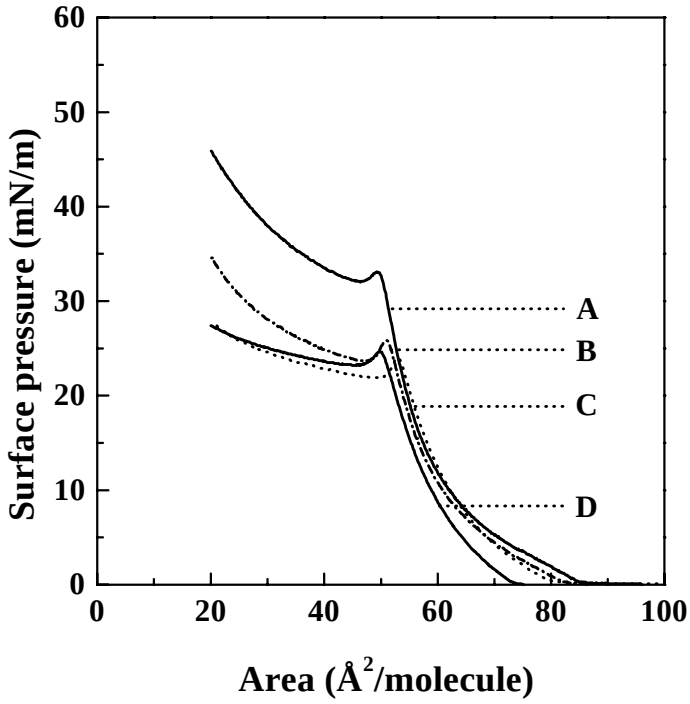

Figure 2.3: *Surface pressure-area isotherms of the amphiphile on a 5 mM $CuCl_2$ subphase at 9.2 (A), 18.7 (B), 27.9 (C) and 37.0 ^oC (D).*

The effect of the subphase temperature can clearly be seen in Figure 2.3, in which the temperature of the subphase, containing 5 mM $CuCl_2$, is varied between 9.1 and 37.0 ^oC. At

low temperatures (2.3A) a collapse pressure of 33.6 $mN \cdot m^{-1}$ is found which decreases when the subphase temperature increases. So, upon raising the subphase temperature, a less stable monolayer is formed. The limiting area remains roughly 62 $Å^2 \cdot molecule^{-1}$, irrespective of the temperature of the subphase, indicating that the coordination polymer is formed at all subphase temperatures.

When the Cu(II) ion concentration of a $CuCl_2$ subphase was varied between 0.5 mM and 10 mM, limiting areas of about 58 $Å^2 \cdot molecule^{-1}$ up to about 62 $Å^2 \cdot molecule^{-1}$ were found, respectively. Already at a Cu(II) ion concentration of 5 mM, a limiting area of about 62 $Å^2 \cdot molecule^{-1}$ was found. A further increase of the Cu(II) ion concentration of the subphase did not result in an increase of the limiting area, suggesting that already on a 5 mM $CuCl_2$ subphase a complete coordination takes place. At concentrations lower that 0.5 mM $CuCl_2$, no reproducible isotherms could be recorded and the limiting areas were smaller than 50 $Å^2 \cdot molecule^{-1}$ which indicates that not all the amphiphiles take part in the formation of the coordination polymer at these low Cu(II) ion concentrations.

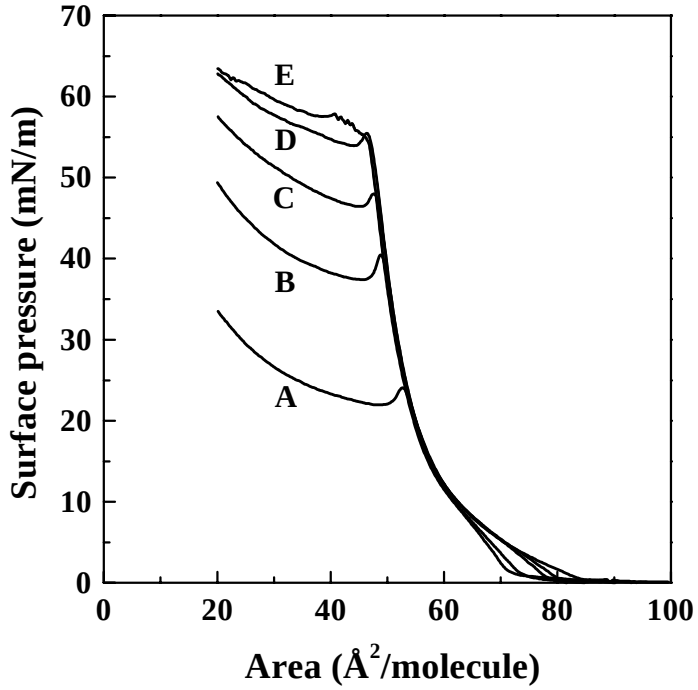

Figure 2.4: *Surface pressure-area isotherms of the amphiphile at 18.7 °C on a 5 mM $CuCl_2$ subphase at different complexation times: 1 (A), 15 (B), 30 (C), 60 (D) and 90 min (E).*

In Figure 2.4 the effect of the complexation time, that is the time between the spreading of the amphiphile at the air-water interface and the time at which the barrier starts to move when the isotherms are recorded, on the isotherms can be seen. Upon increasing the

complexation time, the collapse pressure increases until about 60 minutes of complexation time, after which no further increase in collapse pressure can be observed. So, at longer complexation times, a more stable monolayer is formed with a limiting area of about 57 $Å^2 \cdot molecule^{-1}$.

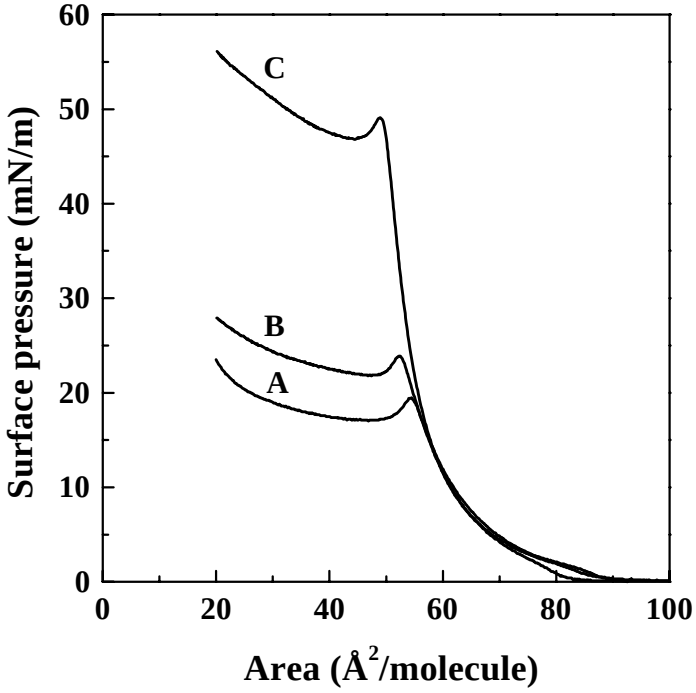

Figure 2.5: *Surface pressure-area isotherms of the amphiphile at 18.7 ^oC on a 0.5 mM $Cu(ClO_4)_2$ subphase at pH values of 4.00 (A), 5.30 (B) and 6.20 (C).*

In Figure 2.5 the effect of the pH of a 0.5 mM $Cu(ClO_4)_2$ subphase on the isotherms can be seen. Normally, the pH of a 0.5 mM $Cu(ClO_4)_2$ subphase is 5.30 and when the pH is lowered to 4.00, the collapse pressure drops from 24.3 to 19.6 $mN \cdot m^{-1}$. So, by decreasing the pH of the subphase a less stable monolayer is formed. But when the pH of the subphase had increased to about 6.2, an enormous increase of the collapse pressure can be seen up to 49.5 $mN \cdot m^{-1}$. It is assumed that at higher pH value the dissociation equilibrium [20] ($LH_2 \leftrightarrow LH^- + H^+ \leftrightarrow L^{2-} + 2H^+$) of the ligand shifts to the right and consequently, a stronger network can be formed after complexation with Cu(II) ions.

Although in solution dithiooxamides do form coordination polymers with Ni(II) and Co(II) [22], formation of a coordination polymer was not observed at the air-water interface with concentrations up to 50 mM for these metal ions. It is already known from literature [20], that dithiooxamides can only form coordination polymers with Co(II) ions in an alkaline solution due to the dissociation of the ligand. So, when in the case of the Co(II) ion, the pH of the subphase had increased to about 8.0, the formation of a coordination polymer could be

observed at elevated temperatures of 37.4 ^{0}C with a limiting area of about 68 Å^2·molecule^{-1}. The formed coordination polymer was very brittle and could not be transferred onto solid substrates.

Morphology of the monolayer

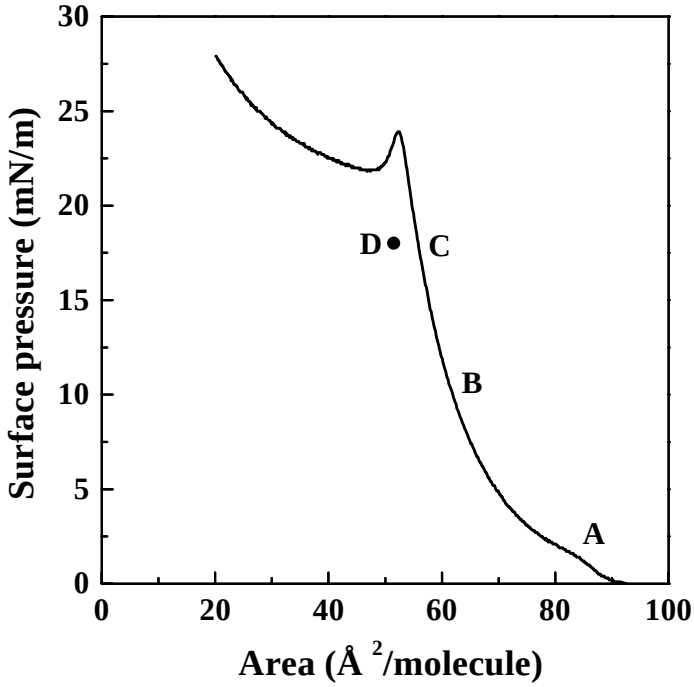

Figure 2.6: *Surface pressure-area isotherm of the amphiphile at 18.7 ^{o}C on a 0.5 mM $Cu(ClO_4)_2$ subphase. The points indicated in this figure correspond to the TEM micrographs of Figure 2.7.*

The transmission electron microscopy (TEM) pictures of Figure 2.7 correspond to the points indicated in Figure 2.6. From Figure 2.7 can be seen that on a 0.5 mM $Cu(ClO_4)_2$ subphase, at very low pressures (2.7A, 2 mN·m^{-1}) a monolayer with loosely packed islands is formed with free space in between. Upon increasing the surface pressure up to 10 (2.7B) and 18 mN·m^{-1} (2.7C), the islands are pushed towards each other and a more homogeneous monolayer is formed with some small holes. When the monolayer is stabilised at a surface pressure of 18 mN·m^{-1} for about 3 hours, the area per molecule drops till 51.5 Å^2 and a homogeneous monolayer without any holes is formed (2.7D).

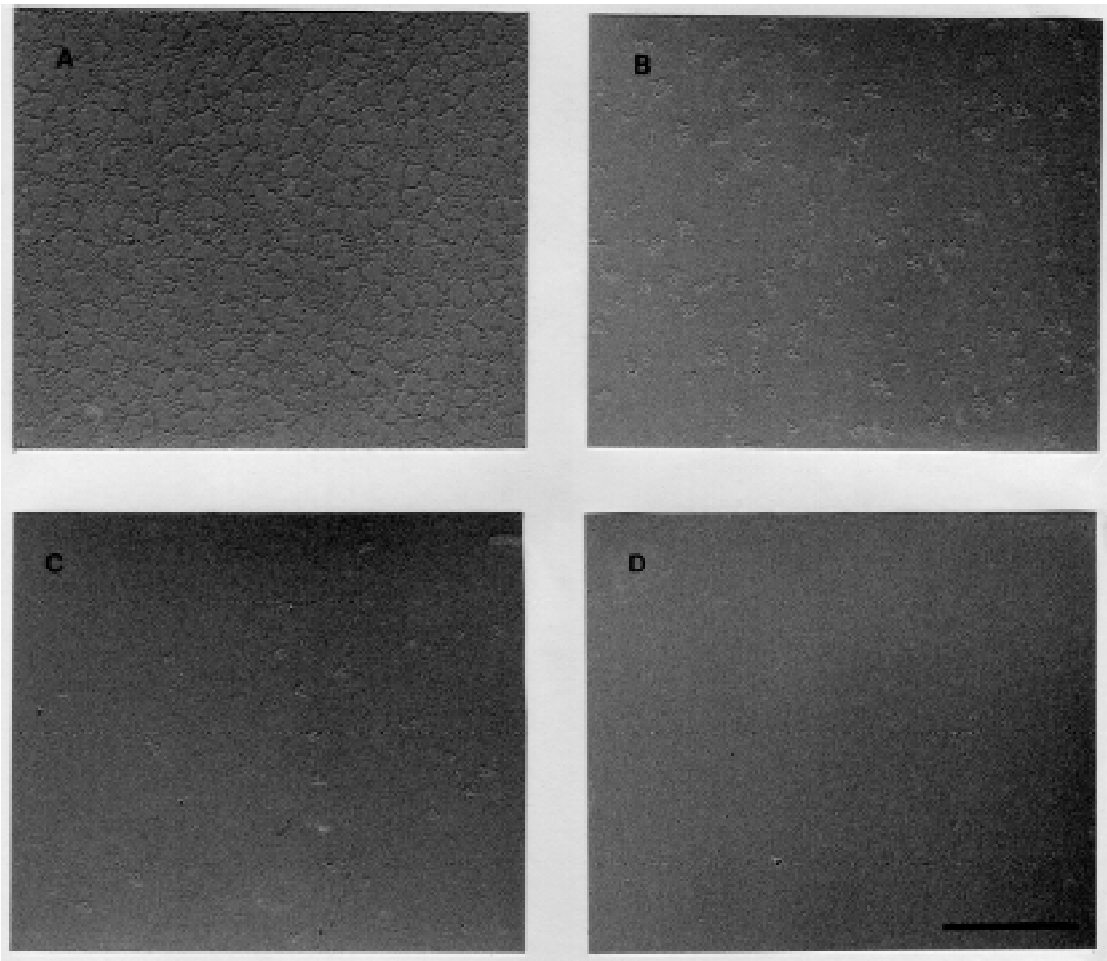

Figure 2.7: *Transmission electron micrographs of a monolayer of the amphiphile at 18.7 ^{0}C on a 0.5 mM $Cu(ClO_4)_2$ subphase at surface pressures of 2 $mN \cdot m^{-1}$ (A), 10 $mN \cdot m^{-1}$ (B), 18 $mN \cdot m^{-1}$ (C) and after 3 hours of stabilisation at 18 $mN \cdot m^{-1}$ (D). The scale bar corresponds to 0.90 μm.*

Multilayer formation

The amphiphile forms stable monolayers at the air-water interface when the subphase contains Cu(II) ions at concentrations between 0.5 and 10 mM at surface pressures of 16 till 25 $mN \cdot m^{-1}$ when the subphase has a temperature of approximately 10 ^{o}C. When the pH has dropped to approximately 4.00, a stable monolayer cannot be formed and when the pH has increased to 6.20, indeed stable monolayers are formed, but these are very stiff, resulting in a

Z-type transfer with transfer ratios of 0.0 on the downstroke and between 0.8 and 1.0 on the upstroke, which gives an inhomogeneous multilayer film. The best transfer was observed when the subphase contained 0.5 mM $Cu(ClO_4)_2$ at about 10 ^oC and at a surface pressure of 24 $mN \cdot m^{-1}$. At these conditions almost a Y-type transfer is observed with a transfer ratio of 0.8 on the downstroke and 1.0 on the upstroke.

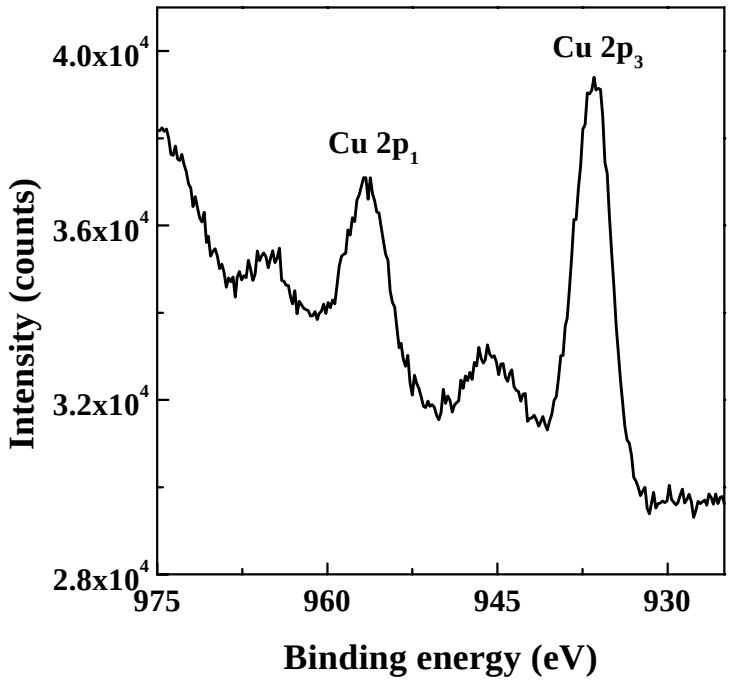

Figure 2.8: *The copper region of a XPS spectrum of a multilayer consisting of 20 layers of the amphiphile on silicon, built up from a 0.5 mM $Cu(ClO_4)_2$ subphase at 10 ^oC and 24 $mN \cdot m^{-1}$.*

XPS measurements were performed on these multilayers in order to establish if these multilayer indeed contained Cu(II) ions. Figure 2.8 shows the copper region of a XPS spectrum of a multilayer consisting of 20 layers of the amphiphile on silicon, built up from a 0.5 mM $Cu(ClO_4)_2$ subphase at 10 ^oC and 24 $mN \cdot m^{-1}$. The Cu $2p_3$ (936.2 eV) and Cu $2p_1$ (956.6 eV) peaks can be seen clearly together with their corresponding satellite peaks which are characteristic for Cu(II) ions. Therefore, the XPS spectrum gives direct proof that a copper coordination polymer is formed at the air-water interface. From the ratio of S to Cu (2:1) it is established that the ratio of amphiphile to Cu(II) ions is 1:1, as expected.

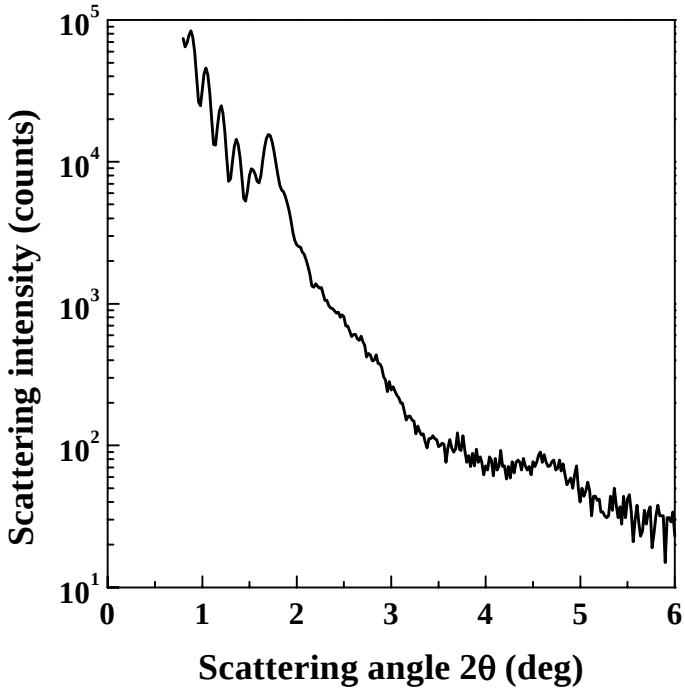

Figure 2.9: *SAXR curve of a multilayer consisting of 20 layers of the amphiphile on silicon, built up from a 0.5 mM $Cu(ClO_4)_2$ subphase at 10 ^oC and 24 $mN \cdot m^{-1}$.*

The SAXR measurement of Figure 2.9 shows only one weak Bragg peak and some Kiessig fringes for a multilayer consisting of 20 layers of the amphiphile on silicon, built up from a 0.5 mM $Cu(ClO_4)_2$ subphase at 10 ^oC and 24 $mN \cdot m^{-1}$. So, the LB film has not a very regular layer pattern. The weak Bragg peak corresponds to a bilayer distance of 51.7 Å, which indicates that the aliphatic tail has a large tilt angle (α) with respect to the surface normal, because the aliphatic tails alone already have a length of about 30 Å in a fully stretched conformation. The presence of the Kiessig fringes indicates that the multilayer film is rather smooth. From the position of the maxima of these fringes the total film thickness can be calculated using the Bragg equation (2.1) [30]:

$$n\lambda = 2d\sin\theta \qquad \textbf{(2.1)}$$

in which d is the total film thickness, θ is the angle of the incident X-ray beam, n is the order of the maxima of the Kiessig fringes and λ is the wavelength of the X-rays (1.542 Å). Using this equation a thickness of 519 Å can be calculated. This value corresponds well with the found bilayer distance from the Bragg peak (51.7 Å) taking into account that the multilayer film consists of 10 bilayers.

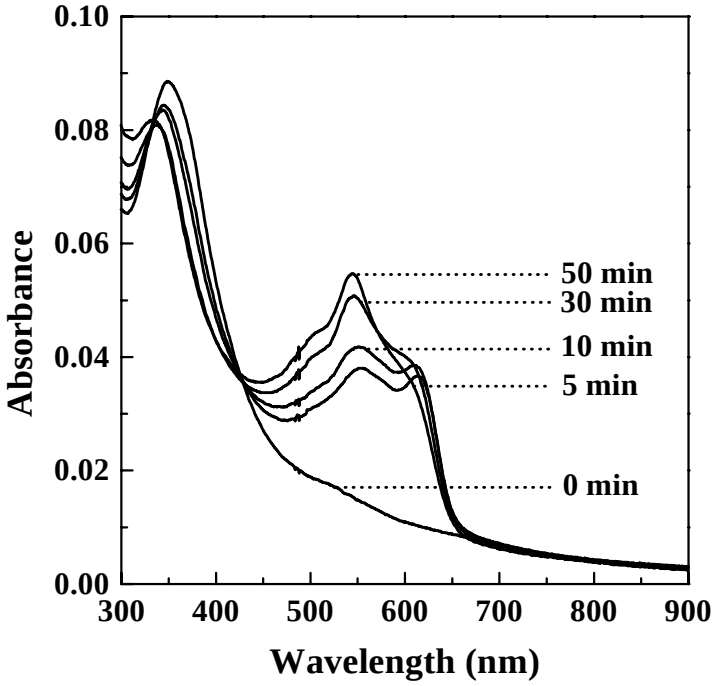

Figure 2.10: *UV/Vis absorption spectral changes of a LB film consisting of 20 layers of the amphiphile on glass, built up from a 0.5 mM $Cu(ClO_4)_2$ subphase at 10 ^oC and 24 $mN \cdot m^{-1}$ at different times of exposure to UV light (λ = 300 nm).*

In Figure 2.10, the absorption spectral changes of a multilayer, consisting of 16 layers of the amphiphile on glass, built up from a 0.5 mM $Cu(ClO_4)_2$ subphase at 10 ^oC and 24 $mN \cdot m^{-1}$, can be seen at different times of exposure to UV light (λ = 300 nm). Before exposure to UV light, a strong absorption with a maximum at 370 nm can be seen, due to the π to π^* absorption which arises from the strong conjugation over the carbon-carbon bond [18]. Upon exposure to UV light, small domains of polydiacetylene are formed which appear purple (λ_{max} = 544 and 620 nm) and at longer irradiation times the red form (λ_{max} = 540 nm) of the polymer is formed. A homogeneous polymer multilayer is not formed as can be seen from the formation of the polydiacetylene domains. Moreover, the absorption of the conjugated polydiacetylene backbone is rather low, indicating that only a small part of the diacetylene groups are converted into the corresponding polydiacetylene. Furthermore, the absorption at 370 nm decreases and shifts to lower wavelengths when the LB film is irradiated with UV light, indicating that the coordination polymer is partly destroyed upon exposure to UV light.

Conclusions

The amphiphile forms only stable, transferable monolayers at the air-water interface when the subphase contained Cu(II) ions at a minimum concentration of 0.5 mM. During the complexation process a coordination polymer network is formed. The counter ion, the temperature and the pH of the subphase have an enormous influence on the stability of the monolayer. Multilayers of the coordination polymer can easily be built up by a Y-type transfer and XPS measurements confirmed the presence of Cu(II) ions inside the LB films. The LB films have a rather weak layer structure with a bilayer distance of approximately 51.7 Å as was shown by means of SAXR measurements. Exposure of the LB films to UV light results in a partly conversion of the diacetylene groups in the aliphatic tail into the corresponding polydiacetylene. Furthermore, the coordination polymer network was partly destroyed upon exposure of the LB film to UV light.

References

1. K.B. Blodgett, *J. Am. Chem. Soc.* **1935**, *57*, 1007.
2. K.B. Blodgett and I. Langmuir, *Phys. Rev.* **1937**, *51*, 964.
3. T. Miyashita, *Prog. Polym. Sci.*, **1993**, *18*, 263.
4. J.D. Swalen, D.L. Allara, J.D. Andrade, E.A. Chandross, G. Garoff, J. Israelachvili, T.J. McCarthy, R. Murray, R.F. Pease, J.F. Rabolt, K.J. Wynne and H. Yu, *Langmuir* **1987**, *3*, 932.
5. G. Roberts (Ed.), *Langmuir-Blodgett films*, Plenum Press, New York and London **1990**.
6. A. Ulman, *An introduction to ultra thin organic films: from Langmuir-Blodgett to to self assembly*, Academic Press, inc., San Diego and London **1991**.
7. G. Caminati, E. Margheri and G. Gabrielli, *Thin Solid Films* **1994**, *244*, 905.
8. G. Caminati, E. Margheri and G. Gabrielli, *Prog. Colloid. Polym. Sci.* **1994**, *97*, 12.
9. G. Caminati, D. Berti, G. Gabrielli, S. Leporatti, R. Rolandi, M.G. Ponzi-Bossi and B. Yang, *Thin Solid Films* **1996**, *284-285*, 181.
10. J.H. van Esch, R.J.M. Nolte, H. Ringsdorf and G. Wildburg, *Langmuir* **1994**, *10*, 1955.
11. I.K. Lednev and M.C. Petty, *Adv. Mater.* **1996**, *8*, 615.
12. L. Kalvoda and E. Brynda, *Thin Solid Films* **1993**, *232*, 120.
13. E. Satori, M.P. Fontana, M. Costa, E. Dalcanale and V. Paganuzzi, *Thin Solid Films* **1996**, *284-285*, 204.
14. M. Gay-Lussac, *Annu. Chim.* **1815**, *95*, 136.
15. M.R. Green, N. Jurban, B.E. Bursten ad D.H. Busch, *Inorg. Chem.* **1987**, *26*, 2326.

16. S. Kanda, K. Ito and T. Nogaito, *J. Poly. Sci.: Part C* **1967**, *17*, 151.
17. S. Kanda, A. Suzuki and K. Ohkawa, *Ind. Eng. Chem. Prod. Res. Develop.* **1973**, *12*, 88.
18. H. Hofmans, H.O. Desseyn and M.A. Herman, *Spectrochimica Acta* **1982**, *38A*, 1213.
19. B. Slootmakers, S.P. Perlepes and H.O. Desseyn, *Spectrochimica Acta* **1989**, *45A*, 1211.
20. S.P. Perlepes, M. Bellaihou and H.O. Desseyn, *Spectrochimica Acta* **1993**, *26*, 751.
21. Z.H. Chohan and A. Rauf, *J. Inorg. Biochemistry* **1992**, *46*, 41.
22. R.N. Hurd, G. DeLaMater, G.C. McElheny and L.V. Peiffer, *J. Am. Chem. Soc.* **1960**, *82*, 4454.
23. A. Suzuki, K. Okhawa, S. Kanda, M. Emoto and S. Watari, *Bull. Chem. Soc. Japan*, **1975**, *48*, 2634.
24. K. Sasakawa and S. Iwata, *Annu. Rep. Res. Reactor Inst. Kyoto Univ.* **1984**, *17*, 146.
25. R. Burzynski, P. Prasad, J. Biegajski and D.A. Cadenhead, *Macromolecules* **1986**, *19*, 1059.
26. H.D. Göbel, *Thesis*, Universität München, Germany **1989**.
27. G.L. Gaines, *Insoluble monolayers at liquid-gas interface*, Wiley-Intersciences, New York **1966**.
28. S.P. Walsh and J.B. Lando, *Langmuir* **1994**, *10*, 252.
29. P. Hiemenz, *Principles of Colloid and Surface Chemistry*, Marcel Dekker, New York and Basel **1977**.
30. A.C. Zeppenfield, S.L Fiddler, W.K. Ham, B.J. Klopfenstein and C.J. Page, *J. Am. Chem. Soc.* **1994**, *116*, 9158.

Chapter 3

Langmuir monolayer formation of metal complexes from a polymerisable amphiphilic ligand

Summary

The monolayer behaviour of 4-(10,12-pentacosadiynamidomethyl)pyridine at the air-water interface has been studied by measuring the surface pressure-area isotherms. The amphiphile forms stable monolayers with a clear liquid-expanded (LE) to liquid-condensed (LC) phase transition at various temperatures. Upon addition of transition metal ions to the subphase complexation at the air-water interface takes place causing an increase of the pressure (Π_c) at which the phase transition appears. Upon complete complexation the phase transition disappears and the monolayer has only the characteristics of a LE phase. The extent of complexation depends strongly on the transition metal used. Moreover, the metal ion concentration, complexation time, temperature, counter ion and the ionic strength of the subphase have a great effect on the complexation behaviour of this amphiphile.

Introduction

Ultra-thin films of polymer metal complexes have potential applications as sensors, catalytic systems and in microelectronical devices. One method to obtain these films is the Langmuir-Blodgett (LB) technique, with which highly ordered monolayers can be formed which in turn can produce multilayers of any desired structure and thickness [1,2].

Recently, several reports [3-9] have been published on the incorporation of metal ions in LB films, which showed all kinds of interesting properties. However, not much effort has been made on the monolayer [10] properties of amphiphilic ligands spread on a subphase containing transition metal ions. A good insight in the complexation behaviour of these ligands at the air-water interface under various conditions will offer a valuable tool to find the optimal conditions for the formation of stable, metal complex containing, monolayers.

This Chapter describes the monolayer characteristics of 4-(10,12-pentacosadiynamidomethyl)pyridine (Scheme 3.1) at the air-water interface by measuring the surface pressure-area isotherms.

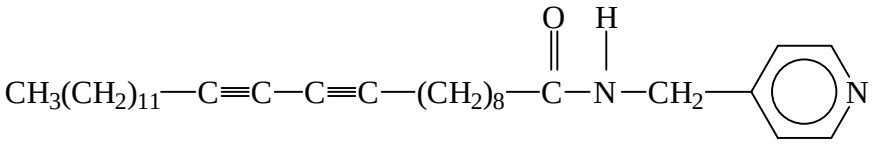

Scheme 3.1

The effects of different transition metal ions, metal ion concentration, complexation time, counter ion, temperature and ionic strength on the complexation process were investigated.

Experimental

Materials

10,12-Pentacosadiynoic acid (Hüls-Petrarch, > 99%) was reacted with thionyl chloride (Merck, > 99%) to obtain the corresponding acid chloride. The amide derivative, 4-(10,12-pentacosadiynamidomethyl)pyridine, was obtained in good yields (70 %) by reaction of 4-(aminomethyl)pyridine (Acros, 98%) with the acid chloride in dry benzene (Merck p.a.) under

nitrogen atmosphere. Triethylamine (Merck, > 99%), distilled under nitrogen atmosphere from CaH_2, was added as a HCl scavenger. The crude product was purified by a twofold crystallisation from acetone (Merck p.a.).
Elemental analysis: Calc. for $C_{31}H_{48}N_2O$: C 80.17; H 10.34; N 6.03. Found: C 80.05; H 10.33; N 6.03.
IR: ν (cm^{-1}) 3294 (ν NH), 2919 (ν_a CH_2), 2849 (ν_s CH_2), 1644 (amide I), 1600 (ν C=N, aromatic ring), 1561 (ν C=C, aromatic ring), 1545 (amide II), 1465 (δ CH_2).
^{1}H NMR (200 MHz): δ 0.87 (t, 3H), 1.24-1.31 (br, 26H), 1.46 (m, 4 H), 1.66 (m, 2H), 2.19 (t, 2H), 2.26 (t, 4H), 4.44 (d, 2H), 6.00 (s, 1H), 7.17 (d, 2H), 8.53 (d, 2H).
T_m = 76 ^oC, T_c = 51 ^oC.

All transition metal salts (BDH Chemicals Ltd, Merck, Acros and Fluka) were used as received. NaOH (Merck p.a.) and HCl (37%, Merck) were used to adjust the pH. Variation in the ionic strength was achieved by adding KCl (Merck p.a.) or $NaClO_4$ (Merck p.a.) to the subphase

The general procedures have been outlined in the experimental section of Chapter 2. The surface pressure-area isotherms were obtained with a standard compression speed of 10 $Å^2 \cdot molecule^{-1} \cdot min^{-1}$. For all complexation experiments a complexation time of 1 minute is used, unless mentioned otherwise.

Results and discussion

Monolayer behaviour of the 4-(10,12-pentacosadiynamidomethyl)pyridine

Figure 3.1 shows surface pressure-area isotherms of the amphiphile at various temperatures on an aqueous subphase. The compound forms a condensed monolayer film at 18.7 ºC and at lower temperatures with a limiting area of 29.3 $Å^2 \cdot molecule^{-1}$. At higher temperatures a phase transition of the liquid-expanded (LE) to liquid-condensed (LC) state is observed; we believe that the raise in surface pressure at 63.5 $Å^2 \cdot molecule^{-1}$ (A_{fl}) is the onset of the LE phase as was shown for a comparable compound by another research group [10] by means of fluorescence microscopy. Upon raising the temperature from 27.7 to 36.6 ºC the pressure at which the phase transition (Π_c) occurs, increases from 2.4 to 13.1 $mN \cdot m^{-1}$. Variation of the pH from 4.0 till 9.0 had no influence on the isotherms of the amphiphile.

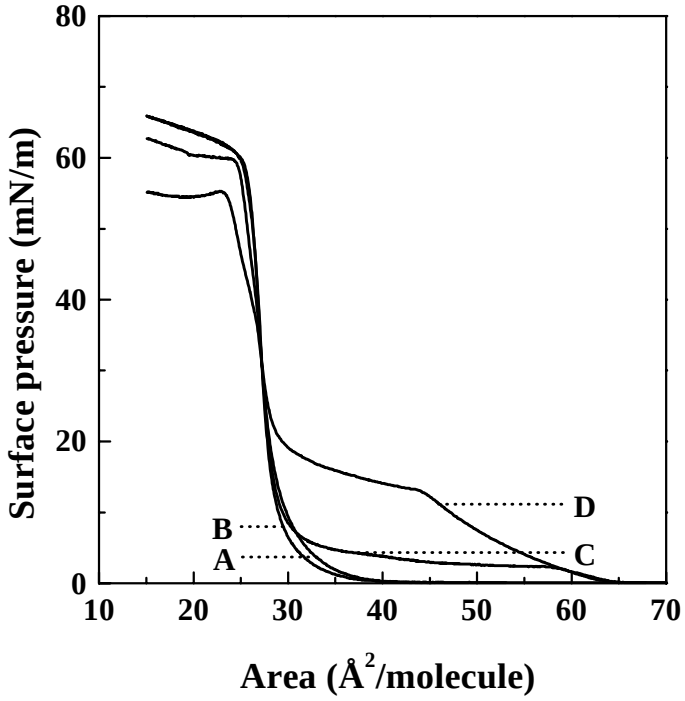

Figure 3.1: *Surface pressure-area isotherms of the amphiphile on an aqueous subphase at 9.4 ºC (A), 18.7 ºC (B), 27.7 ºC (C) and 36.6 ºC (D).*

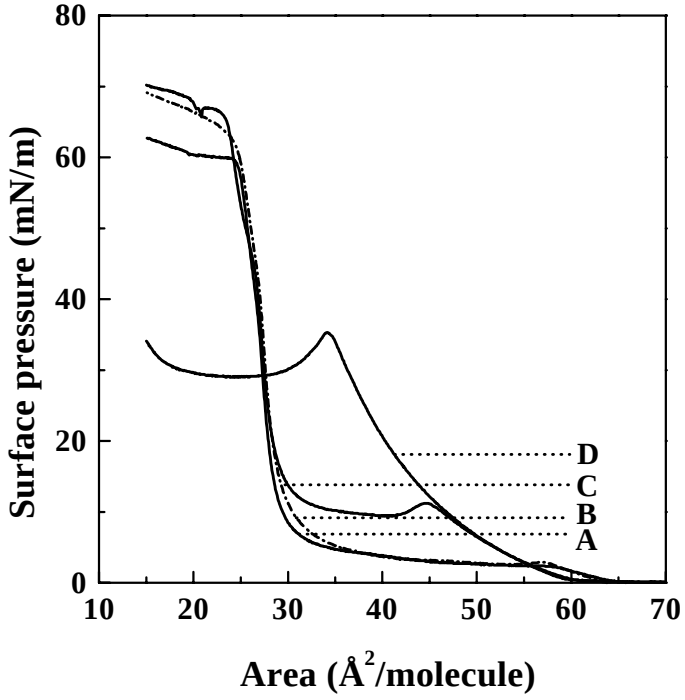

Figure 3.2: *Surface pressure-area isotherms of the amphiphile at 27.7 ºC on a subphase without $CuCl_2$ (A) and with $CuCl_2$ at concentrations of 0.5 mM (B), 5 mM (C) and 50 mM (D).*

Complexation behaviour in the monolayers

Figure 3.2 clearly shows the effect of the addition of $CuCl_2$ to the subphase. At a concentration of 0.5 mM $CuCl_2$ very little or no complexation takes place at all but after increasing the Cu(II) ion concentration, complexation takes place as can be seen from an increase of Π_c. The phase transition totally disappears at a Cu (II) ion concentration of 50 mM and the isotherm only shows LE phase characteristics probably due to the formation of metal complexes with a ratio copper to amphiphile of about 1:1, as will be discussed in more detail in Chapter 4 [11].

For 4-(10,12-pentacosadiynamidomethyl)pyridine no increase in Π_c was observed when other metal chlorides (Cd (II), Co (II), Mn (II), Ni (II) and Zn (II)) were dissolved in the subphase even when concentrations of 100 mM were used. There might be some complexation but not to such an extent that the Π_c increases

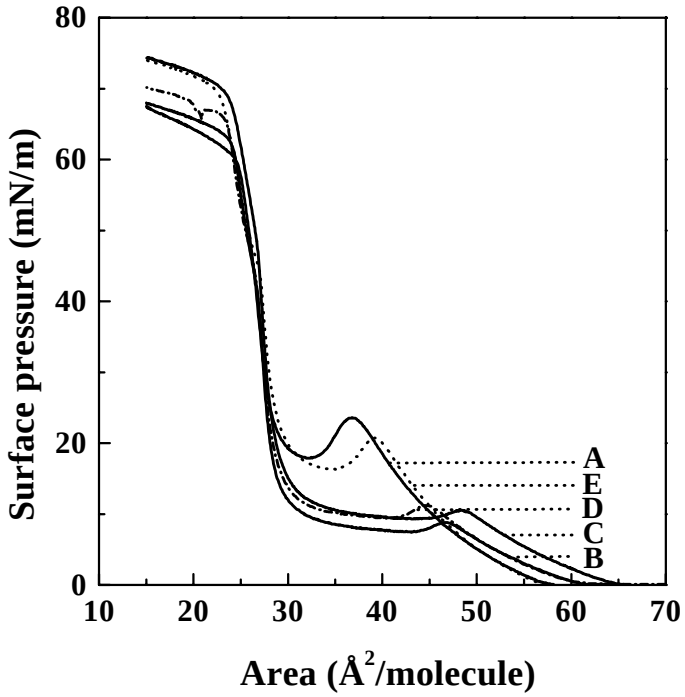

Figure 3.3: *Surface pressure-area isotherms of the amphiphile at 27.7 ºC on a 5 mM Cu (II) subphase with different counter ions: ClO_4^- (A), NO_3^- (B), CH_3COO^- (C), Cl^- (D) and Br^- (E).*

The complexation behaviour of the amphiphile is influenced strongly by changing the counter ion of the Cu (II) ions (Fig. 3.3). Upon complexation a positively charged layer is formed and to meet the condition of electroneutrality, negatively charged anions adsorb to the

positively charged metal complex layer and a Stern layer is formed [12]. The specific interaction energy (ϕ) increases for anions when they are larger, more easily polarisable and have a lower hydration number and consequently their specific adsorption is enhanced, so, a more complete complexation can take place [12]. When the small Cl^- is replaced by the bigger and more easily polarisable Br^- ion, Π_c increases, so, more complexation takes place in the monolayer. Also a big hard base and weakly coordinating counter ion as ClO_4^- causes a large increase of Π_c. The increase in Π_c follows the series: $NO_3^- < Cl^- \cong CH_3COO^- < Br^- < ClO_4^-$. This counter ion effect was found also with Cd(II) ions.

In the case of Cu(II) with ClO_4^- as counter ion even at 18.7 ºC complexation occurs while with Cl^- no LE phase could be observed at this temperature. Upon lowering the temperature even further also with ClO_4^- no complexation is observed. Thus, not at all subphase temperatures complexation takes place. Besides the kind of transition metal and the right counter ion, the temperature of the subphase is also of great importance to achieve complexation in the monolayer.

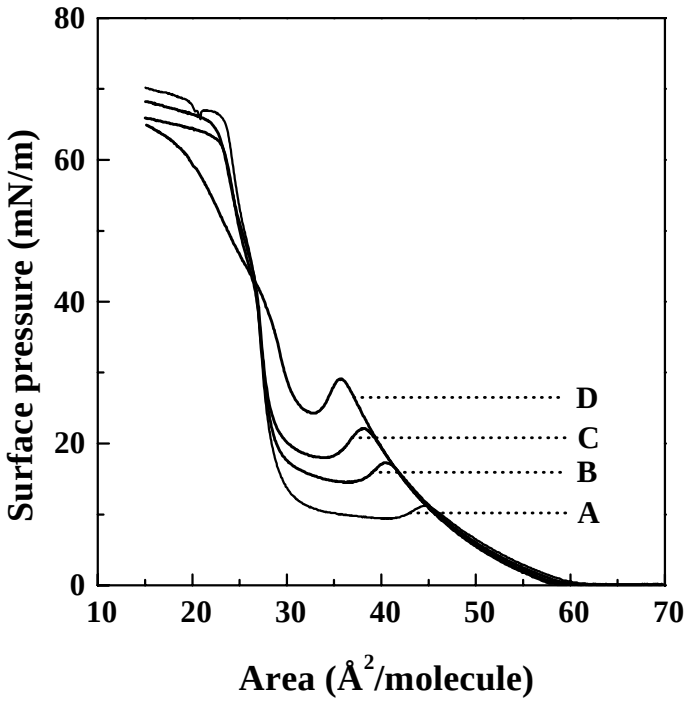

Figure 3.4: *Surface pressure-area isotherms of the amphiphile at 27.7 ºC on a 5 mM $CuCl_2$ subphase with ionic strengths of 0.015 (A), 0.025 (B), 0.035 (C) and 0.065 (D).*

Another important parameter influencing the extent of complexation is the ionic strength (I) of the subphase. As can be seen in Figure 3.4, by raising I from 0.015 to 0.065 by addition of KCl to the subphase, the extent of complexation increases. At higher ionic

strengths the amphiphilic ligands and the transition metals are more shielded from each other by the electrolytes and complexation takes place much more easily. An attempt was also made to force Co (II) on a $CoCl_2$ subphase to form complexes with the amphiphile by increasing the ionic strength but even when I was increased up to 0.215 no complexation could be observed. So, the ionic strength of the subphase only influences the rate of complexation, it can not force a complexation reaction to occur.

When the complexation time is varied, that is the time between the spreading of the amphiphiles and the compression of the monolayer, an increase in Π_c can be seen with increasing complexation time. Therefore, a more complete complexation takes place when the complexation time is increased.

Formation of multilayers

The amphiphile forms stable monolayers at 18.7 ºC on a subphase with and without Cu(II) ions at a surface pressure of 30 $mN \cdot m^{-1}$. Only when the subphase contained Cu(II) ions, these monolayers can be deposited onto solid substrates with transfer ratios of 1.0 on the upstroke and 0.0 on the downstroke. In Chapter 4, a more detailed description on the preparation and investigation of the multilayer structure will be given.

Conclusions

The amphiphile used in this study forms stable monolayers at the air-water interface with a well-defined LC and LE phase transition.

The amphiphile forms complexes with transition metal ions when these are added to the subphase. At high Cu(II) ion concentrations (50 mM or higher), a totally expanded monolayer film is formed which can not be deposited onto solid substrates. When the Cu (II) ion concentration is 5 mM, the monolayer film exhibits a condensed phase and can form stable monolayers. The extent of complexation of a certain transition metal ion can be tuned by the proper choice of metal ion concentration, complexation time, temperature, counter ion and ionic strength of the subphase.

Multilayers can only be built up when the subphase contains Cu(II) ions with a Z-type of transfer.

References

1. G. Roberts (Ed.), *Langmuir-Blodgett films*, Plenum Press, New York **1990**.
2. T. Miyashita, *Prog. Poym. Sci.* **1993**, *18*, 263.
3. B. Tieke and K. Weiss, *Colloid Polym. Sci.* **1985**, *263*, 576.
4. G. Caminati, E. Margheri and G. Gabriëlli, *Thin Solid Films* **1944**, *245*, 202.
5. F. Armand, H. Sakurogi, K. Tokumaru, S. Okada, K. Yase, H. Matsuda, H. Nakanishi, T. Yamada, K. Kajikawa and H. Takezoe, *Thin Solid Films* **1994**, *245*, 202.
6. J. Nagel and U. Oertel, *Polymer* **1995**, *36*, 381.
7. C. W. Yuan, C. L. Lu, L. Wang, N. Gu and Y. Wei, *Polymer* **1992**, *33*, 3525.
8. A. Fukuda, T. Koyama, K. Hanabusa, H. Shirai, H. Nakahara and K. Fukuda, *J. Chem. Soc., Chem. Commun.* **1988**, 1104.
9. K. Z. Wang, C. H. Huang, D. J. Zhou, G. X. Xu, Y. Xu, Y. Q. Liu, D. B. Zhu, X. S. Zhao and X. M. Xie, *Solid State Commun.* **1995**, *93*, 189.
10. J. H. van Esch, R. J. M. Nolte, H. Ringsdorf and G. Wildburg, *Langmuir* **1994**, *10*, 1955.
11. P. J. Werkman, R.H. Wieringa, E.J. Vorenkamp and A. J. Schouten, submitted for publication in Langmuir.
12. P.C. Hiemenz, *Principles of Colloid and Surface Chemistry*, Marcel Dekker, New York and Basel **1977**.

Chapter 4

Langmuir-Blodgett films of metal complexes of 4-(10,12-pentacosadiynamidomethyl)pyridine: a structural investigation

Summary

Complex formation between of 4-(10,12-pentacosadiynamidomethyl)pyridine and metal ions in the subphase results in stable Langmuir monolayers up to surface pressures of 35 $mN \cdot m^{-1}$. Before polymerisation electron microscopy micrographs reveal a flat monomer monolayer and after polymerisation a polymer monolayer with a more striated structure was formed. Multilayers of the amphiphile can only be built up after complexation with metal ions. XPS measurements definitely confirm the presence of metal ions in the multilayers and the molar ratio between metal ion and amphiphile is derived from these spectra. These multilayers are further characterised by means of small angle X-ray reflection measurements and FT-IR spectroscopy, which show that the amphiphile has a large tilt angle (α) with respect to the surface normal.

The multilayers are polymerised by means of UV irradiation. UV/Vis spectroscopy is used to study the polymerisation process. The structural changes during polymerisation are deduced from small angle X-ray reflection measurements and FT-IR spectroscopy. In all cases the bilayer spacing decreases during the polymerisation process, while in some cases the regular plane of the all-trans conformation of the alkyl chains is converted to an irregular one containing gauche conformations. For multilayers built up from a $CuCl_2$ containing subphase, the whole distinct layer structure is destroyed during the polymerisation process.

Introduction

The interaction of metal ions in the subphase with amphiphiles is well known. The metal ions were mostly used to stabilise the monolayer [1,2,3], for example a monolayer of cadmium arachidate is much more stable than an arachidic acid monolayer alone, due to the crosslinking action of the Cd^{2+} ions, but other divalent cations like Pb^{2+}, Ca^{2+}, Ba^{2+}, etc. also have a stabilising effect on the fatty acid monolayers as was already shown by Katherine Blodgett [4,5]. The interactions are of major importance for the manufacture of high-quality Langmuir-Blodgett (LB) films, even small amounts of cations enhance the stability of these fatty acid monolayers and condense them over a particular pH range characteristic for the metal ion dissolved in the subphase. The interaction of the metal ions with the acids depends largely on the physical and chemical properties of the metal ion. Triple valent cations for instance, like Fe^{3+} and Al^{3+}, in the subphase, tend to produce extremely rigid monolayer films with fatty acids which can hardly be transferred onto substrates [1].

Nowadays there is a growing interest in making functional Langmuir-Blodgett films in which the metal ions introduce special semiconducting, magnetic or quantum physical properties into this multilayer films [1,6,7], and these films have potential applications as sensors, for chemical modification of electrodes, in catalytic systems and in microelectronical devices.

In principle the metal ions can be incorporated into the monolayer film in two ways. Firstly, by means of salt or complex formation by the amphiphile from the subphase wherein the metal ions are dissolved and secondly the metals can be bound to the amphiphile before spreading the formed salt or the metal complex at the air-water interface [8,9]. Dithiooxamides [10,11], pyridines [12,13], porphyrins [14], and phthalocyanines[15,16] are often used as ligands for complex formation with metal ions. When crown ethers and imidazoles are used as a ligand units in amphiphiles, even at very low subphase concentrations (10^{-6} M), metal ions are incorporated into the floating monolayer at the air-water interface as was shown by Lednev and Petty [17] and van Esch et al. [18]. Also metal ions could be incorporated into floating polymer monolayers with an amphiphilic character which have ligand groups like pyridine [19], bipyridine [20] or crown ethers [17].

As has been shown in Chapter 3 [21], the amphiphile 4-(10,12-pentacosadiynamido-methyl)pyridine (Scheme 4.1) can form coordination complexes with Cu(II) at the air-water interface when the copper ions are dissolved in the subphase.

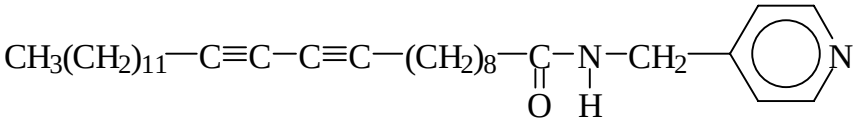

Scheme 4.1

It has been shown that the extent of complexation could easily be tuned by choosing the proper complexation conditions. This amphiphile contains a diacetylene functionality in the aliphatic tail, which can be polymerised upon UV irradiation, resulting in a polymer multilayer with enhanced thermal and mechanical stability. In addition to these favourable mechanical properties, polydiacetylenes are highly conjugated, linear polymers, that exhibit thermo- and solvatochromism, semiconducting as well as strong third-order nonlinear optical properties [22-25]. In principle, polydiacetylenes might find applications as ultra thin resins, protective coatings or in integrated optical devices.

In the present Chapter the morphology of the monolayer, before and after exposure to UV light, will be studied by means of electron microscopy. Furthermore, it will be shown that multilayers could only be built up of monomer monolayers, when the subphase contained Cu^{2+} or Cd^{2+} cations. The structure of these multilayers was deduced from XPS, small angle X-ray reflection and FT-IR measurements, revealing major changes when the cation or counter ions dissolved in the subphase were changed. Polymerisation of the multilayers was followed by UV/Vis spectroscopy. The structural changes during the polymerisation process were studied by means of small angle X-ray reflection and FT-IR measurements. From these studies it is concluded that the layer structure is preserved well with one exception: in the case of multilayers built up from a $CuCl_2$ containing subphase, the layer structure is destroyed during exposure to UV light.

Experimental

The synthesis and characterisation of the amphiphile have been outlined in the experimental section of Chapter 3.

Langmuir-Blodgett films

The monolayer properties were studied by measuring pressure-area isotherms using a commercially available computer controlled Lauda-Filmbalance (FW 2). The water used for the subphase, was purified by a Milli-Q filtration system preceded by a reversed osmosis filtration (Elgastat spectrum SC30). The amphiphile was dissolved in chloroform (Merck, spectroscopic quality), with a concentration of 0.1 wt%, and the isotherms were recorded with a compression speed of 10 $Å^2 \cdot (molecule \cdot min)^{-1}$ at different temperatures. Glass slides, quartz slides and silicon wafers, used as substrates, were subsequently treated with a mixture of H_2O_2 (30%) / NH_3 (25%) / H_2O (1:1:5 v/v) for 30 minutes at 60 ^oC, ultrasonically treated with a mixture of HCl (37%) / H_2O (1:6 v/v) for 15 minutes, washed several times with Milli-Q water, again ultrasonically cleaned with methanol (Merck p.a.), methanol / chloroform (3:1 v/v) mixture and chloroform (Merck p.a.) for 15 minutes, and finally stored in methanol. Before use the substrates were hydrophobised by treating them with a mixture of chloroform and hexamethyldisilazane (Acros, 98%) (4:1 v/v) at 50 ^oC, and finally rinsed with chloroform. Gold substrates were obtained by sputtering a 250 nm thick gold layer onto the cleaned glass slides. A dipping speed of 2 $mm \cdot min^{-1}$ was used for both the down and upstroke transfer.

Polymerisation

The multilayers were polymerised using a Rayonette Photochemical Reactor, which contained UV lamps (254 nm, 16 W). The polymerisation was carried out under an argon atmosphere. The distance of the lamps to the centre of the photochemical reactor was 12 cm. After a constant flow of argon for 40 minutes, the polymerisation of the monolayer at the air-water interface was carried out at a surface pressure of 30 $mN \cdot m^{-1}$, using a small UV lamp (254 nm, 1.6 W) at a 5 cm distance.

Infrared measurements

The transmission infrared measurements were carried out with a Mattson Galaxy 6021 while the grazing incidence reflection measurements were performed on a Bruker IFS-88 FT-IR spectrophotometer equipped with a Spectra-Tech fixed angle (80^o) GIR accessory. Spectra were recorded with a 4 cm^{-1} resolution.

IR spectra at elevated temperatures were recorded with the Mattson Galaxy 6021 equipped with a custom made AABSPEC multi-mode FTIR cell, model #95S-E with a transmission and GIR probe (80^o).

UV/Vis spectroscopy

UV/Vis absorption spectra of the multilayers on glass slides, were recorded on a SLM-Aminco 300 diode-array UV/Vis spectrophotometer.

XPS measurements

XPS spectra were obtained using a X-Probe 300 of Surface Sciences Instruments spectrometer with monochromated AlK_α radiation with energy of 1486.6 eV. Measurements were carried out with a resolution of 1.8 eV and 0.4 eV for the overall and narrow scan, respectively, and take-off angle of 45^o. Binding energy values are referred to the aliphatic carbon 1S line, taken as 287.0 eV.

Small angle X-ray reflection measurements

Small angle X-ray reflection measurements were performed with a Philips PW1830 generator and a Philips PW1820 diffractometer in a $\theta/2\theta$ geometry, using CuK_α radiation (λ=1.542 Å).

Electron microscopy

Samples for transmission electron microscopy (TEM) were prepared by transferring the monolayer, stabilised at a surface pressure of 30 $mN \cdot m^{-1}$, onto a carbon-coated copper grid, which has been made hydrophilic by glow discharge in air under reduced pressure, by a manual horizontal lifting method. The samples were Pt-shadowed at an angle of 20 ^{o}. TEM micrographs were recorded with a Philips EM 300 instrument using an acceleration voltage of 80 kV at a magnification of 10000×.

Results and discussion

Monolayer

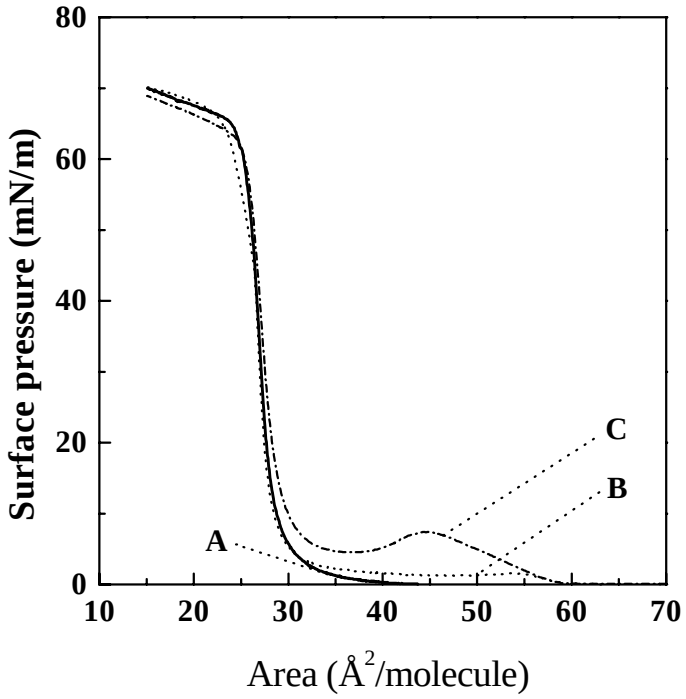

Figure 4.1: *Surface pressure-area isotherms of the amphiphile at 18.7 ^{o}C on an aqueous subphase (A) and on a subphase containing 5 mM $CuCl_2$ (B) and 5 mM $Cu(ClO_4)_2$ (C).*

Figure 4.1 clearly shows the effect of the addition of Cu(II) ions with different counter ions (Cl^- and ClO_4^-) to the subphase. On an aqueous subphase the compound forms a condensed monolayer film at 18.7 ^{o}C. When the subphase contains Cu(II) ions a liquid-expanded (LE) to liquid-condensed (LC) phase transition can be observed which indicates that complexation has taken place at the air-water interface. Upon complexation a charged monolayer is formed in which the amphiphiles start to repel each other resulting in an expanded monolayer [21]. When ClO_4^- was used as counter ion the surface pressure at which the phase transition (Π_c) from the LE to LC phase appears was higher than in the case when Cl^- was used as counter ion. This indicates that when ClO_4^- is used as counter ion a more complete complexation takes place as has already been pointed out in Chapter 3 [21].

With or without metal ions in the subphase, these monolayers could be stabilised at surface pressures up to 35 $mN \cdot m^{-1}$ with subphase temperatures up to 25 ^{o}C and form stable monolayers within 30 minutes at a surface area of about 27 $Å^2 \cdot molecule^{-1}$.

These monolayers could be polymerised at the air water interface after 40 minutes of a constant flow of argon, by means of a small UV lamp (254 nm, 1.6 W) for 2 minutes, resulting in a small contraction of the monolayer. The polymerised monolayer was very brittle and appeared blue which could be seen by the naked eye. Figure 4.2 shows the transmission electron micrographs of the monomer (4.2A) and polymer (4.2B) monolayers picked up at a surface pressure of 30 $mN \cdot m^{-1}$ on a 5 mM $Cu(ClO_4)_2$ subphase.

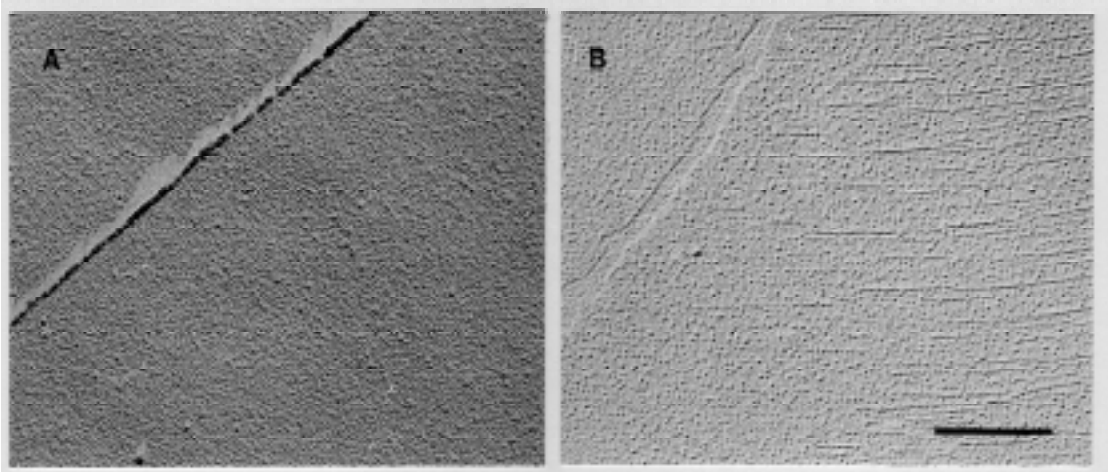

Figure 4.2: *Transmission electron micrographs of transferred monomer (A) and polymer (B) monolayers at a subphase temperature of 19 ^{o}C and a surface pressure of 30 $mN \cdot m^{-1}$. The polymer monolayer was formed after UV irradiation of the monomer monolayer at the air-water interface for 2 minutes under an argon atmosphere. The scale bar corresponds to 0.2 μm.*

The monomer monolayer appeared to be very smooth, the fold on the left upper side of Figure 4.2A, is formed during the preparation of the sample, and will therefore not be present in the monolayer at the air-water interface. The polymer monolayer has a striated texture, which is often seen for polydiacetylene monolayers (Sarkar et al. [26], Putman et al. [27]). The crack on the upper left side of Figure 4.2B, again was formed during the preparation. This crack was exactly formed on the border of two crystals as can be seen from direction of the striations, indicating the chain direction of the polymer backbone [26]. From picture 4.2B it is possible to estimate the thickness of one polymer monolayer, by measuring the length of the shadow. From the equation $h = l \times \tan\alpha$ in which h is the thickness of the

monolayer, l is the length of the shadow and α is the angle at which the samples were Pt-shadowed, the monolayer thickness can be calculated. The estimated thickness is in the order of 33 Å ± 8 Å.

Multilayer formation

Transfer experiments were carried out at surface pressures between 18 and 30 $mN \cdot m^{-1}$ and with a subphase temperature of 19 ^{o}C. The polymer monolayer could not be transferred onto solid substrates because it was too brittle and too stiff. When the monolayers were deposited onto a solid substrate (glass, quartz, gold or silicon), Z-type transfer was observed with transfer ratios of 0.0 on the downstroke and 1.0 on the upstroke, irrespective of the counter ions used (Cl^-, ClO_4^- or Br^-). In Table 4.1 the different samples used in this study are listed.

Table 4.1: *Samples used in this study.*[a,b]

Sample	Substrate	Subphase	Surface pressure ($mN \cdot m^{-1}$)
A	Silicon	5 mM $Cu(ClO_4)_2$	30
B	Glass	5 mM $Cu(ClO_4)_2$	30
C	Au with 3 layers of cadmium arachidate	5 mM $Cu(ClO_4)_2$	30
D	Au with 3 layers of cadmium arachidate	1 mM $Cu(ClO_4)_2$	30
E	Silicon	5 mM $CuCl_2$	30
F	Silicon	5 mM $CdBr_2$	19

[a] *All samples consisted of 16 layers of the amphiphile.*
[b] *Subphase temperature is 19 ^{o}C.*

Cu(II) containing multilayers

XPS measurements were performed on these multilayers to confirm the presence of metal ions in these samples and to give quantitative information about the amount of metal ions incorporated into the LB films. The XPS spectrum of a multilayer built up from a 5 mM $Cu(ClO_4)_2$ subphase (Sample A), is shown in Figure 4.3.

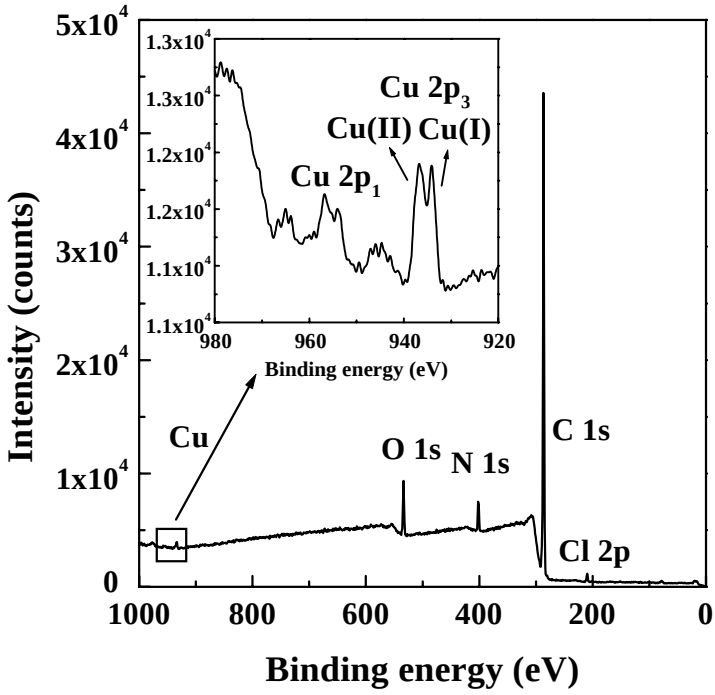

Figure 4.3: *XPS spectrum of 16 layers of amphiphile, transferred from a $Cu(ClO_4)_2$ subphase at 19 ^oC and 30 $mN \cdot m^{-1}$ on silicon (sample A).*

The copper peaks can clearly be seen, but it appeared to be a mixture of Cu (II) (peaks at 936.5 and 956.5 eV with the associated satellites) and Cu (I) (peaks at 933.5 and 954.0 eV). This is somewhat surprising because only Cu(II) was expected in the multilayers and no reduction to Cu (I). So, the behaviour of these multilayers inside the XPS spectrometer was studied more closely. Upon longer exposure of the multilayer to soft X-rays, the Cu(I) peaks increased in time while the Cu(II) peaks decreased in intensity, also the satellites associated with Cu(II) disappeared. Finally, after 20 hours of exposure to X-rays, almost all the Cu(II) is reduced to Cu(I). In Figure 4.4 the Cu(II) and Cu(I) fractions are plotted as function of the exposure time to the soft X-rays in the XPS apparatus. It can be seen clearly that the fraction of Cu(I) increases at longer irradiation time and the Cu(II) ions are reduced.

This phenomena has been described before for Cu^{2+} and some other metal ions (like Cr^{6+} and Fe^{3+}) in the literature [28-33]. This reduction is mainly caused by secondary electrons, those produced inside the sample by slowing down of primary electrons and those falling on the sample from the surroundings [30]. When the multilayers were built up from a 5 mM $CuCl_2$ subphase, it could be seen that the initial X-ray induced reduction of Cu(II) proceeded much slower than when ClO_4^- was used as a counter ion (Figure 4.4, curve B). After 1 hour of exposure to X-rays only a weak shoulder of Cu(I) can be seen in the case of Cl^- containing multilayers (about 7%), whereas in the case of ClO_4^- containing multilayers

there is already a pronounced amount of Cu(I) present after 1 hour of exposure to the soft X-rays. This lower reduction rate of the Cu(II) ions, is probably caused by the difference in packing of multilayers which contain Cl^- or ClO_4^- as counter ion. Probably, the multilayers which contain Cl^- as counter ion, have a more dense packing than the multilayers which contain ClO_4^- as a counter ion, causing a slower reduction of the Cu(II) ions upon exposure to soft X-rays. This was also the case for the X-ray induced Cu(II) reduction inside α- and γ-zirconium phosphates [33]. These layered compounds differ in structure and packing sequence of layers, resulting in a different reduction rate of Cu(II) during the XPS experiments. In α-zirconium phosphate (which has the less dense structure of the two zirconium phosphates) the Cu(II) ions are reduced much faster than in γ-zirconium phosphate. When the floodgun was used for compensation of charging effects, immediately a total reduction of Cu(II) could be observed for multilayers which contain ClO_4^- as counter ions, whereas with Cl^- as counter ion the reduction still appeared very slow.

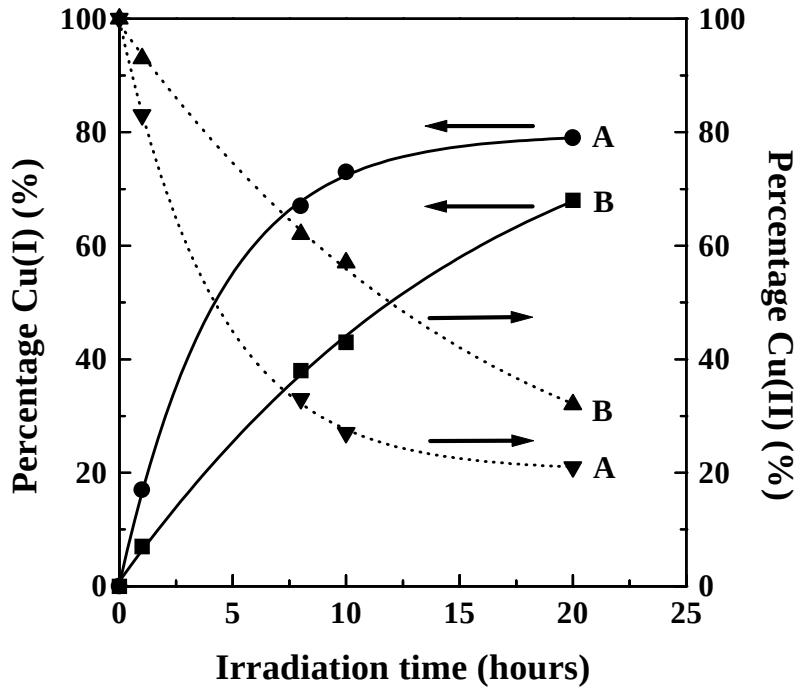

Figure 4.4: *Percentage of Cu(I), calculated by the formula: [Cu(I) $2p_3$ / (Cu(I) $2p_3$ + Cu(II) $2p_3$)] × 100%, at different irradiation times for Cu(II) containing multilayers, built up from a 5 mM $Cu(ClO_4)_2$ (A, sample A) and 5 mM $CuCl_2$ (B, sample E) subphase at 19 ^oC at 30 $mN{\cdot}m^{-1}$ on silicon. In determining the amount of Cu(II), the integrated area of the satellite was also taken into account and the deconvolutions were performed by a best-fit Gaussian computer program.*

The amount of Cu(II) ions incorporated in the multilayers can easily be varied by changing the subphase concentration of Cu(II) ions, as can be seen in Table 4.2.

Table 4.2: *The ratio N:Cu of the multilayers, calculated from the XPS spectra, as a function of the $Cu(ClO_4)_2$ concentration in the subphase.*[a]

$[Cu(ClO_4)_2]$ (mM)	ratio N:Cu
10	4.2
5	4.7
1	17.2
0.5	25.8

[a] *For all multilayers the ratio of Cu:Cl was 1:2.*

Stable monolayers can be formed on a $Cu(ClO_4)_2$ containing subphase up to concentrations of 10mM. When the subphase contained more than 10 mM $Cu(ClO_4)_2$, stable monolayers cannot be formed anymore, probably because too much Cu(II) ions are coordinated to the monolayer, forming a heavily charged monolayer and on compression molecules are probably forced to dissolve in the subphase.

The maximum amount of Cu(II) ions in the multilayers (built up from a 10 mM $Cu(ClO_4)_2$ containing subphase) with ClO_4^- as counter ion was about 1 Cu(II) ion to 2 amphiphiles, because each amphiphile contains 2 nitrogen atoms. When the subphase contained 5 mM $CuCl_2$, the multilayer contained about 1 Cu(II) ion to 3 amphiphiles. Thus, the ClO_4^- counter ion causes a better complexation in the monolayer to occur, as has been discussed already in Chapter 3 [21].

In Figure 4.5, the GIR spectra of sample C and D are shown. The peak at 1621 cm^{-1} corresponds to the ν_{C-N} of the pyridine moiety coordinated to the metal and the 1600 peak corresponds to ν_{C-N} of a free pyridine ring [34,35]. It can be seen clearly that sample D contains relative high amounts of non-coordinated pyridine ligands. The coordinated and non-coordinated pyridine rings most probably have the same orientation because the bands corresponding to both vibrations appear strongly in the GIR spectrum but can hardly be seen in the transmission IR spectrum. From the XPS experiments it can be calculated that multilayers which were built up from a 1 mM $Cu(ClO_4)_2$ subphase contain 1 Cu(II) ion on about 8.6 amphiphiles (each amphiphile having two nitrogens). Therefore it is assumed that the multilayer built up from a 1 mM $Cu(ClO_4)_2$ subphase (sample D), consists of CuL_4 complexes (L = amphiphile) and free amphiphiles in the ratio CuL_4 : 4L because in the GIR

spectrum of this multilayer the peaks of the coordinated non-coordinated pyridine rings have almost the same intensity.

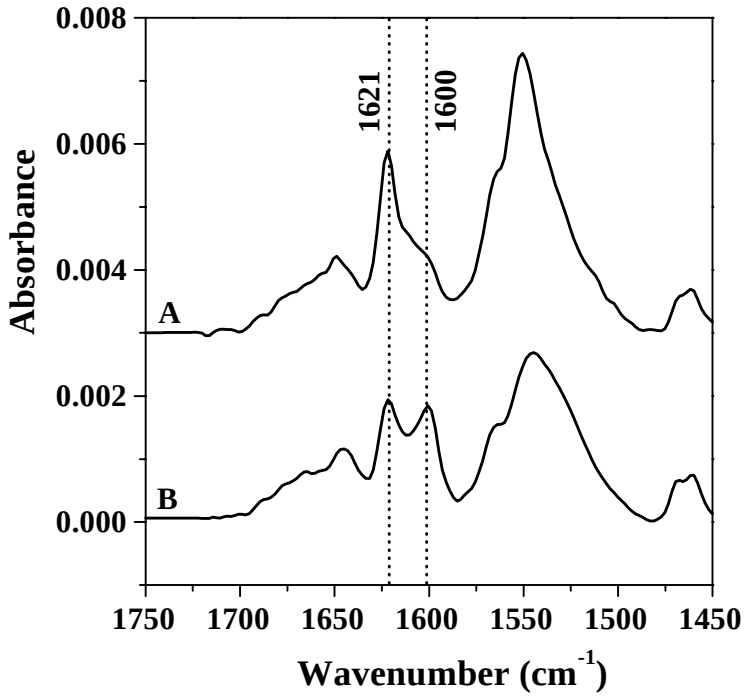

Figure 4.5: *GIR infrared spectra of LB films consisting of 16 layers of the amphiphile on a gold coated glass with 3 layers of cadmium arachidate, built up from a 5 mM (A, sample C) and 1mM (B, sample D) $Cu(ClO_4)_2$ subphase at 19 ^oC and 30 $mN \cdot m^{-1}$.*

The following equations can be considered for complexation of the amphiphile with metal ions.

$$L + M \leftrightarrow ML \quad \textbf{(4.1)}$$

$$L + ML \leftrightarrow ML_2 \quad \textbf{(4.2)}$$

$$L + ML_2 \leftrightarrow ML_3 \quad \textbf{(4.3)}$$

$$L + ML_3 \leftrightarrow ML_4 \quad \textbf{(4.4)}$$

$$nL + M \leftrightarrow ML_n \quad \textbf{(4.5)}$$

At high Cu(II) concentrations (> 10mM $Cu(ClO_4)_2$) the equilibrium is shifted to the copper rich side, forming CuL complexes. This way a heavily charged monolayer is formed which is not stable. At lower Cu(II) concentrations (10 and 5 mM $Cu(ClO_4)_2$) the relative amount of ligands (L) at the air-water interface has increased, so, the equilibrium is shifted

and CuL_2 complexes are formed which is also indicated by the GIR measurements (Figure 4.4) in combination with the XPS measurements. At even lower concentration (1 mM $Cu(ClO_4)_2$ or lower) the equilibrium is totally shifted to the copper deficient side, forming CuL_4 complexes in a matrix of uncoordinated ligands. The composition of the formed complexes at the air-water interface may differ from the structure of the complexes found in the LB films, although the stoichiometry of the complexes will be the same, because during the preparation of the multilayers, the structure of the multilayers is rearranged as will be discussed in the next paragraph. This rearrangement of the multilayer structure may induce the formation of complexes which have a different structure than the complexes formed at the air-water interface.

In order to establish whether the formed multilayers had a distinct layer structure, small angle X-ray reflection measurements were performed. The small angle X-ray reflection patterns of the samples A (Fig. 4.6A) and E (Fig. 4.6B) are shown in Figure 4.6.

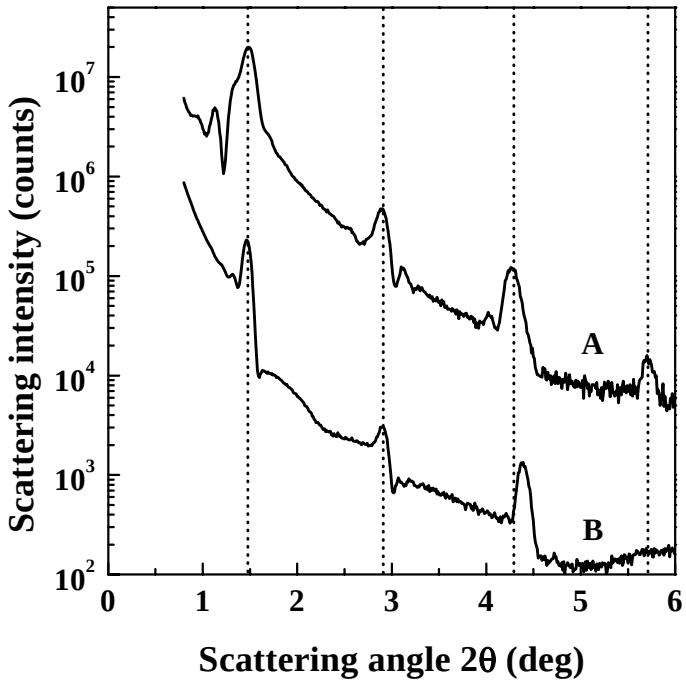

Figure 4.6: *Small angle X-ray reflection curves of 16 layers of the amphiphile built up from (A, sample A) 5mM $Cu(ClO_4)_2$ and (B, sample E) 5mM $CuCl_2$ subphase at 19 ^oC and 30 $mN \cdot m^{-1}$ on silicon.*

A regular layer pattern is observed for these Cu(II) ion containing multilayers, with Bragg peaks representing layer spacings of 59.2 Å and 60.0 Å for the multilayers built up from 5 mM $Cu(ClO_4)_2$ and $CuCl_2$ subphase, respectively. The amphiphile, in fully stretched conformation, has a length of about 36.5 Å, so, the layer spacings found must represent a

bilayer spacing. Because these multilayers were built up by means of a Z-type transfer, a monolayer spacing between 30 and 37 Å was expected. Therefore, a rearrangement to a Y-type structure must have occurred in which the amphiphiles have a large tilt angle with respect to the surface normal, because for a perpendicular orientation of the amphiphiles to the substrate surface a bilayer spacing of about 73 Å should have been found. The rearrangement of a Z-type structure in to a Y-type structure is well-known phenomena for low molecular weight amphiphiles [1,36-39]. The Y-type structure is the thermodynamically most stable structure, with the hydrophobic aliphatic tails and the hydrophilic headgroups facing each other.

To get more information on the orientation of amphiphiles in the LB films, transmission IR spectra (electrical field vector parallel to the substrate surface, so, all individual group vibrations with transition dipole moment components parallel to the substrate surface will absorb maximally in this setup) and grazing incidence reflection (GIR) IR spectra (electrical field vector perpendicular to the substrate surface, so all individual group vibrations with transition dipole moment components perpendicular to the substrate surface will absorb maximally in this setup) were recorded. In Figure 4.7 the different spectra can be seen for a multilayer built up from a 5 mM $Cu(ClO_4)_2$ subphase and the mode assignments are presented in Table 4.3.

Table 4.3: *The IR band assignments [34,35,40-43].*

Wavenumber (cm^{-1})	Assignment	Transition dipole moment, $\bar{M}$
3301	ν (N-H)	∥ N–H bond
2955	ν_a (CH_3)	⊥ C–CH_3
2920	ν_a (CH_2)	⊥ C–C–C chain plane
2871	ν_s (CH_3)	∥ C–CH_3
2850	ν_s (CH_2)	∥ H–C–H plane, bisecting HCH angle
1645	Amide I	∥ C=O bond
1621	ν (C=N_{ar})	∥ ring
1565	ν (C=C_{ar})	∥ ring
1547	Amide II	⊥ C=O bond
1468	δ (CH_2)	∥ H–C–H plane, bisecting HCH angle

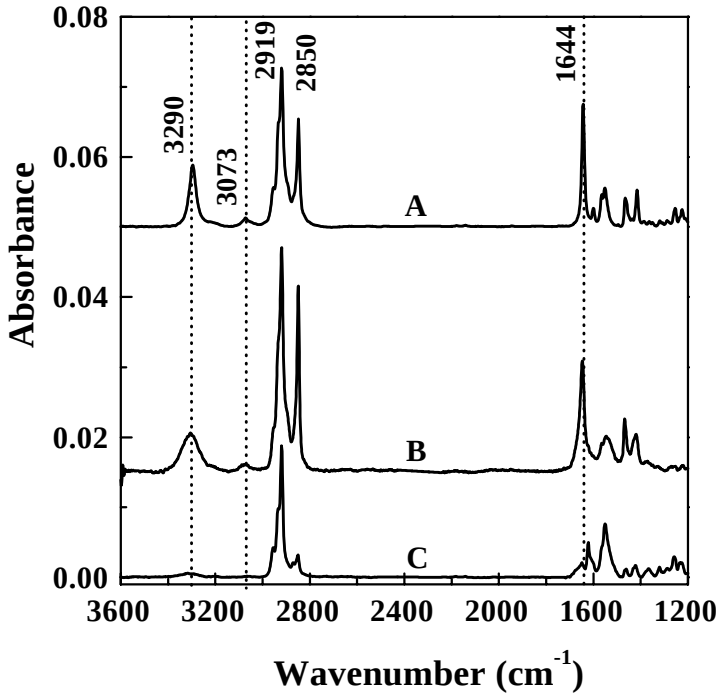

Figure 4.7: *Infrared spectra of the amphiphile: (**A**) powdered in KBr (scale factor: 0.0395×), (**B**) Transmission, (**C**) GIR (scale factor: 0.432×). Samples: In case of GIR, 16 layers transferred onto a gold coated glass slide from a 5mM $Cu(ClO_4)_2$ subphase (sample C) and in case of transmission, 16 layers transferred onto silicon at a subphase concentration of 5 mM $Cu(ClO_4)_2$ (sample A). In both cases the subphase temperature was 19 ^oC and the surface pressure was 30 $mN \cdot m^{-1}$.*

In order to scale the bulk, transmission and GIR spectra in a proper way, transmission and GIR spectra were also recorded at 60 ^oC. At this elevated temperature the side chains are molten and all preferred orientation is lost. Also a bulk spectrum of the amphiphile powdered in KBr was recorded at 80 ^oC, at this temperature the amphiphile is in the molten state. All these spectra were scaled in such a way that the vibrations in the CH stretching vibration region have the same intensity as in the transmission spectrum of sample A at 60 ^oC. These scaling factors were used for the bulk and GIR spectra at room temperature in Figure 4.7.

For the GIR measurements gold substrates were used on which 3 layers of cadmium arachidate were deposited on both the sample and reference side, therefore the 3 cadmium layers make no contribution to the GIR spectrum. 16 monolayer were deposited on top of these 3 cadmium arachidate layers. Furthermore, also a GIR spectrum was recorded when gold substrates were used on which 3 layers of poly((S)-1-acetoxymethylethylethyliso-cyanide) were deposited (sample and reference side) on top of which 16 layers of the

amphiphile from a 5 mM $Cu(ClO_4)_2$ subphase were transferred. This spectrum was identical to the GIR spectrum of Figure 4.7 which indicates that the 3 cadmium arachidate layers probably do not influence the structure of the LB film on top of these layers which allows a proper comparison of the transmission and reflection IR spectra.

In the bulk spectrum of the amphiphile, powdered in KBr, the individual groups have no preferred orientation. In the transmission spectrum (Fig. 4.7B), the N–H (3301 cm^{-1}) and amide I (1645 cm^{-1}) can be clearly seen, while these absorption bands are nearly absent in the GIR spectrum. The integrated area of the amide I peak of the transmission spectrum is one and a half time larger then the amide I peak of the bulk spectrum. The amide II (1545 cm^{-1}) vibration on the contrary is strongly present in the GIR spectrum and very weak in the transmission spectrum. From this it is concluded that the amide groups are oriented parallel to the substrate surface. Furthermore, the pyridine group vibration at 1621 cm^{-1} is strongly absorbing in the GIR spectrum and only weakly in the transmission spectrum, so, the pyridine group is oriented with a small angle with respect to the surface normal. Also in the absorption region of the aliphatic tail vibrations, major differences could be observed. It can be seen that the intensities of the bands at 2920 (ν_a CH_2) and 2850 cm^{-1} (ν_s CH_2) differ tremendously in intensity comparing the transmission and GIR spectra. The asymmetric stretch vibrations of the methylene is absorbing strongly in the GIR spectrum while the symmetric stretch vibration absorptions can hardly be seen. Both vibration absorptions are present in the transmission spectrum. These differences in intensity of the ν_a (CH_2) and ν_s (CH_2) between the GIR and transmission spectra are usually not observed when an all-trans CH_2 chain is oriented with an angle, α, with respect to the surface normal [40-45] and the C–C–C plane in the all-trans alkyl chain can take on any orientation around the chain axis. So, in the normal case, the intensities of ν_a (CH_2) and ν_s (CH_2) in the GIR or transmission spectrum, depend only on the tilt angle, α, and the ratio of their intensities does not change significantly between both spectrum measurement methods.

In the literature [40,46-49], several reports have been published in which comparable changes in intensities of ν_a (CH_2) and ν_s (CH_2) have been described. Those results have been explained by assuming a special packing of the alkyl chains. Nuzzo et al. [46] and Evans et al. [47] interpreted their results as due to a close packing of the CH_2 chains in a triclinic lattice instead of an orthorhombic. This close packing was supposed to be induced by strong dipoles of the sulfone groups incorporated in the alkyl chain. In that way the all-trans C–C–C plane had a preferred orientation, in which this plane was oriented at a certain angle with respect to the substrate surface and could not take on all possible orientations around the chain director. This result was also found by Walsh and Lando [50] for alternating multilayers of

diacetylenes. Figure 4.8 shows a schematic representation of the two extreme orientations of a tilted all-trans aliphatic chain.

From Figure 4.7, it can be deduced that ν_s (CH_2) has a preferred orientation nearly parallel to the substrate surface, because it appeared strong in the transmission spectrum and relatively weak in the GIR spectrum. On the other hand, ν_a (CH_2) was relatively strong in the GIR spectrum, compared with the ν_s (CH_2) vibration in this spectrum. However, the absolute value of the ν_a (CH_2) vibration in the GIR spectrum is smaller as compared to the transmission and bulk spectrum, indicating a large tilt angle (α) of the chain director with respect to the surface normal. Figure 4.8A represents the suggested situation, in which the transition dipole moment of the ν_s (CH_2) vibration is parallel to the substrate surface and the transition dipole of the ν_a (CH_2) vibration has a considerable component perpendicular to the substrate surface.

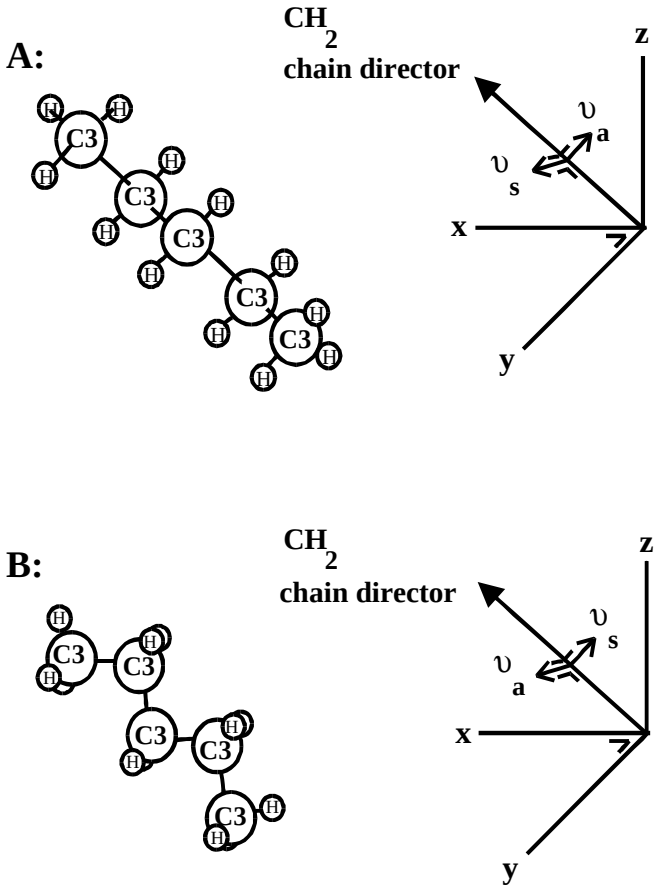

Figure 4.8: *Schematic representation of the two extreme orientations of an all-trans aliphatic chain.*

From the results obtained from the small angle X-ray reflection measurements together with the result from the FT-IR spectra a model for the multilayer film (Figure 4.9), built up from a 5 mM $Cu(ClO_4)_2$ subphase, is proposed.

α is the tilt angle relative to the surface normal. From the experimental data, a value of 35^o was found for α, taking into account a bilayer spacing of 59.2 Å and a large tilt angle of the aliphatic tail as is deduced from the IR spectra, which is not unusual for diacetylenes, where normally values between 20 and 45^o are found [51]. The C–C–C plane of the aliphatic tail has a preferred orientation in which the transition dipole moment of the ν_s (CH_2) vibration must lie nearly in the plane of the substrate [47].

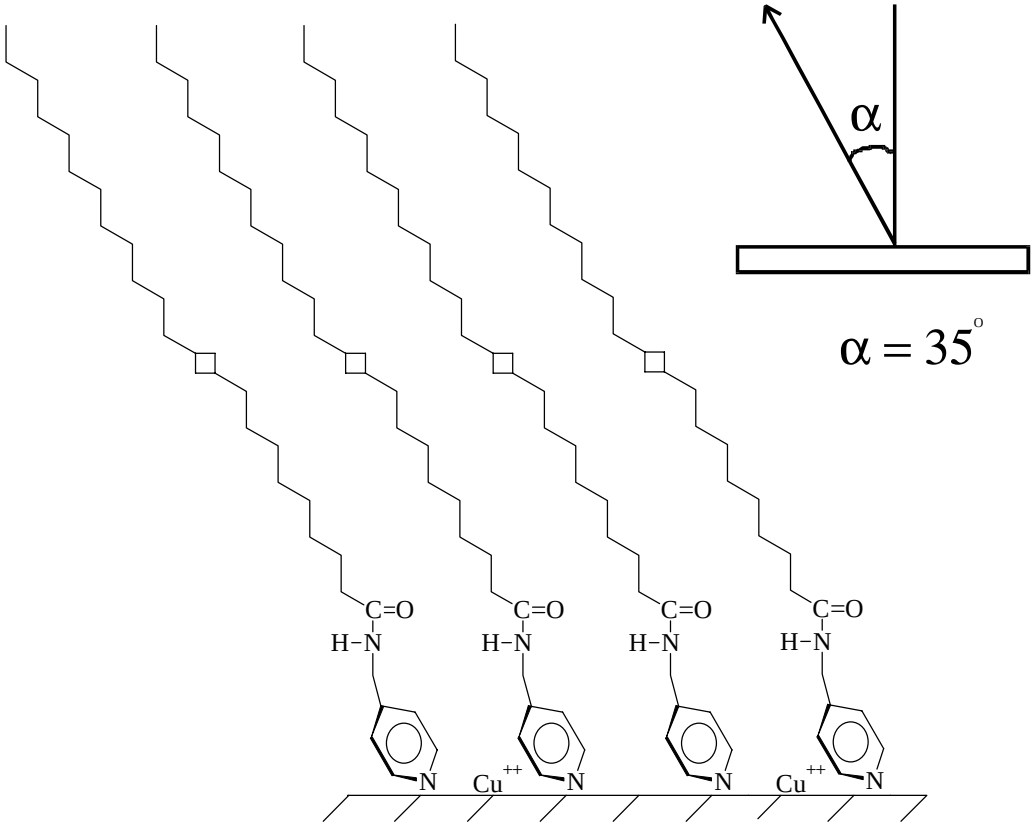

Figure 4.9: *Schematic representation of the structure of amphiphiles inside the multilayers.*

When the subphase contained 5 mM $CuCl_2$, monolayers could only be transferred onto silicon or glass substrates and not onto gold substrates. That is why only transmission IR spectra could be recorded. These spectra (not shown here) closely resemble the transmission spectra of multilayers built up from a 5mM $Cu(ClO_4)_2$ subphase. Furthermore, the multilayers built up from both subphases have nearly the same bilayer spacing as was derived from the

small angle X-ray reflection measurements, so, it is assumed the multilayers built up from both subphases nearly have the same structure.

Cd(II) containing multilayers

Multilayers could also be built up from a 5mM $CdBr_2$ subphase by Z-type transfer at a subphase temperature of 20 ^oC and surface pressures between 15 and 20 $mN \cdot m^{-1}$.

XPS measurements were performed for a direct observation of Cd(II) ions in these LB films. The Cd(II) peaks can be seen clearly at about 405 ($3d_5$) and 412 ($3d_3$) eV [52]. The amount of Cd(II) incorporated is about 1 Cd(II) to 2 amphiphiles, as calculated from the ratio of the integrated peak areas of Cd(II) to N.

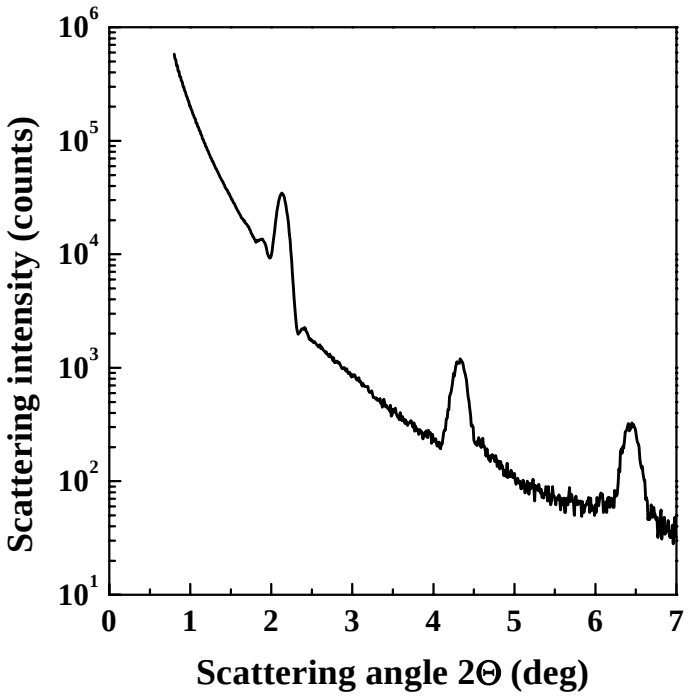

Figure 4.10: *Small angle X-ray reflection curve of a LB film consisting of 16 layers of the amphiphile on silicon, built up from a 5 mM $CdBr_2$ subphase (sample F) at 19 ^oC and 19 $mN \cdot m^{-1}$.*

Small angle X-ray reflection measurements (Fig. 4.10), showed a regular layer structure with a layer spacing of about 42 Å. This might be ascribed to a monolayer spacing, assuming that the amphiphiles are oriented perfectly perpendicular to the substrate ($\alpha = 0^o$) or

it represents a bilayer spacing with a very large tilt angle, α, of the chain director with respect to the surface normal.

In Figure 4.11, the transmission IR spectrum of sample F can be seen. It was not possible to transfer monolayers onto gold or silver coated glass substrates even when these substrates were covered first with 5 layers cadmium arachidate or 4 layers of amylose-acetate [40] or poly((S)-1-acetoxymethylethylisocyanide) [53], so GIR spectra could not be recorded.

For the bulk spectrum, the same scaling factor was used as in Figure 4.7. In the transmission spectrum (fig. 4.11 B), the N-H (3290 cm^{-1}) and Amide I (1644 cm^{-1}) absorption bands can clearly be seen but their relative intensity is weaker than in the bulk spectrum indicating, that the amide bond has a large tilt angle with respect to the surface normal. Also the aliphatic tail vibrations (2920 cm^{-1} for ν_a (CH_2) and 2850 ν_s (CH_2)) should have a much stronger absorption in the transmission spectrum when the aliphatic tails were oriented almost perpendicular to the substrate. However from Figure 4.11 it can be concluded that the aliphatic tail has a large tilt angle (α) with respect to the substrate surface. The carbon-nitrogen stretch vibration absorption is present at 1618 cm^{-1}, indicating that the Cd(II) ions are indeed coordinated to the pyridine ring of the amphiphile.

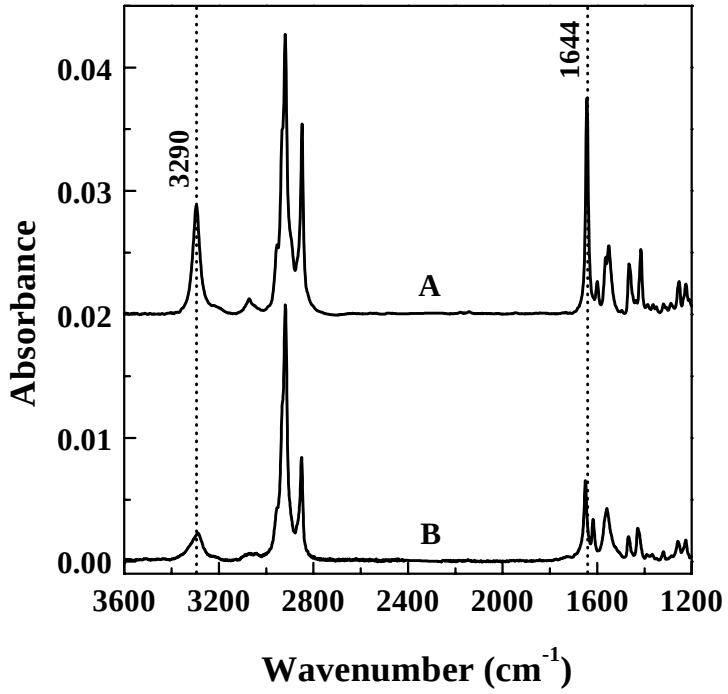

Figure 4.11: *Infrared spectra of the amphiphile: (A) bulk spectrum of the amphiphile, powdered in KBr (scale factor: 0.0395×), (B) transmission, 16 layers of the amphiphile on silicon built up from a 5mM $CdBr_2$ subphase (sample E) at 19 ^oC and 19 $mN \cdot m^{-1}$.*

The transmission spectrum suggests a large tilt angle (α), so from the IR spectrum it can be concluded that the spacing of 42 Å, represents a bilayer spacing. Again a "turnover" from a Z-type structure to a Y-type structure must have occurred, because these multilayers were also built up with a Z-type transfer. From these results a structure for the multilayer is proposed which deviates a little from the LB film built up from a Cu(II) subphase. The tilt angle (α) of the chain director with respect to the surface normal is approximately 55^{o}.

Thus, when the multilayers contain Cd(II) ions the amphiphiles have a larger tilt angle with respect to the surface normal than in the case when the multilayers contain Cu(II) ions.

Polymerisation in the multilayers

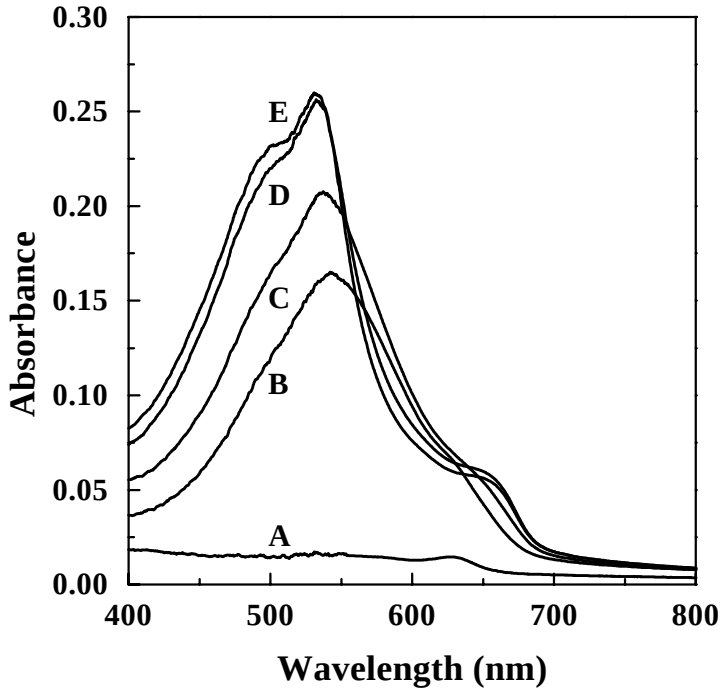

Figure 4.12A: *UV/Vis spectra of a LB film of 16 layers of the amphiphile built up from a 5mM $Cu(ClO_4)_2$ subphase (sample B) at 19 ^{o}C and 30 mN·m^{-1} on glass, at different UV ($\lambda = 254$ nm) irradiation times: (A) 0 min., (B) 2 min., (C) 5 min., (D) 20 min. and (E) 30 min.*

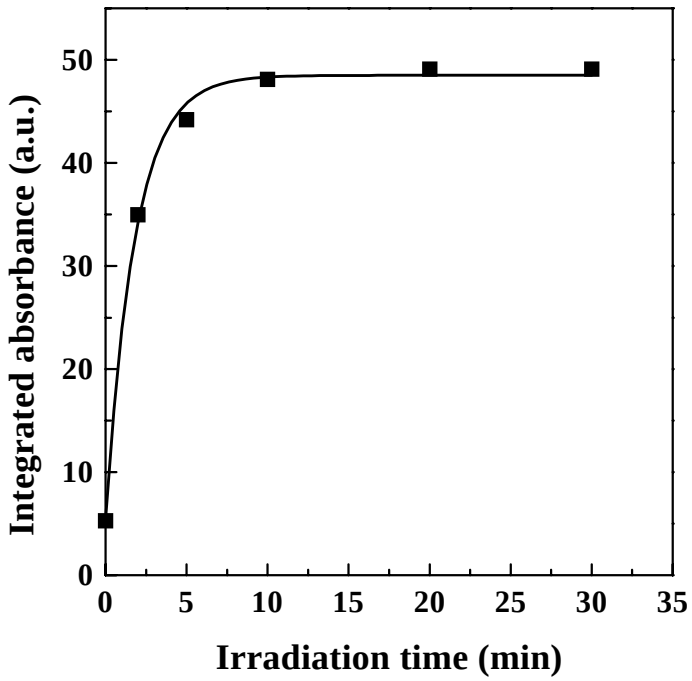

Figure 4.12B: *Integrated absorbance from the UV/Vis spectra of Figure 4.12A, between 400 and 800 nm, at different times of exposure to UV light.*

The LB films were polymerised by means of exposure to UV light (λ = 254 nm) under argon atmosphere. The polymerisation process was followed by UV/Vis spectroscopy. Figure 4.12A exhibits absorption spectrum changes during the UV irradiation of the LB film consisting of 16 layers, built up from 5 mM $Cu(ClO_4)_2$ subphase. Several minutes of exposure to UV light resulted in a red form of the polymer with λ_{max} = 540 nm. Upon UV irradiation a rigid polymer with a one dimensional, conjugated backbone is formed. The conjugation resulted in the strong π to π^* absorption [54,55] shown in Figure 4.11A. In Figure 4.12B, the integrated area of absorbance between 400 and 800 nm as function of the polymerisation time is shown. Apparently the polymerisation is complete after 20 minutes of exposure to UV light. The optical density at 540 nm is about 0.008 per diacetylene monolayer. This is about the maximum obtainable optical density for a polydiacatylene monolayer [24]. Therefore, the polymerisation was more or less complete after 20 minutes of UV irradiation. In the case of the multilayers built up from a 5 mM $CuCl_2$ subphase, however, the polymerisation was complete only after about 50 minutes of exposure to UV light. Thus, by changing the counter ion, the polymerisation properties can be influenced, probably caused by a slightly different packing of the monomers. The polymerisation of diacetylenes is a topochemical reaction where a slightly different packing of the amphiphiles can have enormous influence on the polymerisation behaviour [56].

Upon exposure of the LB films to UV light no reduction of the Cu(II) ions inside these multilayer films to Cu(I) ions is observed as has been proven by means of XPS measurements (not shown here).

In order to examine whether the regular layer pattern was preserved during the polymerisation process, small angle X-ray reflection (SAXR) measurements were performed. In Figure 4.13 (A and B), SAXR measurements are shown of sample A (subphase: 5 mM $Cu(ClO_4)_2$) before and after 30 minutes of UV irradiation.

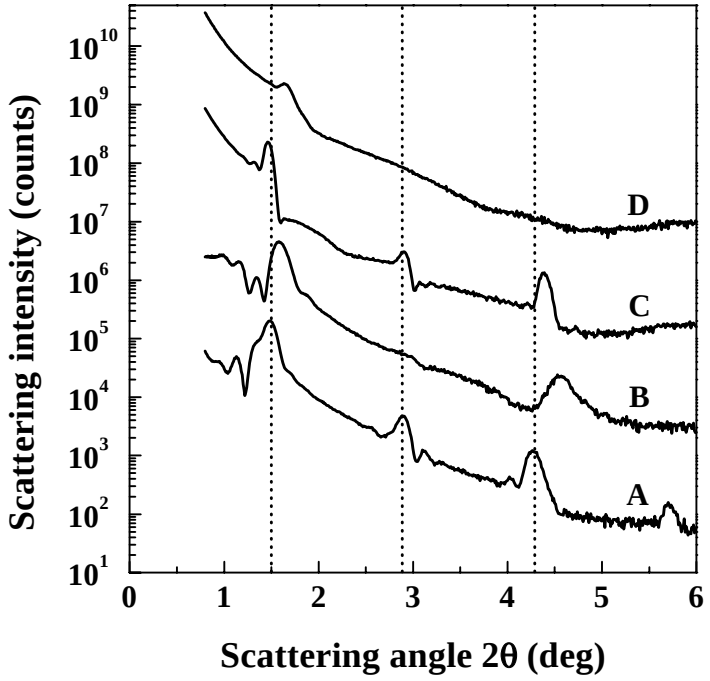

Figure 4.13: *Small angle X-ray reflection curves of a LB film of 16 layers of the amphiphile built up from a 5mM $Cu(ClO_4)_2$ subphase (sample A) at 19 ^oC and 30 $mN{\cdot}m^{-1}$ on silicon, before (A) and after 20 minutes of UV irradiation (B) and SAXR curves of a LB film consisting of 16 layers of amphiphile, built up from a 5 mM $CuCl_2$ subphase (sample E) at 19 ^oC and 30 $mN{\cdot}m^{-1}$ on silicon, before (C) and after 50 minutes of exposure to UV light (D).*

From these measurements it can be concluded that the layer structure is preserved during UV irradiation, although the bilayer spacing decreased from 59.2 down to 57.4 Å and the second order Bragg peak disappeared. The latter phenomenon can be explained by means of the well-known odd-even intensity oscillations of X-ray diffraction profiles [57-60]. In Y-type multilayer films, the juxtaposition of the two hydrophobic ends of the amphiphiles can give rise to a electron-deficient layer which will influence the intensity of the diffraction

peaks. By variation of the layer thickness of this electron-deficient layer, the intensities of the diffraction peaks can be varied which was already shown in 1977 by Matsuda et al. [57], who found that the best agreement between the calculated and experimental diffraction patterns for LB films of cadmium salts of fatty acids, was found when an electron-deficient layer of about two CH_2 groups thick was taken into account. As can be seen from Figure 4.6A and 4.13A, already before exposure to UV light the second Bragg peak had a relatively weaker intensity than the third one, which is additional proof of the existence of a Y-type structure in the LB film [60]. The shift of the Bragg peak to higher angles indicates an increased tilt of the amphiphiles inside the multilayer.

Contrary to LB films prepared from a $Cu(ClO_4)_2$ containing subphase, the layer structure of the LB film built up from a $CuCl_2$ subphase was destroyed after exposure to UV light, which is clearly demonstrated in Figure 4.13 (curves C and D).

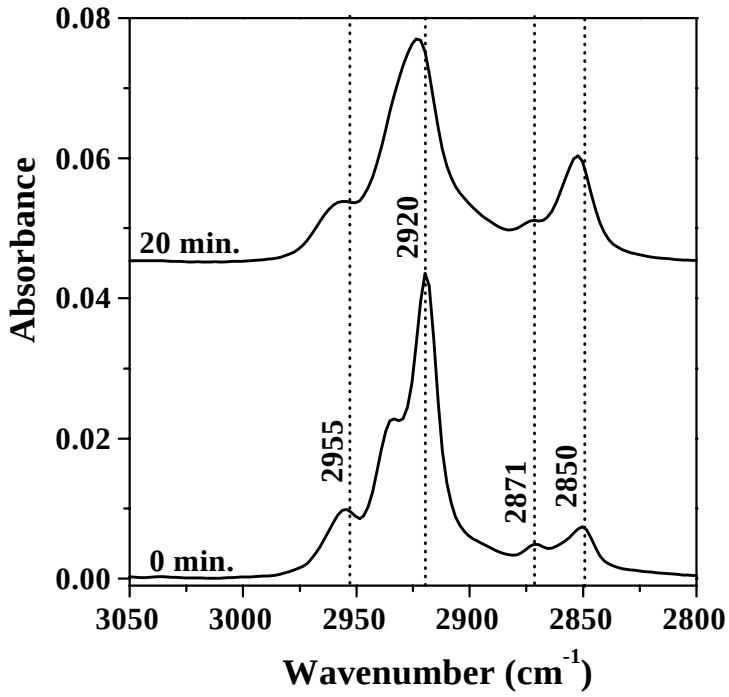

Figure 4.14A: *GIR infrared spectra of a LB film of 16 layers of the amphiphile built up from a 5mM $Cu(ClO_4)_2$ subphase (sample C) at 19 ^oC and 30 $mN \cdot m^{-1}$ on gold-coated glass with 3 layers of cadmium arachidate, before and after 20 minutes of exposure to UV light. The CH_2 and CH_3 stretching vibration region.*

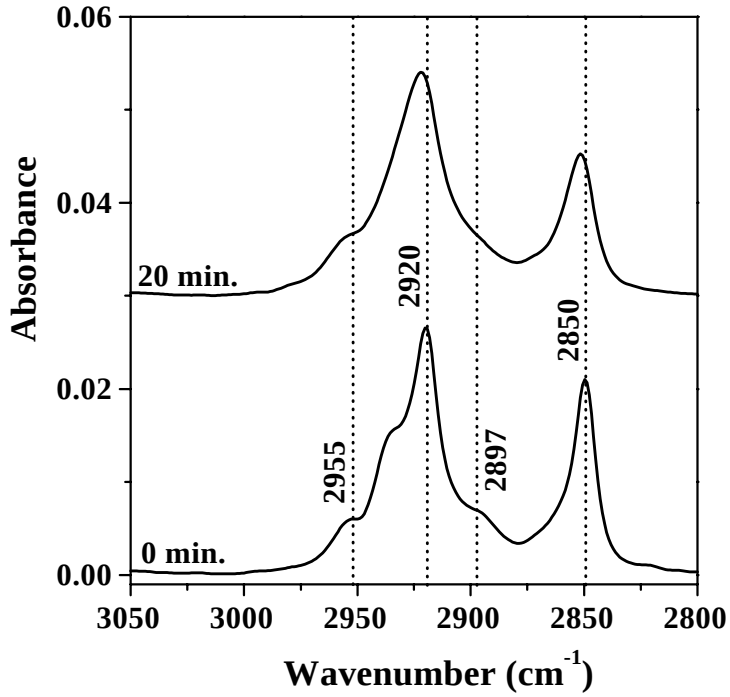

Figure 14.4B: *Transmission infrared spectra of a LB film of 16 layers of the amphiphile built up from a 5 mM $Cu(ClO_4)_2$ subphase (sample A) at 19 ^oC and 30 $mN{\cdot}m^{-1}$ on silicon, before and after 20 minutes of exposure to UV light. The CH_2 and CH_3 stretching vibration region.*

To get more insight into the structural changes during the polymerisation process inside the multilayer, FT-IR spectroscopy measurements were performed. Major changes were found in the CH stretching region for multilayers built up from a 5 mM $Cu(ClO_4)_2$ subphase, as can be seen in the Figures 4.14A (sample C) and 4.14B (sample B). The vibration bands near 2850, 2871, 2920 and 2955 cm^{-1} are due to ν_s (CH_2), ν_s (CH_3), ν_a (CH_2) and ν_a (CH_3) respectively [61,62]. The vibration band near 2934 cm^{-1} arises from the Fermi resonance between the ν_a (CH_3) band and the overtone of the CH_3 asymmetric deformation vibration near 1450 cm^{-1} [61]. The weak vibration near 2897 cm^{-1} was assigned to a Fermi resonance component arising from the ν_s (CH_2) band and an overtone of the CH_2 scissoring vibration [61]. After UV irradiation the ν_s (CH_2) and ν_a (CH_2) bands were slightly shifted to higher frequencies, 2852 and 2922 cm^{-1}, respectively. This indicated that the all-trans alkyl chain is partly converted into an alkyl chain containing gauche conformations. Because for an alkyl chain containing all-trans conformations, the ν_s (CH_2) and ν_a (CH_2) are situated at 2849 and 2919 cm^{-1}, respectively, while for an irregular alkyl chain containing only gauche conformations these vibrations are situated at 2854 and 2924 cm^{-1} [61]. Furthermore, the ν_s

(CH_3) and the ν_a (CH_3) vibrations are situated at 2871 and 2955 cm^{-1}, respectively, irrespective of the alkyl chain conformation. This is consistent with our observations. The intensity of the ν_a (CH_2) band decreased in the GIR spectrum while the intensity of the ν_s (CH_2) band increased upon UV irradiation (Fig 4.14A). This fact together with the slight shift of these vibration bands to higher wavenumbers, could be explained by considering that the all-trans conformation of the alkyl is converted into an irregular one containing gauche conformations.

The same phenomena appeared in multilayers built up from a 5mM $CuCl_2$ subphase. But for these multilayers the intensities of the ν (N-H) and amide I absorptions also decrease in intensity and the peaks become broader, indicating that not only the structure of the aliphatic tail changes upon UV irradiation, but also the amide bond and pyridine rings are reoriented. This explains why the layer structure almost completely disappeared in the SAXR measurement (Fig. 4.13, curve D), upon exposure to UV light.

Polymerisation of Cd(II) containing multilayers

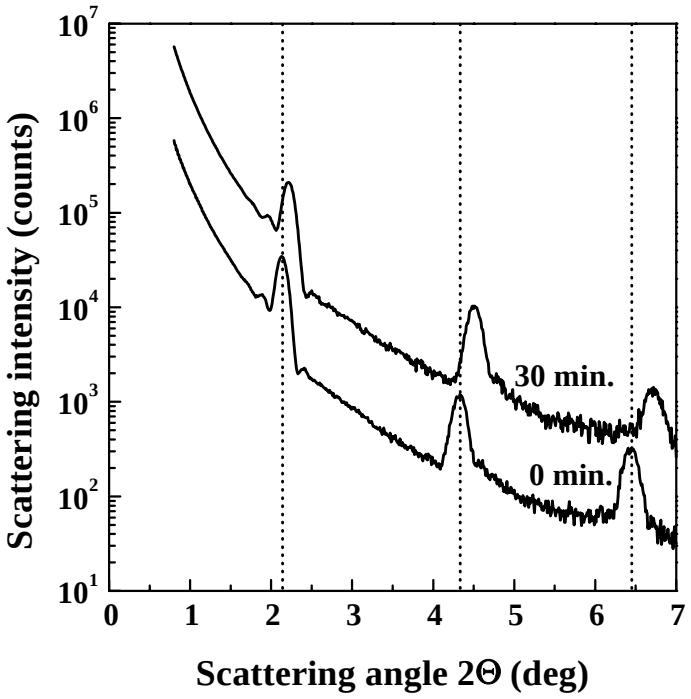

Figure 4.15: *Small angle X-ray reflection curves of a LB film of 16 layers of the amphiphile built up from a 5 mM $CdBr_2$ subphase (sample F) at 19 ^oC and 19 $mN \cdot m^{-1}$ on silicon, before and after irradiation with UV light.*

Upon exposure to UV light (254 nm), the multilayer film built up from a 5 mM $CdBr_2$ subphase, formed a red phase polydiacetylene film. The polymerisation was complete within 30 minutes as could be seen by UV/Vis spectroscopy, in which the absorption at λ_{max} = 540 nm did not increase anymore after 30 minutes of exposure to UV light.

Small angle X-ray reflection measurements revealed that the layer structure was preserved well during the UV irradiation (Fig. 4.15). The bilayer spacing decreased from 42 to 40.5 Å, again indicating that upon polymerisation the amphiphiles make a larger tilt with respect to the surface normal. It can also be seen that the second Bragg peak is present before and after UV irradiation in contrast to the LB films built up from a Cu(II) subphase where the second Bragg peak was already somewhat weaker in intensity before UV irradiation (the well-known odd-even effect) and in the case of ClO_4^- as counter ion totally disappeared upon exposure to UV light. This was a strong indication that the Cu(II) and Cd(II) ions multilayers had different layer structure.

Spectral changes in the transmission IR spectra showed up only in the CH stretching vibration region. The ν_a (CH_2) and ν_s (CH_2) absorptions did not shift to higher wavenumbers as was the case for the Cu(II) containing multilayers (Fig 4.14B). Thus, during the polymerisation process the alkyl chains maintain the all-trans conformation. Furthermore, upon polymerisation the ν_a (CH_2) absorption decreases in intensity while the ν_s (CH_2) absorption show a slight increase in intensity. These spectral changes in the transmission spectrum can only be ascribed to a larger tilt angle (α) of the alkyl chain director with respect to the surface normal, which is in good agreement with the observed decrease in bilayer spacing derived from the SAXR measurements (Fig. 4.15).

Conclusions

Langmuir-Blodgett multilayers of 4-(10,12-pentacosadiynamidomethyl)pyridine could only be built up when the subphase contained Cu(II) or Cd(II) ions. XPS measurements confirmed that complexation had occurred in the monolayer because the multilayers contained metal ions. Care must be taken in drawing conclusions about the valence of the copper ions inside these multilayers from data deduced by XPS measurements, because upon exposure to X-rays the Cu(II) ions undergo a X-ray induced reduction to Cu(I). Small angle X-ray reflection measurements revealed that the formed multilayers had a regular layer structure with a bilayer spacing of approximately 60 Å and 42 Å for the Cu(II) and Cd(II) ions containing multilayers, respectively, although these multilayers were built up by a Z-type transfer. Therefore, a rearrangement to a Y-type structure had occurred.

Changes of metal ion had a great effect on the structure and polymerisation properties of these multilayers. Multilayers built up from a $Cu(ClO_4)_2$ and $CdBr_2$ containing subphase, preserve their regular layer structure during the polymerisation process. But after polymerisation, the all-trans alkyl aliphatic tail of the amphiphile in a Cu(II) ion containing multilayer, is converted into a more irregular alkyl chain, containing gauche conformations. This did not occur in the Cd(II) containing multilayers. For LB films built up from a $CuCl_2$ subphase, the regular layer structure was not preserved during the polymerisation process.

To summarise, the properties of LB film of metal complexes, largely depend on the metal and counter ions used in the subphase, from which the multilayers are built up.

References

1. G. Roberts (Ed.), *Langmuir-Blodgett films*, Plenum Press, New York **1990**.
2. A. Ulman, *An introduction to ultra thin organic films: from Langmuir-Blodgett to self assembly*, Academic Press, San Diego and London **1991**.
3. D.J.M. Linden, J.P. Peltonen and J.B. Rosenholm, *Langmuir* **1994**, *10*, 1592.
4. K.B. Blodgett, *J. Am. Chem. Soc.* **1935**, *57*, 1007.
5. K.B. Blodgett and I. Langmuir, *Phys. Rev.* **1937**, *51*, 964.
6. T. Miyashita, *Prog. Polym. Sci.* **1993**, *18*, 263.
7. J.D. Swalen, D.L. Allara, J.D. Andrade, E.A. Chandross, G. Garoff, J. Israelachvili, T.J. McCarthy, R. Murray, R.F. Pease, J.F. Rabolt, K.J. Wynne and H. Yu, *Langmuir* **1987**, *3*, 932.
8. K.Z. Wang, C.H. Huang, D.J. Zhou, G.X. Xu, Y. Xu, Y.Q. Liu, D.B. Zhu, X.S. Zhao and X.M. Xie, *Solid State Comm.* **1995**, *93*, 189.
9. F. Bonsoni, F. Lely, G. Ricciardi, M. Romanelli and G. Martini, *Langmuir* **1993**, *9*, 268.
10. A. Suzuki, K. Ohkawa, S.Kanda, M. Emoto and S. Watari, *Bull. Chem. Soc. Japan* **1975**, *48*, 2634.
11. K. Sasakawa and S. Iwata, *Annu. Rep. Res. Reactor Inst. Kyoto Univ.* **1984**, *17*, 146.
12. G. Caminati, E. Margheri and G. Gabrielli, *Thin Solid Films* **1994**, *244*, 905.
13. G. Caminati, E. Margheri and G. Gabrielli, *Prog. Colloid Polym. Sci.* **1994**, *97*, 12.
14. E. Satori, M.P. Fontana, M. Costa, E. Dalcanale and V. Paganuzzi, *Thin Solid Films* **1996**, *284-285*, 204.
15. M. Gobernado-Mitre and R. Aroca, *Langmuir* **1993**, *9*, 2185.
16. L. Kalvoda and E. Brynda, *Thin Solid Films* **1993**, *232*, 120.
17. I.K. Lednev and M.C. Petty, *Adv. Mater.* **1996**, *8*, 615.
18. J.H. van Esch, R.J.M. Nolte, H. Ringsdorf and G. Wildburg, *Langmuir* **1994**, *10*, 1955.

19. J. Nagel and U. Oertel, *Polymer* **1995**, *36*, 381.
20. T. Miyashita, S. Saito and M. Matsuda, *Chem. Lett.* **1991**, 859.
21. P.J. Werkman and A.J. Schouten, *Thin Solid Films* **1996**, *284-285*, 24.
22. B. Tieke, H.-J. Graf, G. Wegner, B. Naegele, H. Ringsdorf, A. Banerjie, D. Day and J.B. Lando, *Colloid & Polym. Sci.* **1977**, *255*, 521.
23. R. Burzynski, P.Prasad, J. Biegajski and D.A. Cadenhead, *Macromolecules* **1986**, *19*,1059.
24. C. Bubeck, *Thin Solid Films* **1980**, *160*, 1.
25. H.D. Göbel, *Thesis*, Technische Universität München **1989**.
26. M. Sarkar and J.B. Lando, *Thin Solid Films* **1983**, *99*, 119.
27. C.A.J. Putman, H.G. Hansma, H.E. Gaub and P.K. Hansma, *Langmuir* **1992**, *8*, 3014.
28. B. Wallbank, C.E. Johnson and I.G. Main, *J. Electron Spectrosc.* **1974**, *4*, 263.
29. J.F. Gilp and I.G. Main, *J. Electron Spectrosc.* **1975**, *6*, 397.
30. B.A. Angelis, *J. Electron Spectrosc.* **1976**, *9*, 81.
31. G. Schön, *Surface Science* **1973**, *35*, 96.
32. R.G. Copperthwaite, *Surface Interface Anal.* **1980**, *2*, 17.
33. G. Martella, O. Puglisi, S. Pignataro, G. Alberti and U. Costantino, *Chem. Phys. Lett.* **1982**, *89*, 333.
34. J. Ruokolainen, J. Tanner, G. ten Brinke, O. Ikkala, M. Torkkeli and R. Serimaa, *Macromolecules* **1995**, *28*, 7779.
35. J. Ruokolainen, G. ten Brinke, O. Ikkala, M. Torkkeli and R, Serimaa, *Macromolecules* **1996**, *29*, 3409.
36. J.F. Stephens, *J. Colloid Interface Sci.* **1972**, *38*, 557.
37. E.P Honig, *J. Colloid Interface Sci.* **1973**, *43*, 66.
38. E.P. Honig, J.H. Hengst and D. den Engelsen, *J. Colloid Interface Sci.* **1973**, *45*, 92.
39. M.T. Flanagan, *Thin Solid Films* **1983**, *99*, 133.
40. M. Schoondorp, A.J. Schouten, J.B.E. Hulshof and B.L. Feringa, *Langmuir* **1992**, *8*, 1852.
41. D.L. Allara and R.G. Nuzzo, *Langmuir* **1986**, *1*, 52.
42. J.F. Rabolt, F.C. Burns, N.E. Schlotter and J.D. Swalen, *J. Electron Spectrosc.* **1983**, *30*, 29.
43. D.L. Allara and J.D. Swalen, *J. Phys. Chem.* **1992**, *86*, 2700.
44. C. Naselli, J.F. Rabolt and J.D. Swalen, *J. Chem. Phys.* **1985**, *82*, 2136.
45. G. Duda, A.J. Schouten, T. Arndt, G. Lieser, G.F. Smidt, C. Bubeck and G. Wegner, *Thin Solid Films* **1988**, *159*, 221.
46. R.G. Nuzzo, A. Fusco and D.L. Allara, *J. Am. Chem. Soc.* **1987**, *109*, 2358.
47. S.D. Evans, K.E. Goppert-Berarducci, E. Urankan, L.J. Gerenser, A. Ulman and R.G. Snyder, *Langmuir* **1991**, *7*, 2700.

48. R. Popovitz-Biro, D.J. Hung, E. Shavit, M. Lahav and L. Leiserowitz, *Thin Solid Films* **1989**, *178*, 203.
49. R. Popovitz-Biro, K. Hill, E. Shavit, D.J. Hung, M. Lahav, L. Leiserowitz, J. Sagiv, H. Hsiung, G.R. Meredith and H. Vanherzeele, *J. Am. Chem. Soc.* **1990**, *112*, 2498.
50. S.P. Walsh and J.B. Lando, *Langmuir* **1994**, *10*, 246.
51. B. Tieke, G. Lieser and K. Weiss, *Thin Solid Films* **1983**, *99*, 95.
52. D. Briggs and M.P. Seah (Ed.), *Practical surface analysis*, John Wiley, Chichester and New York **1984**.
53. M. Teerenstra, E.J. Vorenkamp, R.J.M. Nolte and A.J. Schouten, *Thin Solid Films* **1991**, *196*, 153.
54. A.A.D. Deckert, L. Fallon, L. Kiernan, C. Cashin, A. Perrone and T. Encalarde, *Langmuir* **1994**, *10*, 1948.
55. A.A. Deckert, J.H.C. Horne, B. Valentine, I. Kiernan and L. Fallon, *Langmuir* **1994**, *11*, 643.
56. B. Tieke, *Adv. Polym. Sci.* **1985**, *71*, 79.
57. A. Matsuda, M. Sugi, T. Fukui, S. Izima, M. Miyahara and Y. Otsubo, *J. Appl. Phys.* **1977**, *48*, 771.
58. M. Pomerantz and A. Segmüller, *Thin Solid Films* **1980**, *60*,33.
59. P. He, Q. Tian and X. Chen, *New Polymeric Mater.* **1991**, *3*, 19.
60. J.P.K. Peltonen, P. He and J.B. Rosenholm, *Langmuir* **1993**, *9*, 2363.
61. A. Saito, Y. Urai and K. Itoh, *Langmuir* **1996**, *12*, 3938.
62. J.F. Rabolt, F.C. Burns, N.E. Schlotter and J.D. Swalen, *Chem. Phys.* **1983**, *78*, 946.

Chapter 5

Formation of mono- and multilayers of metal complexes of 4-(10,12-pentacosadiynoatomethyl)pyridine

Summary

The monolayer properties of the amphiphile, 4-(10,12-pentacosadiynoato-methyl)pyridine have been studied by measuring the surface pressure-area isotherms. The amphiphile forms stable monolayers at the air-water interface and protonation of the monolayers takes place at pH values of 3.00 or lower. Addition of Cu(II) to the subphase (0.5 - 50 mM) causes an increase of the pressure (Π_c) at which the phase transition from the liquid-expanded (LE) to liquid-condensed (LC) phase shows up, suggesting that complexation in the monolayer has occurred. This complexation behaviour is strongly influenced by the Cu(II) concentration, the kind of counter ion and the ionic strength of the subphase. Multilayers of the amphiphile can only be built up when the subphase contains Cu(II) ions. The presence of Cu(II) ions was confirmed by means of XPS measurements, from which it can be concluded that indeed complexation in the monolayer has taken place. FT-IR and small angle X-ray reflection (SAXR) measurements revealed that the multilayers have a regular layer structure with a bilayer spacing of 41.3 Å. Upon polymerisation by means of exposure to UV light, the regular layer structure of the multilayers is preserved but the layer spacing decreased to 40.5 Å. Upon polymerisation a maximum conversion is reached after 30 minutes of UV irradiation.

Introduction

In Chapter 3 [1] the monolayer behaviour of an amphiphile with a pyridine group as ligand has been described upon complexation with Cu(II) ions dissolved in the subphase. The pyridine group was connected via an amide bond to an aliphatic tail containing a diacetylene functionality. It was shown that the extent of complexation can easily be controlled by changing the subphase conditions like pH, temperature, ionic strength and types of counter ions. Multilayers of these complexes can easily be built up [2] and these LB films can be polymerised by means of UV irradiation. The multilayers, which contained Cu(II) or Cd(II) ions, had a regular layer structure. It was further shown that the structure of these multilayers was strongly influenced by the kind of metal ion incorporated but also by the counter ion, resulting in different polymerisation behaviour.

This Chapter describes the monolayer properties of the amphiphile 4-(10,12-pentacosadiynoatomethyl)pyridine (Scheme 5.1) upon complexation with Cu(II) ions under various conditions.

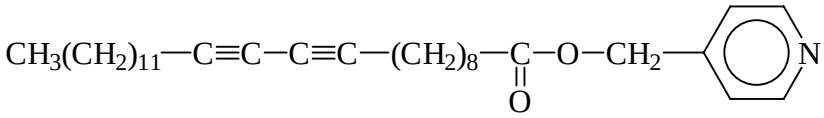

Scheme 5.1

The amphiphile differs from the one described in the Chapters 3 and 4 [1,2] in having an ester bond instead of an amide bond. In this case, it is expected that a less stable monolayer will be formed, because the ester cannot form hydrogen bonds with its neighbouring amphiphiles, whereas the amide can [3,4]. The ester pyridine amphiphile forms metal complexes with Cu(II) ions when copper salts are dissolved in the subphase. Also LB films could be built up from a $Cu(ClO_4)_2$ containing subphase and the structure of these multilayers will be discussed before and after polymerisation by means of exposure to UV light. XPS measurements were performed in order to demonstrate the presence of Cu(II) ions in these multilayer films. Furthermore, small angle X-ray reflections (SAXR) measurements and FT-IR measurements were performed to establish structure of the LB film. To monitor the polymerisation process, UV/Vis absorbance measurements were performed.

Experimental

Materials

10,12-pentacosadiynoic acid (Hüls-Petrarch, 99%) was reacted with thionyl chloride (Merck, > 99%) at about 50 ^{0}C under nitrogen atmosphere to form the corresponding acid chloride. The ester derivative, 4-(10,12-pentacosadiynoatomethyl)pyridine, was obtained by reaction of 4-(hydroxymethyl)pyridine (Acros, 98%) with the acid chloride in dry THF (Acros, > 99%) with equimolar amounts of freshly distilled triethylamine (Merck, > 99%) (as HCl scavenger) under nitrogen atmosphere. The crude product was purified by column chromatography ($CHCl_3$ (Merck p.a.), silicagel 60 (Merck)) followed by a twofold crystallisation from n-hexane (Merck p.a.) (yield: 50%).
Elemental analysis: Calc. for $C_{31}H_{47}NO_2$: C 80.00; H 10.11; N 3.01. Found: C 79.69; H 10.27; N 3.01.
IR: ν (cm^{-1}) 2919 (ν_a CH_2), 2849 (ν_s CH_2), 1734 (ν C=O), 1609 (ν C=N, aromatic ring), 1560 (ν C=C, aromatic ring), 1470 (δ CH_2), 1215 (ν_a C–O–C), 1172 (ν_s C–O–C).
^{1}H NMR (200 MHz): δ 0.87 (t, 3H), 1.25-1.30 (br, 26H), 1.47 (m, 4H), 1.66 (m, 2H), 2.23 (t, 4H), 2.40 (t, 2H), 5.12 (s, 2H), 7.25 (d, 2H), 8.60 (d, 2H).
T_m=36.7 ^{o}C, T_c= 14.0 ^{o}C.

The general procedures have been outlined in the experimental sections of the Chapters 2 and 4.

Results and discussion

Monolayer behaviour

The monolayer properties of the amphiphile were studied by measuring the surface pressure-area isotherm at different temperatures and pH values of the aqueous subphase. Figure 5.1A indicates that at low subphase temperatures (5.2 ^{o}C) a liquid-condensed (LC) monolayer is formed with a limiting area of 30.0 Å^2·molecule^{-1} and a collapse pressure of approximately 50 mN·m^{-1}. Upon rising the subphase temperature, a phase transition from liquid-expanded (LE) to liquid-condensed (LC) state is observed and the collapse pressure decreases, indicating that at higher temperatures a less stable monolayer is formed. When the subphase temperature has increased from 10.4 to 19.1 ^{o}C, the pressure at which the phase transition occurs (Π_c) increases from 2.4 to 13.2 mN·m^{-1}. The monolayers of the ester

amphiphile are less stable than the monolayers of the amide amphiphile [1]. The ester amphiphile has a lower collapse pressure and the phase transition from LE to LC phase takes place already at 10.4 ^{o}C, whereas for the amide amphiphile this phase transition appeared only at elevated temperatures, namely 27 ^{o}C or higher. This reduced monolayer stability of the ester compared to the amide was already predicted, because the ester amphiphile cannot form hydrogen bonds between the molecules, whereas the amide amphiphile can. Changes in the pH of the subphase also influence the monolayer properties of the amphiphile, as can be seen in Figure 5.1B. Increasing the pH from 5.7 to 8.7 does not alter the monolayer behaviour in a dramatic way, only the collapse pressure has slightly decreased, but when the pH of the subphase is lowered to 3.0, Π_c increases and the area per molecule at which the surface pressure begins to rise (A_{fl}) has shifted to a higher value, indicating that the monolayer is partly protonated. Upon protonation the monolayer is charged, which results in an enhanced repulsion between the molecules in the monolayer, which in turn leads to an increase in Π_c and A_{fl}. At a pH of 2.0 the monolayer is totally protonated, resulting in a shift of A_{fl} to high values and an enormous increase in Π_c.

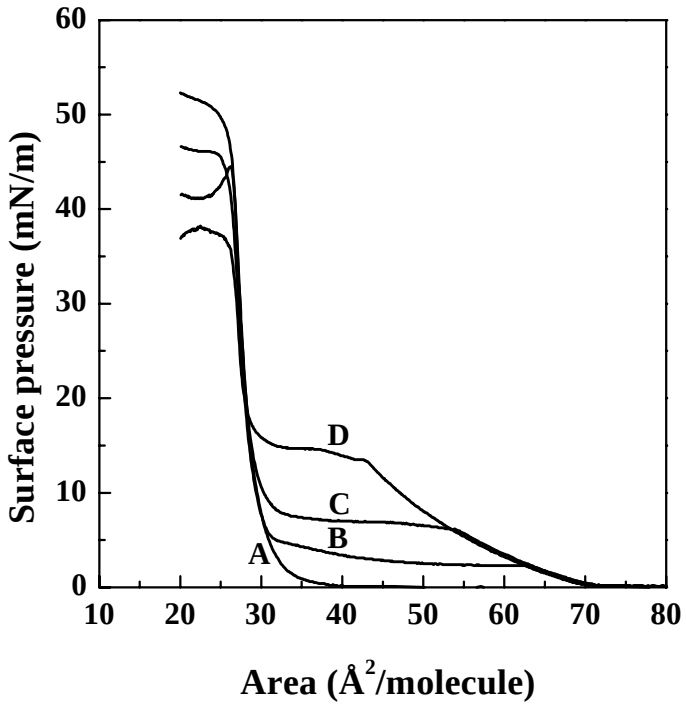

Figure 5.1A: *Surface pressure-area isotherms of 4-(10,12-pentacosadiynoatomethyl)-pyridine on an aqueous subphase at 5.2 ^{o}C (A), 10.4 ^{o}C (B), 14.8 ^{o}C (C) and 19.1 ^{o}C (D).*

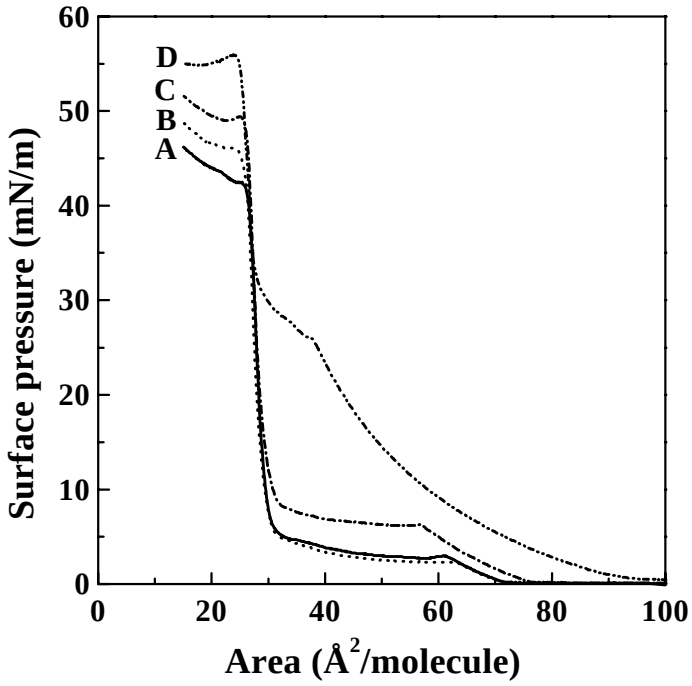

Figure 5.1B: *Surface pressure-area isotherms of the amphiphile on an aqueous subphase at pH values of 8.7 (A), 5.7 (B), 3.0 (C) and 2.0 (D). Subphase temperature: 10.4 ^{o}C.*

Complexation behaviour

Figure 5.2A clearly shows the effect of addition of Cu(II) ions to the subphase. At low Cu(II) concentrations (0.5 mM $CuCl_2$) only a slight increase in collapse pressure can be observed, whereas at a 5 mM $CuCl_2$ subphase, Π_c increases, suggesting that complexation in the monolayer has occurred while upon complexation a charged monolayer is formed, resulting in an increase in Π_c. The collapse pressure also increases upon complexation, so a more stable monolayer is formed, probably due to the crosslinking action of the Cu(II) ions in analogy to the salt formation of metal ions with fatty acids. At high $CuCl_2$ concentrations (50 mM) A_0 has shifted from 30 to 36 $Å^2 \cdot molecule^{-1}$, which could be the result of the formation of "1 to 1" (1 Cu(II) to amphiphile) complex. The "1 to 1" coordination complex forms a heavily charged monolayer at the air-water interface, in which the amphiphiles repel each other strongly, resulting in a shift of A_0 to higher values and a lower collapse pressure indicating that the monolayer is less stable. No increase in Π_c could be observed when other metal chlorides (like Mn(II), Cd(II), Co(II) and Zn(II)) were added to the subphase up to concentrations of 50 mM, indicating that complexation has not occurred.

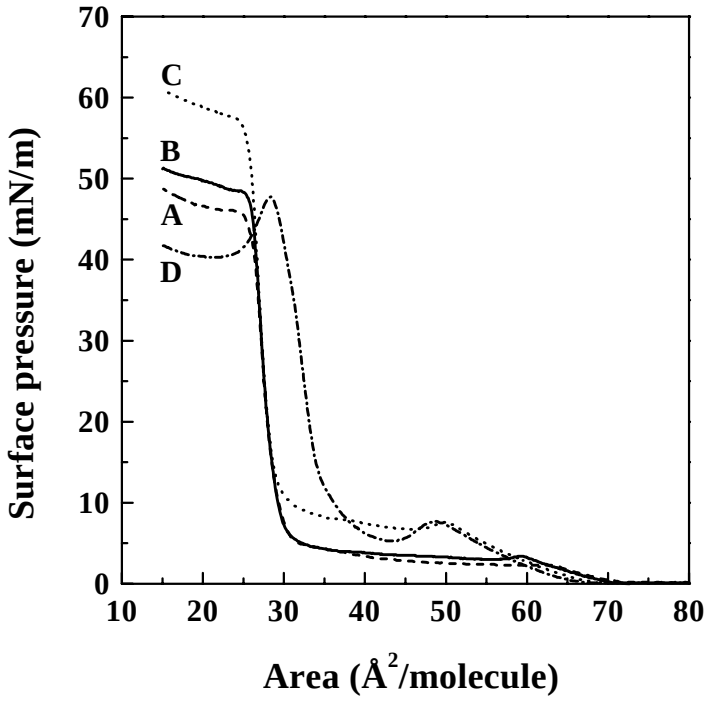

Figure 5.2A: *Surface pressure-area isotherms of the amphiphile at 10.4 ^{o}C on a subphase without (A) and with $CuCl_2$ at concentrations of 0.5mM (B), 5 mM (C) and 50 mM (D).*

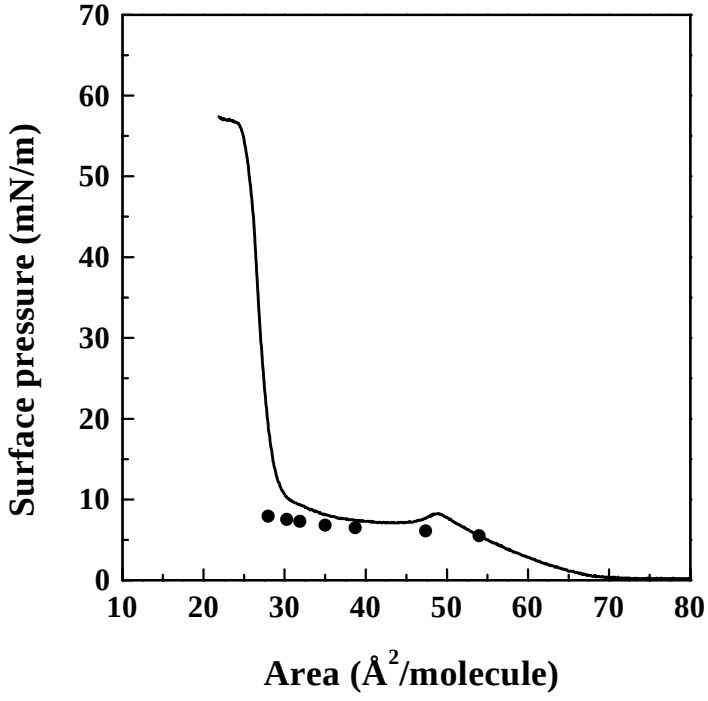

Figure 5.2B: *Surface pressure-area isotherm of the amphiphile at 10.4 ^{o}C on a 5 mM $CuCl_2$ subphase. The points represent the areas found after stabilisation of the monolayer at 5.5, 6.1, 6.5, 6.9, 7.3, 7.5 and 7.9 mN·m^{-1}.*

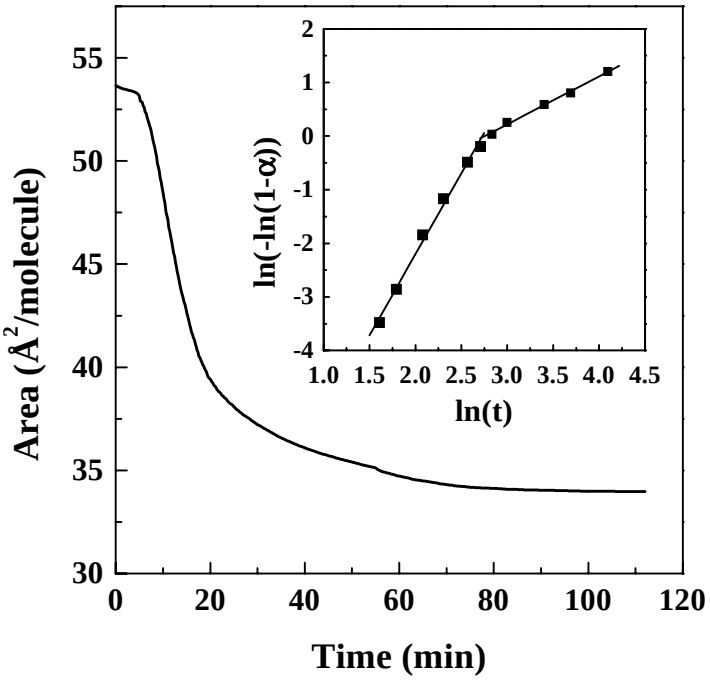

Figure 5.2C: *Isobaric stabilisation curve of the amphiphile at 10.4 °C on a 5 mM $CuCl_2$ subphase and a surface pressure of 6.9 mN·m^{-1}. In the inset the result of the Avrami analysis of the isobaric stabilisation experiments is shown.*

When the monolayer on a 5 mM $CuCl_2$ subphase is stabilised at a surface pressure of 7.8 mN·m^{-1}, just below Π_c (8.2 mN·m^{-1}), the area per molecule decreases from approximately 50 Å^2·molecule^{-1} to approximately 28 Å^2·molecule^{-1}, as can be seen in Figure 5.2B. This decrease in area per molecule is probably caused by a crystallisation process forming a condensed monolayer. When the monolayer on this subphase is stabilised at a surface pressure of 6.9 mN·m^{-1}, which is just below the surface pressure of the coexistence region of the isotherm (7.3 mN·m^{-1}), again a decrease in area per molecule is observed as can be seen in Figure 5.2C. The crystallisation process can be studied by means of the well-known Avrami analysis [5-9] of time-conversion plots. The following equation for the time dependence of the crystalline fraction during isothermal crystallisation was proposed by Avrami [5-7]:

$$1-\alpha = \exp(-Kt^n) \qquad \textbf{(5.1)}$$

in which α is the fraction of crystalline material, K is a constant, t is the time and n is the so-called Avrami exponent. To ensure a constant, thermodynamic driving force, isothermal and isobaric conditions should be used during the crystallisation process at the air-water interface. The fraction of crystalline material can easily be obtained by calculating the area loss referred

to the beginning of the crystallisation process, divided by the area loss associated with the completed crystallisation process. The result is shown in the inset of Figure 5.2C. From the slope of the straight line the Avrami exponent can be calculated. Up to a conversion of approximately 60 % this Avrami exponent (n) has a value of 3.0 [8,9], indicating that the nucleation is sporadic and that disc-like crystals are formed (two-dimensional growth) with a contact-controlled growth. After about 60 % conversion the slope of the line has changed. At this stage of the crystallisation process, n has a value of approximately 0.95. This indicates that after 60 % conversion no new nuclei are formed and that the growth of the disc-like crystals is diffusion-controlled [8,9]. At surface pressure of 5.5 $mN \cdot m^{-1}$ or lower no crystallisation takes place, indicating that the LE phase is thermodynamically stable at low surface pressure.

When the counter ion Cl^- is replaced by another counter ion an enormous effect on the complexation behaviour can be seen (Fig. 5.3A/B).

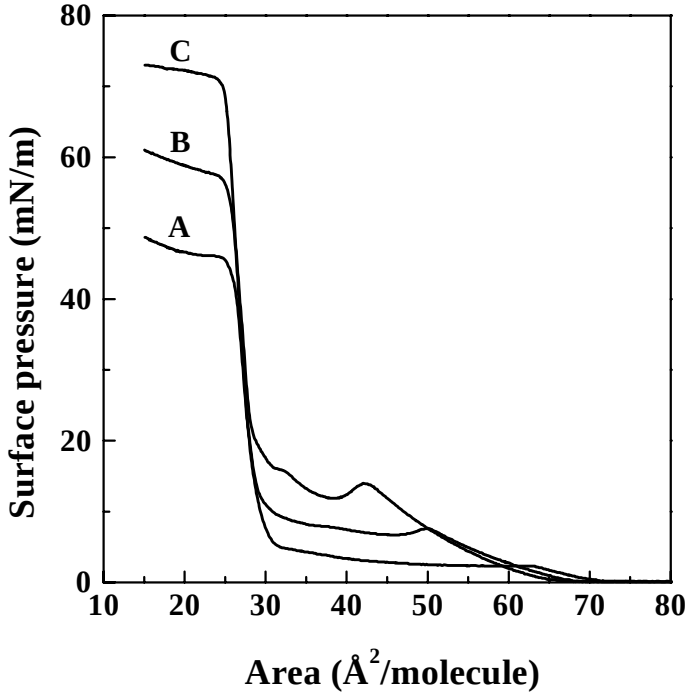

Figure 5.3A: *Surface pressure-area isotherms of the amphiphile at 10.4 ^oC on a subphase without Cu(II) ions (A), with 5mM $CuCl_2$ (B) and 5 mM $CuBr_2$ (C).*

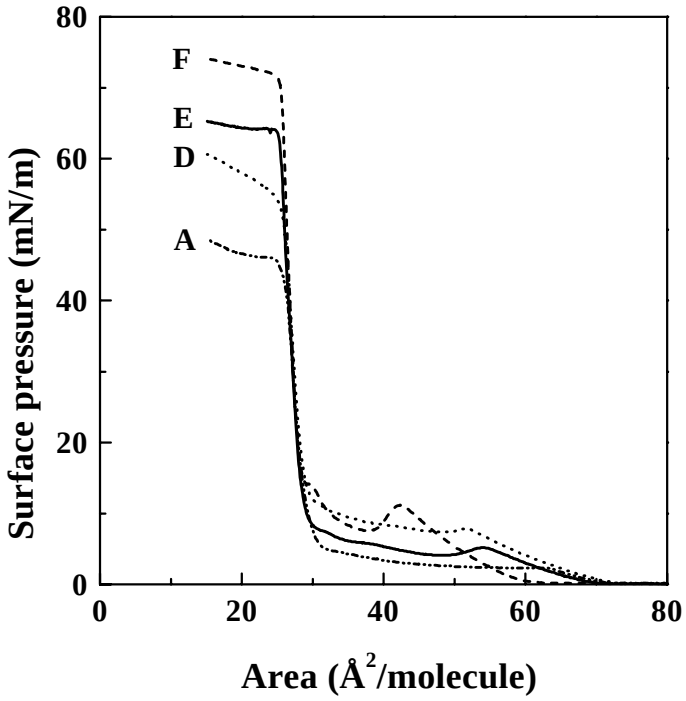

Figure 5.3B: *Surface pressure-area isotherms of the amphiphile at 10.4 ^{o}C on a subphase without Cu(II) ions (A) and on a 5 mM Cu(II) subphase with different counter ions: NO_3^- (D), CH_3COO^- (E) and ClO_4^- (F).*

When complexation occurs, a positively charged monolayer is formed and to meet the condition of electroneutrality, negatively charged anions absorb to the positively charged metal complex monolayer at the air-water interface, forming a Stern layer [10]. The specific interaction energy (ϕ) increases for anions which are larger, more easily polarisable and have a lower hydration number. In that case their specific absorption is enhanced and a more complete complexation may occur. This effect can clearly be seen in Figure 5.3A. When the Cl^- anion is replaced by the bigger more easily polarisable Br^- anion, Π_c increases, so a more complete complexation takes place in the monolayer. From the increase in Π_c and collapse pressures (Fig. 5.3A/B) the following series is deduced of the counter ions, for the complexation of the amphiphile with Cu(II): $NO_3^- < Cl^- \approx CH_3COO^- < Br^- \approx ClO_4^-$. This series was also found for the complexation of Cu(II) with the amide amphiphile [1].

Also the ionic strength of the subphase influences the complexation behaviour of the amphiphile in the monolayer, as can be seen in Figure 5.4. By adding KCl to the subphase, the ionic strength of the subphase has increased. At high ionic strengths Π_c increases, indicating, that the extent of complexation has increased. Probably the metal ions and

amphiphilic ligands are more shielded from each other by the electrolytes, and complexation can take place more easily [11].

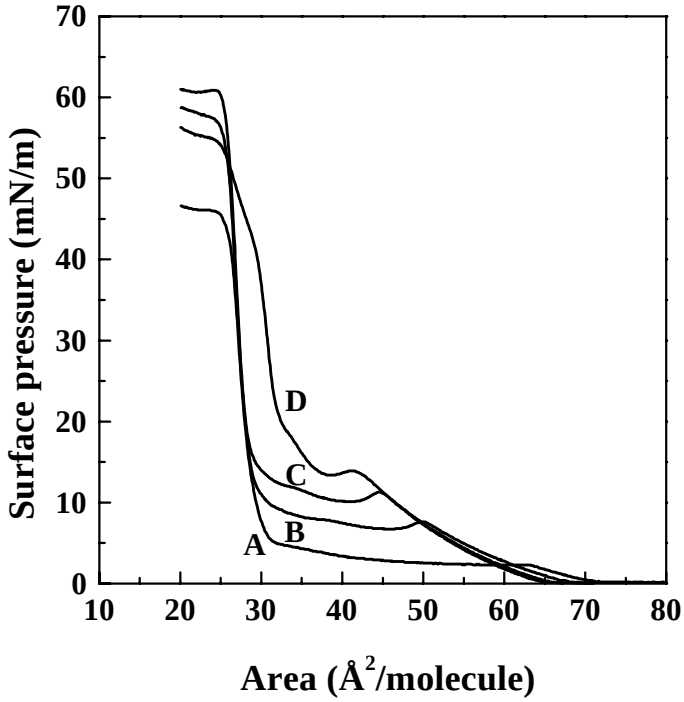

Figure 5.4: *Surface pressure-area isotherms of the amphiphile at 10.4 ^{o}C on a subphase without Cu(II) ions (A) and on a 5 mM $CuCl_2$ subphase with ionic strengths of 0.015 (B), 0.030 (C) and 0.045 (D).*

Multilayer formation

Monolayers of the amphiphile could be stabilised at the air-water interface at surface pressures up to 20 $mN \cdot m^{-1}$ and a subphase temperature of approximately 4 ^{o}C. When the subphase contained $Cu(ClO_4)_2$, up to concentrations of 2.5 mM Cu(II) and up to temperatures of approximately 10 ^{o}C, stable monolayers could be formed at surface pressures up to 28 $mN \cdot m^{-1}$. $CuCl_2$ concentrations up to 5 mM also lead to the formation of stable monolayers.

Only when the subphase contained $Cu(ClO_4)_2$, monolayers could be transferred onto glass slides and silicon wafers with a Z-type transfer and transfer ratios of 0.0 on the downstroke and 1.0 on the upstroke. Regular layer structures were not formed on gold-coated substrates even when these substrates were first covered with 5 layers cadmium arachidate or 4 layers of amylose-acetate [12] or poly((S)-acetoxymethylethylisocyanide) [13]. Moreover, when the subphase contained $CuCl_2$, a regular layer structure could not be built up because the monolayer was too brittle and at elevated temperatures a stable monolayer could not be

formed. Apparently, the counter ions have a great effect on the structure of the multilayer film, which was also the case for the amide amphiphile [2].

XPS measurements

XPS measurements were performed on the multilayers in order to confirm complexation, because XPS measurements can give direct evidence for the presence of Cu(II) in the LB films. It can also give quantitative information about the amount of Cu(II) incorporated into these multilayer films. In this way, XPS measurements prove whether complexation in the monolayers has occurred.

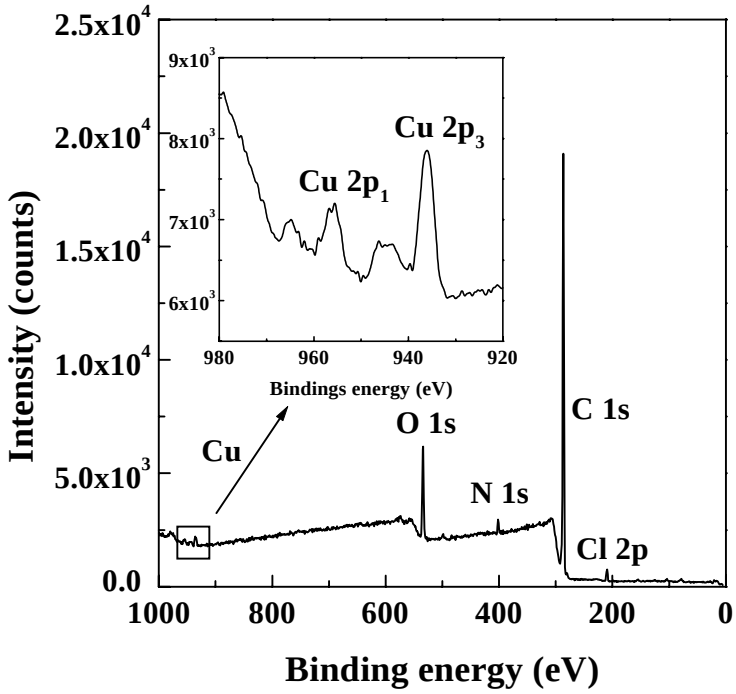

Figure 5.5: *XPS spectrum of a LB film consisting of 16 layers of the amphiphile on silicon, built up from a 2.5 mM $Cu(ClO_4)_2$ subphase at 4.4 ^oC and 25 $mN{\cdot}m^{-1}$.*

Figure 5.5 shows the XPS measurement of a multilayer of the amphiphile built up from a 5 mM $Cu(ClO_4)_2$ subphase. The Cu 2p peaks are clearly present (the Cu $2p_3$ peak at 936.1 eV and the Cu $2p_1$ peak at 955.6 eV) and the ratio of Cu to N is about 1:2. Because every amphiphile contains 1 nitrogen atom the stoichiometry of the metal complex is 1 Cu(II) ion to 2 amphiphiles. In addition, the Cl 2p peak can be seen at 209.3 eV. The ratio Cu to Cl is 1 : 2, as expected.

Small angle X-ray reflection (SAXR) measurements

In order to establish whether the multilayers have a regular layer structure, SAXR measurements were performed on a multilayer built up from a 2.5 mM $Cu(ClO_4)_2$ subphase, as is shown in Figure 5.6.

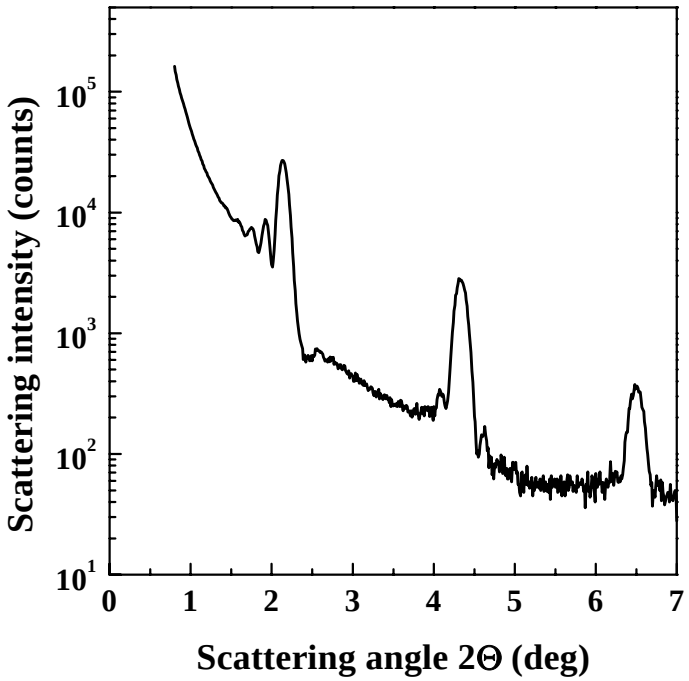

Figure 5.6: *SAXR curve of a LB film consisting of 16 layers of the amphiphile on silicon, built up from a 2.5 mM $Cu(ClO_4)_2$ subphase at 4.4 ^oC and 25 $mN{\cdot}m^{-1}$.*

From the reflection curve a layer spacing of 41.3 Å is deduced. The obtained spacing corresponds to the bilayer spacing of Cd(II) containing multilayers of the amide amphiphile [2]. In a fully stretched conformation the amphiphile has a length of 36.7 Å. When the spacing found is considered as a bilayer spacing in analogy with our previous finding or the amide amphiphile [2], it can be concluded that the amphiphile has a large tilt angle (α) with respect to the surface normal. A rough calculation reveals a value of approximately 55^o for α. Because the multilayers were built up by a Z-type of transfer, a rearrangement to a Y-type of structure must have occurred, which is frequently found in literature, because the Y-type structure is the thermodynamically most stable structure [14-16].

FT-IR measurements

Unfortunately, multilayers could only be built up onto glass and silicon substrates and not onto gold-coated glass slides, so only transmission spectra could be recorded (Fig. 5.7).

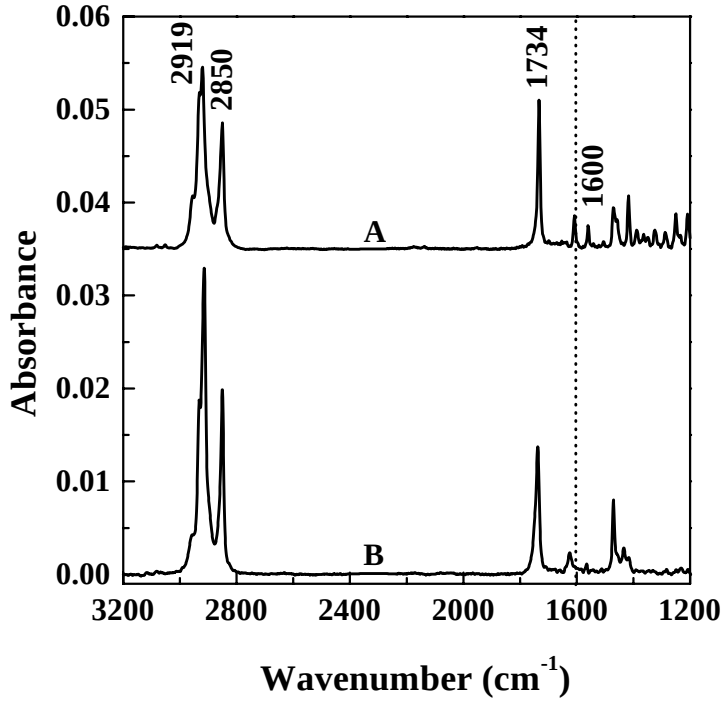

Figure 5.7: *Infrared spectra of the amphiphile:* ***(A)*** *powdered in KBr,* ***(B)*** *transmission spectrum of a LB film consisting of 16 layers of the amphiphile on silicon, built up from a 2.5 mM $Cu(ClO_4)_2$ subphase at 4.4 ^oC and 25 $mN \cdot m^{-1}$.*

In the transmission mode, the electrical field vector is parallel to the substrate, so all individual group vibrations with a transition dipole moment components parallel to the substrate surface will absorb maximally in this mode. In Figure 5.7, a bulk spectrum of the amphiphile, powdered in KBr (no preferred orientation of the individual groups) and a transmission spectrum of a multilayer built up from a 2.5 mM $Cu(ClO_4)_2$ subphase can be seen. The band assignments are presented in Table 5.1.

Table 1: *The IR band assignments [12,17-22].*

Wavenumber (cm^{-1})	Assignment	Transition dipole moment, $\vec{M}$
2954	ν_a (CH_3)	$\perp$ C–CH_3
2919	ν_a (CH_2)	$\perp$ C–C–C chain plane
2871	ν_s (CH_3)	$\parallel$ C–CH_3
2850	ν_s (CH_2)	$\parallel$ H–C–H plane, bisecting HCH angle
1734	ν (C=O)	$\parallel$ C=O bond
1622	ν (C=N_{ar})	$\parallel$ ring
1560	ν(C=C_{ar})	$\parallel$ ring
1470	δ (CH_2)	$\parallel$ H–C–H plane, bisecting HCH angle
1251	ν_a (C–O–C)	$\parallel$ C–O–C bond
1172	ν_s (C–O–C)	$\parallel$ C–O–C bond

The transmission spectra of the multilayers of Figure 5.7, strongly resemble the transmission spectra of a Cd(II)-containing multilayer of the amide amphiphile in Chapter 4 [2]. Moreover, the SAXR and transmission IR spectra of the ester amphiphile strongly correspond to the SAXR measurement and IR spectra of the Cd(II)-containing LB films of the amide amphiphile [2] suggesting that these LB films have the same structure. In Figure 5.7 the CH stretching vibrations of the aliphatic tail, ν_a (CH_2) at 2919 cm^{-1} and ν_s (CH_2) at 2850 cm^{-1}, can be seen clearly and also the ν (C=O) at 1734 cm^{-1} can be seen in the transmission spectrum, so these vibrations have a large transition dipole moment component parallel to the substrate surface. Furthermore, the vibrations of the pyridine ring at 1622 and 1560 cm^{-1} can be seen, indicating that the pyridine ring has a large tilt angle with respect to the surface. When the pyridine ring had an orientation perpendicular to the substrate, no vibrations would be seen at 1622 and 1560 cm^{-1} in the transmission mode. The location of $\nu_{C\text{-}N}$ of the pyridine at 1622 cm^{-1} corresponds to pyridine which is coordinated to metal ions, otherwise the $\nu_{C\text{-}N}$ would absorb at 1600 cm^{-1}. The fact that no shoulder can be detected at 1600 cm^{-1} indicates that all the pyridine moieties of the amphiphiles are coordinated to the Cu(II) ions. The transmission IR spectra together with the SAXR measurement, suggest that the amphiphile has a large tilt angle (α) with respect to the surface normal and, therefore, the following structure for the amphiphiles in these multilayers (Fig. 5.8) is proposed.

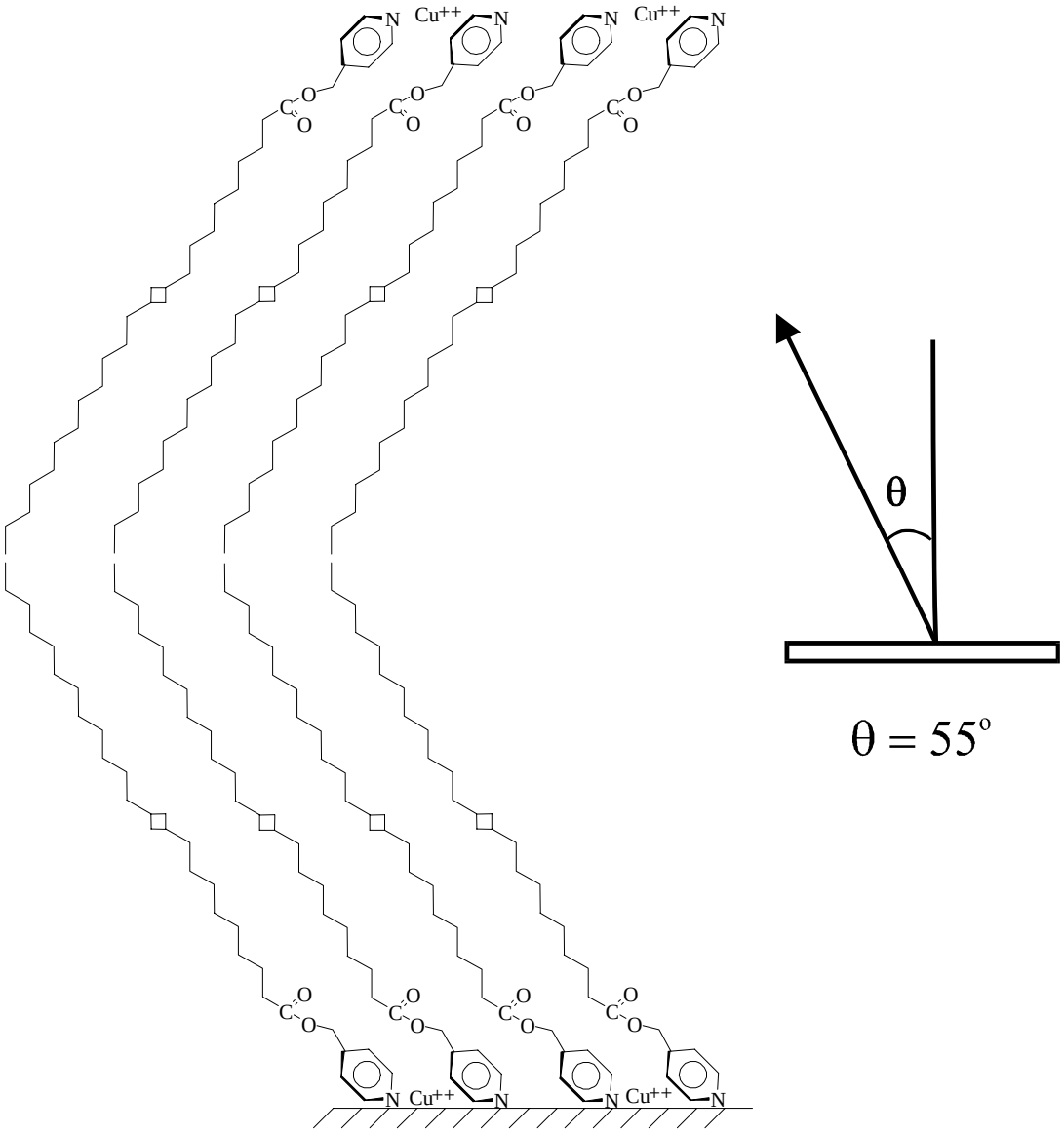

Figure 5.8: *Schematic representation of the structure of the multilayer film.*

Polymerisation of the multilayers

The LB films were polymerised under argon atmosphere by means of UV irradiation (λ = 254 nm). The progress of the polymerisation process was studied by means of UV/Vis spectroscopy because upon polymerisation a highly conjugated linear polymer is formed which strongly absorb in the visible region with λ_{max} = 630 nm for the blue form and λ_{max} = 500 and 540 nm for the red form [23,24].

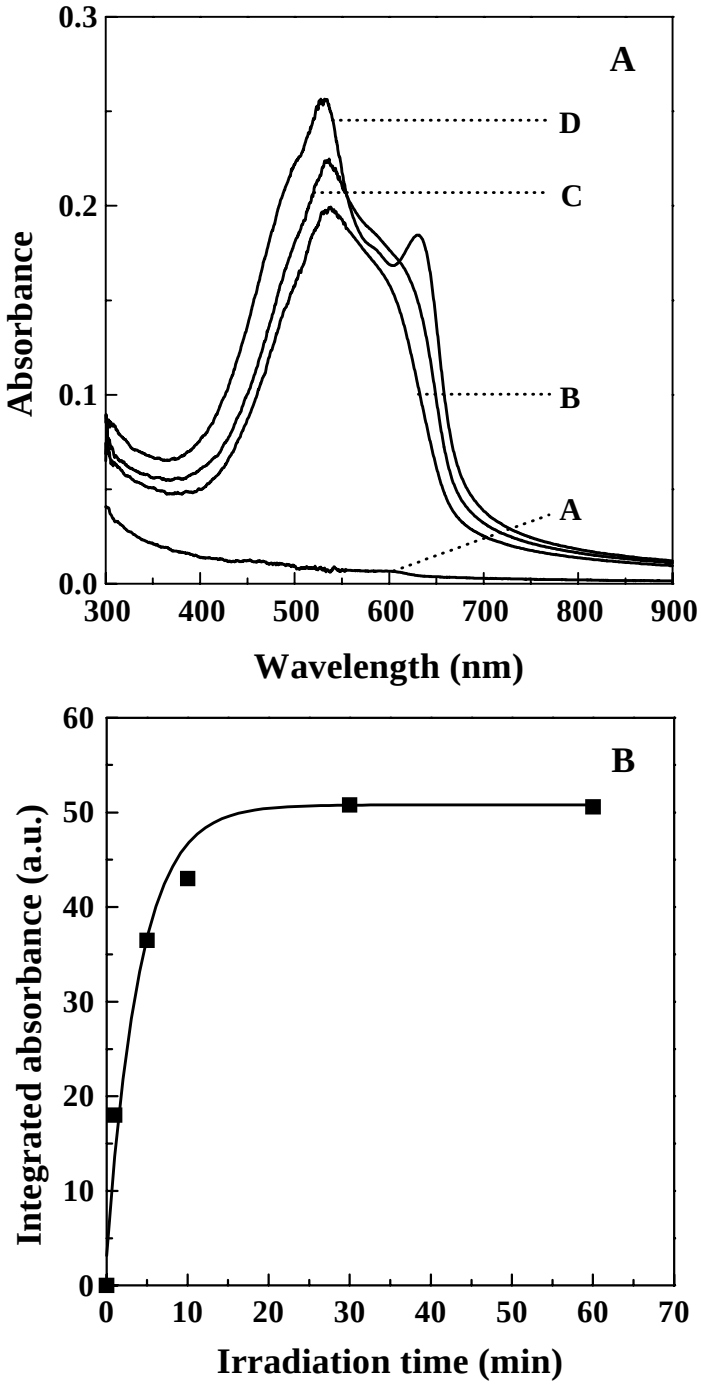

Figure 5.9: ***A.*** *UV/Vis spectra of a LB film consisting of 16 layers of the amphiphile on glass, built up from a 2.5 mM $Cu(ClO_4)_2$ subphase at 4.4 ^oC and 25 $mN \cdot m^{-1}$, at different UV (λ = 254 nm) irradiation times: 0 min. (A), 5 min. (B), 10 min. (C) and 30 min. (D).* ***B.*** *Integrated absorbance of the UV/Vis spectra of Figure 5.9A between 400 and 800 nm, at different times of exposure to UV light.*

UV/Vis spectroscopy

In Figure 5.9A the absorption spectra of the multilayer consisting of 16 layers, built up from a 2.5 mM $Cu(ClO_4)_2$ subphase can be seen at different times of exposure to UV light. Several minutes of irradiation with UV light resulted in the formation of the red form of the polymer with λ_{max} = 540 nm. A maximum conversion is reached after 30 minutes of UV irradiation, which can also be seen in Figure 5.9B, in which the integrated area of absorbance between 400 and 800 nm is shown at different times of exposure to UV light. Here it can be seen that the integrated area remains constant after 30 minutes of exposure to UV light indicating that no further polymerisation takes place.

SAXR measurements

In order to investigate whether the regular layer was preserved during exposure to UV light, SAXR measurements were performed on a multilayer consisting of 16 layers, built up from a 2.5 mM $Cu(ClO_4)_2$ subphase, as can be seen in Figure 5.10.

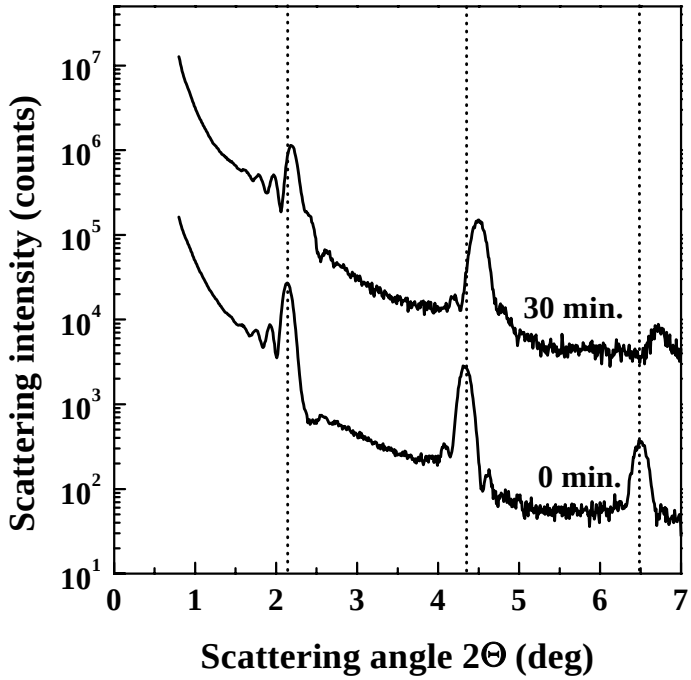

Figure 5.10: *SAXR curves of a LB film consisting of 16 layers of the amphiphile on silicon, built up from a 2.5 mM $Cu(ClO_4)_2$ subphase at 4.4 ^oC and 25 $mN \cdot m^{-1}$, at different UV irradiation times.*

Apparently the layer structure is preserved during the polymerisation process. The bilayer spacing decreases somewhat from 41.3 to 40.5 Å, probably due to the formation of a more irregular alkyl chain containing gauche conformations [2]. Before exposure to UV light the alkyl chains had an all-trans conformation as is shown by IR spectroscopy (Fig. 5.7) which showed that ν_a (CH_2) is located at 2919 cm^{-1} and that ν_s (CH_2) is located at 2850 cm^{-1}. These locations are characteristic for an all-trans aliphatic chain [25]. Upon polymerisation the ν_a (CH_2) and ν_s (CH_2) bands are shifted to 2922 and 2852 cm^{-1}, respectively, indicating that the all-trans alkyl chain is converted to a more irregular one containing gauche conformations. For an alkyl chain containing only gauche conformations the ν_a (CH_2) and ν_s (CH_2) bands are located at 2924 and 2855 cm^{-1}, respectively [25]. These spectral changes in the IR spectra upon polymerisation were also found for multilayers of the amide amphiphile built up from a Cu(II) ions containing subphase [2] as has been described in Chapter 4.

Conclusions

The monolayer behaviour studies of the ester amphiphile show that when the subphase contains Cu(II) ions, complexation in the monolayers occurs. The complexation behaviour is strongly influenced by the kind of counter ion, the Cu(II) ions concentration and the ionic strength of the subphase. In addition, protonation of the monolayer occurs at pH values of 3.00 or lower. Regular multilayer structures can be built up when the subphase contains $Cu(ClO_4)_2$, which is confirmed by SAXR and FT-IR measurements. Direct evidence for the complexation came from XPS measurements, which reveals the presence of Cu(II) ions incorporated into the multilayers. These multilayers can be polymerised upon exposure to UV light, maintaining their layer structure, as is shown by SAXR measurements.

References

1. P.J. Werkman and A.J. Schouten, *Thin Solid Films* **1996**, *284-285*, 24.
2. P.J. Werkman, R.H. Wieringa, E.J. Vorenkamp and A.J. Schouten, submitted for publication in Langmuir.
3. E.M. Landau, S. Grayer Wolf, M. Levanon, L. Leiserowitz, M. Lahav and J. Sagiv, *J. Am. Chem. Soc.* **1989**, *111*, 1436.
4. E.M. Landau, S. Grayer Wolf, J. Sagiv, M. Deutsch, K. Kjaer, J. AlsNielsen, L.Leiserowitz and M. Lahav, *Pure Appl. Chem.* **1989**, *61*, 673.
5. M. Avrami, *J. Chem. Phys.* **1939**, *7*, 1103.

6. M. Avrami, *J. Chem. Phys.* **1940**, *8*, 212.
7. M. Avrami, *J. Chem. Phys.* **1941**, *9*, 177.
8. P.C. Hiemenz, *Polymer Chemistry, The Basic Concepts*, Marcel Dekker, New York and Basel **1984**.
9. J.M.G. Cowie, *Polymers: Chemistry & Physics of Modern Materials*, 2nd ed., Blackie, Glasgow and London **1991**.
10. P.C. Hiemenz, *Principles of Colloid and Surface Chemistry*, Marcel Dekker, New York and Basel **1977**.
11. R.G. Wilkens, *Kinetics and Mechanism of Reactions of Transition Metal Complexes*, 2nd ed., VCH Verlagsgeselschaft GmbH, Weinheim **1991**.
12. M. Schoondorp, A.J. Schouten, J.B.E. Hulshof and B.L. Feringa, *Langmuir* **1992**, *8*, 1852.
13. M.N. Teerenstra, E.J. Vorenkamp, R.J.M. Nolte and A.J. Schouten, *Thin Solid Films* **1991**, *196*, 153.
14. G. Roberts (Ed.), *Langmuir-Blodgett films*, Plenum Press, New York and London **1990**.
15. J.F. Stephens, *J. Colloid Interface Sci.* **1972**, *38*, 557.
16. E.P. Honig, *J. Colloid Interface Sci.* **1973**, *43*, 66.
17. J. Ruokolainen, J. Tanner, G. ten Brinke, O. Ikkala, M. Torkkeli and R. Serimaa, *Macromolecules* **1995**, *28*, 7779.
18. J. Ruokolainen, G. ten Brinke, O. Ikkala, M. Torkkeli and R. Serimaa, *Macromolecules* **1996,** *29*, 3409.
19. D.L. Allara and R.G. Nuzzo, *Langmuir* 1986, *1*, 52.
20. J.F. Rabolt, F.C. Burns, N.E. Schlotter and J.D. Swalen, *J. Electron. Spectrosc.* **1983,** *30*, 29.
21. D.L. Allara and J.D. Swalen, *J. Phys. Chem.* **1992**, *86*, 2700.
22. C. Naselli, J.F. Rabolt and J.D. Swalen, *J. Chem. Phys.* **1985**, *82*, 2136.
23. C. Bubeck, *Thin Solid Films* **1988**, *160*, 1.
24. H.D. Göbel, *Thesis*, Technische Universität München **1989**.
25. A. Saito, Y. Urai and K. Itoh, *Langmuir* **1996**, *12*, 3938.

Chapter 6

Morphological changes of monolayers of two polymerisable pyridine amphiphiles upon complexation with Cu(II) ions at the air-water interface

Summary

In this Chapter the monolayer behaviour of two amphiphilic, diacetylenic units containing, pyridine ligands at the air-water interface is studied by measuring the surface pressure-area isotherms and by Brewster angle microscopy (BAM). On a pure water subphase, Brewster angle microscopy of the monolayer of the ester containing ligand, shows the formation of spiral dendritic crystalline domains at the plateau in the isotherm near the solid state region. The formation of spiral crystalline domains indicates that the LC phase is L_1'. The amide containing ligand however, forms two-dimensional crystalline domains directly after spreading at the air-water interface, which are pushed together upon compression. No chiral domains are observed for this amphiphile indicating that the ester and amide amphiphile have a different LC phase. Both amphiphiles spread uniformly when the subphase contains $CuCl_2$ and upon compression crystalline domains are formed which grow when the area per molecule is reduced further, till a condensed monolayer film is formed. The shape of the crystalline domains on a Cu(II) ion containing subphase changes by replacing the Cl^- counter ion by a ClO_4^- anion. The size of the crystalline nuclei decreases when the Cu(II) concentration increases.

Introduction

In Chapter 3, the monolayer characteristics of 4-(10,12-pentacosadiynamido-methyl)pyridine at the air-water interface upon complexation with Cu(II) have been investigated by measuring the surface pressure-area isotherms [1]. It has been shown that the extent of complexation could be tuned by the proper choice of metal ion concentration, complexation time, temperature, ionic strength of the subphase and the type of counter ion. In Chapter 5, more or less the same complexation behaviour was found for the amphiphile 4-(10,12-pentacosadiynoatomethyl)pyridine (an ester) [2]. XPS measurements confirmed the presence of Cu(II) ions in the multilayers of this ester.

Brewster angle microscopy (BAM) allows direct visualisation of changes in the morphology of the monolayers during compression at the air-water interface [3-9]. Unlike fluorescence microscopy no additional probe has to be introduced in the monolayer which may cause artifacts [10,11]. The domains of the condensed (C) phase surrounded by the liquid-expanded (LE) or gas (G) phase, have been observed by Brewster angle microscopy with a great variety of sizes and shapes [12] like, circular, spiral and dendritic structures. These shapes depend on a variety of parameters, like: type of amphiphilic molecule, temperature, modification of the water subphase, impurity content, spreading technique and compression rate.

In this Chapter a morphological study on the monolayer behaviour of two polymerisable amphiphilic ligands (Scheme 6.1) is presented: 4-(10,12-pentacosa-diynamidomethyl)pyridine (A) and 4-(10,12-pentacosadiynoatomethyl)pyridine (B).

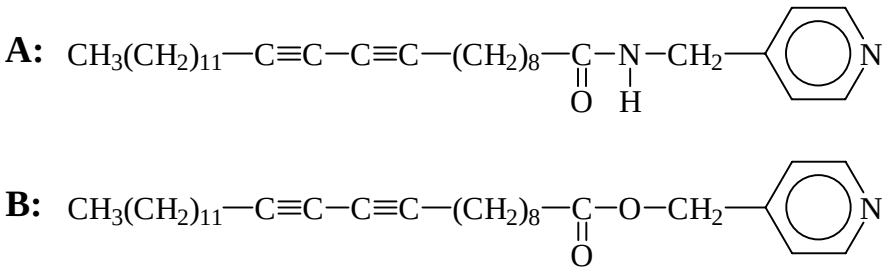

Scheme 6.1

It is known from the literature that amphiphilic amides form much more stable monolayers than ester compounds [13] due to additional stabilisation by hydrogen bonding. In this Chapter the effect of hydrogen bonding upon the morphology of the monolayer and the influence of Cu(II) ions added to the subphase has been studied. To investigate the influence

of the Cu(II) ions dissolved in the subphase on the monolayer characteristics and morphology of amphiphile A, isotherms and BAM images were recorded at a subphase temperature of 19.8 ^{o}C. At lower subphase temperature no phase transition from the LE to LC phase could be observed. Therefore, at lower subphase temperatures the crystallisation process of the formed Cu(II) ion complex of amphiphile A could not be studied. At a subphase temperature of 19.8 ^{o}C amphiphile B forms a totally expanded monolayer film. At a subphase temperature of 9.4 ^{o}C a clear phase transition from the LE to LC phase could be observed. For this reason all the experiments of amphiphile B were carried out at a subphase temperature of 9.4 ^{o}C.

It appeared that on a Cu(II) ions containing subphase the crystalline domains have a different shape than on a pure water subphase. Upon complexation with the Cu(II) ions, amphiphile A spreads homogenously at the air-water interface, while on a subphase without Cu(II) ions, crystalline domains were formed, which moved towards each other upon compression. At high Cu(II) concentration more, but smaller, crystalline domains were formed at the liquid-expanded (LE) to liquid-condensed (LC) phase transition. Also the type of counter ion had a great influence on the shape of the crystalline domains.

Experimental

The synthesis and characterisation of both amphiphiles have been described in Chapter 3 and 5 [2,14]. $Cu(ClO_4)_2$ (Acros, 98%) and $CuCl_2$ (Merck, 99%) were used as received.

The monolayer properties were studied by measuring surface pressure-area isotherms on a computer controlled Lauda-Filmbalance (FW 2) with water, purified by a Milli-Q filtration system, as the subphase. A Langmuir through (custom made by Riegler & Kirstein (GmbH), Ultrathin Organic Film Technology) equipped with a Brewster Angle Microscope was used to study the morphology of the monolayers. The light source of the BAM was a small diode laser (LaserMax MDL-200-680-35, 34 mm long, 11 mm diameter) which emitted 35 mW at 680 nm. The BAM setup has been described elsewhere in more detail [15].

The amphiphiles were dissolved in chloroform (Merck, spectroscopic quality), with a concentration of 0.1 wt% and the isotherms were recorded at a barrier speed of 10 $Å^2 \cdot molecule^{-1} \cdot minute^{-1}$.

For all complexation experiments a complexation time of 1 minute was used.

Results and discussion

Isotherms

The surface pressure-area isotherms of the two amphiphiles at 9.4 ^{o}C are shown in Figure 6.1. It can be seen that the amide (compound A) forms a condensed monolayer at the air-water interface with a limiting area of approximately 29 Å^{2}·molecule^{-1} and a collapse pressure of approximately 60 mN·m^{-1}, whereas the ester (compound B) shows a phase transition from the LE to the LC phase. The ester has a limiting area of approximately 30 Å^{2}·molecule^{-1} and a collapse pressure of about 45 mN·m^{-1}, so the monolayer of the ester is less stable than the monolayer of the amide, probably because in the amide monolayer hydrogen bonds are formed between the molecules (Figure 6.2) which stabilise the monolayer [13,16,17] additionally.

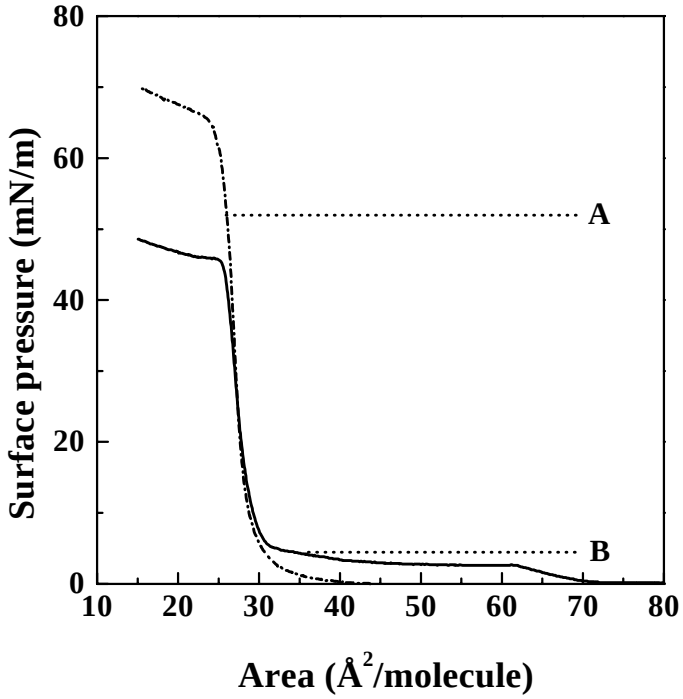

Figure 6.1: *Surface pressure-area isotherms of the amide (**A**) and the ester (**B**) amphiphiles on an aqueous subphase at 9.4 ^{o}C.*

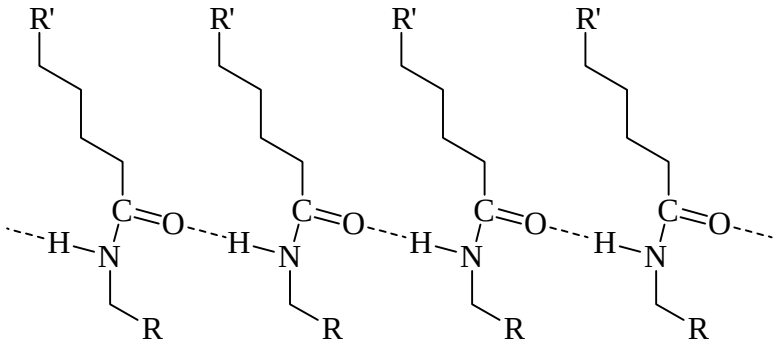

Figure 6.2: *Schematic representation of the hydrogen bonds between the amide amphiphiles in a monolayer.*

4-(10,12-pentacosadiynamidomethyl)pyridine

Figure 6.3 shows surface pressure-area isotherms of the amphiphile at a temperature of 19.8 ^{o}C on a subphase with (5 and 10 mM) and without $Cu(ClO_4)_2$. On a subphase with $Cu(ClO_4)_2$, a phase transition from LE to LC state can be observed, indicating that complexation takes place, because upon complexation charged molecules are formed which start to repel each other [17].

With increasing $Cu(ClO_4)_2$ concentration, Π_c increases from about 7 to about 13 $mN \cdot m^{-1}$, indicating that the monolayer becomes more charged at higher Cu(II) concentrations, because more Cu(II) ions bind to the pyridine group of the amphiphiles [14] as has been shown in Chapter 4.

The isotherms were recorded simultaneously with BAM imaging. These images are shown in Figure 6.4. The pictures correspond to the points indicated in Figure 6.3. When the subphase does not contain Cu(II) ions, no homogeneous monolayer is formed (6.4a), but the molecules formed crystalline domains. Upon compression, the domains are pushed towards each other and the surface pressure starts to rise. At point 6.4b a homogeneous condensed monolayer is formed and when the area per molecule has decreased further the monolayer starts to collapse.

The amphiphile spreads homogeneously when the subphase contains 5 mM $Cu(ClO_4)_2$. No crystalline domains are formed but the gas and liquid-expanded phase coexist (6.4c). Upon compression a LE monolayer is formed. The surface pressure rises gradually till point 6.4d is reached, where crystalline nuclei appear and the surface pressure decreases again. The whole

air-water interface was covered with nuclei, so the dip in the isotherm corresponds to a nucleation and crystallisation process in the monolayer. The formed crystalline nuclei have a dendritic structure. Dendritic structures are metastable structures formed by a diffusion-limited growth of the crystalline phase as is shown by various research groups by means of fluorescence microscopy or BAM [12,15,18-20]. The number of nuclei increases as the area per molecule is decreased (6.4e) and the surface pressure starts to rise. At high surface pressures (about 50 $mN \cdot m^{-1}$) a pure condensed film is formed (6.4f). When the $Cu(ClO_4)_2$ concentration has increased up to 10 mM, more crystalline nuclei are formed at the dip in the isotherm (image 6.4g), but the nuclei are smaller in size as compared to the nuclei formed on a 5 mM $Cu(ClO_4)_2$ subphase. At higher Cu(II) ion concentrations in the subphase Π_c increases (Fig. 6.3). This increase in Π_c causes a decrease in nucleation energy as is shown by Helm et al. [21,22]. They found that Π_c increased for different phospholipids when the subphase temperature increased or when the NaCl concentrations of the subphase increased. At higher subphase temperatures or higher NaCl concentrations of the subphase, fluorescence microscopy showed that more and smaller crystalline domains were formed due to the decreased nucleation energy at higher values of Π_c.

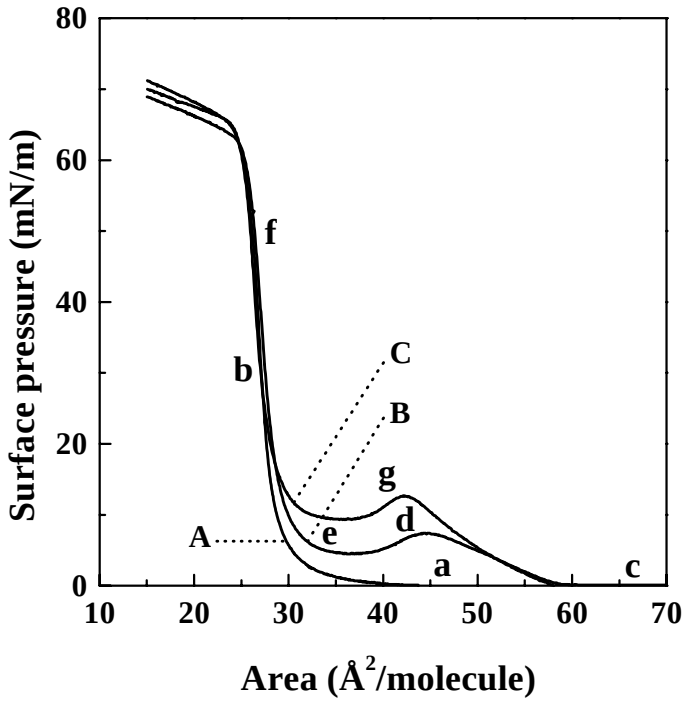

Figure 6.3: *Surface pressure-area isotherms of the amide amphiphile at 19.8 ^oC on an aqueous subphase (**A**), a 5mM (**B**) and a 10mM $Cu(ClO_4)_2$ subphase (**C**).*

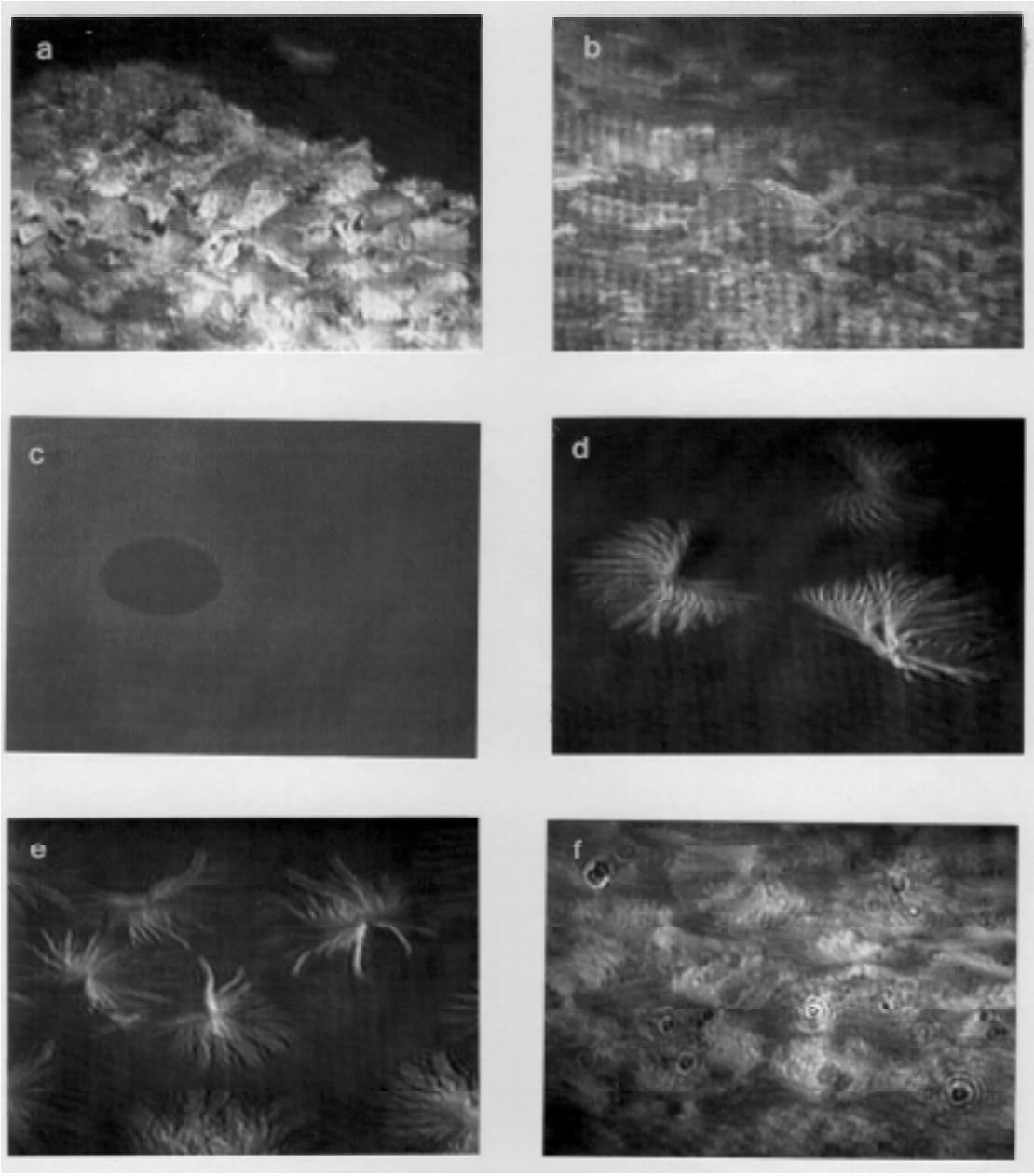

Figure 6.4: *BAM images of the amide monolayer at 19.8 ^{o}C corresponding to the points of the Π-A isotherms for the amide compound (Fig. 6.3). Image size: 350 × 480 μm^2.*

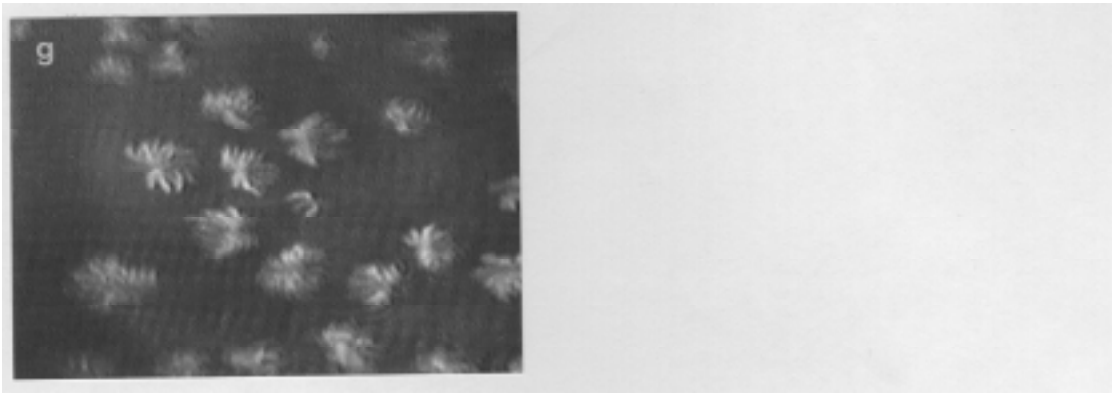

Figure 6.4, continued: *BAM images of the amide monolayer at 19.8 ^{o}C corresponding to the points of the Π-A isotherms for the amide compound (Fig. 6.3). Image size: 350 × 480 μm^2.*

Figure 6.5 shows the surface pressure-area isotherms of the amide amphiphile at a temperature of 19.8 ^{o}C on a subphase containing 5 and 10 mM $CuCl_2$. Both isotherms exhibit a LE to LC phase transition suggesting complexation has taken place. At higher copper concentrations the surface pressure at which the phase transition LE to LC phase (Π_c) appears, increases again, indicating that more copper ions bind to the monolayer film [14]. The BAM images of Figure 6.6 represent the points indicated in Figure 6.5. At large areas (more than 63 $Å^2 \cdot molecule^{-1}$) the monolayer appears to be homogeneous. The reflectivity of the monolayer changes when Π_c, is reached (6.6a). Crystalline nuclei are also formed here and upon further compression of the monolayer the nuclei grow (6.6b). In this case we see crystallisation of the amphiphiles in dendritic structures which may originate from a diffusion-limited growth mechanism. The nuclei differ in shape from the nuclei formed on a $Cu(ClO_4)_2$ subphase. At a surface pressure of 30 $mN \cdot m^{-1}$ a homogeneous condensed monolayer has been formed without any pinhole (6.6c). At surface pressures of about 60 $mN \cdot m^{-1}$, the monolayer starts to collapse (6.6d). At higher copper concentrations (10 mM), much more nuclei are formed at the phase transition (6.6e) with more arms but smaller in size as in the case of a $Cu(ClO_4)_2$ subphase. Moreover, these nuclei grow upon decreasing the area per molecule till a complete condensed film is formed.

So, by using ClO_4^- as a counter ion instead of Cl^- more complexation takes place in the monolayer as indicated by the higher Π_c at the same Cu(II) ion concentration [1] (Figure 6.3 and 6.5). Furthermore, the shape of the crystalline domains changes when ClO_4^- is used as an anion instead of Cl^-.

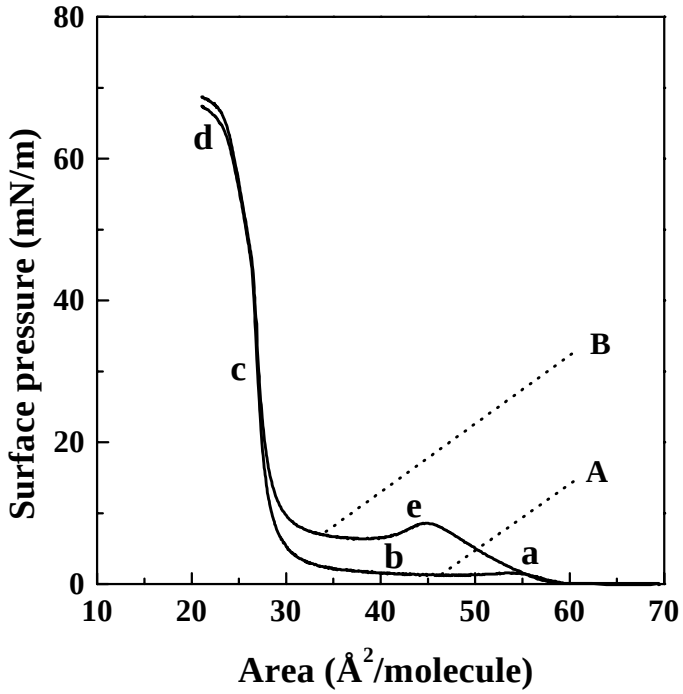

Figure 6.5: *Surface pressure-area isotherms of the amide amphiphile at 19.8 ^{o}C on a subphase with 5 mM (**A**) and 10 mM $CuCl_2$ (**B**).*

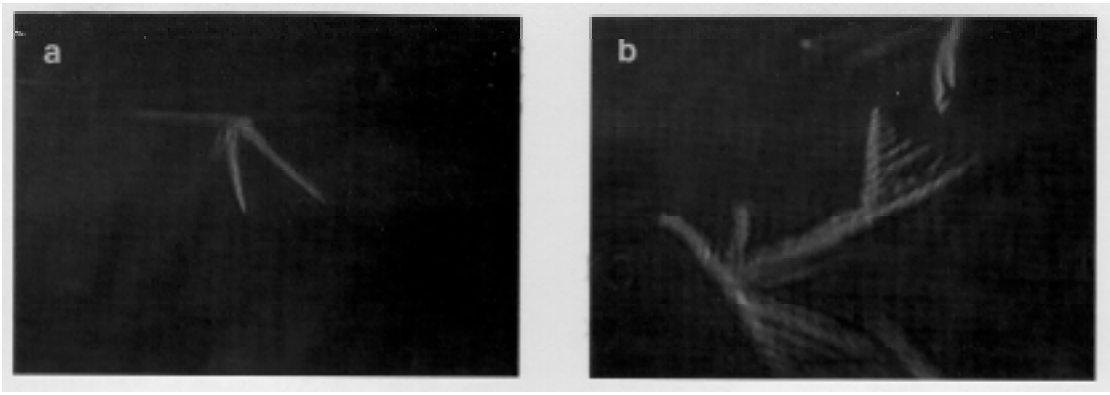

Figure 6.6: *BAM images of the amide monolayer at 19.8 ^{o}C corresponding to the points of the Π-A isotherms for the amide compound (Fig. 6.5). Image size: 350 × 480 μm^2.*

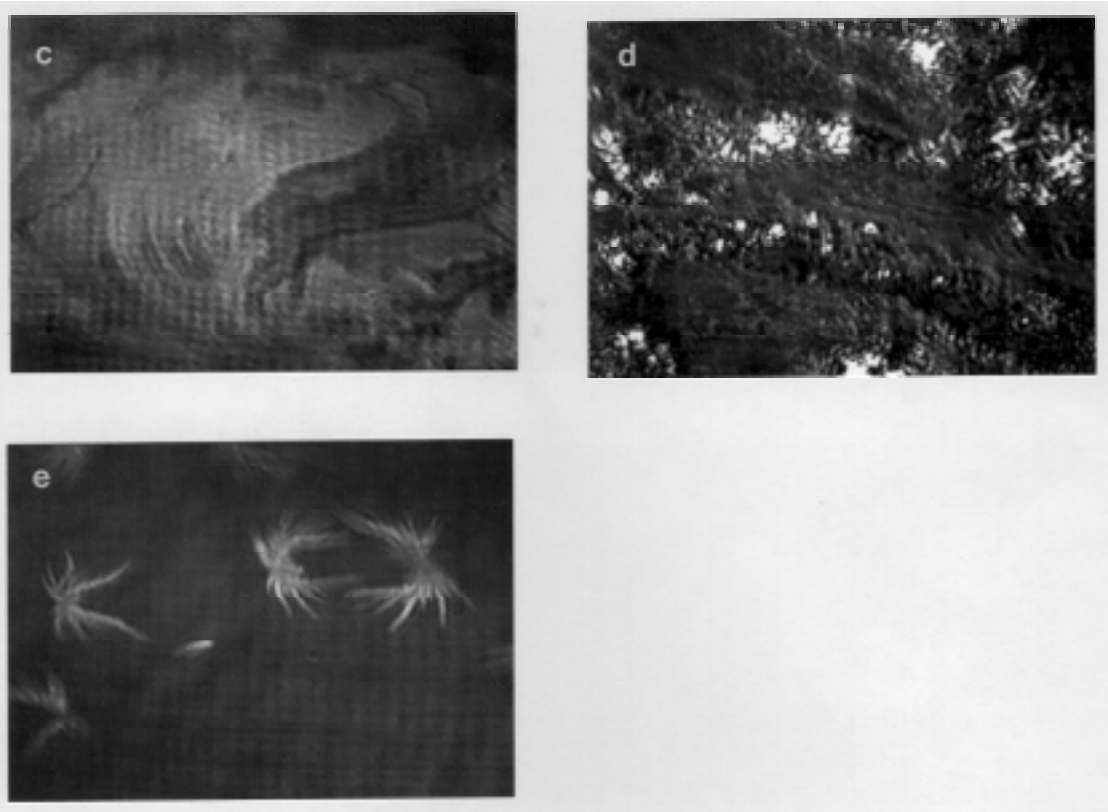

Figure 6.6, continued: *BAM images of the amide monolayer at 19.8 ^{o}C corresponding to the points of the Π-A isotherms for the amide compound (Fig. 6.5). Image size: 350 × 480 μm^2.*

4-(10,12-pentacosadiynoatemethyl)pyridine

As can be seen from Figure 6.7, the collapse pressure of the monolayer film of the ester increases drastically (from 45 to about 70 $mN \cdot m^{-1}$) on a $Cu(ClO_4)_2$ containing subphase in contrast to the amide where only a slight increase in collapse pressure can be observed. Moreover, the Π_c of the ester increases from 3 to 12 $mN \cdot m^{-1}$ upon complexation with Cu(II) ions, forming a much more stable monolayer film. When the subphase contains $CuCl_2$, an increase in collapse pressure (from 45 to about 58 $mN \cdot m^{-1}$) compared to the pure aqueous subphase, is also observed, but this value is lower than the collapse pressure on a $Cu(ClO_4)_2$ containing subphase. Also the Π_c increases compared to the pure aqueous subphase, but again the value is lower than the Π_c of the monolayer on a $Cu(ClO_4)_2$ subphase, indicating that on a $Cu(ClO_4)_2$ subphase more Cu(II) ions bind to the pyridine group of amphiphile B at the air-water interface at the same Cu(II) ion concentration.

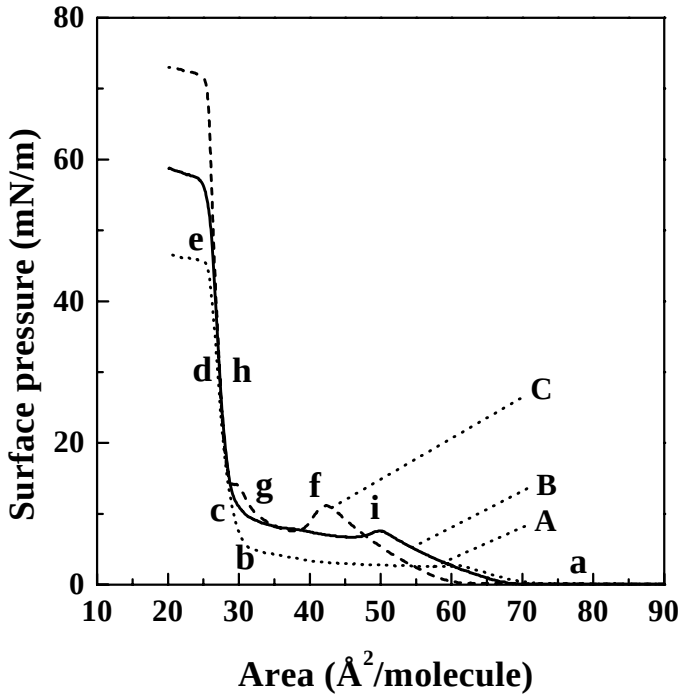

Figure 6.7: *Surface pressure-area isotherms of the ester amphiphile at 9.4 ^oC on an aqueous subphase (**A**), a 5 mM $CuCl_2$ (**B**) and a 5 mM $Cu(ClO_4)_2$ (**C**) subphase.*

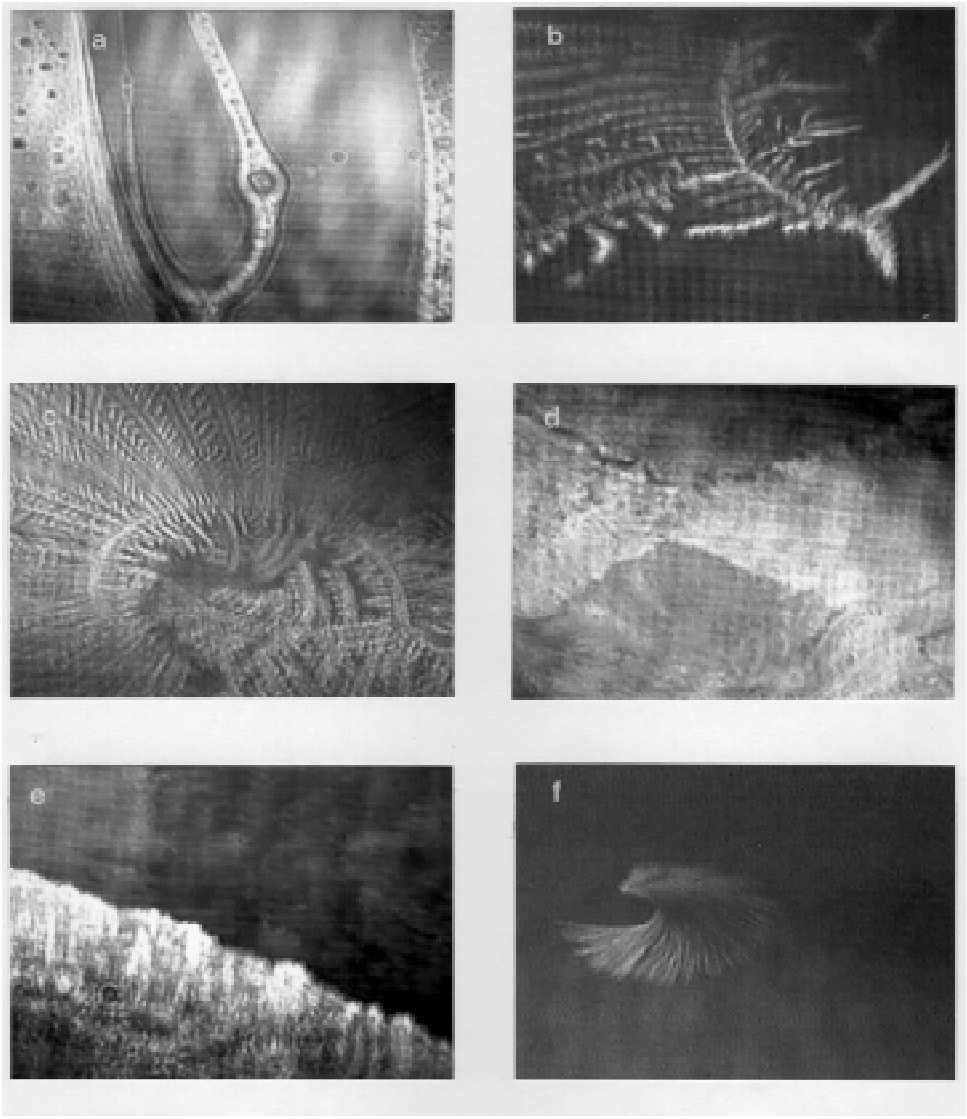

Figure 6.8: *BAM images of the ester monolayer at 9.4 ^{o}C corresponding to the points of the Π-A isotherm of the ester compound (Fig. 6.7). Image size: 350 × 480 μm^2.*

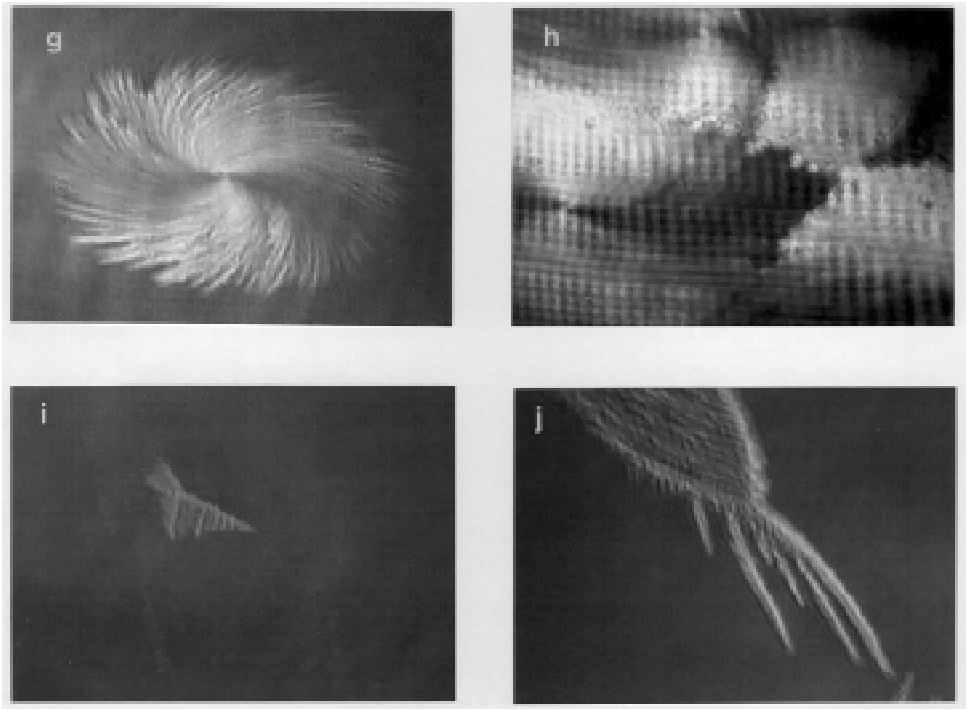

Figure 6.8, continued: *BAM images of the ester monolayer at 9.4 ^{o}C corresponding to the points of the Π-A isotherm of the ester compound (Fig. 6.7). Image size: 350 × 480 μm^2.*

Figure 6.8 shows BAM images of the ester compound upon compression on a water subphase at 9.4 ^{o}C. The images correspond to the points in Figure 6.7. At low surface pressure the LE and G phases coexist (6.8a). When the monolayer is compressed a homogeneous LE phase is formed. At Π_c no nuclei can be seen, probably because the dimensions of the crystallites of the newly formed condensed phase do not exceed the lateral resolution of the BAM (about 5 μm). At the beginning of the solid state region of the isotherm however, suddenly big dendritic crystals are formed (> 200 μm) (6.8b). Again these dendritic structures suggest a diffusion-limited growth mechanism as in the case of amphiphile A. Upon further compression these nuclei grow very fast in a circular way (6.8c). The spiral growth of the crystalline domains is somewhat surprising because it suggests that these domains are chiral although amphiphile B is achiral. This behaviour was also observed by other research groups [23-26] for achiral fatty acids and their esters. The spiral effects can only be accounted for when it is assumed that the liquid-condensed phase is the so-called L_1' phase. This phase is a tilted mesophase in which the molecules have a tilt azimuth in a direction intermediate between the nearest neighbour and the next-nearest neighbour [25,26]. The L_1' phase has a

broken reflection symmetry [23] which causes the spiral structures observed by fluorescence microscopy [23,24] and BAM [25,26] for achiral compounds.

At high pressures, about 30 $mN \cdot m^{-1}$, a homogeneous condensed phase (6.8d) is reached. At 45 $mN \cdot m^{-1}$ the monolayer starts to collapse and the monolayers start to shift over each other, which can be seen nicely in image 6.8e.

When $Cu(ClO_4)_2$ is added to the subphase, again at large surface areas (> 61 $Å^2 \cdot molecule^{-1}$) the LE and G phases coexist, but at Π_c (6.8f) circular domains are formed, which grow when the surface area is decreased (6.8g). Again, the appearance of chirality identifies the LC phase as L_1' [24]. Following the growing process, we observe that the point on the edge is the nucleus of the domain. Upon further compression the domains start to deform each other and at high surface pressures (30 $mN \cdot m^{-1}$) crystalline domains with different orientations are formed (6.8h).

When the subphase contains 5mM $CuCl_2$, crystalline nuclei start to grow at Π_c (6.8i), but again these nuclei differ in shape from the nuclei formed on a $Cu(ClO_4)_2$ subphase. The nuclei formed on a $CuCl_2$ subphase have a dendritic structure. On this subphase no chiral crystalline domains are formed which indicates that the LC phase is not L_1' [24]. Thus, by changing the counter ion of the Cu(II) ions the LC phase changes. Upon further compression these nuclei grow (6.8j) and at high surface pressures a homogeneous LC phase was formed again.

Therefore, both the presence of Cu(II) ions and the type of counter ion used, have an enormous influence on the nucleation and crystallisation process and consequently on the shape of the crystalline domains formed during compression of the monolayer.

Conclusions

The features of the isotherms of both amphiphiles correspond to a two-dimensional nucleation and crystallisation process.

The morphology of the monolayer can be studied nicely by means of BAM. It shows that upon complexation the amide amphiphile is spread homogeneously at the air-water interface, but when the subphase does not contain Cu(II) ions crystalline domains are formed and a homogeneous condensed film is obtained upon compression. Moreover, it can be seen that for both amphiphiles crystalline nuclei start to appear at Π_c, which grow upon further compression. The shape of these crystalline nuclei depend strongly on the counter ion, whereas the size of these nuclei can be varied by changing the Cu(II) ion concentration of the subphase. Furthermore, it is shown that amphiphile B forms chiral crystalline domains on an

aqueous subphase and on a 5 mM $Cu(ClO_4)_2$ subphase which identifies the LC phase as L_1'. By changing the counter ion from ClO_4^- to Cl^-, the LC phase changes from a phase with a broken reflection symmetry to a phase with a reflection symmetry and no chiral crystalline domains can be observed anymore. Moreover, also the crystalline domains of amphiphile A have no chirality on an aqueous subphase as well as on a Cu(II) ion containing subphase. This indicates that the 2 amphiphiles have at least different LC phases on an aqueous and $Cu(ClO_4)_2$ containing subphase.

References

1. P.J. Werkman and A.J. Schouten, *Thin Solid Films* **1996**, *284-285*, 24.
2. P.J. Werkman, H. Wilms, R.H. Wieringa and A.J. Schouten, submitted for publication in Thin Solid Films.
3. D. Hönig and D. Möbius, *J. Phys. Chem.* **1991**, *95*, 4590.
4. S. Hénon and J. Meunier, *Rev. Sci. Instrum.* **1991**, *62*, 936.
5. D. Hönig and D. Möbius, *Thin Solid Films* **1992,** *210-211*, 64.
6. S. Rivière, S. Hénon, J. Meunier, D.K. Schwartz, M.-W. Tsao and C.M. Knobler, *J. Chem. Phys.* **1992**, *101*, 10045.
7. R.C. Ahuja, P-.L. Caruso and D. Möbius, *Thin Solid Films* **1994**, *242*, 195.
8. S. Hénon and J. Meunier, *Thin Solid Films* **1993**, *243*, 471.
9. V. Melzer and D. Vollhardt, *Phys. Rev. Lett.* **1996**, *76*, 3770.
10. M. Lösche, E. Sackmann and H. Möhwald, *Ber. Bunsen. Ges. Phys. Chem.* **1983**, *87*, 848.
11. N. Sommerdijk, *Ph. D Thesis*, University of Nijmegen, Nijmegen, The Netherlands **1995**.
12. U. Gehlert and D. Vollhardt, *Langmuir* **1997**, *13*, 277.
13. G. Roberts (Ed.), *Langmuir-Blodgett films*, Plenum Press, New York and London **1990**.
14. P.J. Werkman, R.H. Wieringa, E. J. Vorenkamp and A.J. Schouten, submitted for publication in Langmuir.
15. M.A. Cohen Stuart, R.A.J. Wegh, J.M. Kroon and E.J.R. Sudhölter, *Langmuir* **1996**, *12*, 2863.
16. R. Popovitz-Biro, K. Hill, E. Shavit, D.J. Hung, M. Lahav, L. Leiserowitz, J. Sagiv, H. Hsiung, G.R. Meredith and H. Vanherzeele, *J. Am. Chem. Soc.* **1990**, *112*, 2498.
17. R. Popovitz-Biro, D.J. Hung, E. Shavit, M. Lahav and L. Leiserowitz, *Thin Solid Films* **1989**, *178*, 203.
18. K.A. Suresh, J. Nittmann and F. Rondelez, *Europhys. Lett.* **1988**, *6*, 437.
19. S. Akamatsu, O. Bouloussa, K. To and F. Rondelez, *Phys. Rev. A* **1992**, *46*, 4504.

20. G. Weidemann and D. Vollhardt, *Thin Solid Films* **1995**, *264*, 94.
21. C.A. Helm, L. Laxhuber, M. Lösche and H. Möhwald, *Colloid & Polymer Sci.* **1986**, *264*, 55.
22. C.A. Helm and H. Möhwald, *J. Phys. Chem.* **1988**, *92*, 1262.
23. X. Qiu, J. Ruiz-Garcia, K.J. Stine and C.M. Knobler, *Phys. Rev. Lett.* **1991**, *67*, 703.
24. X. Qiu, J. Ruiz-Garcia and C.M. Knobler, *Prog. Colloid & Polymer Sci.* **1992**, *89*, 197.
25. T.M. Fisher, R.F. Bruinsma and C.M. Knobler, *Phys. Rev. E* **1994**, *50*, 413.
26. S. Rivière, S. Hénon and J. Meunier, *Phys. Rev. E* **1994**, *49*, 1375.

Chapter 7

An investigation on the formation of mono- and multilayers of metal complexes of N-(10,12-pentacosadiynamidopropyl)imidazole at the air-water interface

Abstract

The monolayer characteristics of N-(10,12-pentacosadiynamidopropyl)-imidazole have been studied at the air-water interface by measuring surface pressure-area isotherms. The amphiphile forms stable monolayers with a well-defined liquid-expanded (LE) to liquid-condensed (LC) phase transition. The liquid-expanded (LE) phase of this monolayer film is thermodynamically not stable. As can be seen by changes in the isotherms metal complexes at the air-water interface are formed even when the subphase has a metal ion concentration as low as $5 \cdot 10^{-7}$ M. The extent of complexation can easily be tuned by variation of metal ion concentration, the counter ion, the temperature and ionic strength of the subphase. Transmission electron microscopy (TEM) revealed that the monomer monolayer has a smooth appearance while upon UV irradiation at the air-water interface, the red form of the polymer is formed, which has a striated structure.

Multilayers with a regular layer structure can be built up when the subphase contained $CuCl_2$, with a Z-type transfer. These multilayers, however, have a Y-type structure as was shown by small angle X-ray reflection (SAXR) measurements, therefore the molecules have "turned over" to form a Y-type structure. XPS measurements confirmed the presence of Cu(II) ions in these multilayers, giving a direct proof of the formation of metal complexes at the air-

water interface. The structure of the multilayers was examined more closely by FT-IR measurements. The multilayers can easily be polymerised by exposure to UV light. SAXR and FT-IR measurements revealed that the layer structure is preserved during the polymerisation process, although the alkyl side chains loose their all-trans conformation.

Introduction

In the Chapters 3, 5 and 6 [1-3] the monolayer behaviour of 2, diacetylene group containing amphiphilic ligands, with a pyridine group as ligand, linked with an amide or ester bond to the aliphatic tail, has already been studied. The amide formed the most stable monolayers, due to hydrogen bonding between the amide bonds of the molecules. Both amphiphiles formed metal complexes at the air-water interface and multilayers of these metal complexes could also be built up. XPS measurements confirmed the presence of metal ions in these multilayer films. The multilayers preserved their regular layer structure upon irradiation with UV light.

Furthermore, van Esch et al. [4] studied the monolayer behaviour of imidazole group containing amphiphiles upon coordination with metal ions at the air-water interface by measuring surface pressure-area isotherms and by means of fluorescence microscopy. They found that metal complexes were most easily formed with Cu(II) ions, already at concentrations as low as 10^{-6} M $CuCl_2$ complexation took place at the air-water interface.

In this Chapter, the complexation behaviour of N-(10,12-pentacosadiyn-amidopropyl)imidazole (Scheme 7.1) at the air-water interface, with various metal ions dissolved in the subphase, is studied by measuring the surface pressure-area isotherms.

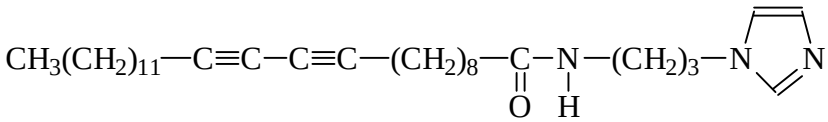

Scheme 7.1

An imidazole headgroup was used as a ligand because imidazole has a much greater equilibrium constant for the formation of metal complexes than pyridine, mainly due to the larger basicity of the imidazole ligand [5]. The imidazole headgroup is linked to the aliphatic

tail via an amide bond, and therefore hydrogen bonds can be formed between the molecules which increases the monolayer stability. The aliphatic tail contains a diacetylene functionality, so the mono- and multilayers can be polymerised [6-8]. The amphiphiles indeed forms metal complexes at the air-water interface and the extent of complexation can easily be controlled by the proper choice of the complexation conditions. Regular multilayers can be built up when the subphase contained $CuCl_2$. The structure of the multilayers is studied by means of SAXR and FT-IR measurements. XPS measurements gave direct proof for the incorporation of Cu(II) ions into the multilayers. The monolayers at the air-water interface and the multilayer films can easily be polymerised by means of UV irradiation, which results in the formation of the red form of the polymer.

Experimental

Materials

10,12-pentacosadiynoic acid (Hüls-Petrarch, 99%) was reacted with thionyl chloride (Merck, > 99%) to obtain the corresponding acid chloride. The amide derivative, N-(10,12-pentacosadiynamidopropyl)imidazole, was obtained in good yields (about 60%) by reaction of 1-(3-aminopropyl)imidazole (Acros, 98%) with the acid chloride in dry benzene (Merck p.a.) under nitrogen atmosphere. Triethylamine (Merck, > 99%), distilled under nitrogen atmosphere from CaH_2 (Acros), was added as a HCl scavenger. The crude product was purified by a twofold crystallisation from n-hexane (Merck p.a.).
Elemental analysis: Calc. for $C_{31}H_{51}N_3O$: C 77.29; H 10.67; N 8.72. Found: C 76.98; H 10.55; N 8.78.
IR: ν (cm^{-1}) 3300 (ν NH), 2920 (ν_a CH_2), 2850 (ν_s CH_2), 1640 (Amide I), 1548 (Amide II), 1508 (ν C=N, imidazole ring), 1466 (δ CH_2).
^{1}H NMR (200 MHz): δ 0.87 (t, 3H), 1.26-1.55 (m, 32H), 2.00 (m, 2H), 2.11-2.27 (m, 6H), 3.27 (m, 2H), 4.00 (t, 2H), 5.58 (s, 1H) 6.96 (s, 1H), 7.07 (s, 1H), 7.50 (s, 1H).
T_m = 54.9 ^{o}C, T_c = 35.4 ^{o}C.

All metal salts (BHD Chemicals, Ltd., Merck, Acros and Fluka) were used as received.

The general procedures have been outlined in the experimental sections of the Chapters 2 and 4.

Electron microscopy

Samples for transmission electron microscopy (TEM) were prepared by a horizontal lifting method of a monolayer, stabilised at a constant surface pressure of 30 $mN \cdot m^{-1}$, onto a carbon-coated copper grid, which was made hydrophilic by glow discharge in air under reduced pressure. The samples were Pt shadowed at an angle of 20^{o}. The samples used for electron diffraction (ED) were not Pt shadowed. TEM micrographs and ED patterns were recorded with a Philips EM300 instrument using an acceleration voltage of 80 kV and for the TEM micrographs a magnification of 10000× was used.

Results and discussion

Monolayer behaviour

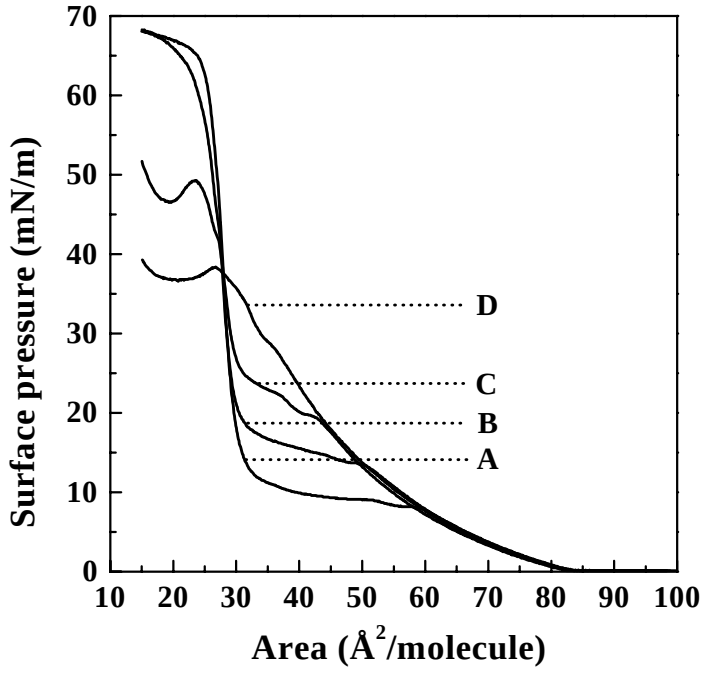

Figure 7.1A: *Surface pressure-area isotherms of the amphiphile on an aqueous subphase at 4.8 ^{o}C (A), 9.3 ^{o}C (B), 13.8 ^{o}C (C) and 18.3 ^{o}C (D).*

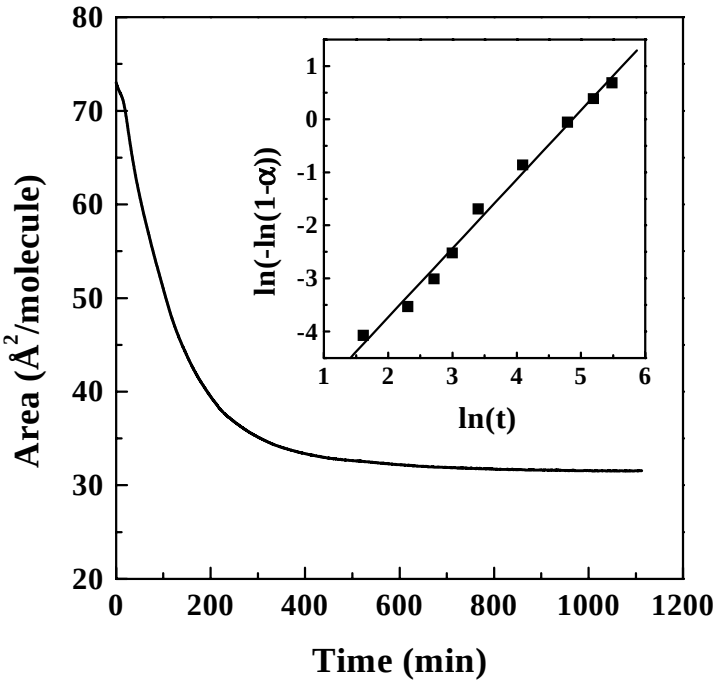

Figure 7.1B: *Isobaric stabilisation curve of the amphiphile on an aqueous subphase at 4.8 °C and a surface pressure of 3 mN·m^{-1}. In the inset the result of the Avrami analysis of the isobaric stabilisation experiment is shown.*

By measuring the surface pressure-area isotherms, the monolayer characteristics of the imidazole amphiphile, at the air-water interface were studied at different temperatures (Fig. 7.1A) and pH (Fig.7.2) values of the subphase.

The amphiphile already has a phase transition from the liquid-expanded (LE) to the liquid-condensed (LC) state at subphase temperatures as low as 4.8 °C, with a limiting area in the condensed state of approximately 32 Å^2·molecule^{-1} (Fig. 7.1A). The liquid-expanded (LE) state is thermodynamically not stable. When the monolayer is stabilised at a surface pressure of 3 mN·m^{-1} and a subphase temperature of 4.8 °C, the area per molecule decreases from about 73 Å^2·molecule^{-1} to about 31 Å^2·molecule^{-1} as is shown in Figure 7.1B. This decrease in area per molecule is probably caused by a slow crystallisation process forming a condensed monolayer film at a surface pressure of 3 mN·m^{-1}. The crystallisation process can be studied by using the well-known Avrami analysis [9-13] of the conversion-time plots. Avrami proposed the following equation for the time dependence of the crystalline fraction during isothermal crystallisation [9-11]:

$$1-\alpha = \exp(-Kt^n) \qquad \textbf{(7.1)}$$

in which α is the fraction of crystalline material, K is a constant, t is the time and n is the so-called Avrami exponent. When isobaric and isothermal conditions are used, the Avrami equation is expected to describe the crystallisation process of the amphiphile at the air-water interface. The fraction of crystalline material can easily be calculated by calculating the area loss, referred to the beginning of the crystallisation process, divided by the area loss associated with the completed crystallisation process. The result of the Avrami analysis is shown in the inset of Figure 7.1B. From the slope of the straight line the Avrami exponent can be calculated. This Avrami exponent (n) has a value of approximately 1.3, indicating that probably two crystallisation processes take place at the same time. One in which the nucleation is simultaneous and where disc-like crystals are formed with a diffusion-controlled growth (n = 1) [12,13]. In the other process, the nucleation is sporadic, so during the whole crystallisation process new nuclei are formed. In the latter process, there are also disc-like crystals formed with a diffusion-controlled growth (n = 2) [12,13].

Upon raising the temperature of the subphase, the pressure at which the phase transition occurs (Π_c), increases while the collapse pressure decreases, indicating that a less stable, more expanded monolayer is formed. At a temperature of 18.7 ^{o}C a totally expanded monolayer is formed.

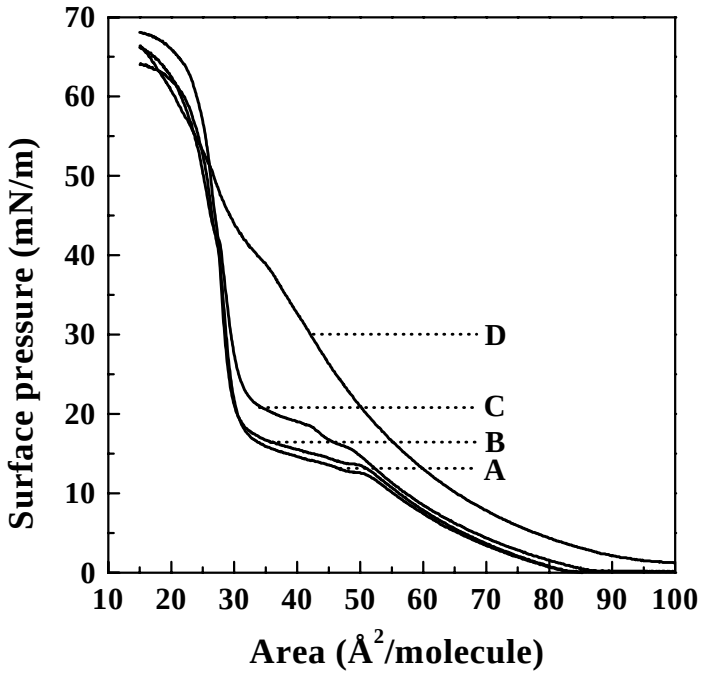

Figure 7.2: *Surface pressure-area isotherms of the amphiphile at 9.3 ^{o}C on an aqueous subphase at pH values of 9.00 (A), 5.70 (B), 4.15 (C) and 3.00 (D).*

The pH of the subphase also influences the monolayer characteristics of the amphiphile (Fig. 7.2). Increasing the pH from 5.70 (normal pH of the water used as subphase) up to 9.00 does not alter the monolayer properties but when the pH was decreased to 4.15, the monolayer became more expanded, indicating that protonation of the monolayer takes place, which is consistent with the observations of van Esch et al. [4]. Upon protonation a charged monolayer is formed leading to an enhanced repulsion between the charged amphiphiles, causing an increase in Π_c and an increase in the onset of the LE phase (A_{fl}). At even lower pH values (3.00), the monolayer becomes totally protonated forming a totally expanded monolayer film without a LE to LC phase transition. Also the A_{fl} increases upon protonation from about 83 $Å^2 \cdot molecule^{-1}$ at pH = 5.70 to about 87 $Å^2 \cdot molecule^{-1}$ at pH = 4.15 to very large values at lower pH values of the subphase.

Complexation behaviour in the monolayer

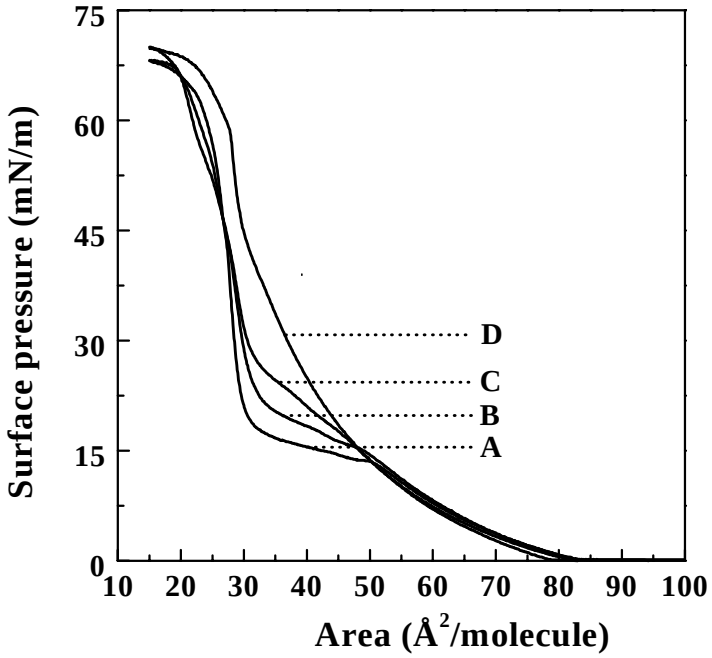

Figure 7.3: *Surface pressure-area isotherms of the amphiphile at 9.3 ^oC on a subphase without $CuCl_2$ (A) and with $CuCl_2$ at concentrations of $5 \cdot 10^{-7}$ M (B), $5 \cdot 10^{-6}$ M (C) and $5 \cdot 10^{-5}$ M (D).*

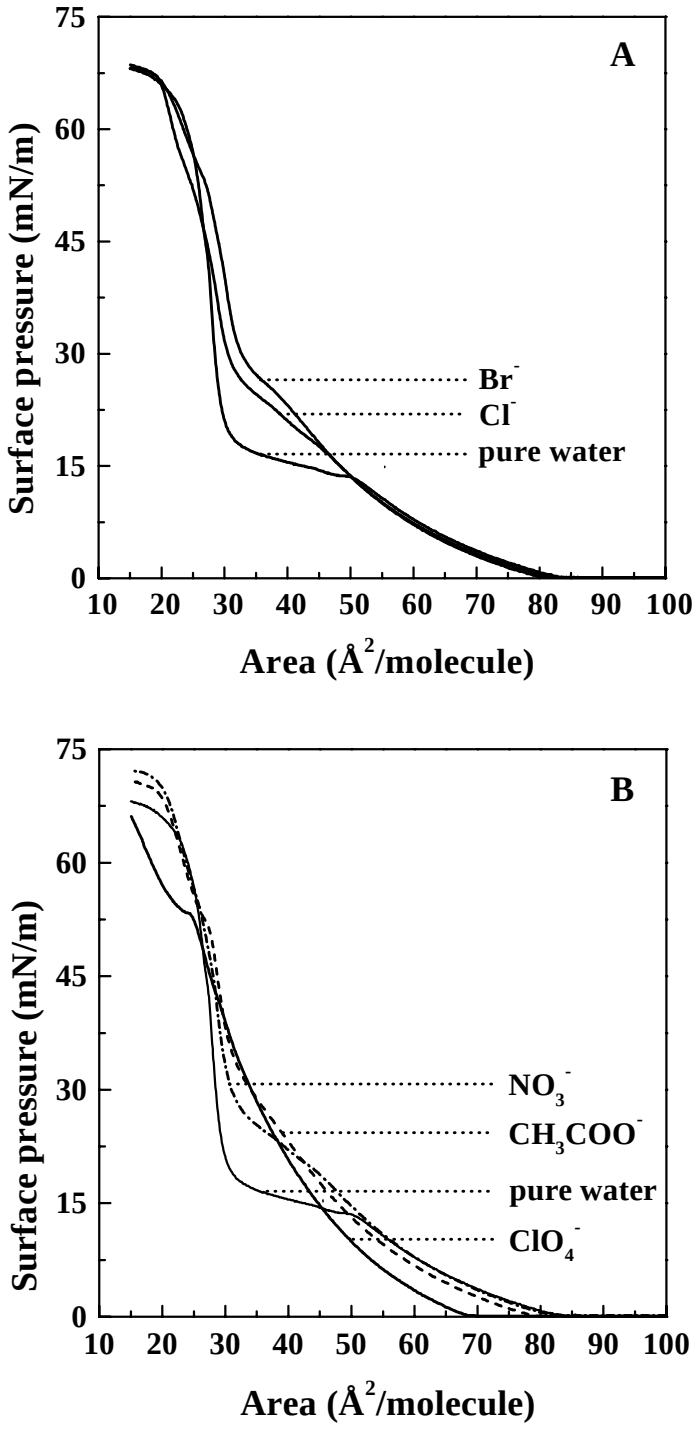

Figure 7.4A/B: *Surface pressure-area isotherms of the amphiphile at 9.3 ^{o}C on a subphase without $CuCl_2$ and on a $5 \cdot 10^{-6}$ M Cu(II) subphase with different counter ions.*

Even small amounts of $CuCl_2$, dissolved in the subphase, have an enormous effect on the isotherms of the amphiphile, as can be seen in Figure 7.3. Upon addition of Cu(II) ions to the subphase, Π_c increases, suggesting that complexation has occurred, while upon complexation charged molecules are formed which results in an increased repulsion between neighbouring molecules which may retard the crystallisation process, causing the increase in Π_c. At Cu(II) concentrations as high as $5 \cdot 10^{-5}$ M, a totally expanded monolayer is formed. Also A_{fl} is shifted from about 83 to about 78 $Å^2 \cdot molecule^{-1}$. Apparently, upon complexation a thicker monolayer film is formed in which the amphiphiles have a different orientation compared to a pure water subphase.

The effect of the counter ion on the complexation process can be seen clearly in the Figures 7.4A and B. When the Cl^- counter ion is replaced by the bigger more easily polarisable Br^- anion, an increase in Π_c can be observed (Fig. 7.4A), and the monolayer becomes more expanded. This counter ion effect was also observed for the pyridine amphiphiles and more extensively described in the Chapter 3 and 5. The increase in Π_c follows the series: $Cl^- \cong NO_3^- < CH_3COO^- \cong Br^- < ClO_4^-$.

Also other metal ions do form metal complexes with the amphiphile at the air-water interface, as can be seen in Figure 7.5. Addition of $5 \cdot 10^{-4}$ M metal chlorides to the subphase causes an increase in Π_c. The isotherm of $CuCl_2$ is not shown in Figure 7.5, because at concentrations of $5 \cdot 10^{-5}$ M $CuCl_2$, the monolayer is already totally expanded, which is not the case for the other metal chlorides. The increase in Π_c depends on the metal ion dissolved in the subphase and follows the series: Mn(II) < Ni (II) < Cd(II) ≅ Co(II) < Zn(II) < Cu(II). This is the same order of binding of the metal ions to the amphiphiles as was found by van Esch et al. [4].

The ionic strength of the suphase has an enormous influence on the monolayer characteristics, as can be seen in Figure 7.6. The ionic strength of the subphase was increased by adding KCl to the $5 \cdot 10^{-6}$ M $CuCl_2$ subphase, which causes an increase in Π_c indicating that the extent of complexation is increased at higher ionic strengths of the subphase. At higher ionic strengths of the subphase, the metal ions and amphiphiles are more shielded from each other by the electrolytes and complexation can occur more easily [15].

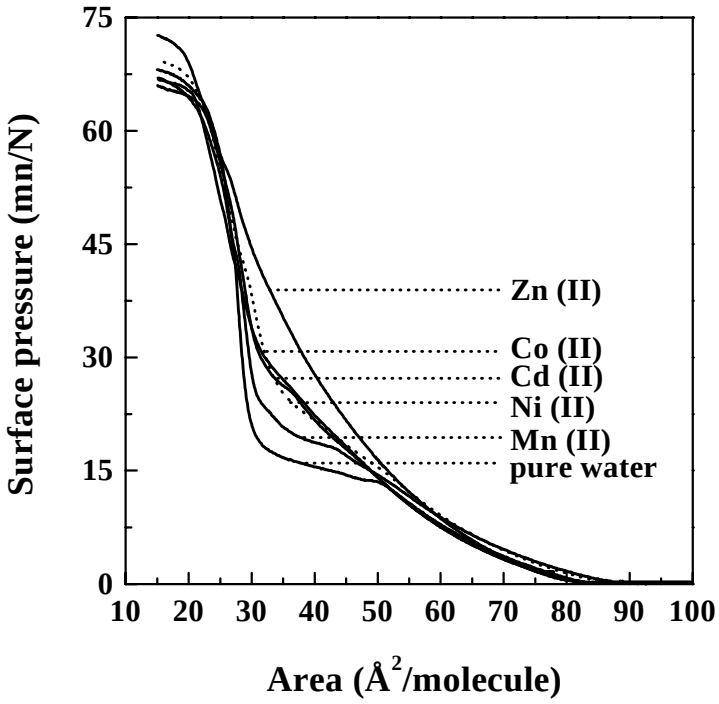

Figure 7.5: *Surface pressure-area isotherms of the amphiphile at 9.3 ^{o}C on a subphase without metal ions and on a $5 \cdot 10^{-4}$ M subphase of different metal chlorides.*

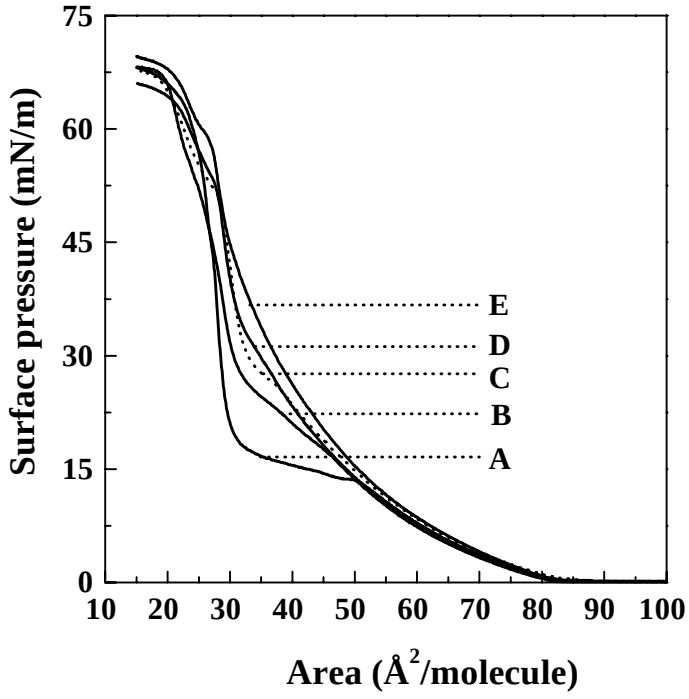

Figure 7.6: *Surface pressure-area isotherms of the amphiphile at 9.3 ^{o}C on a subphase without $CuCl_2$ (A) and on a $5 \cdot 10^{-6}$ M $CuCl_2$ subphase with different ionic strengths: $1.5 \cdot 10^{-5}$ (B), $3.0 \cdot 10^{-5}$ (C), $6 \cdot 10^{-5}$ (D) and $1.5 \cdot 10^{-4}$ (E).*

Morphology of the monolayers

The monolayers could be stabilised at the air-water interface in the condensed phase at surface pressures up to 40 $mN \cdot m^{-1}$ on a subphase containing water without Cu(II) ions at a temperature of about 5 ^{o}C, forming a stable monolayer within 60 minutes with an area of about 28.0 $Å^2 \cdot molecule^{-1}$. These monolayers could easily be polymerised at the air-water interface after 40 minutes of a constant flow of argon, by means of a small UV lamp (254 nm, 1.6 W) for 2 minutes, resulting in a small contraction of the monolayer (about 8 %). The polymerised monolayer of the amphiphiles appeared as the red form of the polymer, as could be seen by the naked eye. In Figure 7.7 the TEM micrographs of the monomer (7.7A) and polymerised (7.7B) monolayer can be seen, which were picked up at a surface pressure of 30 $mN \cdot m^{-1}$ on an aqueous subphase.

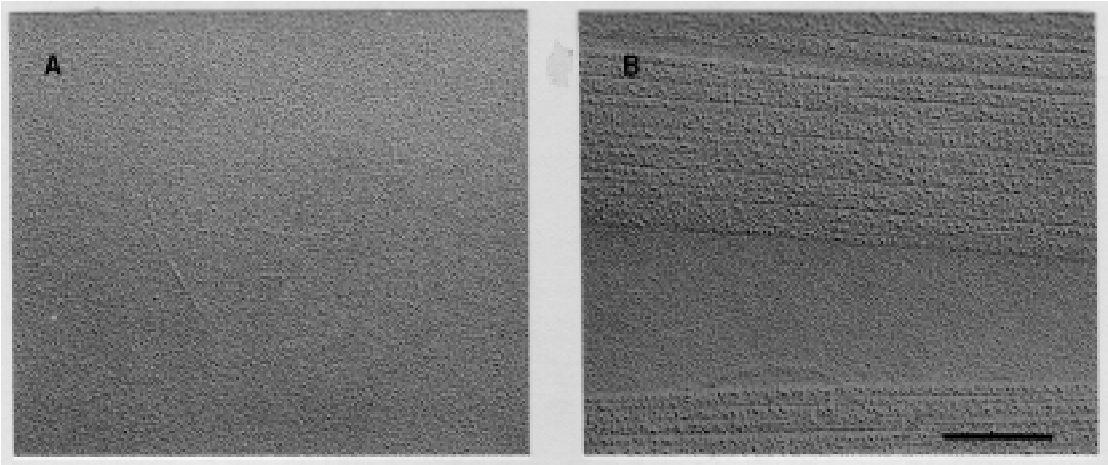

Figure 7.7: *Transmission electron micrographs of a monomer (**A**) and polymer (**B**) monolayer of the amphiphile at 9.3 ^{o}C on an aqueous subphase at a surface pressure of 30 $mN \cdot m^{-1}$. The polymer monolayer was formed after UV irradiation of the monomer monolayer at the air-water interface for 2 minutes under argon atmosphere. The scale bar corresponds to 0.2 μm.*

The monomer monolayer has a very smooth appearance while the polymer monolayer on the other hand has a striated texture which is often observed for polydiacetylene monolayers [16,17]. The crack in the middle of the micrograph of the polymer monolayer (7.7B) has to be ascribed to the preparation of the sample. Apparently, this crack is formed

along the direction of the fibres, indicating the chain direction of the polymer backbone [16]. From picture 7.7B it is possible to estimate the thickness of one polymer monolayer, by measuring the length of the shadow. From the equation $h = 1 \times \tan\alpha$, in which h is the thickness of the polymer monolayer, l is the length of the shadow and α is the angle at which the samples were Pt-shadowed, a monolayer thickness of 34 Å ± 8 Å can be calculated.

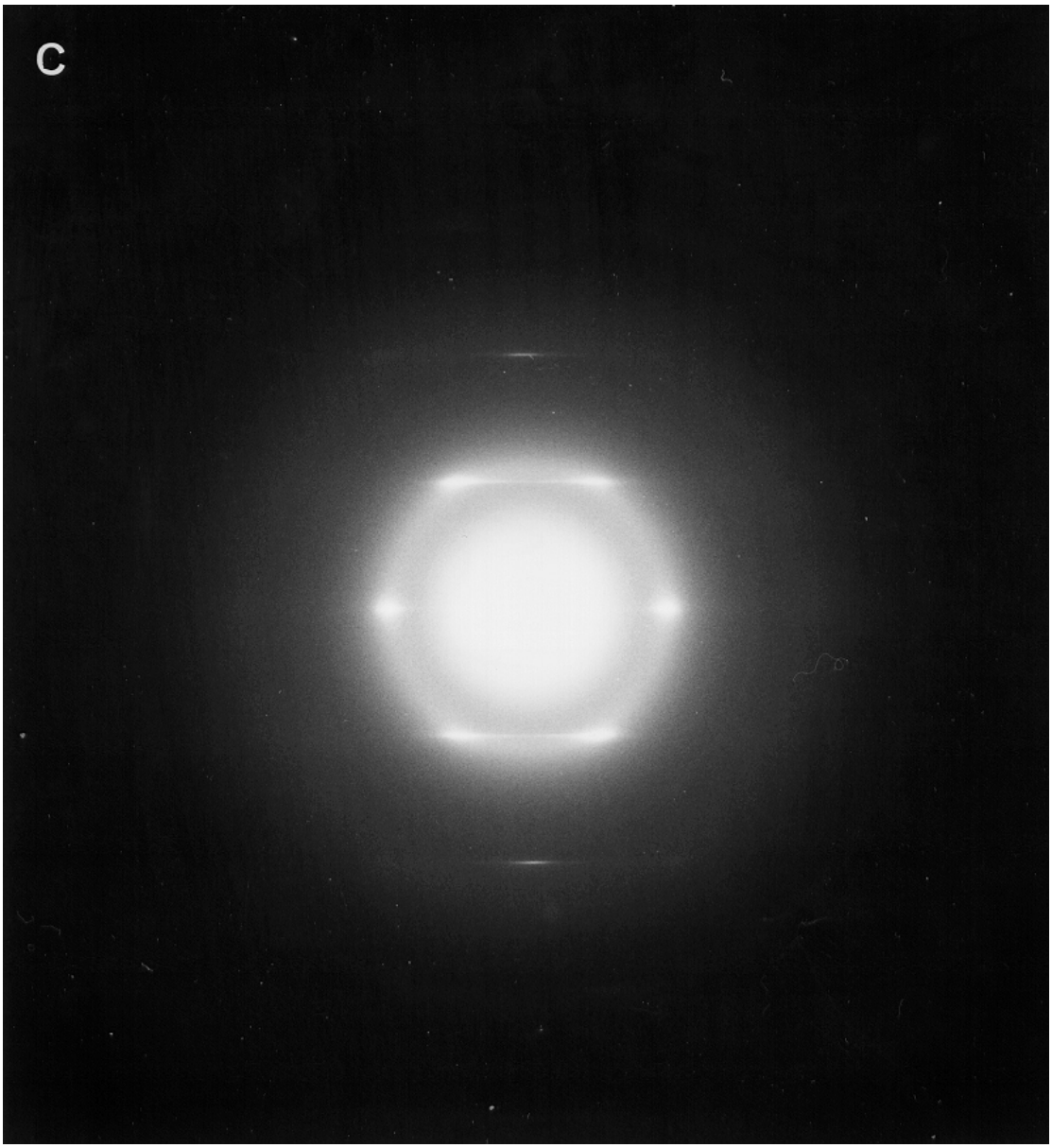

Figure 7.7C: *ED pattern of the polymerised monolayer of the amphiphile at the air-water interface at 9.3 ^{o}C on a aqueous subphase at a surface pressure of 30 $mN \cdot m^{-1}$ by means of UV irradiation for 2 minutes under argon atmosphere.*

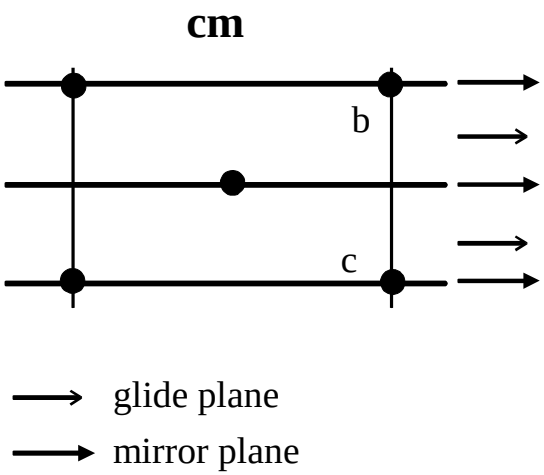

Figure 7.7D: *Schematic representation of the deduced plane group from the ED pattern of Figure 7.7C. Plane group cm.*

Figure 7.7C shows the electron diffraction (ED) pattern of the polymer monolayer. The streaking in the c^* direction can be attributed to the limited number of unit cells (5-10) within a crystalline fibre in the direction perpendicular to the fibre axis. The fibres are stabilised by an intramolecular hydrogen bonding network between the amide bonds nearly parallel to the polydiacetylene backbone [18,19]. From the ED pattern the lattice of Figure 7.7D is deduced. It shows a cm plane group symmetry with b = 4.84 Å and c = 8.85 Å. The lattice has 3 mirror planes and 2 glide planes over which the polydiacetylene backbones are shifted parallel to the chain direction with respect to each other by 1/2b. The surface area of the unit cell is 42.83 $Å^2$ with 2 molecules per unit cell. So, every molecule in the crystalline state occupies about 21.4 $Å^2$. From these data and in analogy with Kanetake et al. [18], the molecular packing shown in Figure 7.8 is proposed, in which the separated sheets are shifted with respect to each other, parallel to the direction of the polymer backbone.

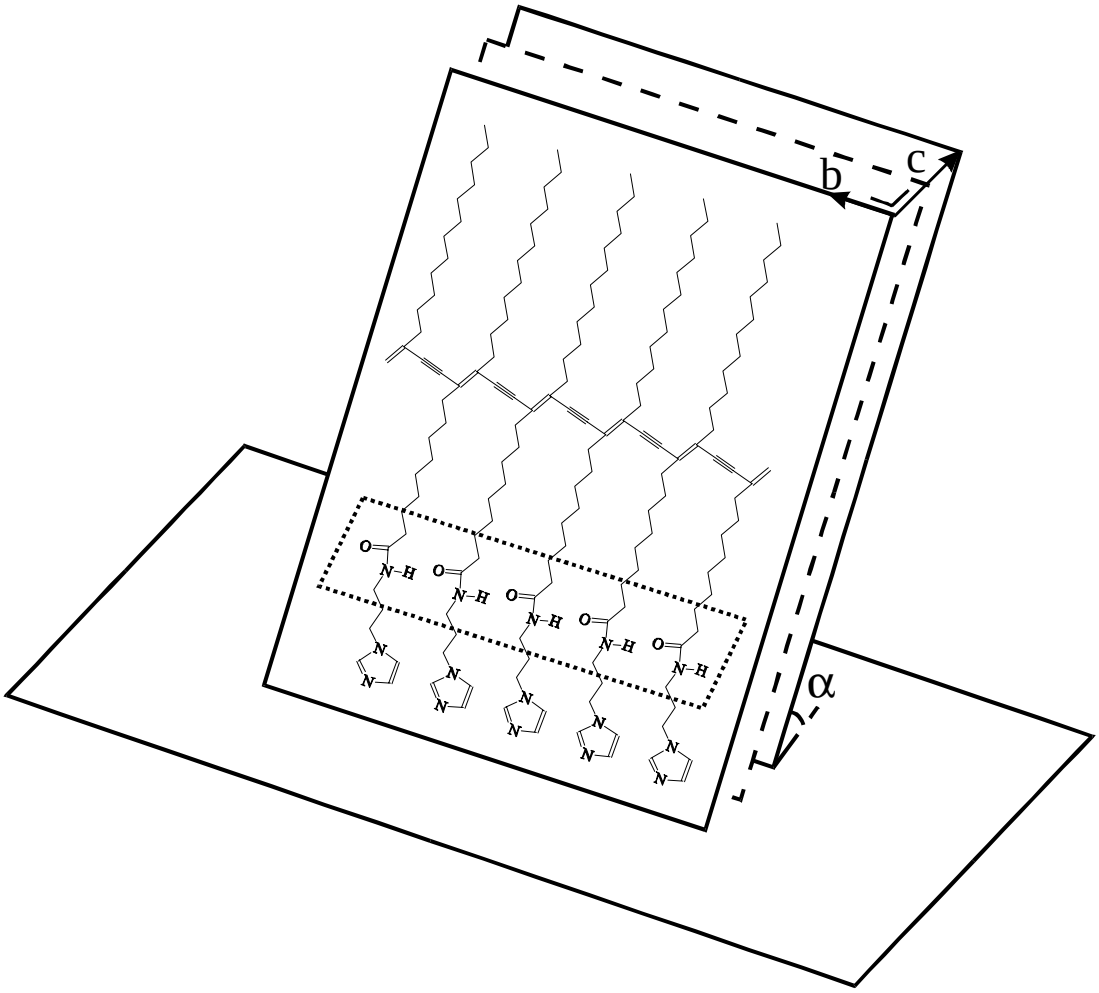

Figure 7.8: *Schematic representation of the polymerised monolayer of the amphiphile.*

Multilayer formation

Multilayers of the amphiphile were built up when the subphase contained $5 \cdot 10^{-5}$ M $CuCl_2$ at a subphase temperature of 4.5 ^{o}C and a surface pressure of 30 $mN \cdot m^{-1}$. Upon stabilisation the area decreases very rapidly from the LE phase, of about 36 $Å^2 \cdot molecule^{-1}$ (Fig. 7.3) to an area of about 29 $Å^2 \cdot molecule^{-1}$, because crystallisation takes place and a homogeneous condensed monolayer is formed which can be transferred onto solid substrates. Z-type transfer is observed with transfer ratios of 0.0-0.1 on the downstroke and 1.0 on the upstroke. When other metal ions or counter ions were used, a more Y-type transfer was observed with transfer ratios of 0.2-0.6 on the downstroke and 1.0 on the upstroke, so these multilayers had no regular layer structure. Also the polymerised monolayers could be

deposited onto solid substrates, again a more or less Y-type transfer was observed (transfer ratio on the downstroke: 0.5-0.7; transfer ratio on the upstroke: 0.9-1.0). In this way, irregular multilayers were built up.

Therefore only multilayers consisting of 16 layers layers, built up from a $5 \cdot 10^{-5}$ M $CuCl_2$ subphase, will be discussed in the present work.

Structural investigation of the multilayers

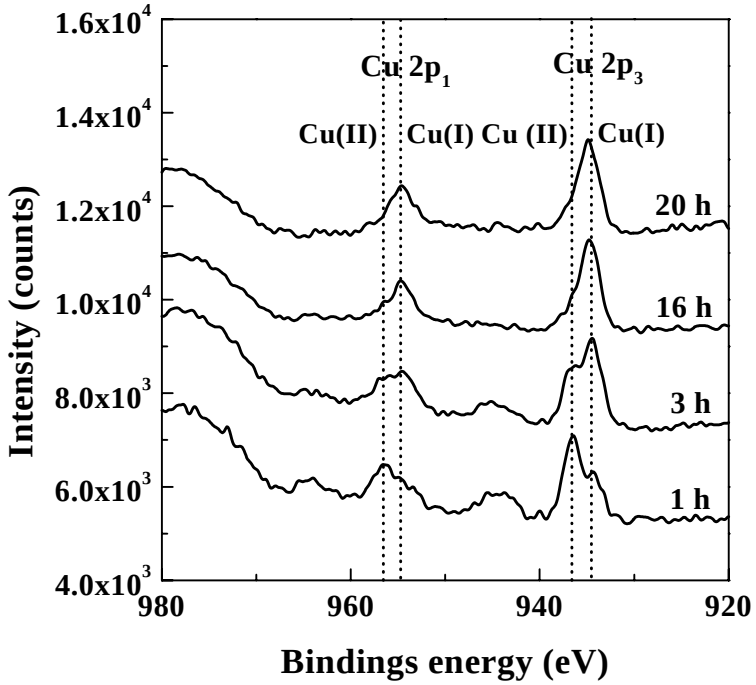

Figure 7.9: *The copper region of XPS spectra of a multilayer consisting of 16 layers of the amphiphile on silicon, built up from a $5 \cdot 10^{-5}$ M $CuCl_2$ subphase at 4.5 ^{o}C and 30 $mN \cdot m^{-1}$.*

XPS measurements were performed on these multilayers in order to confirm the presence of Cu(II) ions in the multilayers and to give some quantitative information about the formed metal complexes. In Figure 7.9, XPS spectra of the copper region of a multilayer consisting of 16 layers, built up from a $5 \cdot 10^{-5}$ M $CuCl_2$ subphase can be seen. After 1 hour of exposure to the soft X-rays, the presence of the copper peaks located at 936.5 eV (Cu $2p_3$) and 956.5 eV (Cu $2p_1$) and their satellites which are characteristic for Cu(II), can be seen clearly. Also Cu(I) peaks can be observed (934.5 eV Cu $2p_3$ and 954.6 eV Cu $2p_1$). As is already pointed out in Chapter 4 [2], upon longer exposure times of the multilayers to soft X-rays

(Fig. 7.9), the Cu(I) peaks increase in intensity while the Cu(II) peaks and their satellites decrease in intensity and finally after 20 hours of exposure to X-rays almost all Cu(II) is reduced to Cu(I). This phenomena is commonly observed in the literature [20-24] for transition metal ions and in the case of copper it is called X-ray induced copper reduction. From the ratio between the areas of the N and Cu $2p_3$ peak (including the satellite peak), the amount of Cu(II) ions incorporated into the multilayers could be calculated. The ratio N to Cu was approximately 7:1, because every amphiphile contained 3 nitrogen atoms, the ratio of amphiphile to copper in these multilayers is approximately 2:1. Furthermore the ratio Cu to Cl is 1:2, as expected.

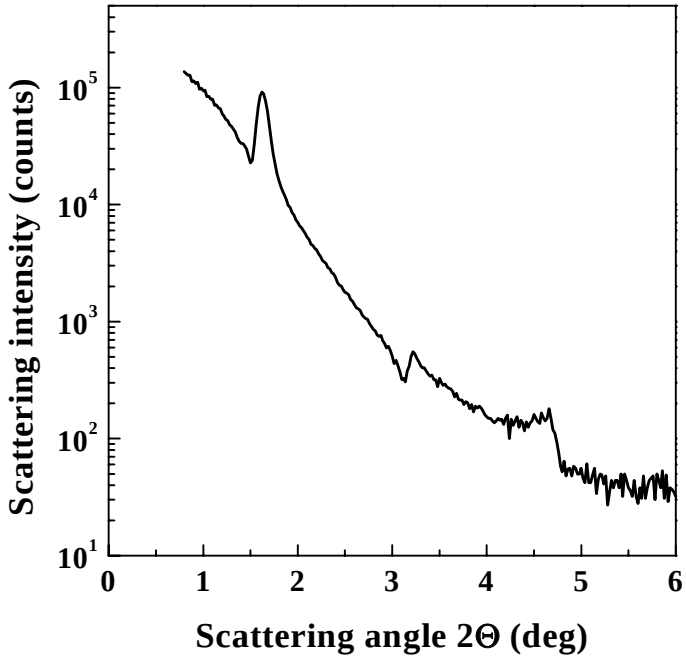

Figure 7.10: *Small angle X-ray reflection curve of a multilayer consisting of 16 layers of the amphiphile on silicon, built up from a $5 \cdot 10^{-5}$ M $CuCl_2$ subphase at 4.5 ^{o}C and 30 $mN \cdot m^{-1}$.*

SAXR measurements were performed on the multilayers in order to establish if these multilayers had a regular layer structure. The SAXR curve of a multilayer consisting of 16 layers, built up from a $5 \cdot 10^{-5}$ M $CuCl_2$ subphase (Fig. 7.10) has one clear Bragg peak which corresponded to a bilayer spacing of about 54.6 Å. Very weak second an third order Bragg peaks can also be seen. Because the multilayers were built up with a Z-type transfer, a Bragg peak corresponding to monolayer distance (about 27 to 37 Å, depending on the tilt angle with

respect to the surface normal) was expected. Apparently the molecules have "turned over" to form a Y-type structure, which is the thermodynamically most favourable structure [25,26].

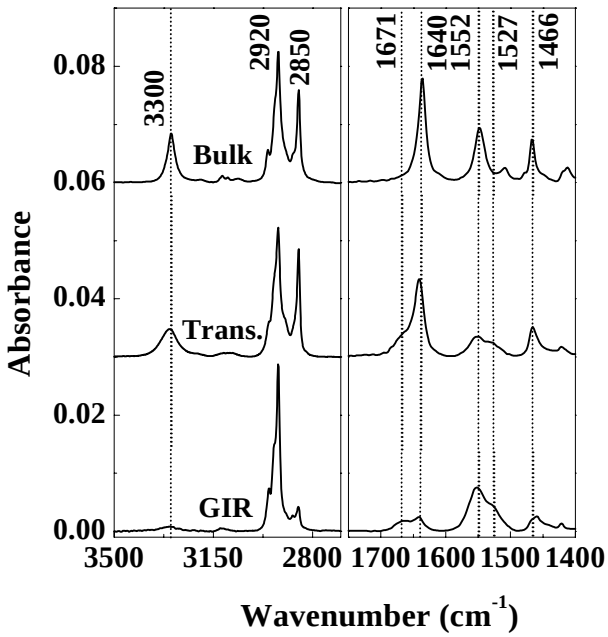

Figure 7.11: *Bulk (scale factor: 0.0310×), transmission and GIR (scale factor: 0.432×) infrared spectra of the amphiphile. Samples: In the case of the transmission spectrum, 16 layers of the amphiphile transferred onto silicon from a $5 \cdot 10^{-5}$ M $CuCl_2$ subphase and in the case of GIR, 16 layers of the amphiphile transferred onto a gold coated glass slide from a $5 \cdot 10^{-5}$ M $CuCl_2$ subphase. Subphase temperature was 4.5 ^{o}C and the surface pressure was 30 $mN \cdot m^{-1}$. The bulk and transmission spectra were y-shifted by 0.06 and 0.03 absorbance units, respectively.*

In order to examine the structure of the multilayers in more detail, FT-IR measurements were performed as shown in Figure 7.11. The band assignments are listed in Table 7.1. The same scaling factors were used for the bulk, transmission and GIR spectra as in Chapter 4 [2] for a proper comparison of the 3 spectra.

Table 7.1: *The IR band assignments [27-32].*

Wavenumber (cm^{-1})	Assignment	Transition dipole moment, $\bar{M}$
3300	ν (NH)	$\parallel$ N–H bond
2954	ν_a (CH_3)	$\perp$ C–CH_3
2920	ν_a (CH_2)	$\perp$ C–C–C chain plane
2871	ν_s (CH_3)	$\parallel$ C–CH_3
2850	ν_s (CH_2)	$\parallel$ H–C–H plane, bisecting HCH angle
1640	Amide I	$\parallel$ C=O bond
1548	Amide II	$\perp$ C=O bond
1508	ν (C=N_{imid})	$\parallel$ ring
1466	δ (CH_2)	$\parallel$ H–C–H plane, Bisecting HCH angle

As is shown in Figure 7.11, a bulk infrared spectrum of an uncoordinated amphiphile is recorded, powdered in KBr, in which the individual groups have no preferred orientation. Also transmission and GIR spectra were recorded of multilayer films consisting of 16 layers of the amphiphile, built up from a $5 \cdot 10^{-5}$ M $CuCl_2$ subphase. In the transmission mode, the electrical field vector is parallel to the substrate surface, so, all individual group vibrations with a transition dipole moment parallel to the substrate surface will absorb maximally in this mode while in the GIR mode, the electrical field vector is perpendicular to the substrate surface, so, all individual group vibrations with a transition dipole moment perpendicular to the substrate surface will absorb maximally in the GIR mode. In Figure 7.11, it can clearly be seen that the N-H (3300 cm^{-1}) and amide I (1642 cm^{-1}) bands are strongly present in the transmission spectrum while their intensity is much weaker in the GIR spectrum. The amide II band (1552 cm^{-1}) is strongly present in the GIR spectrum. The integrated area of the amide I peak in the transmission spectrum is larger than the integrated area of the amide I peak in the bulk spectrum. From these observations it can be concluded that the amide bond has a small tilt angle with respect to the surface normal. Closer examination (Fig. 7.11) of the amide I vibration reveals that there is also a vibration at 1671 cm^{-1} of much smaller intensity. From this second, much weaker, vibration it can be concluded that there is a small number of free amide groups which are not hydrogen bonded to their neighbouring molecules [27]. The

imidazole vibration is shifted completely to 1527 cm^{-1}, indicating that free ligands are no longer present [27,28] and all imidazole headgroups are involved in the complexation process because a free imidazole ligand shows a vibration at 1508 cm^{-1} (Fig. 7.11 bulk spectrum). The imidazole vibration can be seen in both the transmission and GIR spectra, although its intensity is somewhat stronger in the GIR spectrum, indicating that the imidazole group also makes a rather small tilt angle with respect to the surface normal. Major differences between the 2 IR methods can be observed in the CH stretching region, in which the symmetric methylene stretch (ν_s (CH_2) at 2850 cm^{-1}) is strongly present in the transmission spectrum but has a weak intensity in the GIR spectrum and the asymmetric methylene stretch (ν_a (CH_2) at 2920 cm^{-1}) appears relatively strong in the GIR mode. These observations in the CH stretching region suggest, as is already pointed out in Chapter 4 [2], that the C–C–C plane of the all-trans alkyl chain has a preferred orientation around the chain director, because when the all-trans alkyl chain can freely rotate around the C–C–C plane the ratio of the intensities of ν_a (CH_2) and ν_s (CH_2) will be about 2 in both the transmission and GIR spectrum. This is not the case for the multilayers of the imidazole amphiphile, so, the orientation of the all-trans alkyl chain is not random.

From Figure 7.11 it can be deduced that ν_s (CH_2) has a preferred orientation nearly parallel to the substrate surface, because it appears strong in the transmission spectrum and relatively weak in the GIR spectrum. On the other hand, ν_a (CH_2) is relatively strong in the GIR spectrum, compared to the transmission spectrum, indicating a large tilt angle (α) of the chain director with respect to the surface normal. Furthermore, the transition dipole moment of the ν_s (CH_2) vibration must lie nearly parallel to the substrate surface because this vibration strongly absorbs in the transmission spectrum but has a very weak intensity in the GIR spectrum. These results were also found by Walsh and Lando [33] for alternating multilayers of diacetylene group containing amphiphiles.

From the SAXR and FT-IR measurements a model (Fig. 7.12) is proposed for the multilayer film of the imidazole amphiphile, built up from a $5 \cdot 10^{-5}$ M $CuCl_2$ subphase. From the experimental data, a value of about 45^o has been found for α, taking into account a bilayer spacing of 54.6Å, a length of about 37 Å for the amphiphile in a fully stretched conformation and a large tilt angle of the aliphatic tail as is deduced from the IR spectra.

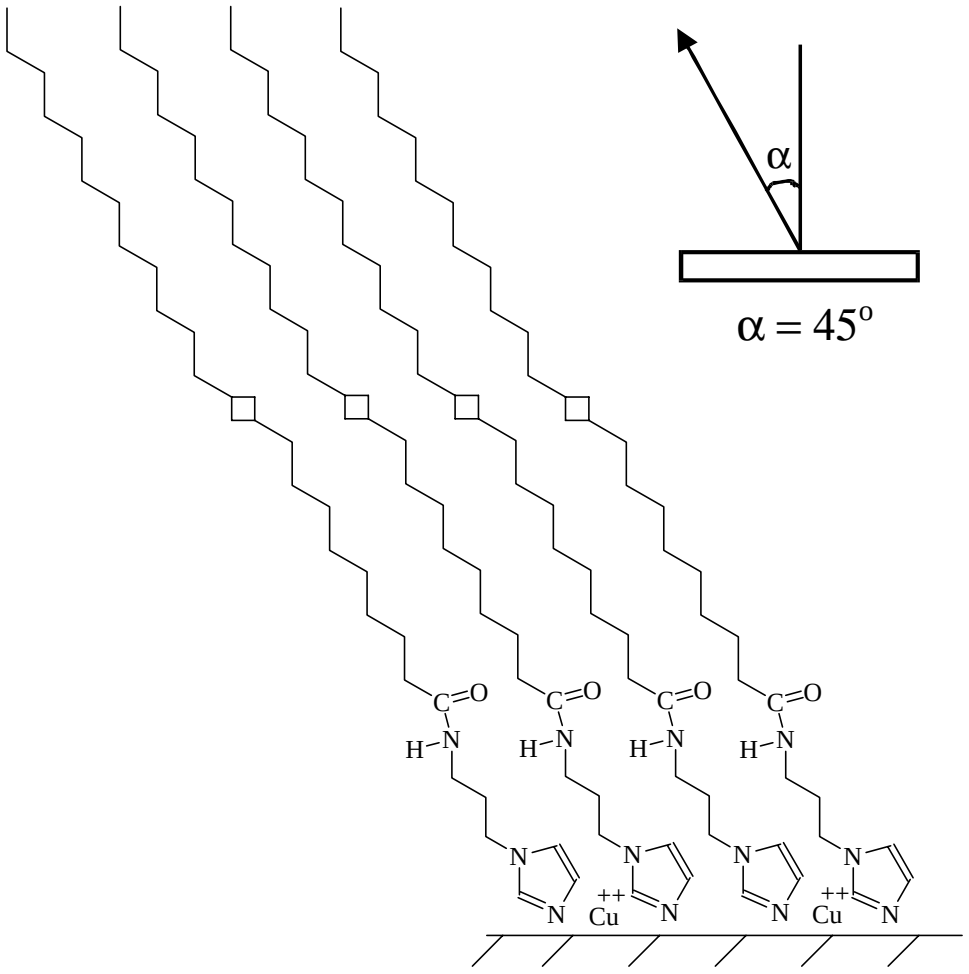

Figure 7.12: *Schematic representation of the structure of the amphiphiles inside the multilayers.*

Polymerisation in the multilayers

The LB films were polymerised by means of exposure to UV light (λ = 254 nm) under argon atmosphere. The polymerisation process was followed by UV/Vis spectroscopy as can be seen in Figure 7.13A. After several minutes of UV irradiation a red form of the polymer is formed with λ_{max} = 540 nm and after 30 minutes of exposure to UV light a maximum degree of polymerisation is reached because the absorption at 540 nm does not increase anymore. This can also be seen in Figure 7.13B, where the integrated absorbance, between 400 and 800 nm, is plotted as function of UV irradiation times. Apparently, a maximum conversion is reached after 30 minutes of exposure to UV light.

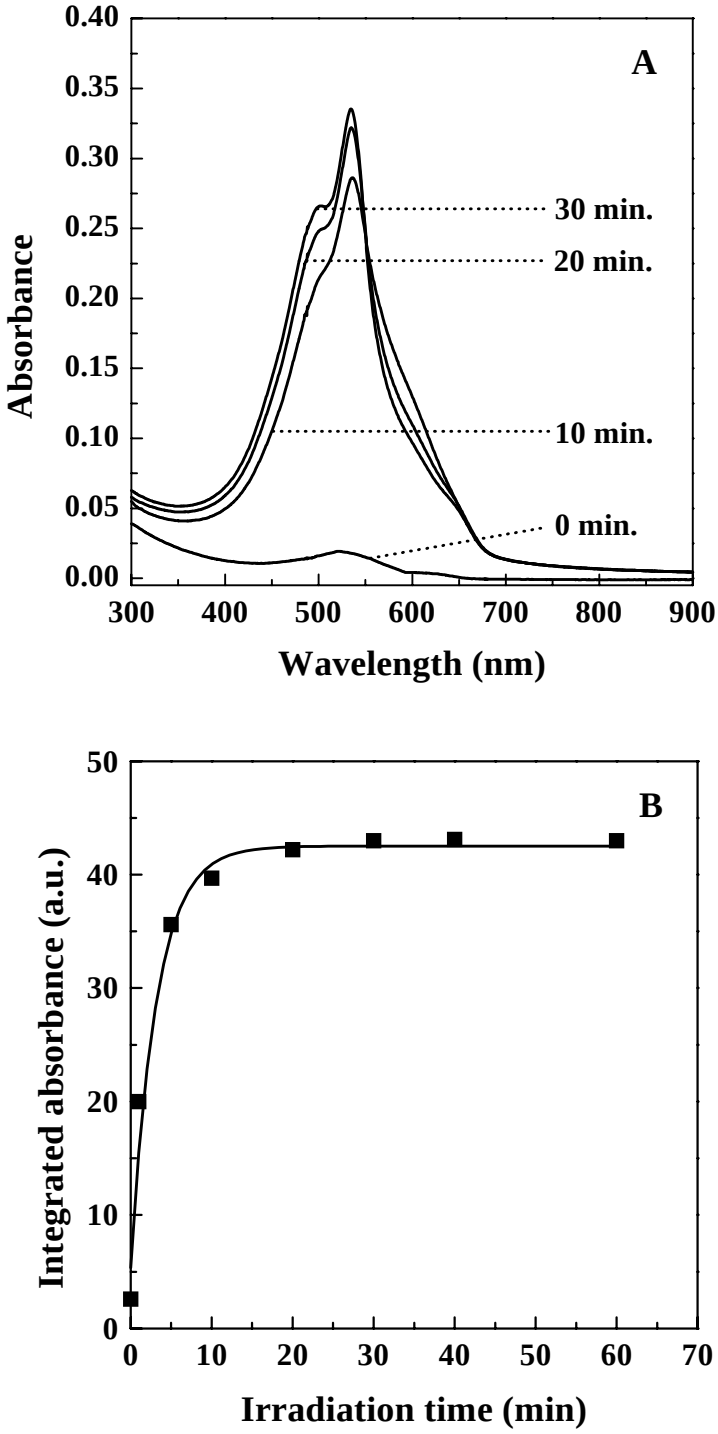

Figure 7.13: ***A****, UV/Vis absorption spectra of a multilayer of the amphiphile on glass, consisting of 16 layers, built up from a* $5 \cdot 10^{-5}$ *M* $CuCl_2$ *subphase at 4.5* ^{o}C *and 30* $mN \cdot m^{-1}$*, at different UV irradiation times.* ***B****, Integrated absorbance, between 400 and 800 nm, from the UV/Vis spectra of Figure 7.13A at different times of exposure to UV light.*

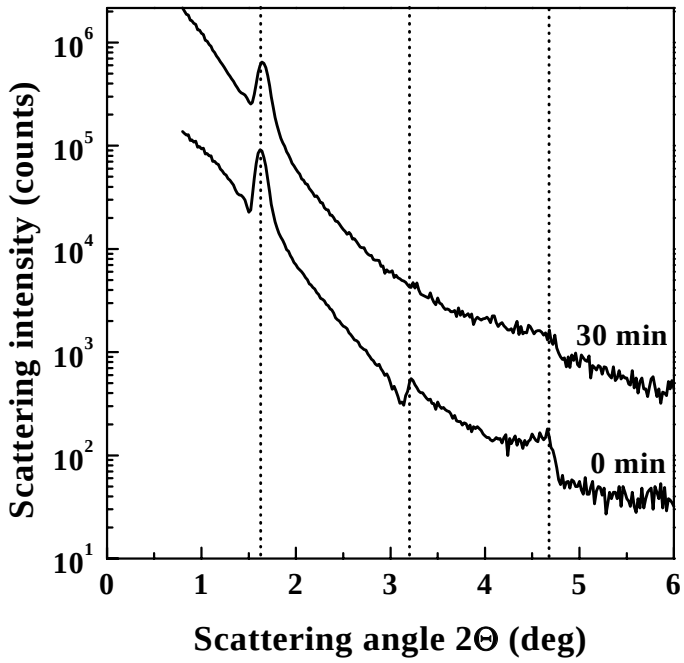

Figure 7.14: *Small angle X-ray reflection curves of a LB film consisting of 16 layers of the amphiphile on silicon, built up from a $5 \cdot 10^{-5}$ M $CuCl_2$ subphase at 4.5 ^{o}C and 30 $mN \cdot m^{-1}$, before and after 30 minutes of exposure to UV light.*

The layer structure of the multilayer, consisting of 16 layers of amphiphile, built up from a $5 \cdot 10^{-5}$ M $CuCl_2$ subphase is preserved during the polymerisation process, as can be seen in Figure 7.14, although the bilayer distance decreases from the original 54.6 to 53.5 Å.

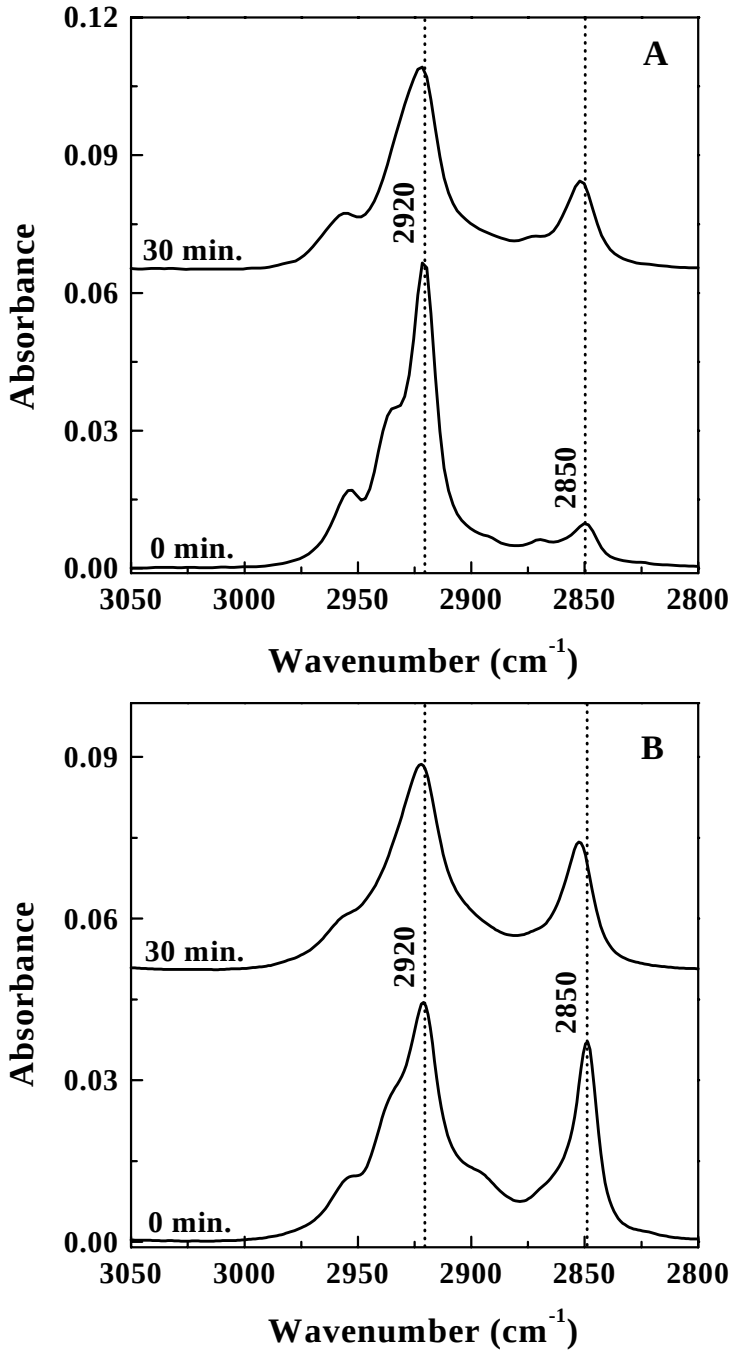

Figure 7.15: A, *GIR infrared spectra of a LB film consisting of 16 layers of the amphiphile, built up from a $5 \cdot 10^{-5}$ M $CuCl_2$ subphase at 4.5 ^{o}C and 30 $mN \cdot m^{-1}$, before and after 30 minutes of exposure to UV light.* **B**, *transmission infrared spectra of a LB film consisting of 16 layers of the amphiphile, built up from a $5 \cdot 10^{-5}$ M $CuCl_2$ subphase at 4.5 ^{o}C and 30 $mN \cdot m^{-1}$, before and after 30 minutes of exposure to UV light. The CH_2 and CH_3 stretching vibration region.*

During the polymerisation process, only in the CH stretching region major structural changes can be observed, as is shown in Figure 7.15A and B. The vibrations, due to ν_s (CH_2) (2850 cm^{-1}) and ν_a (CH_2) (2920 cm^{-1}) stretching vibrations, reveal a small shift to higher wavenumbers: 2852 and 2921 cm^{-1} for ν_s (CH_2) and ν_a (CH_2) respectively, indicating that the all-trans alkyl chain is partly converted to a more irregular one containing gauche conformations as was already described by Saito et al. [34] for the polymerisation of LB films of Cd(II) salts of 10,12-pentacosadiynoic acid. Furthermore, the intensity of the ν_a (CH_2) vibration decreases in the GIR spectrum, while the intensity of the ν_s (CH_2) vibration increases upon polymerisation (Figure 7.15A). This fact, together with the slight shift of the methylene stretch vibrations to higher wavenumbers, can be explained by considering a partial conversion of the all-trans alkyl chain during the polymerisation process into a more irregular alkyl chain containing gauche conformations, thereby loosing the orientation of the C–C–C plane of the aliphatic tail around the chain director.

Conclusions

The diacetylene group containing amphiphile N-(10,12-pentacosadiynamidopropyl)-imidazole, with an imidazole group as ligand, forms metal complexes at the air-water interface with all kinds of metal ions dissolved in the subphase at concentrations as low as $5 \cdot 10^{-7}$ M. The complexation process can easily be controlled by variation of the metal ion concentration, the counter ion, the temperature and ionic strength of the subphase.

The amphiphile forms stable monolayers at the air-water interface at surface pressures up to 40 $mN \cdot m^{-1}$. But only when the subphase contained $CuCl_2$, multilayers with a regular layer structure can be built up, which is confirmed by SAXR and FT-IR measurements. XPS measurements revealed the presence of Cu(II) ions in the multilayers, giving a direct proof that complexation in the monolayer at the air-water interface has occurred. The multilayers can be polymerised by means of UV irradiation, forming the red form of the polymer. During the polymerisation process, the regular layer structure is preserved, although FT-IR measurements show that the all-trans alkyl chains are partly converted to more irregular alkyl chains containing gauche conformations.

References

1. P.J. Werkman and A.J. Schouten, *Thin Solid Films* **1996**, *284-285*, 24.
2. P.J. Werkman, R.H. Wieringa, E.J. Vorenkamp and A.J. Schouten, submitted for publication in Langmuir.
3. P.J. Werkman, H. Wilms, R.H. Wieringa and A.J. Schouten, submitted for publication in Langmuir.
4. J.H. van Esch, R.J.M. Nolte, H. Ringsdorf and G. Wildburg, *Langmuir* **1994**, *10*, 1995.
5. R.J. Sundberg and R.B. Martin, *Chem. Rev.* **1974**, *74*, 471.
6. C. Bubeck, *Thin Solid Films* **1980**, *160*, 1.
7. H.D. Göbel, *Thesis*, Technische Universität München, Germany **1989**.
8. A. Dhanabalan, S.S. Talwar and S. Major, *Thin Solid Films* **1996**, *279*, 221.
9. M. Avrami, *J. Chem. Phys.* **1939**, *7*, 1103.
10. M. Avrami, *J. Chem. Phys.* **1940**, *8*, 212.
11. M. Avrami, *J. Chem. Phys.* **1941**, *9*, 177.
12. P.C. Hiemenz, *Polymer Chemistry, the Basic Concepts*, Marcel Dekker, New York and Basel **1984**.
13. J.M.G. Cowie, *Polymers: Chemistry & Physics of Modern Materials*, 2nd ed., Blackie, Glasgow and London **1991**.
14. I.K. Lednev and M.C. Petty, *Adv. Mater.* **1996**, *8*, 615
15. R.G. Wilkens, *Kinetics and mechanistics of reactions of transition metal complexes*, 2nd. ed., VCH Publishers, New York **1991**.
16. M. Sarkar and J.B. Lando, *Thin Solid Films* **1983**, *99*,19.
17. C.A.J. Putman, H.G. Hansma, H.E. Gaub and P.K. Hansma, *Langmuir* **1992**, *8*, 3014.
18. T. Kanetake, Y. Tomioka, S. Imaseki and Y. Taniguchi, *J. Appl. Phys.* **1992**, *2*, 938.
19. S. Meyer, P. Smith and J-.C. Wittman, *J. Appl. Phys.* **1995**, *77*, 5655.
20. B. Wallbank, C.E. Johnson and I.G. Main, *J. Electron Spectrosc.* **1974**, *4*, 263.
21. J.F. Gilp and I.G. Main, *J. Electron Spectrosc.* **1975**, *6*, 397.
22. R.G. Copperthwaite, *Surface Interface Anal.* **1980**, *2*, 17.
23. G. Schön, *Surface Science* **1973**, *35*, 96.
24. G. Martella, O. Puglisi, S. Pignataro, G. Alberti and U. Costantino, *Chem. Phys. Lett.* **1982**, *89*, 333.
25. G. Roberts (Ed.), *Langmuir-Blodgett films*, Plenum Press, New York and London **1990**.
26. A. Ulman, *An introduction to ultrathin organic films: from Langmuir-Blodgett to self-assembly*, Academic Press, San Diego and London **1991**.
27. N.A.J.M. Sommerdijk, *Thesis*, University of Nijmegen, The Netherlands **1995**.

28. J. Reedijk, *J. Inorg. Chem.* **1971**, *33*, 179.
29. M. Schoondorp, A.J. Schouten, J.B.E. Hulshof and B.L. Feringa, *Langmuir* **1992**, *8*, 1852.
30. D.L. Allara and R.G. Nuzzo, *Langmuir* **1986**, *1*, 52.
31. J.F. Rabolt, F.C. Burns, N.E. Schlotter and J.D. Swalen, *J. Electron Spectrosc.* **1983**, *30*, 29.
32. D.L. Allara and J.D. Swalen, *J. Phys. Chem.* **1992**, *86*, 2700.
33. S.P. Walsh and J.B. Lando, *Langmuir* **1994**, *10*, 246.
34. A. Saito, Y. Urai, and K. Itoh, *Langmuir* **1996**, *12*, 3938.

Chapter 8

Fabrication of alternating multilayers of a diacetylene group containing amphiphilic ligand and acid, using the Langmuir-Blodgett technique

Summary

The structure of alternating multilayers of two diacetylene group containing amphiphiles (an acid (A) and a pyridine ligand (B)), built up from a 5 mM $CdBr_2$ subphase, is examined. SAXR measurements revealed that these multilayers have a regular layer structure with a bilayer spacing of 55.2 Å. From this bilayer spacing in combination with FT-IR measurements, it can be concluded that the aliphatic tails of amphiphile A have a tilt angle (α) of approximately 34^o with respect to the surface normal, while in the case of amphiphile B, α has a value of about 45^o. In the all-trans aliphatic alkyl chains of both amphiphiles, the C-C-C plane has a preferred orientation in such a way that the symmetric stretches of the methylene groups of the aliphatic chain must be close to being in a plane parallel to the substrate.

These multilayers can be partly polymerised by means of UV irradiation, forming the red form (λ_{max} = 540 nm) of the polymer. Upon polymerisation the regular layer structure is preserved and the bilayer spacing increases from 55.2 up to 57.9 Å. The preferred orientation of the C-C-C plane of the aliphatic tail chain around the chain director is lost during the polymerisation process. Also, the all-trans alkyl chain is partly converted in a more irregular one containing gauche conformations.

Introduction

Already in 1935 Katherine Blodgett [1,2] examined the stabilising effect of metal ions (like Pb(II), Ca(II), Cd(II), etc.), dissolved in the subphase on a fatty acid monolayer at the air-water interface due to the crosslinking action of the metal ions. Thus, the interaction between metal ions and amphiphiles at the air-water interface is well-known for many years. Nowadays there is a growing interest in functional Langmuir-Blodgett (LB) films in which the metal ions introduce special semiconducting, magnetic or quantum physical properties into these ultra thin multilayer films [3-6]. For instance, using electron spin resonance, Pomerantz [7] demonstrated that at temperatures near 2K, LB films of fatty acids containing Mn(II) ions, rapidly developed a large internal magnetic field. LB films which contain metal ions have potential applications as sensors, for chemical modification of electrodes, in catalytical systems and in micro-electronic devices [4-6]. However, a number of possible applications of LB films depend on the supramolecular structure of these films and especially the alternate layer structures of 2 different amphiphiles (A and B) are of great interest, while by means of the alternating monolayer deposition technique, stable Y-type structures can be obtained without a plane of symmetry (noncentrosymmetric). These noncentrosymmetric multilayers are useful for or required for different applications like second-order NLO [5,8,9], pyroelectric devices [5,10], piezoelectric devices [5], etc..

Metal ions (dissolved in the subphase) can be introduced into the monolayers at the air-water interface by, firstly, salt formation with acid groups as with fatty acids or, secondly, by complex formation with ligands which are incorporated into amphiphiles [11-16] (ligands as hydrophilic headgroup) or polymers [17,18].

In Chapter 4 [19] the possibility of incorporation of Cd(II) ions into multilayers of 4-(10,12-pentacosadiynamidomethyl)pyridine has already been shown. These multilayers were built up by means of Z-type transfer, but “flip over” to form a Y-type structure as was shown by small angle X-ray reflection (SAXR) and FT-IR measurements. This Chapter describes the preparation of polymerisable, noncentrosymmetric Langmuir-Blodgett superlattices based on 2 diacetylene group containing amphiphiles (Scheme 8.1) using the Langmuir-Blodgett technique. One amphiphile (A) contains an acid headgroup and the other (B) contains a pyridine headgroup.

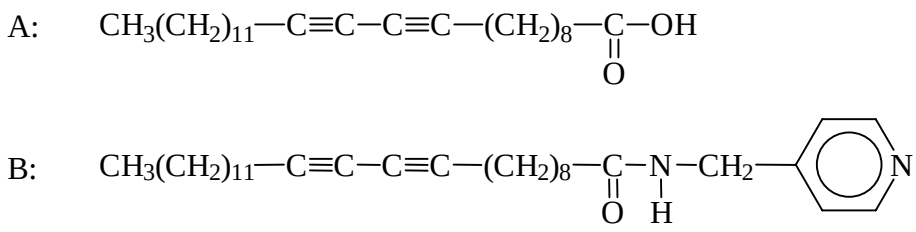

Scheme 8.1

By using the alternating deposition technique, stable ABAB, Y-type films are obtained. These films were built up from a Cd(II) ion containing subphase. XPS measurements confirmed the presence of Cd(II) ions in the multilayers. The structure of these films was studied by means of SAXR and FT-IR measurements. The SAXR curve shows 7 Bragg peaks indicating that the multilayers have a regular layer structure. The multilayers were polymerised by exposure to UV light (λ = 254 nm), maintaining their regular layer structure. Also the structural changes, in the multilayer film, induced by the photopolymerisation process will be shown.

Experimental

Materials

10,12-pentacoadiynoic acid (Hüls-Petrarch, 99%) and $CdBr_2$ (Merck, 98%) were used without further purification. 4-(10,12-pentacosadiynamidomethyl)pyridine was prepared as described in Chapter 3 [19].

Alternating deposition

A commercially available computer controlled KSV-5000 alternate layer system (Figure 8.1), manufactured by KSV Corporation (Finland) was used for the preparation of the alternating LB films. The trough consists of three compartments, two similar sized compartments for two different monolayer films and a small one for a clean water surface. The two identical film surfaces are separated by the small clean surface compartment so mixing of two different films is impossible. The water used for the subphase was purified by a reversed-osmosis system (Elgastat spectrum SC 30) and subsequent filtration through a Milli-Q purification system. The amphiphiles were dissolved at a concentration of 0.1 wt% in chloroform (Merck, spectroscopic quality). For the cleaning procedures of the substrates and

the preparation of the gold-coated glass slides, a standard method was used as described in Chapter 2. The subphase contained 5mM $CdBr_2$ and had a temperature of 20.0 ^{o}C. Amphiphile A was stabilised at a surface pressure of 17 $mN \cdot m^{-1}$ while amphiphile B was stabilised at a surface pressure of 20 $mN \cdot m^{-1}$. Monolayers of both amphiphiles were transferred onto substrates with a dipping speed of 2 $mm \cdot min^{-1}$ for the down- and upstroke. Amphiphile A was transferred at the downstroke with transfer ratios between 0.9 and 1.0 and amphiphile B was transferred at the upstroke with a transfer ratio of 1.0.

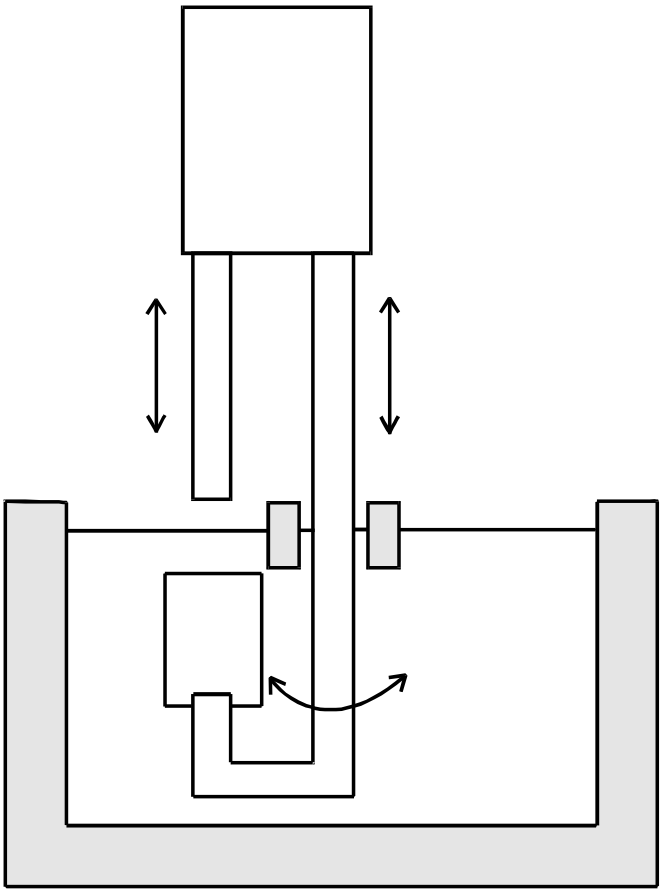

Figure 8.1: *Schematic representation of the KSV-5000 alternate layer system.*

The general procedures have been outlined in the experimental sections of Chapter 2 and 4.

Results and discussion

Alternating multilayer formation

On a subphase containing 5 mM $CdBr_2$ at 20 ^{o}C, amphiphile A was stabilised at a surface pressure of 17 $mN \cdot m^{-1}$ because at higher surface pressures no stable monolayer could be obtained and at lower surface pressures a less complete transfer onto substrates was observed. Amphiphile B was stabilised at a surface pressure of 20 $mN \cdot m^{-1}$ at which the best transfer was obtained. First, a monolayer of the Cd(II) salt of amphiphile A was transferred onto a solid substrate on the upstroke (transfer ratio: 1.0) after which an alternating multilayer was built up with transfer of the Cd(II) salt of amphiphile A on the downstroke and transfer of the Cd(II) complex of amphiphile B on the upstroke until the multilayer contained 18 alternating monolayers. Figure 8.2 shows a simplified schematic illustration of the obtained structure.

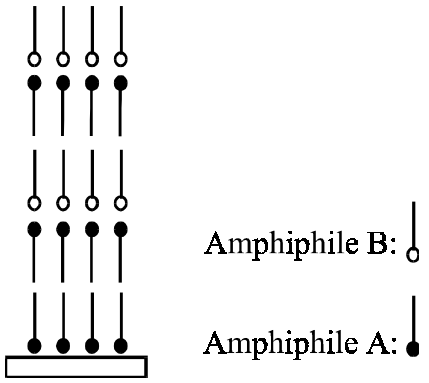

Figure 8.2: *Schematic representation of the alternating multilayer.*

XPS measurements

In order to reveal the presence and amount of incorporation of Cd(II) ions in the multilayers, XPS measurements were performed on an alternating multilayer built up from a 5 mM $CdBr_2$ subphase (Fig. 8.3).

The Cd $3d_3$ and Cd $3d_5$ peaks can clearly be seen in Figure 8.3, also the N 1S peak, originating from amphiphile B can be seen, indicating that indeed both amphiphiles are present in the multilayers, while also a large O 1s peak could be observed. This O 1s peak is much larger than in the case of multilayers composed entirely of amphiphile B [19]. Each Cd(II) ion, coordinated to amphiphile B, has 2 Br^- ions for charge compensation, so from the ratio N to Br^- (about 2:1) it can be concluded that 2 amphiphiles B are coordinated to 1 Cd(II) ion while each amphiphile B contains 2 nitrogen atoms. This Cd(II) ion content in the amphiphile B layer corresponds to the Cd(II) ions content of multilayers of amphiphile B, built up from a 5 mM $CdBr_2$ subphase as has already been shown in Chapter 4 [19]. Furthermore, it was found that 2 amphiphiles A form a salt with 1 Cd(II) ion, which is consistent with the IR measurements (Fig. 8.5) which show no vibrations at 1700 cm^{-1}, indicating complete salt formation of the carboxylic acid groups.

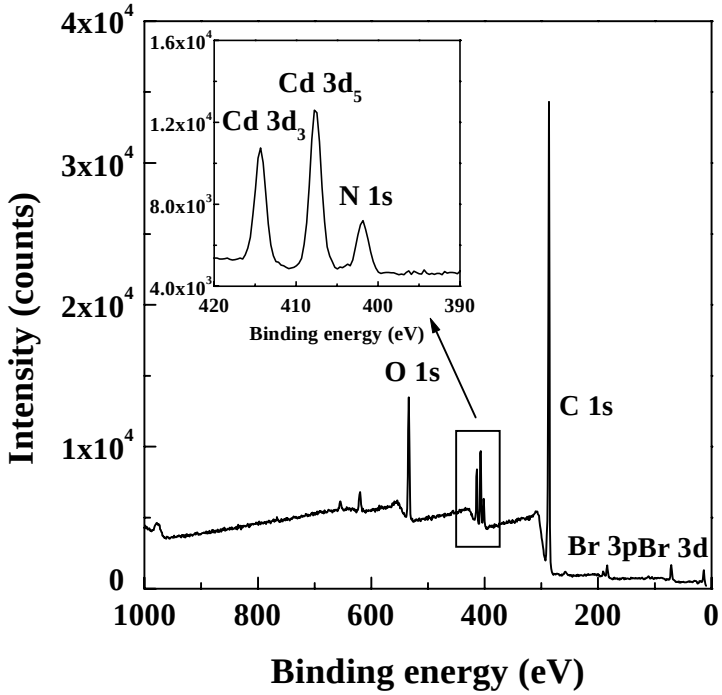

Figure 8.3: *XPS spectrum of an alternating multilayer on silicon of amphiphiles A and B, consisting of 19 layers, built up from a 5 mM $CdBr_2$ subphase at 20 ^0C.*

SAXR measurements

In order to examine if the alternating layer multilayers built up from a 5 mM $CdBr_2$ subphase, had a regular layer structure, SAXR measurements were performed on the alternating multilayers. Figure 8.4 shows that the alternating LB film had a regular layer pattern, indicated by the presence of 7 Bragg peaks, which corresponded to a spacing of 55.2 Å. This spacing corresponds to a bilayer spacing as expected. Also multilayers of pure amphiphile A were built up from a 5 mM $CdBr_2$ subphase. These LB films had a bilayer spacing of 54.9 Å, which corresponds well to values observed in the literature [20-22] for multilayers of the diacetylene acid, in which the aliphatic tails had a tilt angle (α) of about 34^0 with respect to the surface normal. The even order Bragg peaks have a relative weaker intensity then the odd order Bragg peaks. This phenomena can be explained by means of the well-known odd-even intensity oscillations of X-ray diffraction patterns, which is caused by the electron-deficient layer formed due to the juxtaposition of the hydrophobic chains, as has been explained in Chapter 4.

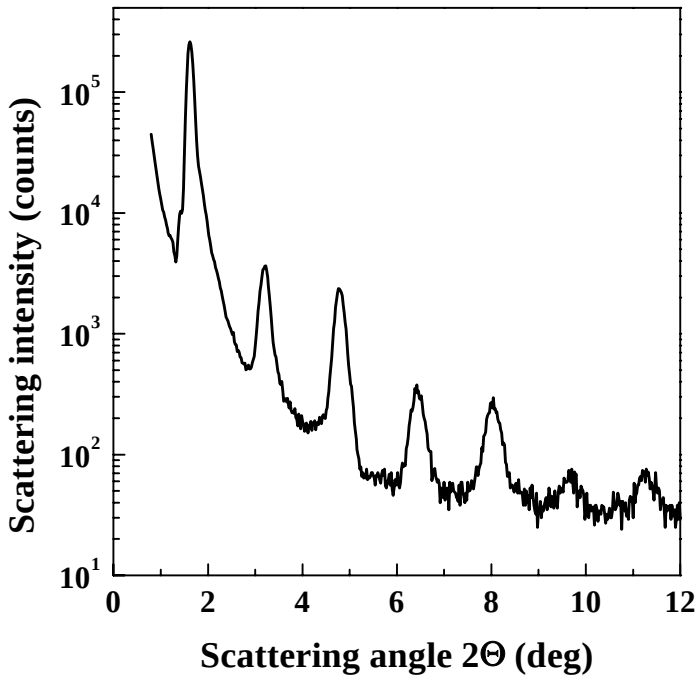

Figure 8.4: *SAXR curve of an alternating multilayer on silicon of amphiphiles A and B, consisting of 19 layers, built up from a 5 mM $CdBr_2$ subphase at 20 ^oC.*

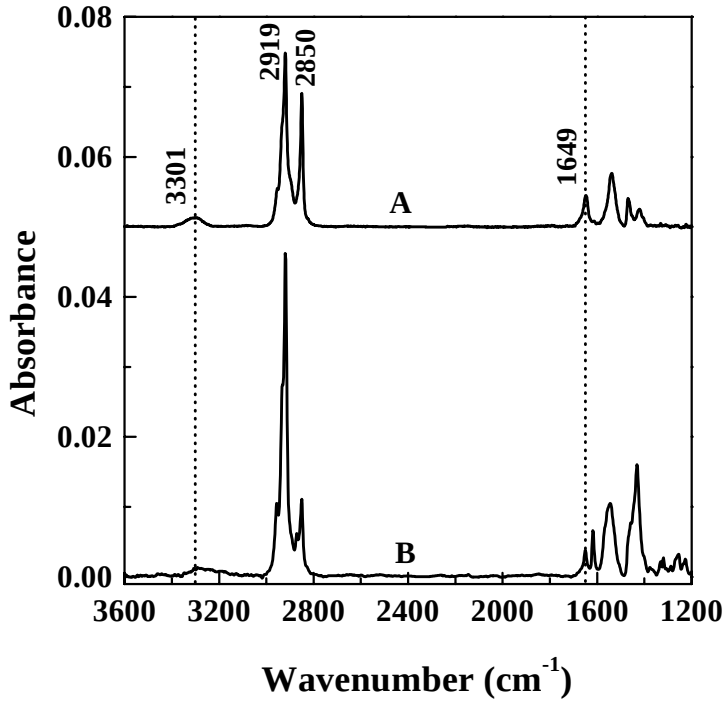

Figure 8.5: *Infrared spectra of alternating multilayers of amphiphile A and B, consisting of 19 layers, built up from a 5 mM $CdBr_2$ subphase at 20 ^{0}C: (A) transmission, silicon as substrate (2 × 19 layers), (B) GIR, gold coated glass slide as substrate.*

Infrared measurements

In order to study the structure of the multilayers in more detail, transmission IR spectra (electrical field vector parallel to the substrate surface, so all individual group vibrations with a transition dipole moment components parallel to the substrate, will absorb in this mode) and grazing incidence reflection (GIR) IR spectra (electrical field vector perpendicular to the substrate surface, so all individual group vibrations with a transition dipole moment components perpendicular to the substrate will absorb in this mode) were recorded. Figure 8.5 shows the transmission and GIR IR spectra of the alternating multilayers built up from a 5 mM $CdBr_2$ subphase. The band assignments are listed in Table 8.1.

Table 8.1: *The IR band assignments [8,9,19, 23]*

Wavenumber (cm^{-1})	Assignment	Transition dipole moment, $\bar{M}$
3301	ν (N–H)	∥ N–H bond
2954	ν_a (CH_3)	⊥ C–CH_3 bond
2919	ν_a (CH_2)	⊥ C–C–C plane
2871	ν_s (CH_3)	∥ C–CH_3 bond
2850	ν_s (CH_2)	∥ H–C–H plane, bisecting HCH angle
1649	Amide I	∥ C=O bond
1615	ν (C=N_{ar})	∥ ring
1539	ν_a (COO^-)	⊥ C–COO^- bond
1465	δ (CH_2)	∥ H–C–H plane, bisecting HCH angle
1434	ν_s (COO^-)	∥ C–COO^- bond

From Figure 8.5 it can be seen that in the transmission mode the N-H (3301 cm^{-1}) and amide I (1649 cm^{-1}) vibrations are present. These vibrations are also present in the GIR spectrum but weaker in intensity, indicating that the amide bond makes a tilt with respect to the surface normal and is not oriented perpendicular to the substrate surface, otherwise these vibrations would not be observed in the GIR spectrum. Furthermore, the pyridine group vibration near 1615 cm^{-1} is clearly present in the GIR spectrum, but very weakly in the transmission mode, from which can be concluded that the pyridine ring has a small tilt angle with respect to the surface normal. The ν_a (COO^-) vibration of amphiphile A at 1539 cm^{-1} is present in both the transmission and GIR spectra while the ν_s (COO^-) vibration at 1434 cm^{-1} is only strongly present in the GIR spectrum.

There are also major differences observed between both IR modes, in the region of the CH stretching vibrations of the aliphatic tail. The intensity of the band at 2919 cm^{-1} (ν_a CH_2) is very strong in the GIR mode while the ν_s (CH_2) band (2850 cm^{-1}) has a much weaker intensity. Both vibrations can be seen clearly in the transmission mode. As already has been discussed in Chapter 4 [19] and by other authors [9,10,23,24], the different ratio of intensities between the ν_a (CH_2) and ν_s (CH_2) bands, comparing the transmission and GIR mode, is usually not observed when the C-C-C plane of the all-trans alkyl chain can take on any

orientation around the chain axis, when this chain axis is oriented with a tilt angle (α) with respect to the surface normal. So, in our case the C-C-C plane has a preferred orientation, in which this plane is oriented almost parallel to the substrate surface and does not take on all possible orientations around the chain director. This way the ν_s (CH_2) vibration has a large component parallel to the substrate and will therefore absorb strongly in the transmission mode and relatively weak in the GIR mode, as can be seen in Figure 8.5. The asymmetric stretch vibration of the methylene (ν_a CH_2) absorbs relatively strong in the GIR mode, which indicates that the chain director has a large tilt angle (α) with respect to the surface normal. These results were also found by Walsh and Lando [10] for alternating multilayers of other diacetylene group containing amphiphiles.

In Figure 8.6 the proposed model for the alternating multilayers can be seen. The model was deduced from SAXR and FT-IR measurements. From the SAXR measurements of multilayers from the pure amphiphile A, built up from a 5 mM $CdBr_2$ subphase, a bilayer spacing of 54.9 Å was found. Therefore the separate monolayers have a thickness of 27.45 Å. The total length of a fully stretched amphiphile A which forms a salt with a Cd(II) ion has a length of approximately 33 Å [21,22]. Assuming that the amphiphiles are fully stretched the found monolayer thickness results in a tilt angle (α) of approximately 34^o with respect to the surface normal. It is assumed that amphiphile has the same orientation in the alternating multilayer as in the LB film of the pure amphiphile A [10] because in both cases the multilayers are built up with Y-type transfer. However, analogous to Ogawa [21], amphiphile B is expected to have a different orientation in the alternating multilayer compared to the LB film of pure amphiphile B, because the latter LB film is built up with Z-type transfer but rearranges to the thermodynamically more stable Y-type structure (see Chapter 4). This multilayer film had a bilayer of approximately 42 Å [19]. The alternating multilayer film is built up with Y-type transfer, so no rearrangement of amphiphile B in this film is expected. The alternating multilayers have a bilayer spacing of about 55.2 Å, leaving about 27.75 Å for the monolayer of amphiphile B. Assuming that amphiphile A has the same orientation in the alternating layers as in multilayer films of the pure amphiphile (monolayer thickness 27.45 Å) it can be calculated easily that a monolayer of amphiphile B is 27.75 Å thick in the alternating multilayer film. From the FT-IR spectra can be seen that the pyridine ring and amide bond have small tilt angles with respect to the surface normal and because amphiphile B has a length of about 36.5 Å in a fully stretched conformation, the aliphatic tail must have a large α with a value of about 45^o. Both amphiphiles have a preferred orientation of the C-C-C plane of the aliphatic tail in which the transition dipole moment of the ν_s (CH_2) vibration must lie nearly in the plane of the substrate.

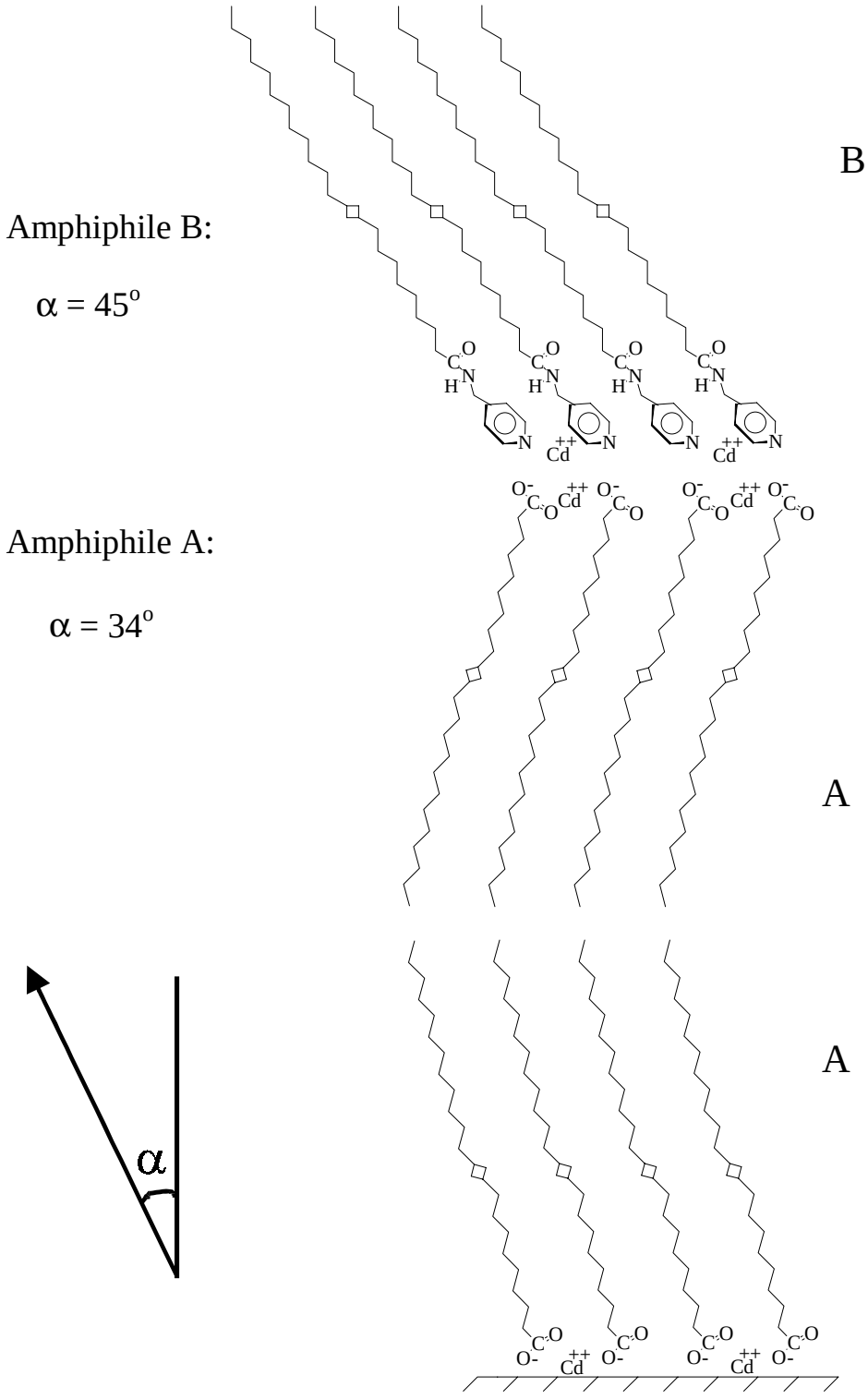

Figure 8.6: *The schematic structure of the amphiphiles in the alternating multilayer.*

Polymerisation in the multilayers

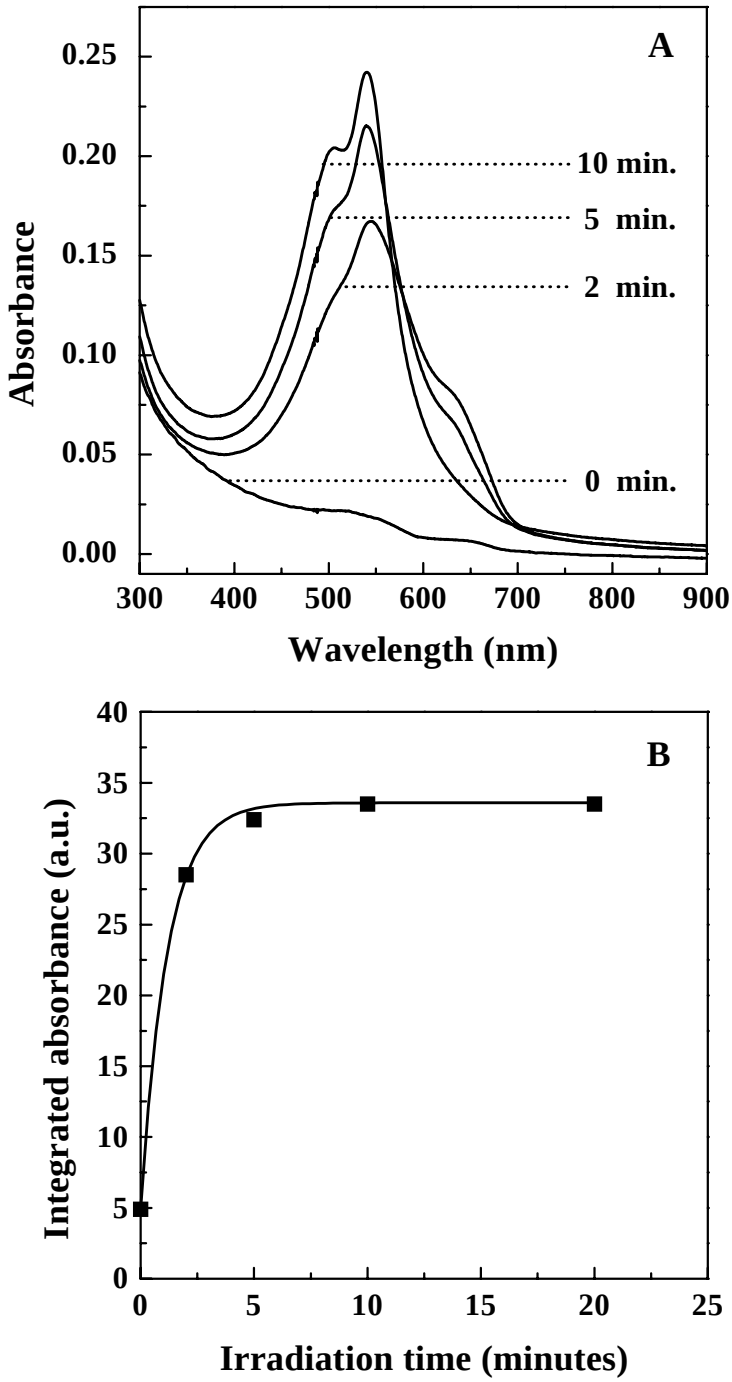

Figure 8.7: A: *UV/Vis absorption spectra of the alternating multilayer on glass of amphiphile A and B, consisting of 19 layers, built up from a 5 mM $CdBr_2$ subphase at 20 ^0C, at different times of exposure to UV light (λ = 254 nm).* **B:** *Integrated absorbance from the UV/Vis spectra of the alternating multilayer of Figure 8.7A, between 400 and 800 nm, at different times of exposure to UV light.*

The LB films were polymerised by means of exposure to UV light (λ = 254 nm) under argon atmosphere. The polymerisation process was followed by means of UV/Vis spectroscopy (Fig. 8.7A/B) because upon polymerisation a rigid, one-dimensional, conjugated backbone is formed. This conjugation results in a strong π to π^* absorption in the visible region [25-27].

In Figure 8.7A, the absorption spectrum changes of the LB film, during exposure to UV light, can be seen. After a few minutes of UV irradiation, the red form (λ_{max} = 540 nm) of the polymer is formed, also a shoulder of the blue form (λ_{max} = 620 nm) of the polymer can be seen. Upon higher conversion, the blue form disappears leaving only the red form of the polymer, which is the form with a reduced conjugation [28]. The integrated absorbance between 400 and 800 nm is plotted against the irradiation time in Figure 8.7B. It can be seen clearly that a maximum degree of polymerisation is reached after 10 minutes of exposure to UV light. This corresponds to a partial conversion, while multilayers of only amphiphile A or B have integrated absorbances between 400 and 800 nm of about 50 for multilayers consisting of 16 layers of amphiphiles. Therefore, the packing of the amphiphiles in the alternating multilayers differs from the packing of the amphiphiles when the multilayers consist only of amphiphile A or B.

SAXR measurements were performed on the alternating multilayers, after different times of UV irradiation, in order to reveal if the regular layer structure was preserved during the polymerisation process. In Figure 8.8, the SAXR curves can be seen of alternating multilayers built up from a 5mM $CdBr_2$ subphase after 0, 5 and 10 minutes of exposure to UV light. Here it can be seen clearly that the layer structure is preserved during the polymerisation process. The bilayer thickness increases from 55.2 till 57.9 Å, as can be concluded from the shift of the Bragg peaks to smaller scattering angles. The SAXR curves of the polymerised alternating multilayer film is assumed to consist of 2 superimposed lattices: one of the polymer lattice and one of the monomer lattice, because the polymerisation is not complete, as we have already pointed out. This is in agreement with the results of Dhanabalan et al. [22]. The shoulder at the low scattering angle side of the first Bragg peak corresponds to the polymer lattice (bilayer spacing = 57.9 Å) while the major peak, which is superimposed on the Bragg peak of the polymer lattice, corresponds to the monomer lattice (bilayer thickness = 55.2 Å). The second Bragg peak clearly consists of 2 reflections, one of the polymer lattice at the lower scattering angle side, which can be seen as a shoulder on which the reflection of the monomer lattice is superimposed. At higher scattering angles only the Bragg peak of the

polymer lattice can be seen clearly. The Bragg peaks, which correspond to the monomer lattice are only weak reflections at the higher scattering angle side of the main reflection.

The increase in bilayer thickness corresponds to a decrease in tilt angle (α) of the chain director of the aliphatic tail with respect to the surface normal [20,21].

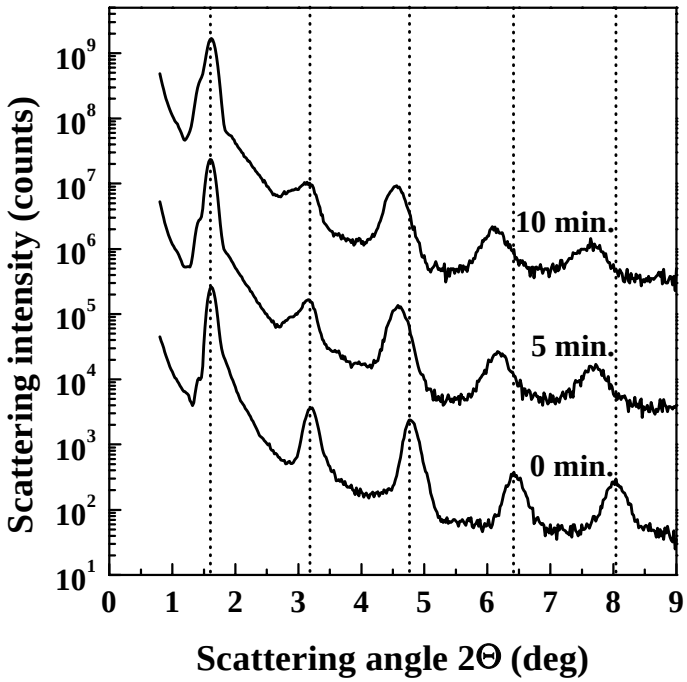

Figure 8.8: *SAXR curves of an alternating multilayer on silicon of amphiphile A and B, consisting of 19 layers, built up from a 5 mM $CdBr_2$ subphase at 20 ^0C, at different times of UV irradiation.*

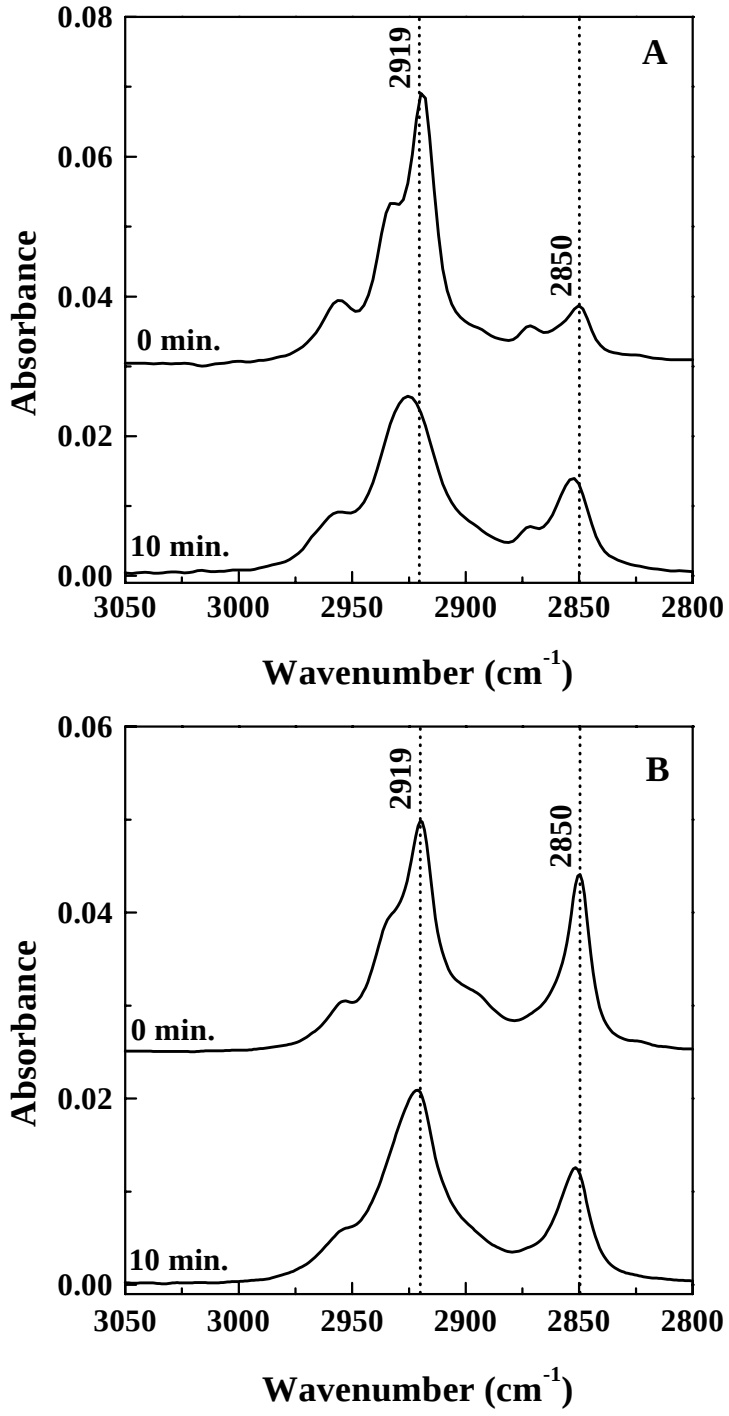

Figure 8.9: A: *GIR infrared spectra of the CH stretching region of an alternating multilayer of amphiphile A and B, consisting of 19 layers on gold, built up from a 5mM $CdBr_2$ subphase at 20 ^oC, before and after 10 minutes of UV irradiation.* **B:** *Transmission infrared spectra of the CH stretching region of an alternating multilayer on silicon of amphiphile A and B, consisting of 2 × 19 layers, built up from a 5 mM $CdBr_2$ subphase at 20 ^oC, before and after 10 minutes of UV irradiation.*

FT-IR measurements were performed in order to study the structural changes during the polymerisation process. During exposure to UV light the major changes can be found in the CH stretching region of the IR spectra. The vibration bands near 2850, 2871, 2919 and 2954 cm^{-1} are due to ν_s (CH_2), ν_s (CH_3), ν_a (CH_2) and ν_a (CH_3) stretching vibrations respectively [29,30]. Upon polymerisation the ν_s (CH_2) and ν_a (CH_2) are slightly shifted to higher wavenumbers, 2922 and 2852 cm^{-1} respectively, indicating that the all-trans alkyl chain is partly converted to a more irregular one containing gauche conformations [19,29]. Furthermore, the intensity of the ν_a (CH_2) band decreases in the GIR spectrum upon polymerisation, while the intensity of the ν_s (CH_2) band increases (Fig. 8.9A) and both the intensities of the ν_s and ν_a (CH_2) bands decrease upon UV irradiation in the transmission mode (Fig. 8.9B). After polymerisation the ratio in intensities between the ν_a and ν_s vibration bands is about 1.80 for both the GIR and transmission mode. Upon polymerisation the preferred orientation of the C-C-C plane of the aliphatic tail around the chain director is lost and the C-C-C plane can take on any orientation around the chain director.

Conclusions

Alternating multilayers of two diacetylene group containing amphiphiles, were built up from a 5 mM $CdBr_2$ subphase with a regular layer pattern. The structure of the multilayers was investigated by means of SAXR and FT-IR measurements and these revealed that the molecular orientation of the amphiphiles is very similar to their orientation in LB films of the parent compounds.

Upon polymerisation, the layer structure is preserved and the bilayer thickness increases from 55.2 up to 57.9 Å due to a change in tilt angle of the aliphatic tail with respect to the surface normal. Also the C-C-C plane of the aliphatic tail of the amphiphiles, loses its preferred orientation (in which the ν_s (CH_2) vibration lies nearly parallel to the plane of the substrate) around the chain director upon polymerisation.

References

1. K. Blodgett, *J. Am. Chem. Soc.* **1935**, *57*, 1007.
2. K. Blodgett and I. Langmuir, *Phys. Rev.* **1937**, *51*, 964.
3. T. Miyashita, *Prog. Polym. Sci.* **1993**, *18*, 263.
4. J.D. Swalen, D.L. Allara, J.D. Andrade, E.A. Chandros, G. Garoff, J. Israelachvili,

T.J. McCarthy, R. Murray, R.F. Pease, J.F. Rabolt, K.J. Wynne and H. Yu, *Langmuir* **1987**, *3*, 932.

5. G. Roberts (Ed.), *Langmuir-Blodgett films*, Plenum Press, New York and London **1990**.
6. U. Ulman, *An introduction to ultrathin organic films: from Langmuir-Blodgett to self assembly*, Academic Press, San Diego and London **1991**.
7. M. Pomerantz, *Phase transitions in surface films*, Plenum Press, New York **1980**.
8. M.N. Teerenstra, E.J Vorenkamp, R.J.M. Nolte and A.J. Schouten, *Thin Solid Films* **1991**, *196*, 153.
9. M.A. Schoondorp, A.J. Schouten, J.B.E. Hulshof and B.L. Feringa, *Langmuir* **1992**, *8*, 1852.
10. S.P. Walsh and J.B. Lando, *Langmuir* **1994**, *10*, 246.
11. G. Caminati, E. Margheri and G. Gabrielli, *Thin Solid Films* **1994**, *244*, 905.
12. G. Caminati, E. Margheri and G. Gabrielli, *Prog. Colloid Polym. Sci.* **1994**, *97*, 12.
13. A. Susuki, K. Ohkawa, S. Kanda, E. Emoto and S. Watari, *Bull. Chem. Soc. Japan* **1975**, *48*, 2634.
14. K. Sasakawa and S. Iwata, *Annu. Rep. Res. Reactor Inst. Kyoto Univ.* **1984**, *17*, 146.
15. L. Kalvoda and E. Brynda, *Thin Solid Films* **1993**, *232*, 120.
16. J.H. van Esch, R.J.M. Nolte, H. Ringsdorf and G. Wildburg, *Langmuir* **1994**, *10*, 1955.
17. J. Nagel and U. Oertel, *Polymer* **1995**, *36*, 381.
18. T. Miyashita, S. Saito and M. Matsuda, *Chem. Lett.* **1991**, 859.
19. P.J. Werkman, R.H. Wieringa, E.J. Vorenkamp and A.J. Schouten, submitted for publication in Langmuir.
20. B. Tieke, G. Lieser and K. Weiss, *Thin Solid Films* **1983**, *99*, 95.
21. K. Ogawa, *J. Phys. Chem.* **1991**, *95*, 7109.
22. A. Dhanabalan, S.S. Talwar and S. Major, *Thin Solid Films* **1996**, *279*, 221.
23. R.G. Nuzzo, A. Fusco and D.L. Allara, *J. Am. Chem. Soc.* **1987**, *109*, 2358.
24. S.D. Evans, K.E. Goppert-Berarducci, E. Urankan, L.J. Gerenser, A. Ulman and R.G. Snyder, *Langmuir* **1991**, *7*, 2700.
25. C. Bubeck, *Thin Solid Films* **1980**, *160*, 1.
26. H.D. Göbel, *Thesis*, Universität München, Germany **1989**.
27. A.A. Deckert, J.C. Horne, B. Valentine, L. Kiernan and L. Fallon, *Langmuir* **1995**, *11*, 643.
28. R. Burzynski, P.N. Prasad, J. Biegajski and D.A. Cadenhead, *Macromolecules* **1986**, *19*, 1059.
29. A. Saito, Y. Urai and N.E. Schlotter, *Langmuir* **1996**, *12*, 3938.

30. J.F. Rabolt, F.C. Burns, N.E. Schlotter and J.D. Swalen, *Chem. Phys.* **1983**, *78*, 946.

Chapter 9

The formation of copper sulphide semiconductors inside Langmuir-Blodgett films of Cu(II) ion complexes

Summary

The fabrication of layers of copper sulphide within multilayers of copper complexes of the amphiphile 4-(10,12-pentacosadiynamidomethyl)pyridine, by diffusion of H_2S into the multilayers, was studied by UV/Vis spectroscopy. XPS measurements revealed that copper sulphides can be synthesised which differ in stoichiometry when multilayers are used which were built up from different subphases ($CuCl_2$ or $Cu(ClO_4)_2$). The distinct layer pattern of the LB films is preserved during the formation of the copper sulphide layers and the bilayer distance increases slightly by approximately 1.8 Å for the multilayers built up from a 5 mM $CuCl_2$ subphase, whereas for the multilayers built up from a 5 mM $Cu(ClO_4)_2$ subphase the bilayer spacing decreases a little by approximately 0.6 Å after the formation of copper sulphide inside these LB films. After polymerisation the multilayer structure is destroyed in the case of LB films built up from the $CuCl_2$ subphase, whereas the layer structure is preserved during the polymerisation process in the case of multilayers built up from a 5 mM $Cu(ClO_4)_2$ subphase.

Introduction

In recent years, there is a growing interest in the construction of inorganic semiconductor particles or layers in Langmuir-Blodgett (LB) films. Barraud et al. [1], recognised the possibility of the formation of metal sulphides inside LB films of behenic acid salts. In these LB films the metal sulphides were prepared by converting the metal ions into their corresponding sulphides by reaction with the gas hydrogen sulphide (H_2S). So, the LB films were used as an organic matrix into which inorganic species could be inserted. On the basis of this concept several reports have been published in which metal ions (like Cd(II)) were converted to their corresponding sulphides (in this case CdS). In this way a wide variety of semiconductor nanoparticles (also called quantum dots, Q-particles, nanocrystals or clusters [2]) have been synthesised. The optical and electronic properties of semiconductor particles start to change when the diameter of the particle is reduced below the average hole-electron distance [2,3,4], the so called "quantum size effect" which could be observed as a blue shift of the band gap. This blue shift is proportional to the size (or smallness) of the particle [2-6]. All kinds of metal ions were incorporated into Langmuir monolayers [7,8] or Langmuir-Blodgett multilayers and subsequent converted with H_2S, H_2Se [9,10] or H_2Te [9] to produce the corresponding metal sulphides, metal selenides or metal tellurides, respectively. In this way CdS [1,9,11-14], PbS [1,15,16], AgS [1], ZnS [1], NiS [1], CoS [17], PtS [18,19] and PdS [18,19] nanoparticles have been prepared. LB films containing these semiconductor particles have potential applications in optoelectronic devices as optical switches, as infrared detectors and in photovoltaics [19,20].

Barraud et al. [1,21] built up multilayers of behenic acid, incorporated Cu(II) ions into these films and exposed the multilayers to H_2S. In this way Cu_2S layers could be formed between the hydrophilic headgroups of the amphiphiles and they measured the electrical properties of these films and showed that these samples were also photoconductive.

From the literature [20,22,23] it is known that copper sulphide exist in a wide variety of compositions ranging from Cu_2S (chalcocite) at the 'copper rich' side to CuS_2 (pyrite) on the 'copper deficient' side. Chen et al. [24] showed that they could influence the composition of the copper sulphide layers, formed in the LB films of copper stearate, by variation of the H_2S pressure and exposure (reaction) time ranging from $CuS_{0.77}$ to $CuS_{1.62}$.

In Chapter 3 [25] the monolayer characteristics of the amphiphile 4-(10,12-pentacosadiynamidomethyl)pyridine (Scheme 9.1) were presented upon complexation with Cu(II) ions under different conditions, like: Cu(II) ion concentration, type of counter ion, complexation time and ionic strength of the subphase. In Chapter 4 [26], multilayers of these metal complexes were built up and it was shown that the structure of these Cu(II) ion containing multilayer films could be altered by changing the counter ion (Cl^- or ClO_4^-). The

amphiphile had a diacetylene functionality in the aliphatic tail, which could be polymerised upon exposure to UV light, forming a polydiacetylene with a one-dimensional, rigid, conjugated backbone [27,28].

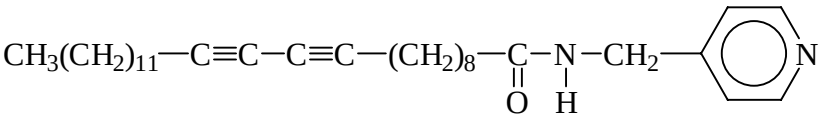

Scheme 9.1

This Chapter describes the formation of copper sulphide layers within LB films of copper complexes of the amphiphile (Scheme 9.1) with Cl^- or ClO_4^- as counter ion. XPS measurements were performed in order to reveal the stoichiometry of the formed copper sulphides. The reaction with H_2S was followed by means of UV/Vis spectroscopy and the structural changes due to the copper sulphide formation were studied by small angle X-ray reflection (SAXR) measurements. Furthermore, these multilayers with copper sulphide particles were polymerised by means of UV irradiation. This polymerisation process was studied by means of UV/Vis spectroscopy and SAXR measurements.

Experimental

The synthesis of the amphiphile, 4-(10,12-pentacosadiynamidomethyl)pyridine and the general procedures have been outlined in the experimental sections of the Chapters 2, 3 and 4.

Generation of copper sulphide

The LB films were placed in a cylindrical glass cell, which was connected to a dry N_2 and H_2S cylinder and disconnected from the outer atmosphere by a dressel bottle with paraffin oil. First, the glass cell was purged with N_2 for 15 minutes after which H_2S was passed slowly for 15 minutes. For longer gassing times, the H_2S flow was stopped after 15 minutes and the multilayer films were left in the H_2S atmosphere for the desired time.

Results and discussion

As is already described in Chapter 4 [26], multilayers of the amphiphile can only be built up when the subphase contains Cu(II) ions. The studied multilayers consist of 16 layers of the amphiphile, built up from a 5 mM $CuCl_2$ or 5 mM $Cu(ClO_4)_2$ subphase at 18.7 ^oC and 30 $mN \cdot m^{-1}$, by means of Z-type transfer with transfer ratios of 0.0-0.1 on the downstroke and 1.0 on the upstroke. SAXR measurements [26] revealed that the multilayers have a Y-type structure, so, the amphiphiles must have "turned over" to form the thermodynamically more favourable Y-type of structure, because the multilayers were built up with a Z-type transfer. In the Y-type structure, the Cu(II) ion rich plane is centred between the hydrophilic headgroups and upon exposure to H_2S this Cu(II) ion rich plane is converted into a semiconductor copper sulphide layer.

In Figure 9.1 the copper and sulphur regions of a XPS spectrum of a LB film, consisting of 16 layers of the amphiphile on silicon, built up from a 5 mM $CuCl_2$ subphase, is shown. The Cu(II) ions are indeed incorporated in the multilayers as can be seen by the presence of the copper peaks (936.5 eV, Cu $2p_3$ and 956.5 eV, Cu $2p_1$) (Fig. 9.1A) and their corresponding satellites which are characteristic for Cu(II) [22-24]. From the ratio between N to Cu it is concluded that the multilayers contain 1 Cu(II) ion to 3 amphiphiles [26]. Furthermore, it can be seen that no sulphur was present in the LB films (Fig. 9.1B) before exposure to H_2S .

After 30 minutes of exposure to the H_2S gas, the copper peaks shifted to lower bindings energy values (933.5 and 954.0 eV for Cu $2p_3$ and Cu $2p_1$, respectively) (Fig. 9.1A), the satellites disappeared and the full width at half-maximum (FWHM) became smaller. All these changes in the copper region indicated that upon exposure to H_2S, the Cu(II) ions are reduced to Cu(I) which is consistent with the results of Chen et al. [24]. Also Folmer et al. [22,23] concluded that no Cu(II) ions were present in copper sulphides (ranging in composition from CuS_2 to Cu_2S), but that all the copper was in the monovalent state. After the reaction with H_2S, the multilayers contain sulphur, as can be seen in Figure 9.1B. From the ratio Cu:S (1.05), we propose that CuS is formed in the multilayers. Upon longer gassing times, the ratio Cu:S did not change anymore. When the multilayers, built up from a $Cu(ClO_4)_2$ subphase, were exposed to H_2S, the same phenomena could be observed, again Cu(II) was reduced to Cu(I) but the stoichiometry of the formed copper sulphide layers was different. In this case, the ratio Cu:S was 0.61. Thus, in the case of multilayers built up from a $Cu(ClO_4)_2$ subphase, $Cu_{1.64}S$ is formed. Depending on the structure of the multilayer film (which is different for multilayers built up from a Cu(II) ions containing subphase with Cl^- or ClO_4^- as counter ion [26]), different copper sulphides can be obtained when multilayers which

contain Cu(II) ions are exposed to H_2S. Furthermore, upon exposure the Cl^- peaks which were present before exposure to H_2S for charge compensation, disappear after 30 minutes of exposure to H_2S, indicating that indeed all the Cu(II) ions are converted to copper(I) sulphide.

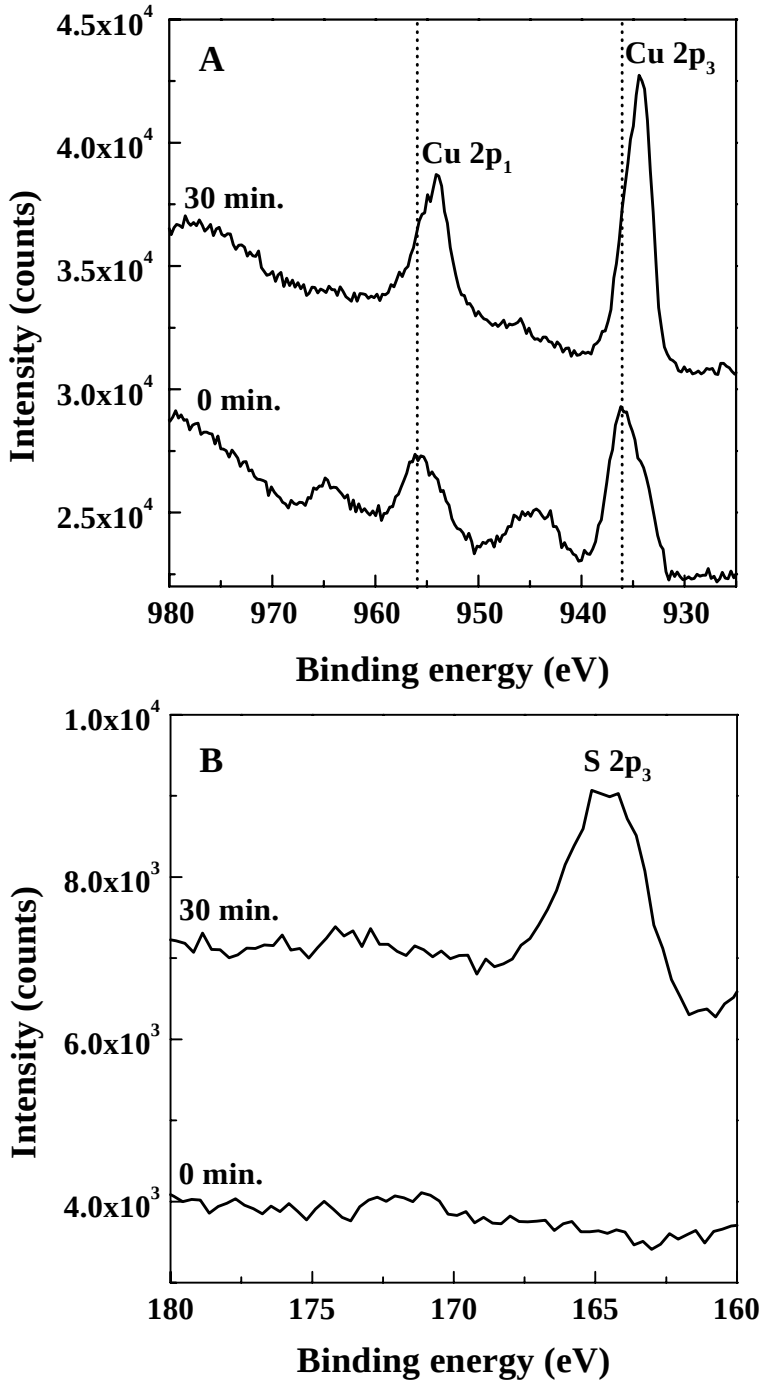

Figure 9.1: *XPS spectra of LB films, consisting of 16 layers of the amphiphile on silicon built up from a 5 mM $CuCl_2$ subphase at 18.7 ^oC and 30 $mN{\cdot}m^{-1}$, before and after 30 minutes of exposure to H_2S: A, the copper region and B, the sulphur region.*

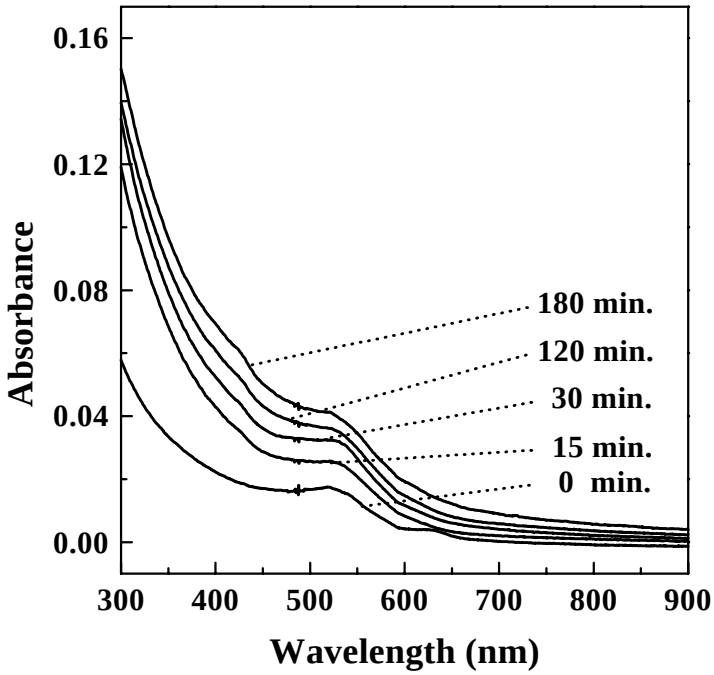

Figure 9.2: *UV/Vis absorption spectra of a LB film on glass, consisting of 16 layers of the amphiphile, built up from a 5mM $CuCl_2$ subphase at 18.7 ^oC and 30 $mN \cdot m^{-1}$, at different times of exposure to H_2S.*

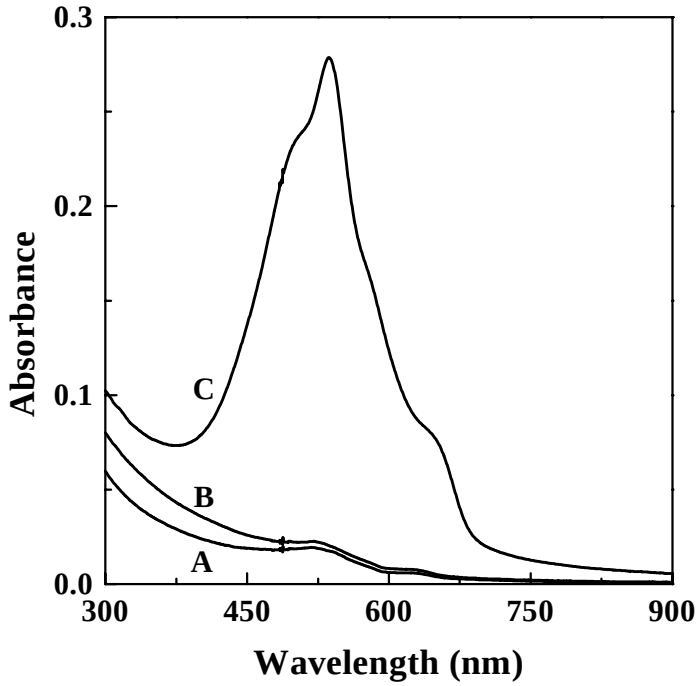

Figure 9.3: *UV/Vis absorption spectra of a LB film on glass, consisting of 16 layers of the amphiphile, built up from a 5 mM $Cu(ClO_4)_2$ subphase at 18.7 ^oC and 30 $mN \cdot m^{-1}$: (A) 0 min. H_2S, (B) 30 min. H_2S and (C) 30 min. H_2S and 20 min. UV irradiation (254 nm).*

In Figure 9.2, the absorption spectra of a LB film, consisting of 16 layers of the amphiphile, built up from a 5 mM $CuCl_2$ subphase, can be seen after different times of exposure to H_2S. The absorption of the formed copper sulphide layers increases at longer gassing times but after 180 minutes no further increase in absorption can be observed. This gassing time is much longer than the time needed for a maximum amount of incorporation of sulphur into the LB films, as was deduced by the XPS experiments while the XPS measurements give information about the first 50 to 100 Å at the surface of the LB film. So, the copper sulphide formation in the top layers is completed within 30 minutes while, due to diffusion, the copper sulphide formation near the substrate surface was completed after 180 minutes of exposure to H_2S. In Figure 9.2 an absorption onset of the copper sulphide layers at about 600 nm can be observed, which is in agreement with the results of Barraud et al. [21].

The absorption onset of copper sulphides strongly depends on the stoichiometry of the semiconductor. Cu_2S has an absorption onset at about 1050 nm [29]. The exact position of the absorption onset depends on the method of preparation of copper sulphide films. When the copper content of the copper sulphides is lowered the absorption onset shifts to lower wavenumbers. For instance, $Cu_{1.8}S$ and copper sulphides which are more copper deficient have an absorption onset at about 600 nm [29-31]. Therefore the found absorption onset at approximately 600 nm already indicates that the formed copper sulphide inside the LB films of the copper complex is not Cu_2S but is more copper deficient. Furthermore, absorption spectra of copper sulphide nanoparticles show a sharp blue shifted peak [32,33]. Therefore it can be assumed that the formed copper sulphides in the LB films are arranged as layers between the hydrophilic headgroups of the amphiphilic ligands because an absorption onset at about 600 nm is found and no sharp absorption peak is observed.

In Figure 9.3 the absorption spectra of a LB film on glass, built up from a 5 mM $Cu(ClO_4)_2$ subphase, before and after 30 minutes of exposure to H_2S can be seen. Moreover, the absorption of the formed copper sulphide layers did not increase anymore after 30 minutes of exposure to H_2S. Apparently the H_2S gas diffuses much faster into multilayer films built up from a 5 mM $Cu(ClO_4)_2$ than in the case of LB films built up from a $CuCl_2$ subphase. This phenomena is in agreement with the results from Chapter 4 [26], in which was concluded (from the much faster reduction of the Cu(II) ions to Cu(I) ions inside LB films built up from 5 mM $Cu(ClO_4)_2$ subphase, due to the soft X-rays in the XPS apparatus) that the LB films built up from a 5 mM $Cu(ClO_4)_2$ subphase have a more open structure than multilayer films built up from a $CuCl_2$ subphase.

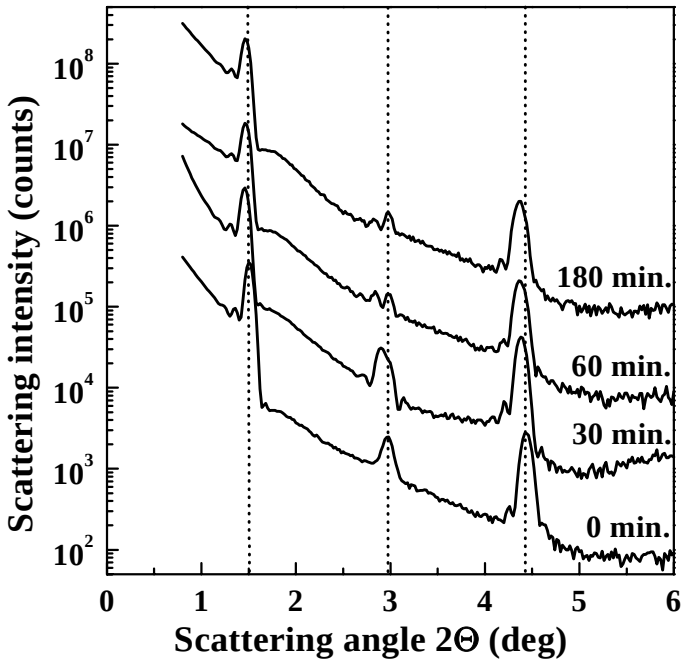

Figure 9.4: *Small angle X-ray reflection curves of a LB film on silicon, consisting of 16 layers of the amphiphile built up from a 5 mM $CuCl_2$ subphase at 18.7 ^oC and 30 $mN \cdot m^{-1}$, at different times of exposure to H_2S.*

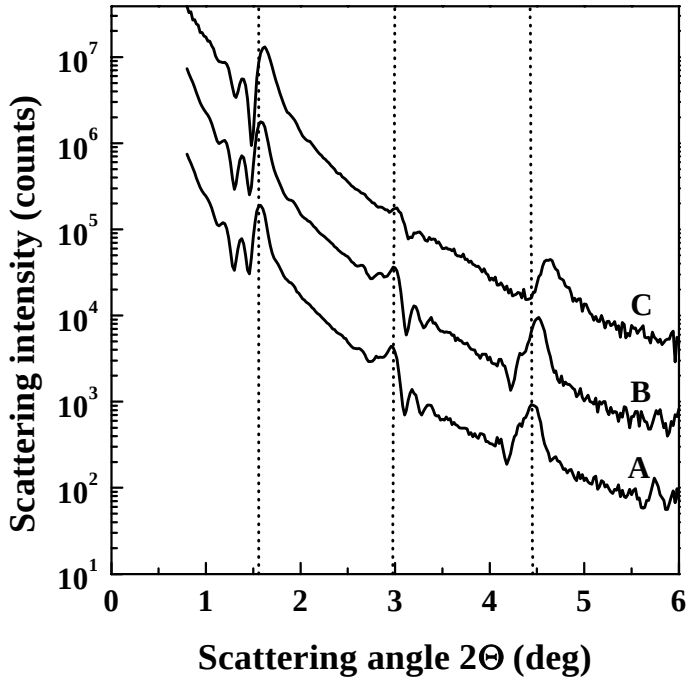

Figure 9.5: *Small angle X-ray reflection curves of a LB film on silicon, consisting of 16 layers of the amphiphile built up from a 5 mM $Cu(ClO_4)_2$ subphase at 18.7 ^oC and 30 $mN \cdot m^{-1}$: (A) 0 min. H_2S, (B) 30 min. H_2S and (C) 30 min. H_2S and 20 min. UV irradiation.*

Figure 9.4 shows the SAXR measurements of a multilayer film, consisting of 16 layers of the amphiphile on silicon, built up from a 5 mM $CuCl_2$ subphase, at different times of exposure to H_2S. The multilayer film has a regular layer pattern with a bilayer spacing of 60.0 Å as can be calculated from the positions of the Bragg peaks. After 180 minutes of exposure to H_2S, the second Bragg peak disappears and the first and third Bragg peak shift to slightly lower reflection angles, indicating an increase in bilayer distance after formation of the copper sulphide layers. The multilayer now has a bilayer spacing of 61.8 Å. Thus, upon formation of the copper sulphide layers the bilayer distance increases 1.8 Å. From the disappearance of the second Bragg peak can be concluded that the even harmonics make no contribution to the electron density profile, which was also found by Facci et al. [11], who claimed that the disappearance of the even peaks is consistent with the marked decrease in electron density in the middle of the bilayer planes upon formation of the metal sulphide particles.

In Figure 9.5 the SAXR measurements of a multilayer film consisting of 16 layers of the amphiphile from a 5 mM $Cu(ClO_4)_2$ subphase on silicon, before and after 30 minutes of exposure to H_2S, can be seen. The Bragg peaks have shifted slightly to higher scattering angles indicating that the bilayer spacing has decreased upon exposure to the reducing gas. After exposure to H_2S the bilayer is 58.6 Å. Thus, upon exposure to H_2S the bilayer spacing has decreased with 0.6 Å. Probably the formation of the copper sulphide layers induces a slightly different packing of the aliphatic tails in such a way that the aliphatic tails make a larger tilt angle with respect to the surface normal. This phenomena was also found by Luo et al. [17] for cobalt stearate multilayer film. They found that after exposure to H_2S, the bilayer spacing of the LB films decreased from about 50 Å to 40 Å, in this case the hexagonal packing of the amphiphiles was transformed into an orthorhombic one, due to exposure to H_2S.

The multilayer films can easily be polymerised by exposure to UV light (λ = 254 nm) under argon atmosphere. However, the regular layer structure of the LB film built up from a $CuCl_2$ subphase is completely destroyed, as has already been described in Chapter 4 [26], for LB films which were not exposed to H_2S. Figure 9.3 shows the UV/Vis spectral changes of a multilayer film, consisting of 16 layers of the amphiphile on glass, built up from a 5 mM $Cu(ClO_4)_2$ subphase after 20 minutes of exposure to UV light. The red form of the polymer with λ_{max} = 540 nm is formed and after 20 minutes no further increase in absorption could be observed, indicating that the maximum degree of polymerisation is reached after 20 minutes of exposure to UV light which was also the case for multilayers built up from a 5 mM $Cu(ClO_4)_2$ which were not treated with H_2S [26]. From the SAXR measurement of Figure 9.5 it can be seen that the layer structure of a LB film built up from a 5 mM $Cu(ClO_4)_2$ subphase

after the H_2S treatment is preserved during the polymerisation process, although the bilayer distance decreases from 58.6 Å till 56.6 Å upon exposure to UV light. This decrease in layer thickness is probably caused by a conversion of the all-trans alkyl chain into a more irregular one containing gauche conformations during the polymerisation process, as has already been pointed out in Chapter 4 [26] by means of FT-IR measurements.

Conclusions

It has been shown that it is possible to fabricate semiconductive copper sulphide layers between planes of hydrophilic headgroups of amphiphilic ligands in a LB film without disturbing the regular layer structure. XPS measurements showed that Cu(II) ion containing multilayers, with different counter ions (ClO_4^- or Cl^-) can produce copper sulphide layers which differ in stoichiometry. The formation of copper sulphide can nicely be followed by UV/Vis spectroscopy. Furthermore, the layer structure of the LB film is completely destroyed when the LB film (containing Cl^- as anion) is exposed to UV light, whereas in the case of multilayers with ClO_4^- as counter ion, the layer structure is preserved during the polymerisation process.

References

1. A. Ruaudel-Tiextier, J. Leloup and A. Barraud, *Mol. Cryst. Liq. Cryst.* **1986**, *134*, 347.
2. Y. Wang and N. Herron, *J. Chem. Phys.* **1991**, *95*, 525.
3. W. Mahler, *Inorg. Chem.* **1988**, *27*, 435.
4. A. Henglein, *Chem. Rev.* **1989**, *89*, 1861.
5. Z. Du, Z. Zhang, W. Zhao, Z. Zha, J. Zhang, Z. Jin and T. Li, *Thin Solid Films* **1992**, *210-211*, 404.
6. Y. Wang, N. Herron, W. Mahler and A. Suna, *J. Opt. Soc. Am. B* **1989**, *6*, 808.
7. J.H. Fendler and F. Meldrum, *Adv. Mater.* **1995**, *7*, 607.
8. K.C. Yi and J.H. Fendler, *Synthetic Metals* **1995**, *71*, 2109.
9. F. Griezer, D.N. Furlong, D. Scoberg, I. Ichinose, N. Kimizuka and T. Kunitake, *J. Chem. Soc. Faraday Trans.* **1992**, *88*, 2207.
10. R.S. Urquhart, D.N. Furlong, T. Gengenbach, N.J. Geddes and F. Griezer, *Langmuir* **1995**, *11*, 1127.
11. P. Facci, V. Erokhin, A. Tronin and C. Nicolini, *J. Chem. Phys.* **1994**, *98*, 13323.
12. X.K. Zhao, S. Xu and J.H. Fendler, *Langmuir* **1991**, *7*, 520.

13. C.T. Ewins and B. Stewart, *Thin Solid Films* **1996**, *284-285*, 49.
14. R. Zhu, Y. Wei, C. Yu, S. Xiao and Z. Lu, *Solid State Communications* **1992**, *84*, 449.
15. X. Peng, S. Guan, X. Chai, J. Jiang and T. Li, *J. Phys. Chem.* **1992**, *96*, 3170.
16. X.Peng, H. Chen, S. Kan, T. Bai and T. Li, *Thin Solid Films* **1994**, *242*, 118.
17. X. Luo, Z. Zhang and Y. Liang, *Langmuir* **1994**, *10*, 3213.
18. D.J. Elliot, D.N. Furlong, T.R. Gengenbach, F. Griezer, R.S. Urquhart, C.L. Hoffman and J.F. Rabolt, *Colloid Surfaces A: Physicochem. Eng. Aspects* **1995**, *103*, 207.
19. D.J. Elliot, D.N. Furlong, T.R. Gengenbach, F. Griezer, R.S. Urquhart, C.L. Hoffman and J.F. Rabolt, *Langmuir* **1995**, *11*, 4773.
20. M.T.S. Nair and P.K. Nair, *Semicond. Sci. Technol.* **1989**, *4*, 191.
21. J. Leloup, A. Ruaudel-Teixtier and A. Barraud, *Thin Solid Films* **1992**, *210-211*, 407.
22. J.C.W. Folmer and F. Jellinek, *J. Less-Common Metals* **1980**, *76*, 153.
23. J.C.W. Folmer, *Thesis*, University of Groningen, The Netherlands **1981**.
24. H. Chen, X. Chai, Q. Wei, Y. Jiang and T. Li, *Thin Solid Films* **1989**, *178*, 535.
25. P.J. Werkman and A.J. Schouten, *Thin Solid Films* **1996**, *284-285*, 24.
26. P.J. Werkman, R.H. Wieringa, E.J. Vorenkamp and A.J. Schouten, submitted for publication in Langmuir.
27. H. Göbel, *Thesis*, Technische Universität München, Germany **1989**.
28. C. Bubeck, *Thin Solid Films* **1980**, *160*, 1.
29. R. Marshall and S.S. Mitra, *J. Appl. Phys.* **1965**, *36*, 3882.
30. N. Nakayama, *J. Phys. Soc. Japan* **1968**, *25*, 290.
31. J. George and K.S. Joseph, *Solid State Comm.* **1983**, *48*, 601.
32. V.I. Klimov and V.A. Karavanskii, *Phys. Rev. B* **1996**, *54*, 8087.
33. S.K. Haram, A.R. Mahadeshwar and S.G. Dixit, *J. Phys. Chem.* **1996**, *100*, 5868.

Summary

Thin molecular films have potential applications in electronic and optical devices and have regenerated interest in the classical Langmuir-Blodgett (LB) film technique. The easy monolayer and multilayer preparation and the wide variety of organic compounds available, make this method particularly attractive. Classical LB films of low molecular weight amphiphiles often have poor mechanical and thermal stability or poor resistance to dissolution by organic solvents. These problems are major obstacles for applications in practical devices. In order to overcome these problems, polymer LB films have been employed to improve the thermal and mechanical stability of LB films. Polymer LB films can be prepared from amphiphilic monomers which are polymerised by conventional polymerisation methods after which LB films are prepared from polymerisable amphiphiles. These are spread at the air-water interface after which multilayers are built up and the amphiphiles in these multilayers are subsequently polymerised by means of UV or γ-irradiation or thermally. The latter approach is used in this thesis.

The extension of the LB technique to include functional metal complexes can result in a substantial expansion of the variety of functional films. These metal complex film systems have potential applications as sensors, in nonlinear devices, in energy conversion and storage devices, in optical computing and information storage media.

This thesis describes the formation and detailed characterisation of LB films of metal complexes of polymerisable amphiphiles of the following general structure with X being the hydrophilic headgroup containing a ligand and n = 1 or 2.

$$[CH_3—(CH_2)_{11}—C{\equiv}C—C{\equiv}C—(CH_2)_8]_n—X$$

The influence of different ligands (dithiooxamide, pyridine and imidazole) used as hydrophilic headgroup upon the complexation process at the air-water interface with metal ions, has been studied by measuring the surface pressure-area characteristics. In the case of the pyridine group containing amphiphiles, also Brewster angle microscopy (BAM) has been used to visualise morphological changes of the monolayers during the complexation process at the air-water interface. Furthermore, the influence of hydrogen bonding upon the stability and morphology of the monolayers is studied. Multilayers of all the amphiphiles have been built

up and their structure has been investigated by means of XPS, small angle X-ray reflection (SAXR) measurements and FT-IR spectroscopy. The LB films have been polymerised by means of irradiation with UV light under an argon atmosphere. This process has been studied by means of UV/Vis and FT-IR spectroscopy and by means of SAXR measurements. For a number of possible applications of noncentrosymmetric LB films are useful or required. For this reason alternating multilayers were prepared. The structure and polymerisation behaviour of these noncentrosymmetric superlattices is discussed in great detail.

In recent years there is a growing interest in the preparation of inorganic semiconductor particles or layers in LB films. These films have potential applications in optoelectronic devices as optical switches, as infrared detectors and in photovoltaics. For this reason, semiconductor copper sulphide layers have been prepared in LB films of a pyridine group containing amphiphilic ligand, by exposing the Cu(II) ions in these multilayers to H_2S.

In *Chapter 2* the monolayer properties of the amphiphile N,N'-Bis(10,12-pentacosadiynyloxycarbonylmethyl)dithiooxamide (X = O–$COCH_2$–NHC(=S)C(C=S)NH–CH_2CO–O, n = 2) are described. The amphiphile itself does not form stable monolayers at the air-water interface but when Cu(II) ions are added to the subphase, a strongly conjugated coordination polymer is formed. The coordination polymer forms stable monolayers at the air-water interface and the stability of these monolayers is strongly influenced by the counter ion, pH and temperature of the subphase. The morphology of monolayer film is studied by means of electron microscopy. Multilayers of the coordination polymer can easily be built up with a Y-type transfer. Unfortunately, upon irradiation with UV light the diacetylene groups are only partly converted to polydiacetylene and the coordination polymer is partly destroyed.

Chapter 3 describes the monolayer behaviour of the amphiphile 4-(10,12-pentacosadiynamidomethyl)pyridine (X = CONH–CH_2–C_5H_4N, n = 1) at the air-water interface. This amphiphile itself forms stable monolayers with a clear liquid-expanded (LE) to liquid-condensed (LC) phase transition at various temperatures. When Cu(II) ions are added to the subphase an increase in surface pressure (Π_c) at which the phase transition appears, can be observed, which indicates that complexation in the monolayer has occurred. The extent of complexation depends strongly on the metal ion, metal ion concentration, complexation time, counter ion, temperature and ionic strength of the subphase. The appearance of these monolayers at the air-water interface, before and after irradiation with UV light, has been studied by means of electron microscopy, as is described in *Chapter 4*. Furthermore, multilayers of Cu(II) and Cd(II) complexes of the amphiphile have been built up and XPS measurements confirm the presence of these metal ions. It has been found that a maximum amount of 1 metal ion to 2 amphiphiles can be incorporated into these multilayer films. When

the multilayers contain Cu(II) ions, these Cu(II) ions are reduced by X-rays to Cu(I) in the XPS apparatus.

The structure of the multilayers is strongly influenced by the type of metal ion and counter ion incorporated. The multilayers are polymerised by means of UV irradiation forming a strongly conjugated polymer with absorption bands at 540 and 620 nm. Upon polymerisation the bilayer spacing decreases and in the case of the Cu(II) ion containing multilayers, the regular all-trans alkyl chain of the amphiphiles is converted into a more irregular one containing gauche conformations.

Chapter 5 describes the monolayer properties of the amphiphile 4-(10,12-pentacosadiynoatemethyl)pyridine (X = OCO–CH_2–C_5H_4N, n = 1) at different pH values of the aqueous subphase. The complexation process with Cu(II) ions at the air-water interface was studied and again this process is strongly influenced by different factors as already discussed in Chapter 3. Multilayers of the amphiphile can only be built up when the subphase contains Cu(II) ions. These LB films have a regular layer structure and the bilayer spacing decreases during the polymerisation process.

In *Chapter 6* the morphological changes of monolayers of the amide pyridine amphiphile (of Chapter 3 and 4) and the ester pyridine amphiphile (of Chapter 5) during compression are shown by means of Brewster angle microscopy (BAM). On a pure water subphase, Brewster angle microscopy of the monolayer of the ester amphiphile, shows the formation of spiral crystalline domains at the plateau in the isotherm near the solid state region. The amide containing ligand however, forms two-dimensional crystalline domains directly after spreading at the air-water interface, which are pushed together upon compression. The effect of complexation with Cu(II) ions or the effect of different types of counter ions on the morphology of the monolayers of the amphiphiles can be observed nicely. Furthermore, the size of the crystalline nuclei decreases when the Cu(II) ion concentration of the subphase increases.

The monolayer characteristics of N-(10,12-pentacosadiynamidopropyl)imidazole (X = CONH–$(CH_2)_3$-$C_3H_3N_2$, n = 1) is described in *Chapter 7*. This amphiphile already forms complexes with different metal chlorides at very low metal ion concentrations of the subphase ($5 \cdot 10^{-7}$ M). The appearance of the monolayer at the air-water interface before or after irradiation with UV light has been studied by means of electron microscopy. The plane group symmetry of the polymerised monolayers was deduced from electron diffraction measurements. Multilayers with a regular layer structure can be built up when the subphase contains $CuCl_2$. The multilayers were polymerised by exposure to UV light and during this process the bilayer spacing decreases and again the all-trans alkyl chains of the amphiphiles are converted into more irregular ones containing gauche conformations.

The preparation of Y-type alternating multilayer films of two diacetylene group containing amphiphiles (an acid (A in which X = COOH) and the amide (B in which X = CONH–CH_2–C_5H_4N, n = 1) of Chapter 3 and 4) is described in *Chapter 8*. The alternating multilayers have a regular layer structure and the alkyl chains of the amphiphiles have an all-trans conformation. These films can partly be polymerised by means of UV irradiation forming the red form (λ = 540 nm) of the polymer. Upon polymerisation the regular layer structure is preserved and the bilayer spacing increases and the all-trans conformation of the aliphatic chain is partly converted into a more irregular one containing gauche conformations.

Chapter 9 describes the fabrication of copper sulphide layers within multilayers of copper complexes of the amide pyridine amphiphile (Chapter 3 and 4) by diffusion of H_2S into the multilayers. It is shown that copper sulphide layers can be synthesised which differ in stoichiometry when Cu(II) ion containing multilayers are used which are built up from different subphases ($CuCl_2$ or $Cu(ClO_4)_2$). The copper sulphide containing multilayers can be polymerised by exposure to UV light. After polymerisation the regular layer structure is destroyed in the case of LB films built up from a $CuCl_2$ subphase, whereas in the case of multilayers built up from a $Cu(ClO_4)_2$ subphase, the regular layer structure is preserved during the polymerisation process.

It is clear that metal complexes of polymerisable amphiphilic ligands can be formed at the air-water interface. The kind of ligand used as headgroup of the amphiphile has an enormous influence on the complexation behaviour of the amphiphile. Introducing an amide bond into the amphiphile greatly enhances the monolayer stability. LB films of these metal complexes can be prepared, which have a regular layer structure. The structure of the multilayer films is strongly influenced by the metal ion or counter ion incorporated into the LB films. In most cases the regular layer structure is preserved during the polymerisation process although the all-trans aliphatic chains are converted into more irregular ones containing gauche conformation. In this way LB films of polymeric metal complexes are successfully prepared. Also, noncentrosymmetric alternating multilayers can be prepared. Furthermore, the Cu(II) ions inside the multilayers can react with a reducing gas to form semiconductor layers. The acquired knowledge is important for the preparation of other thin molecular films of metal complexes which are suitable for all kinds of applications.

Samenvatting

Dunne molekulaire films hebben potentiële toepassingen in elektronische en optische systemen en hebben opnieuw de aandacht gevestigd op de klassieke Langmuir-Blodgett (LB) techniek. Hierbij wordt een verbinding opgelost in een vluchtig organisch oplosmiddel dat niet met water mengt. Een kleine hoeveelheid van deze oplossing wordt op een wateroppervlak tussen twee barrières gedruppeld. Het oplosmiddel verdampt en de molekulen blijven achter op het wateroppervlak en vormen daar een monomolekulaire laag (een monolaag). Deze molekulen kunnen zich ordenen door de barrières naar elkaar toe te schuiven. Tijdens de verkleining van het wateroppervlak (hetgeen overeenkomt met een verkleining van de beschikbare oppervlak per molekuul (A)) wordt de oppervlaktedruk (Π) gemeten. Wanneer de gemeten oppervlaktedruk tegen het beschikbare oppervlak per molekuul wordt uitgezet, wordt een Π-A isotherm verkregen. In Figuur 1 is een standaardvoorbeeld van een Π-A isotherm weergegeven.

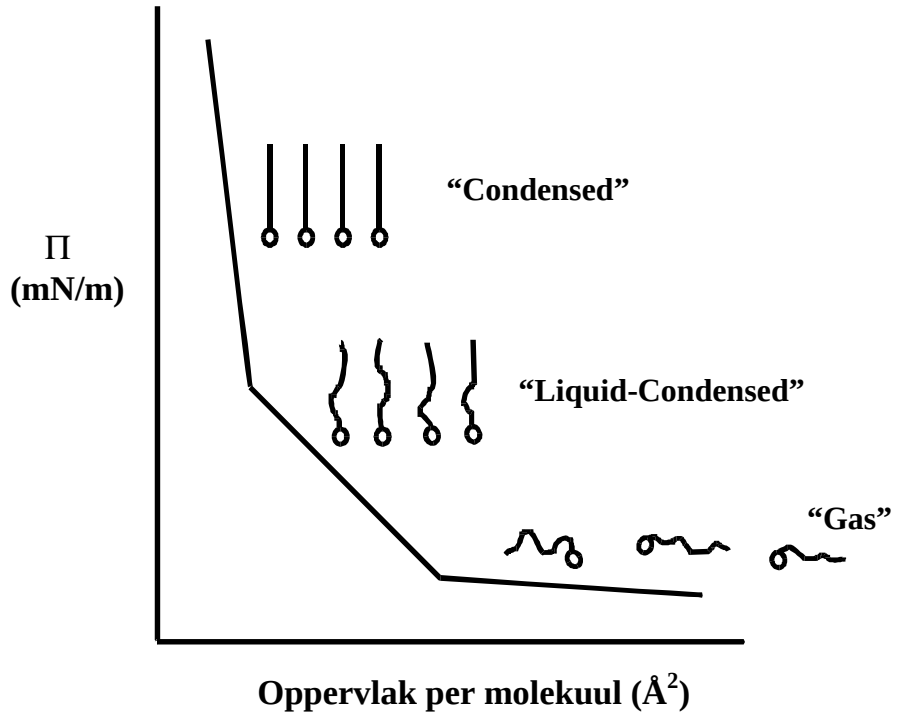

Figuur 1: *Een standaardvoorbeeld van een Π-A isotherm.*

In Figuur 1 is te zien dat bij grote oppervlakken per molekuul de oppervlaktedruk (Π) bijna 0 $mN \cdot m^{-1}$ is omdat de molekulen elkaar niet voelen. Dit gebied wordt de “Gas” fase van de isotherm genoemd. Bij verdere verkleining van het wateroppervlak beginnen de molekulen elkaar te voelen en neemt Π toe. Deze fase van de isotherm wordt de “Liquid-Condensed” fase genoemd. Tenslotte bij nog verdere verkleining van het wateroppervlak wordt de “Condensed” fase van de isotherm bereikt, een kleine verandering van het oppervlak per molekuul heeft enorme verandering in oppervlaktedruk tot gevolg. In deze fase zijn de molekulen in een zeer geordende toestand gebracht.

Zeepachtige molekulen zijn de eerste verbindingen die zijn onderzocht met behulp van de LB techniek. Deze molekulen zijn amfifielen (Figuur 2) met een hydrofiel (waterminnend) gedeelte en een hydrofoob (waterafstotend) gedeelte. Het hydrofiele gedeelte richt zich naar het wateroppervlak terwijl het hydrofobe gedeelte zich van het water af richt tijdens het verkleinen van het wateroppervlak. Hierdoor kunnen goed geordende monolagen op het water worden gevormd.

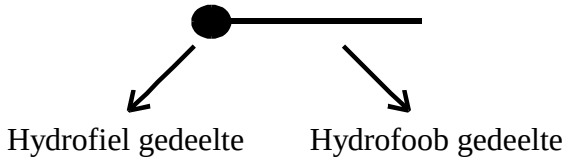

Figuur 2: *Schematische weergave van een amfifiel.*

Wanneer de molekulen op het wateroppervlak in de meest geordende toestand zijn gebracht (de “Condensed” fase) kunnen ze worden overgebracht op een substraat (bijvoorbeeld een glas, goud of silicium plaatje). De overdracht van de monolaag vindt plaats door een substraat verticaal door de monolaag, die onder constante druk staat, te bewegen. Wanneer er zowel tijdens het naar beneden als het omhoog bewegen van het substraat monolaag overdracht plaatsvindt, spreekt men van een Y-type overdracht. In de multilaag komen dan de hydrofiele koppen tegen over elkaar te zitten evenals de hydrofobe staartuiteinden. Dit is de meest stabiele film struktuur. Treedt er alleen overdracht van de monolaag tijdens de omhooggaande beweging op dan spreekt men van een Z-type overdracht, waarbij de kop van het ene amfifiel naar de staart van het volgende amfifiel is gekeerd (kop-staart). Dit film type is minder stabiel. Verder is er nog een X-type overdracht (staart-kop) waarbij alleen bij de neergaande beweging overdracht van de monolaag plaatsvindt. Door nu de op- en neergaande beweging van het substraat verschillende malen te herhalen kan een dunne geordende molekulaire film worden gemaakt waarvan de dikte precies kan worden

ingesteld. Het gemak waarmee mono- en multilaagsystemen gemaakt kunnen worden in combinatie met de grote verscheidenheid aan organische verbindingen, maken de LB techniek tot een aantrekkelijke methode om ultradunne organische films te maken.

De klassieke LB films van laag molekulaire amfifielen hebben vaak een slechte mechanische en thermische stabiliteit. Ook lossen deze films vaak snel op in organische oplosmiddelen. Deze problemen zijn grote obstakels om deze films toe te passen in praktische systemen. Om deze problemen te overwinnen is men er toe overgegaan polymeren te gebruiken als organisch materiaal voor de vervaardiging van LB films. Op die manier krijgen deze ultradunne films betere mechanische en thermische eigenschappen.

Polymere LB films kunnen op verschillende manieren worden vervaardigd. Eén manier is om amfifiele monomeren volgens conventionele polymerisatie methoden te polymeriseren en om de gevormde polymeren vervolgens op het lucht-water grensvlak te spreiden waarna de LB films kunnen worden opgebouwd. Een andere manier is om polymeriseerbare amfifielen op het wateroppervlak te spreiden en ze vervolgens te polymeriseren in de monolaag waarna multilagen kunnen worden opgebouwd. Ook kunnen deze polymeriseerbare amfifielen direkt na spreiding op wateroppervlak worden overgebracht op een substraat zodat een LB film wordt gevormd. Vervolgens kunnen de amfifielen in deze film worden gepolymeriseerd door ze bloot te stellen aan UV of γ-straling. Deze laatste aanpak wordt in dit proefschrift gebruikt.

Wanneer de conventionele organische materialen, die geschikt zijn voor de LB techniek, worden uitgebreid met funktionele metaalkomplexen, kan dat leiden tot een enorme toename in de verscheidenheid van funktionele films. Deze metaalkomplex film systemen hebben mogelijke toepassingen als sensoren, in niet lineair optische systemen, in energie omzetting en opslag systemen en in informatie opslag media.

In dit proefschrift wordt de vorming van polymeriseerbare amfifiele metaalkomplexen aan lucht-water grensvlak behandeld. De invloed van verschillende liganden, metaalionen en tegenionen op het komplexatiegedrag van polymeriseerbare amfifielen met metaalionen aan het lucht-water grensvlak zijn onderzocht. Hiertoe worden metaalionen in het water opgelost en worden de molekulen (zoals verderop weergegeven) op het wateroppervlak gebracht. De metaalionen gaan zich aan de molekulen binden (komplexeren) omdat deze molekulen bepaalde groepen (liganden) bevatten die graag een binding met metaalionen aangaan. Vervolgens worden Π-A isothermen opgenomen en een verandering in de vorm van deze isothermen is een sterke indicatie voor de vorming van metaalkomplexen aan het lucht-water

grensvlak. De polymeriseerbare amfifiele liganden hebben de volgende algemene struktuur waarin X de hydrofiele kopgroep is die een ligand bevat en n kan 1 of 2 zijn.

$$[CH_3—(CH_2)_{11}—C\equiv C—C\equiv C—(CH_2)_8]_n—X$$

Van de gevormde polymeriseerbare amfifiele metaalkomplexen zijn LB films opgebouwd welke zeer gedetailleerd gekarakteriseerd zijn. De invloed van verschillende liganden (dithiooxamide (X = O–$COCH_2$–NHC(=S)C(=S)NH–CH_2CO–O, n = 2), pyridine (X = CONH–CH_2–C_5H_4N of OCO–CH_2–C_5H_4N, n = 1) en imidazole (X = CONH–$(CH_2)_3$–$C_3H_3N_2$, n = 1)) als kopgroep op het komplexatie gedrag met metaalionen (opgelost in de waterfase) aan het lucht-water grensvlak is onderzocht aan de hand van Π-A isothermen. Verder zijn de veranderingen die in de monolaagstruktuur ontstaan door het optreden van komplexatie, onderzocht met behulp van Brewster angle microscopie (BAM) tijdens het samendrukken van de monolaag. Bij deze techniek wordt het wateroppervlak onder een hoek van 53^o (de Brewster angle) bestraald met een laser. Bij deze hoek vindt er geen reflectie van de laser van het wateroppervlak plaats zodat de detector, die onder dezelfde hoek staat opgesteld aan de andere kant van het wateroppervlak, geen signaal opvangt. Wanneer de monolaag zich in de “Liquid-Condensed” (LC) of “Condensed” (C)fase bevindt, treedt er wel reflectie van het laserlicht op omdat de monolaag een andere brekingsindex heeft dan water. Deze reflectie maakt de structuur van de monolaag op het lucht-water grensvlak zichtbaar, zodat de structuur veranderingen door het optreden van komplexatie goed zichtbaar zijn. Verder is de invloed van de vorming van waterstofbruggen tussen pyridine amfifielen op de structuur en stabiliteit van deze monolagen onderzocht.

De verschillende amfifielen blijken goed metaalkomplexen te kunnen vormen op het lucht-water grensvlak. De volgende factoren hebben grote invloed op het komplexatie gedrag: het soort metaalion (bijv. Cu(II), Mn(II), Cd(II), etc.), het type tegenion (Cl^-, Br^-, ClO_4^-, etc.), de temperatuur, pH en de ionsterkte van de waterfase. Het dithiooxamide amfifiel (Hoofdstuk 2) vormt een coördinatie polymeer wanneer koper (Cu(II)) ionen in de waterfase waren opgelost. Verder vormen de twee pyridine amfifielen (Hoofdstuk 3 en 5) metaalkomplexen met Cu(II) ionen bij concentraties vanaf 5 mM. Het imidazole amfifiel (Hoofdstuk 7) vormt al metaalkomplexen met Cu(II) ionen bij concentraties vanaf $5\cdot10^{-7}$ M. Dit komt voornamelijk doordat de imidazole groep een veel grotere basiciteit heeft dan de pyridine groep. Ook kan dit amfifiel met veel meer metaalionen metaalkomplexen vormen aan het lucht-water grensvlak. Van de twee pyridine amfifielen vormt degene met een amide binding tussen de hydrofiele kopgroep en de hydrofobe staart de meest stabiele monolagen, doordat dit amfifiel

waterstofbruggen kan vormen met nabuur amfifielen (Hoofdstuk 6). De struktuur veranderingen die door het plaatsvinden van komplexatie optreden in de monolagen van de pyridine amfifielen op het lucht-water grensvlak, zijn goed te zien aan de hand van de BAM foto's zoals te zien is in Hoofdstuk 6.

Van de verschillende Cu(II) en Cd(II) komplexen zijn multilaagsystemen opgebouwd met behulp van de LB techniek. De struktuur van deze multilaagsystemen is met verschillende technieken bestudeerd. Fourier transform infrarood spectroscopie (FT-IR) is een techniek die veel informatie verschaft over de oriëntatie van molekulen in LB films. X-ray photoelectron spectroscopie (XPS) geeft informatie over welke elementen er in de toplaag (50 tot 100 Å, 1Å = 10^{-10} m)) van de LB film aanwezig zijn. Ook kan de verhouding tussen de verschillende elementen die in deze toplaag aanwezig zijn worden berekend. Verder zijn er veel small angle X-ray reflection (SAXR) metingen uitgevoerd om vast te stellen of de multilaagsystemen wel een goede lagenstruktuur hebben.

Het blijkt dat de structuur van deze LB films sterk wordt beïnvloed door het soort metaalion en type tegenion dat in de waterfase wordt opgelost. Wanneer de LB films zijn opgebouwd met een Z-type overdracht (alleen overdracht met de opgaande beweging van het substraat), blijkt dat deze films toch een Y-type struktuur hebben. Er heeft dus een reorganisatie in de LB film plaatsgevonden om tot de meest stabiele Y-type film te komen. De lange alifatische (CH_2) staarten staan onder een bepaalde hoek t.o.v. het substraat die varieert van 35^o tot 55^o, afhankelijk van het gebruikte amfifiel, metaalion en type tegenion.

De amfifielen bevatten een diacetyleen binding (Figuur 3). Wanneer de amfifielen bestraald worden met UV licht (λ = 254 nm), vindt er een 1,4 additie plaats en wordt het overeenkomstige polymeer gevormd (een polydiacetyleen). Dit polymeer is goed te zien omdat het licht absorbeert in het zichtbare gebied van het licht waardoor het polymeer er rood (λ_{max} = 500 en 540 nm) of blauw ((λ_{max} = 620 nm) uitziet.

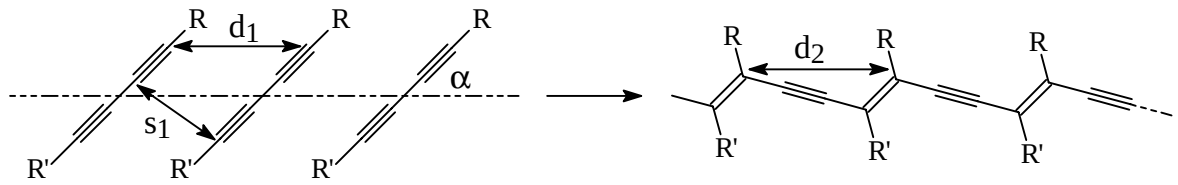

Figuur 3: *Het principe van de diacetyleen polymerisatie.*

Met behulp van elektronen microscopie is goed te zien dat de verschillende amfifielen een homogene vlakke monolaag vormen op het wateroppervlak. Maar na bestraling met UV licht krijgt de monolaag een gestreepte structuur.

Na bestraling met UV licht verandert ook de structuur van de LB films. De lagenstruktuur neemt af in dikte en de alifatische staarten van de amfifielen verliezen de regelmatige all-trans conformatie en krijgen een meer onregelmatige struktuur die gauche conformaties bevat.

Voor veel mogelijke toepassingen van LB films is het van belang dat deze films een niet-centrosymmetrische struktuur hebben (Figuur 4). Eén van de manieren om dit via de LB techniek te bereiken is om alternerende multilaagsystemen te vervaardigen.

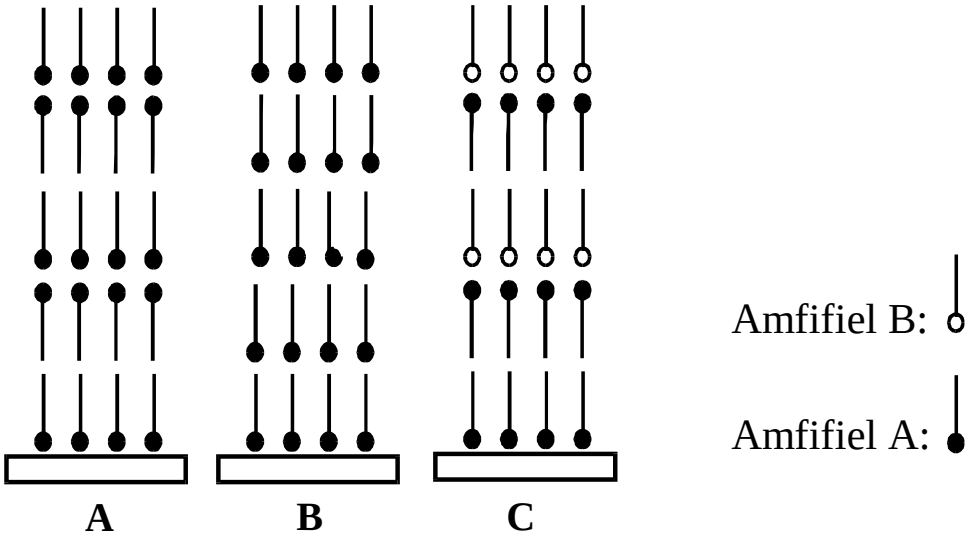

Figuur 4: *Schematische voorstelling van een centrosymmetrisch (A), een niet-centrosymmetrisch (B) en een alternerend niet-centrosymmetrisch (C) systeem.*

Er is een Y-type alternerend multilaagsysteem opgebouwd bestaande uit twee diacetyleen groep bevattende amfifielen (Hoofdstuk 8). Eén met een zuur groep (X = COOH, n = 1) als hydrofiele kop en één met een pyridine groep (X = $CONH–CH_2–C_5H_4N$, n = 1). Deze alternerende LB films hebben een goede regelmatige lagenstructuur die toeneemt in dikte wanneer dit systeem wordt blootgesteld aan UV licht.

De laatste jaren is er een grote belangstelling voor de vervaardiging van anorganische halfgeleider deeltjes of lagen in LB films. Deze LB films hebben mogelijke toepassingen in

opto-electronische systemen als optische schakelaars, als infrarooddetektoren en in fotovoltaïsche cellen. Daarom zijn de LB films van het amide pyridine amfifiel die Cu(II) ionen bevatten blootgesteld aan het gas zwavelwaterstof (H_2S) (Hoofdstuk 9). Hierdoor worden dunne lagen van de halfgeleider kopersulfide gevormd tussen de hydrofiele kopgroepen van de amfifielen. Het blijkt dat de verhouding tussen koper en zwavel in het gevormde kopersulfide sterk afhangt van het tegenion van koper (Cl^- of CLO_4^-). Gedurende de vorming van de kopersulfide lagen blijft de lagenstruktuur van de amfifielen behouden. Maar na bestraling met UV licht verliest de LB film waarin Cl^- het tegenion is van Cu(II), zijn lagenstruktuur terwijl in de LB films die ClO_4^- als tegenion bevatten hun lagenstruktuur tijdens het polymerisatieproces behouden.

De verworven kennis over de vervaardiging van ultradunne molekulaire films van metaalkomplexen en het beïnvloeden van het komplexatiegedrag in de monolaag is van groot belang voor het vervaardigen van andere multilaagsystemen van metaalkomplexen, die geschikt zijn voor allerlei mogelijke toepassingen.